

**Synthesis of cyclitol derivatives and study of
their complexation with ions and small
molecules**

Thesis

Submitted to the

UNIVERSITY OF PUNE

For the degree of

DOCTOR OF PHILOSOPHY

in

CHEMISTRY

By

Shailesh Satish Dixit

Organic Chemistry Division
National Chemical Laboratory
Pune-411008

September 2007

Dedicated to my Beloved Parents...



CERTIFICATE

This is to certify that the work incorporated in the thesis entitled “**Synthesis of cyclitol derivatives and study of their complexation with ions and small molecules**” submitted by **Shailesh S. Dixit** was carried out by him under my supervision at the National Chemical Laboratory, Pune, India. Such materials obtained from other sources have been duly acknowledged in the thesis.

Date: September, 15th 2007
Organic Chemistry Division
National Chemical Laboratory
Pune, 411 008

Dr. M. S. SHASHIDHAR
Research guide

DECLARATION

I hereby declare that the thesis entitled “**Synthesis of cyclitol derivatives and study of their complexation with ions and small molecules**” submitted for Ph. D. degree to the University of Pune has not been submitted by me for a degree to any other University.

Date: September, 15th 2007
Organic Chemistry Division
National Chemical Laboratory
Pune, 411 008

SHAILESH SATISH DIXIT

ACKNOWLEDGEMENT

This thesis is the result of five years of work whereby I have been accompanied and supported by many people. It is a pleasant aspect that I have now the opportunity to express my gratitude for all of them.

I owe the fulfillment of this great endeavour to my research mentor Dr. M. S. Shashidhar who introduced me to this fascinating realm of chemistry. Although any eulogy is insufficient, but I take this opportunity to express my reverence to him for his guidance and excellent work ethics. His systematic working style and humanitarianism is an attribute that I wish to take forward with me along with the chemistry that I learnt from him.

I wish to express my gratitude to Dr. M. M. Bhadbhade and Dr. Rajesh Gonnade for the X-ray analysis. Rajesh is also a good friend of mine and was always there to help me. I thank Dr. V.G. Puranik for constant support. I am grateful to Dr. N. N. Joshi, Dr. B. G. Hazra and Dr. T. Pathak for their help and encouragement.

I also thank Head, Organic Chemistry Division, Dr. Ganesh Pandey, and Director NCL, for infrastructure and facilities. Help rendered by NMR, Microanalysis and library group are gratefully acknowledged. I would like to thank Dr. Peddireddy for TGA/DTA.

I would like to thank DST and CSIR, New Delhi for the financial support.

I was blessed with an opportunity to work in most systematic and well maintained lab. I am very much indebted to my seniors Dr. Praveen, Dr. Sureshan, Dr. Aditya, Dr. Manash, Dr. Sachin, and Dr. Devaraj for their advices, true help, love and care. I enjoyed cheerful and amazing atmosphere with humor in lab with colleagues Murali, Manoj, Gaurav, Madhuri, Rajendra, Shobhana and Bharat. I also thank Sunilji and Moreji for their regular help in laboratory maintenance. Stay in lab 213, 215 and 285 at the end of work, will be always green in my memory.

I wish to thank Dr. Vijay Khanna, Dr. P. H. Ladwa, Dr. Pai, Dr. Pratap, Dr. Reddy, Mr. P. D. Kulkarni and other staff members of Ahmednagar College, for excellent teaching and to understand chemistry in a different way. My special thanks are due to my senior and teacher, Mrs. Saira Pathan for her help and all time encouragement.

I feel great sense of gratitude for Mr. N.V. Jadhav, Mr. S. R. Kankrej, Mr. R. P. Patil, Mr. N. M. Kadam, Mrs. S. P. Nirbhavane, Mrs. S. G. Gaikwad and other staff members of Bhonsala Military College, Nashik for their encouragement, support and inspiration to come to research.

I am indebted to all my teachers who paved the foundation stone to my studies.

My warm thanks are due to my friends Sambhaji, Satpal, Anish, Prashant, Rodney, Manmohan, Sachin, Babu, Namdeo, Nilkanth, Sudhir, Khirud, Gahininath, Jadabsharma, Bala, Keshrinath, Jiten and all other friends and colleagues at NCL who directly or indirectly helped me during doctoral research work.

Special thanks to Dnyandev (Nanu), Dr. Nilesh, Dr. Yogesh, Dr. Praveen, Sandeep, Deepak, Ujwal, Mehraj and Yogesh Waman, who made my stay very comfortable and memorable one.

I would like to extend my thanks to Meeran, Yogesh, Hemant, Sanjay, Dnyaneshwar, Toshal, Vishal, Vaibhav, Sunil and Amit for being with me whenever I needed. Bharat, Amol, Dr. Sachin, Dr. Sanjay, Parikshit, Navneet, Aniket, Sanjay Mhaske, Gokul, Gorakh, Gangadhar, Sunil, Umesh, Prakash, Rahul, Gauri, Pramila, Kalpana, Komal, Pallavi and Rohini are gratefully acknowledged for constant encouragement and support.

I take this opportunity to thank Dr. Mrs. Vidya Shashidhar and Dr. Mrs. Ranjana Bhadbhade for their advice and help. I thank Mr. B. A. Salunke, Mr. S. H. Munot, Mr. V. Balaji and Mr. R. N. Pagire, and their family members for making my family stay memorable in Pune.

I can't find the right words for the one person whom I like most, my wife, Nandini. She could have only experienced all my ups and downs, without her patience, love & endless support this thesis

wouldn't have been written. Special thanks to my daughter Rajeshwari (Sarasi) for making pleasant atmosphere at home and always refreshing me by her smile.

No words would suffice to express my gratitude and love to my parents, sister (Swati), aaji, mama, mami, mavshi, aatya, kaka, kaku, in-laws and all family members for their continuous showering of boundless affection on me and supporting me in whatever I chose or did. It was always a pleasure to share thoughts and discuss with Suhas and Parag. Also, special thanks to my nephew Varad for enjoyable moments which I had with him.

It is my parent's prayer, constant struggle and relentless hard work to overcome the odds of life, which has inspired me to pursue life with a greater optimism. The warmth and moral value of my parent's have stood me in good stead through my life and I would always look up to them for strength no matter what I have to go through. This Ph. D. thesis is a result of the extraordinary will, efforts and sacrifices of my parents. My successes are dedicated to them now and always.

It gives me great strength and belief in presence of **God**; because of his enormous blessings it was possible to bring the completion of my research endeavours in the best possible way. I bow to the divine strength and wish it would dwell throughout my life.

Date: 15th September, 2007

Shailesh

CONTENTS

Title	Page No.
Abbreviations	1
Synopsis of the thesis	5
List of publications	13
PART-A	15
A review of the literature on the complexation behavior of cyclitol and carbohydrate derivatives with metal ions.	
PART-B	66
Chapter 1	66
Synthesis and metal ion binding studies of <i>myo</i>-inositol derived crown ethers.	
Section 1	66
Metal ion binding studies with <i>myo</i>-inositol derived crown-4-ethers.	
1.1 Introduction	67
1.2 Results and discussion	67
1.3 Conclusions	79
Section 2	80
Inositol derived crown ethers: effect of auxiliary protecting groups on their metal ion binding ability.	
1.4 Introduction	81
1.5 Results and discussion	82
1.6 Conclusions	99

Section 3	100
1.7 Experimental section	100
1.8 References	124
1.9 Appendix	130
Chapter 2	197
<i>scyllo</i>-Inositol derived crown ethers: A comparative study with <i>myo</i>-inositol derived crown ethers.	
2.1 Introduction	198
2.2 Results and discussion	199
2.3 Conclusions	211
2.4 Experimental section	212
2.5 References	220
2.6 Appendix	221
Chapter 3	247
Complexation of simple <i>O</i>-substituted inositol derivatives with metal ions and small molecules.	
3.1 Introduction	248
3.2 Results and discussion	251
3.3 Conclusions	271
3.4 Experimental section	272
3.5 References	289
3.6 Appendix	292

Abbreviations

Ac	Acetyl
Ac ₂ O	Acetic anhydride
All	Allyl
anh.	Anhydrous
aq.	Aqueous
Bn	Benzyl
BnBr	Benzyl bromide
BuLi	Butyl lithium
<i>i</i> -BuNH ₂	Iso-butyl amine
Bz	Benzoyl
BzCl	Benzoyl chloride
Calcd.	Calculated
Cat.	Catalytic
Conc.	Concentration
(COCl) ₂	Oxalyl chloride
CSA	Camphorsulfonic acid
D ₂ O	Deuterium Oxide
DAG	Diacylglycerol
DCM	Dichloromethane
DIAD	Diisopropyl azidodicarboxylate
DIBAL	Diisobutyl aluminium

dil.	Dilute
DMAP	Dimethylamino pyridine
DMF	N, N' Dimethylformamide
DMSO	Dimethyl sulfoxide
eq.	Equivalent
EtOAc	Ethyl acetate
Et ₃ N	Triethyl amine
g	Gram
GPI	Glycophosphatidylinositol
h	Hour(s)
Hz	Hertz
Ins (1) P	<i>D-myo</i> -inositol-1-phosphate
Ins (1,2,6) P ₃	<i>D-myo</i> -Inositol-1,2,6-trisphosphate
Ins (1,4,5) P ₃	<i>D-myo</i> -Inositol-1,4,5-trisphosphate
Ins (1,3,5) P ₃	<i>D-myo</i> -Inositol-1,3,5-trisphosphate
Ins (2,4,6) P ₃	<i>D-myo</i> -Inositol-2,4,6-trisphosphate
Ins((1-2 cyc)4,5)P ₃	<i>D-myo</i> -inositol-1,2-cyclic-4,5-trisphosphate
Ins (1,2,3,4,5,6) P ₆	<i>D-myo</i> -Inositol-1,2,3,4,5,6-hexakisphosphate
IR	Infrared
LiH	Lithium hydride
Me	Methyl
MeOH	Methanol

CH ₃ CN	Acetonitrile
Mg	Magnesium
MeI	Methyl iodide
min.	Minute(s)
mL	Milliliter
mmol	Milli mol
m.p.	Melting point
NaH	Sodium hydride
NaOMe	Sodium methoxide
NaBH ₄	Sodium borohydride
NMR	Nuclear magnetic Resonance
ORTEP	Orthogonal thermal ellipsoid plot
Ph	Phenyl
PI-PLC	Phosphatidylinositol-specific phospholipase C
PtdIns	Phosphatidylinositol
rt.	Room temperature (23-30 °C)
Rac.	Racemic
Rf	Retention factor
Satd	Saturated
TBDMS	<i>tert</i> -Butyldimethylsilyl
TFA	Trifluoroacetic acid
THF	Tetrahydrofuran

TLC	Thin layer chromatography
TMS	Trimethyl silyl
TsOH	<i>p</i> -Toluene sulfonic acid
TsCl	<i>p</i> -Toluene sulfonyl chloride

Synopsis of the Thesis



The thesis entitled “**Synthesis of cyclitol derivatives and study of their Complexation with ions and small molecules**” consists of two parts.

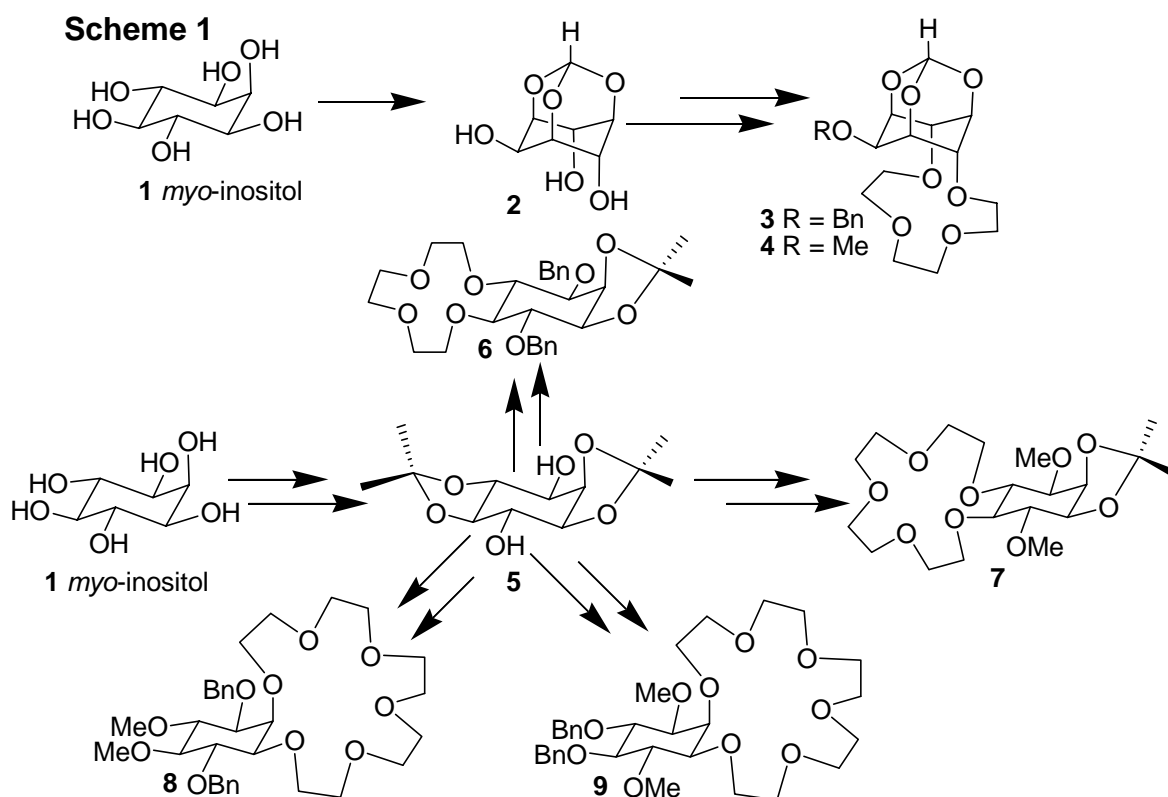
Part A: A review of the literature on the complexation behavior of cyclitol and carbohydrate derivatives with metal ions.

The metal binding properties of multidentate ligands can be influenced by the choice of the donor atoms and by the steric demands of the ligand backbone. A systematic optimization of these two properties can be used for the design of selective chelators for metal ions. Although carbohydrates have been used as scaffolds for the construction of metal ion binding agents, similar efforts using cyclitols as core molecules for the construction of metal ion binding agents started only recently.¹ Due to the presence of six hydroxyl groups in inositols, the hydroxyl groups unutilized for the construction of crown ethers, can be derivatized to modulate the binding efficiency of cations to crown ethers. Cyclitols have been known to form complexes with metal ions for several decades and inositol derivatives were suspected to form chelates with metal ions during chemical reactions. Using these facts as a starting point, this part of the thesis discusses various types of the metal binding molecules derived from carbohydrates and cyclitols, which serves as an introduction to the work described in the Part B of the thesis.

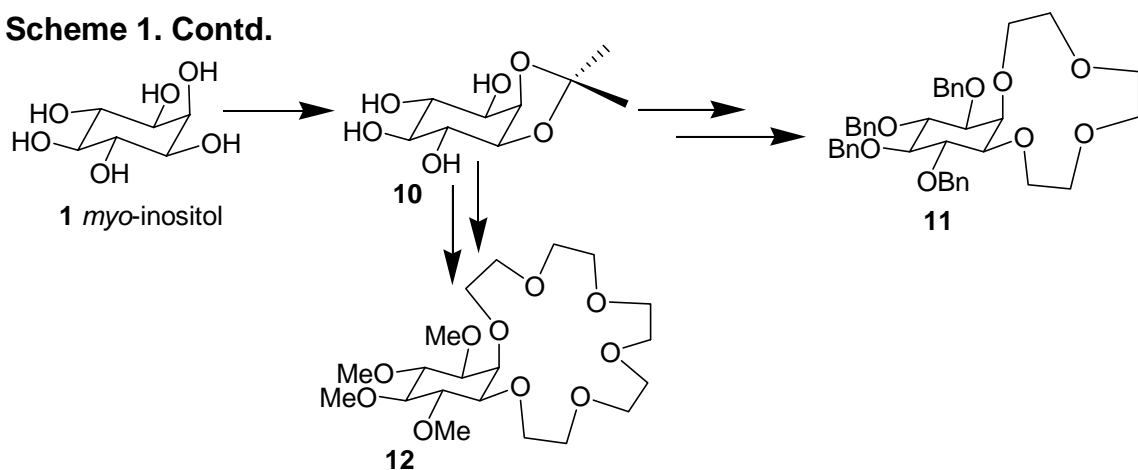
Part B: Chapter 1. Synthesis and metal ion binding studies of *myo*-inositol derived crown ethers.

This chapter describes the preparation of *myo*-inositol derived crown ethers **3, 4, 6, 7, 8, 9, 11** and **12** (Scheme 1) and evaluation of their ability to bind to metal ions by picrate extraction.² All the crown ethers were prepared from commercially available *myo*-inositol by using protection – deprotection strategy of the inositol hydroxyl groups. The

results of picrate binding studies reveal that the crown ether having 1,3-diaxial (**3**) orientation shows the highest selectivity for binding to lithium although the crown ether having 1,2-diequatorial (**6**) orientation exhibited the highest binding constant for lithium picrate. These results suggest that relative binding affinity of metal ions to crown ethers can be tuned by varying the relative orientation of crown ether oxygen atoms. The relevance of these results to the previously observed regioselectivity during the *O*-substitution of *myo*-inositol orthoesters is discussed.³ This work has been published in *Tetrahedron*.⁴



Scheme 1. Contd.

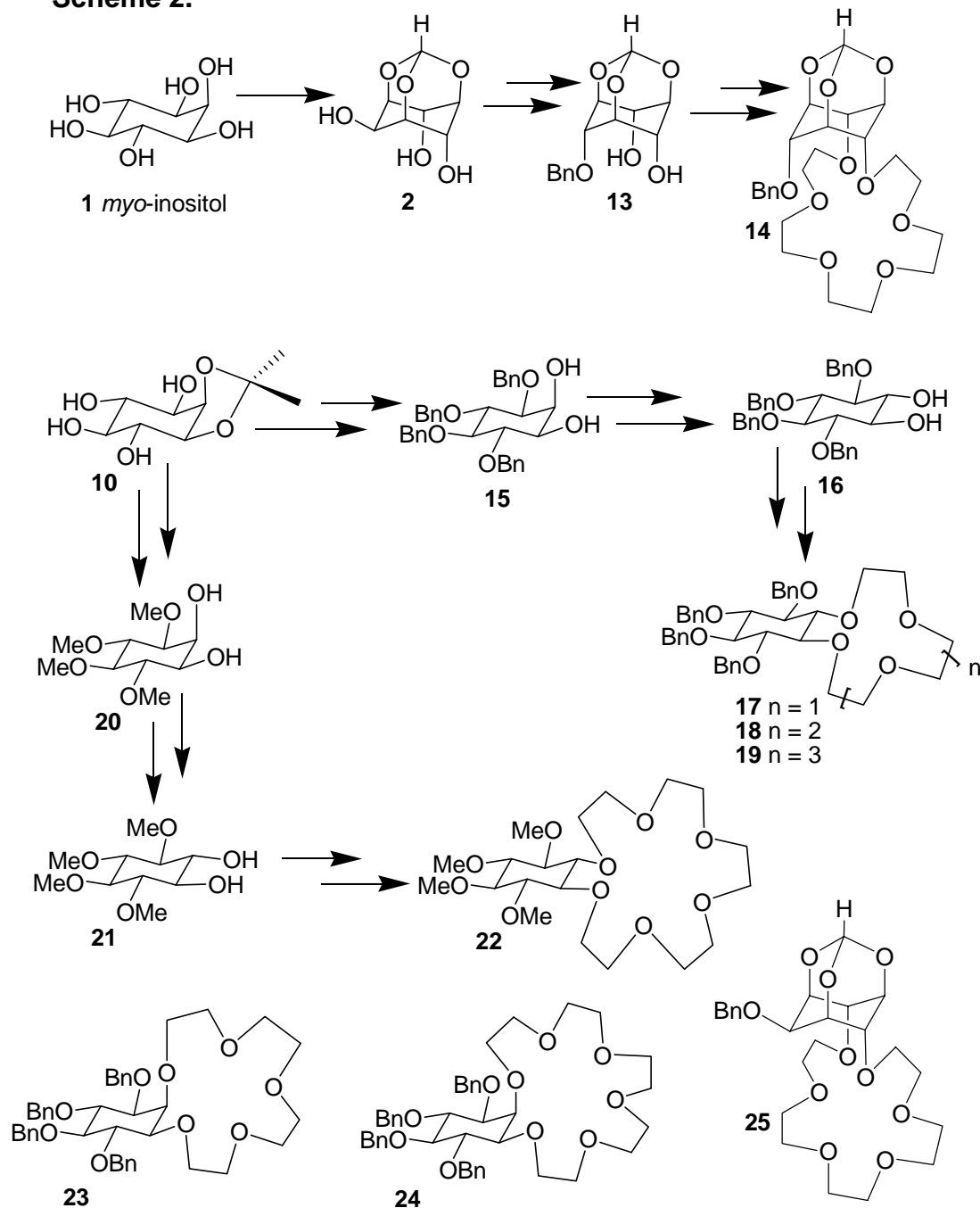


A comparison of the binding constants of crown ethers **4**, **7**, **8**, **9** and **12** with metal picrates showed that the *O*-substituents on the inositol ring contribute significantly for the binding of crown ethers with metal ions. In particular, binding efficiency of *myo*-inositol derived crown ethers to silver and potassium ions could be enhanced by introducing benzyl ethers in the inositol ring. The results obtained in this chapter shows that metal ion binding ability of inositol derived crown ethers vary depending on the relative orientation of crown ether oxygen atoms and on the nature of the auxiliary protecting groups on the hydroxyl groups not involved in crown ether formation. These factors may be exploited to develop selective cyclitol based binding agents for metal ions.

Chapter 2: *scyllo*-Inositol derived crown ethers: A comparative study with *myo*-inositol based crown ethers.

This chapter describes the preparation and evaluation of metal picrate complexing ability of *scyllo*-inositol derived crown ethers. We also give a comparison of these results with those obtained with *myo*-inositol derived crown ethers (Chapter 1) which highlight the significance of relative orientation of oxygen atoms in the crown ethers. *scyllo*-Inositol derived crown ethers **14**, **17**, **18**, **19** and **22** (Scheme 2) were prepared from a suitably protected *myo*-inositol derivative and their metal ion binding ability was

Scheme 2.



estimated by picrate extraction experiments.² The results were compared with the picrate extraction results for the corresponding *myo*-inositol derived crown ether either from previous chapter (11 and 12) or from earlier work (23, 24 and 25) reported from our

laboratory.^{1b} The crown ethers **14**, **17**, **18**, **19** and **25**, **11**, **23**, **24** only differ in the disposition of the C2-oxygen, which is axial in *myo*-inositol derived crowns and equatorial in *scyllo*-inositol derived crowns. In orthoesters **25** and **14** although *myo*-crown as well as *scyllo*-crown have two axial oxygen atoms that form the crown ether, the third in the former is anti- with respect to the crown ether moiety in *myo*-derivative but syn- in *scyllo* derivatives. A comparison of the metal picrate extraction constants show that by and large *myo*-inositol derived crowns extract metal picrate better than the corresponding *scyllo*-derived crown. But, in orthoester based crown, *scyllo*-crown appears to be slightly better for the extraction of metal picrates, (except for potassium-picrate). This stereochemical disposition of one oxygen atom in the inositol ring has very large effect for the extraction of potassium (**24/ 19** \approx 4136) and silver picrate (**23/ 18** \approx 2201; **24/ 19** \approx 2605). For other cations tested, the change in stereochemistry does not appear to have great influence on their binding to crown ethers.

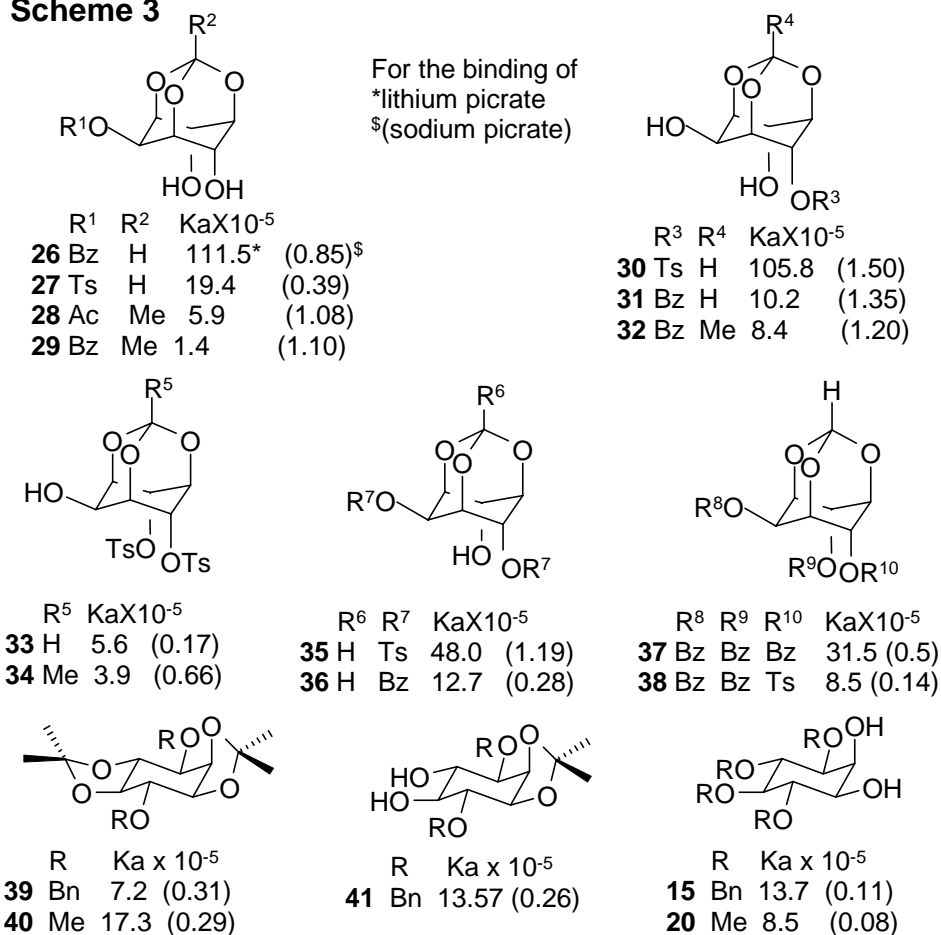
Chapter 3. Complexation of simple *O*-substituted inositol derivatives with metal ions and small molecules.

Selective protection and deprotection of *myo*-inositol hydroxyl groups is known to depend on the reaction conditions and the reagents used.⁵ The unusual selectivity patterns observed during the reaction of *myo*-inositol or its derivatives especially wherein the reagents used involve metal ions have been attributed to the chelation of inositol derivatives with metal ions. These reports prompted us to carry out picrate extraction experiments with simple inositol derivatives (Scheme 3). These extraction experiments suggest that the inositol derivatives bind lithium ions better than sodium ions. Most of the orthoester derivatives shown below bind lithium picrate 10-100 times better than sodium

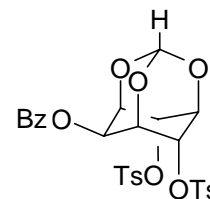
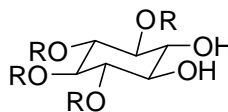
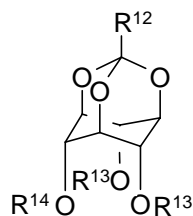
picrate. These results give credence to the suggestion that the extent of chelation of metal ions by inositol derivatives is a major factor in deciding the observed regioselectivity⁴ for the *O*-substitution reactions. This work has been published in *Tetrahedron*⁴

We also screened some of the inositol derivatives (Scheme 3) for their complexation with small organic molecules, since co-crystallization of organic compounds and determination of their physical and chemical properties are of current research interest.⁶ We found that **45**, forms molecular complex with toluene, methanol and naphthalene. X-ray crystal structures of some of these molecular adducts were solved.

Scheme 3



Scheme 3. Contd.



	R ¹²	R ¹³	R ¹⁴	K _a × 10 ⁻⁵	R	K _a × 10 ⁻⁵	
42	H	Ts	H	7.51 (0.28)	21	Me 1.3 (0.11)	45 Inclusion complexes with toluene, methanol and naphthalene
13	H	H	Bn	0.57 (0.27)			
43	H	Bn	H	1.5 (0.05)			
44	H	Bn	Bn	1.6 (0.78)			

References:

1. a) L. A. Paquette, J. Tae, *J. Am. Chem. Soc.*, **2001**, *123*, 4974-4984; b) K. M. Sureshan, M. S. Shashidhar, A. J. Varma, *J. Org. Chem.* **2002**, *67*, 6884-6888; c) D. G. Hilmey, L. A. Paquette, *J. Org. Chem.*, **2004**, *69*, 3262-3270; d) L. A. Paquette, P. R. Selvaraj, K. M. Keller, J. S. Brodbelt, *Tetrahedron*, **2005**, *61*, 231-240
2. S. S. Moore, T. L. Tarnowski, M. Newcomb, D. J. Cram, *J. Am. Chem. Soc.* **1977**, *99*, 6398-6405.
3. S. Devaraj, M. S. Shashidhar, S. S. Dixit, *Tetrahedron* **2005**, *61*, 529-536.
4. S. S. Dixit, M. S. Shashidhar, S. Devaraj, *Tetrahedron* **2006**, *62*, 4360-4363.
5. K. M. Sureshan, M. S. Shashidhar, T. Praveen, T. Das, *Chem. Rev.* **2003**, *103*, 4477-4504.
6. a) K. Manoj, R. G. Gonnade, M. M. Bhadbhade, M. S. Shashidhar, *Cryst. Growth Des.* **2006**, *6*, 1485-1492; b) C. Murali, M. S. Shashidhar, R. G. Gonnade, M. M. Bhadbhade, *Eur. J. Org. Chem.* **2007**, 1153-1159.

Note: Compound numbers in the abstract are different from those in thesis.

References are given separately for each chapter.

List of Publications

1. Chelation controlled regiospecific O-substitution of *myo*-inositol orthoesters allows convenient access to orthogonally protected *myo*-inositol derivatives.

Devaraj, S.; Shashidhar, M. S.; **Dixit, S. S.** *Tetrahedron* **2005**, *61*, 529-536.

2. Cyclitol based metal complexing agents. Preference for the extraction of lithium by *myo*-inositol based crown-4-ethers depends on the relative orientation of oxygen atoms present in the crown ether.

Dixit, S. S.; Shashidhar, M. S.; Devaraj, S. *Tetrahedron* **2006**, *62*, 4360-4363.

3. Inositol derived crown ethers: effect of auxiliary protecting groups and the relative orientation of crown ether oxygen atoms on their metal ion binding ability.

Dixit, S. S.; Shashidhar, M. S. *Tetrahedron* (Accepted).

4. Guest Induced Conformational Polymorphism: Crystal structure analysis of inclusion complexes of 2-O-benzoyl-4,6-di-O-tosyl-*myo*-inositol 1,3,5 orthoformate with methanol and toluene.

Dixit, S. S.; Shashidhar, M. S.; Gonnade, R. G.; Bhadbhade, M. M. (To be communicated).

5. Similarity in the molecular organization of D & L – *chiro*-inositol hexabenzoate with chiral crystals of meso *myo*-inositol hexabenzoate: A detailed crystal structure analysis.

Dixit, S. S.; Shashidhar, M. S.; Gonnade, R. G.; Bhadbhade, M. M. (To be communicated).

6. Crystal structure analysis of selectively protected *scyllo* inositol: structures of mono, di- and tri-O-benzyl *scyllo*-inositol orthoformate.

Dixit, S. S.; Shashidhar, M. S.; Gonnade, R. G.; Bhadbhade, M. M. (To be communicated).

7. Crystal structures of three 13-crown-4 derivative of *myo*-inositol: Intramolecular O-H...O and C-H...O interactions stabilized the conformation of the crown ether.

Dixit, S. S.; Shashidhar, M. S.; Gonnade, R. G.; Bhadbhade, M. M. (Manuscript under preparation).

8. Structural investigations of 1,4,5,6-tetra-O-methyl *myo*-inositol and 2,4,5,6-tetra-O-methyl *myo*-inositol: Single crystal X-ray crystallography study.

Dixit, S. S.; Jagdhane, R. C.; Shashidhar, M. S.; Gonnade, R. G.; Bhadbhade, M. M. (Manuscript under preparation).

9. Influence of isopropylidene substituents on chair conformation of inositol ring: crystal structures of 1,2-4,5-di-O-isopropylidene-3,6-di-O-methyl *myo*- inositol and 1,2-O-isopropylidene-3,6-di-O-methyl *myo*- inositol.

Dixit, S. S.; Shashidhar, M. S.; Gonnade, R. G.; Bhadbhade, M. M. (Manuscript under preparation).

PRESENTATIONS AND POSTERS

ORAL PRESENTATIONS

1. Cyclitol-based metal complexing agents. Effect of the relative orientation of oxygen atoms in the ionophoric ring on the cation-binding ability of *myo*-inositol-based crown ethers.

Talk on the occasion of OCS Day, 2003, at NCL, Pune.

2. Cyclitol-based metal complexing agents. Effect of ring size, hydroxyl protecting groups and relative orientation of oxygen atoms in the ionophoric ring on the cation-binding ability of *myo*-inositol-based crown ethers.

Talk on the occasion of First Junior National Organic Symposium Trust (NOST) Symposium, November, 2004 at NCL, Pune.

POSTERS PRESENTED

1. Effect of Hydroxyl Protecting Groups and Relative Orientation of Oxygen Atoms in the Ionophoric Ring on the Cation-Binding Ability of *myo*-Inositol-Based Crown Ethers.

Poster presented at the 6th National Symposium in Chemistry, 2004. (organized by Chemical Research Society of India), Department of Chemistry, Indian Institute of Technology, Kanpur.

2. Effect of metal ion on regio-selective alkylation and acylation of *myo*-inositol orthoesters.

Poster presented on the occasion of Science Day, 2006 at NCL.

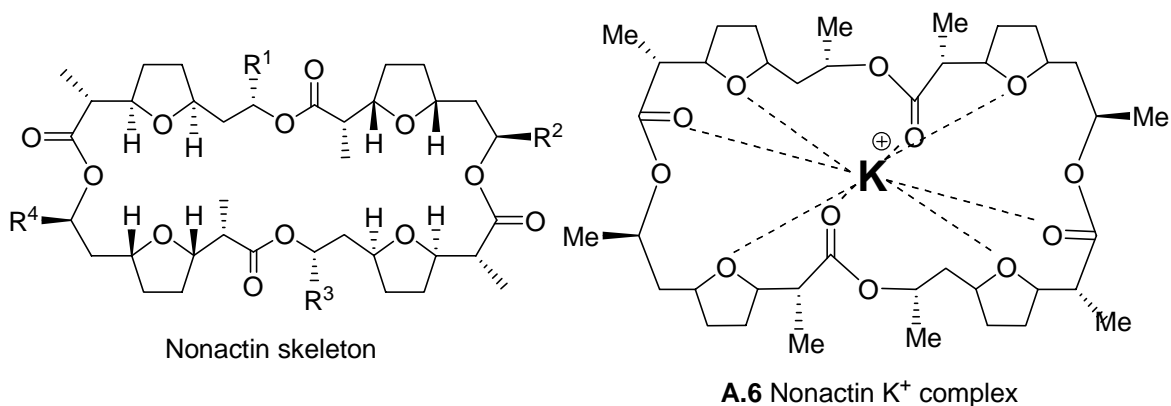
PART-A

A review of the literature on the complexation behavior of cyclitol and carbohydrate derivatives with metal ions.

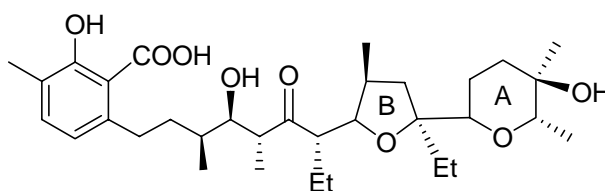
Research is to see what everybody else has seen, and to think what nobody else has thought.

-Albert-Szent-Gyorgi (Biochemist)

Organic compounds that bind specific metal ions have been of interest to chemists for the last several decades. Interest in the study of metal ion binding agents is mainly due to applications that they find in various areas of chemistry, biology, medicine and industry. Interest in the study of metal ion binding agents was aroused, for example, due to the discovery of natural products which form complexes with metal ions and realized¹ to have profound implications in the action of antibiotics. Some of the examples of natural products that bind cations strongly are shown in Figure A1.² The crystal structure of nonactin – potassium ion complex (**A.6**)³ showed that the cation was entrapped in a cavity formed by the 32 membered ring lined with polar groups, and lipophilic groups outside.



Compound	R ¹	R ²	R ³	R ⁴	Compound	R ¹	R ²	R ³	R ⁴
A.1 Nonactin	Me	Me	Me	Me	A.4 Trinactin	Me	Et	Et	Et
A.2 Monactin	Me	Et	Me	Me	A.5 Tetranactin	Et	Et	Et	Et
A.3 Dinactin	Me	Et	Me	Et					

**A.7** Lasalocid

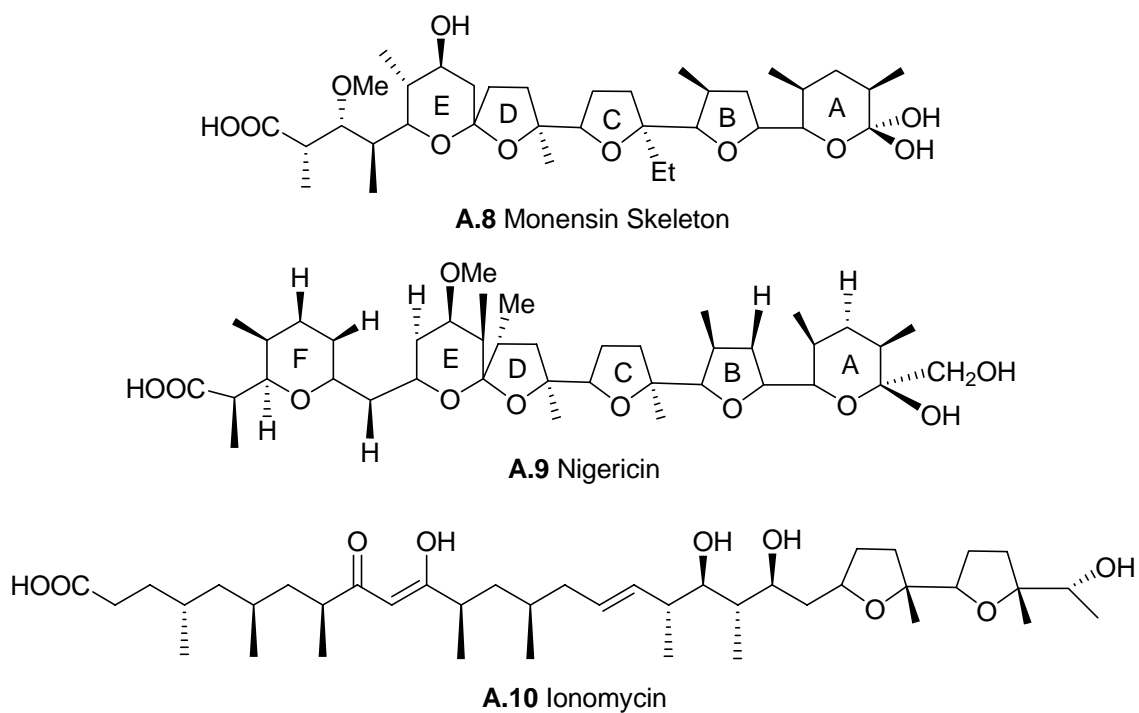


FIGURE A1. Naturally occurring cation binding compounds.

An interesting example of boron-containing marine natural product⁴ is provided by aplasmomycin A, (**A.11**, Figure A2) isolated as a metabolite from the culture of the marine microorganism *Streptomyces griseus*.⁵ Although boron cannot be completely regarded as a metal, its encapsulation by aplasmomycin A results in a structure as rigid as that resulting from the chelation of a metal ion. Other naturally occurring metal complexing agents include enterobactin⁶ **A.12** and muellitol, [**A.13**, 1,3,5-tri(3-methylbut-2-enyl)-*scyllo*-inositol], isolated from the leaves of *Evodiella muelleri*.^{7,8} Enterobactin is a siderophore produced by enteric bacteria to trap ferric ions under iron-deficient conditions.⁹ It exhibits extraordinarily high affinity for ferric ions (stability constant K_f of ferric enterobactin $\approx 10^{49}$).¹⁰

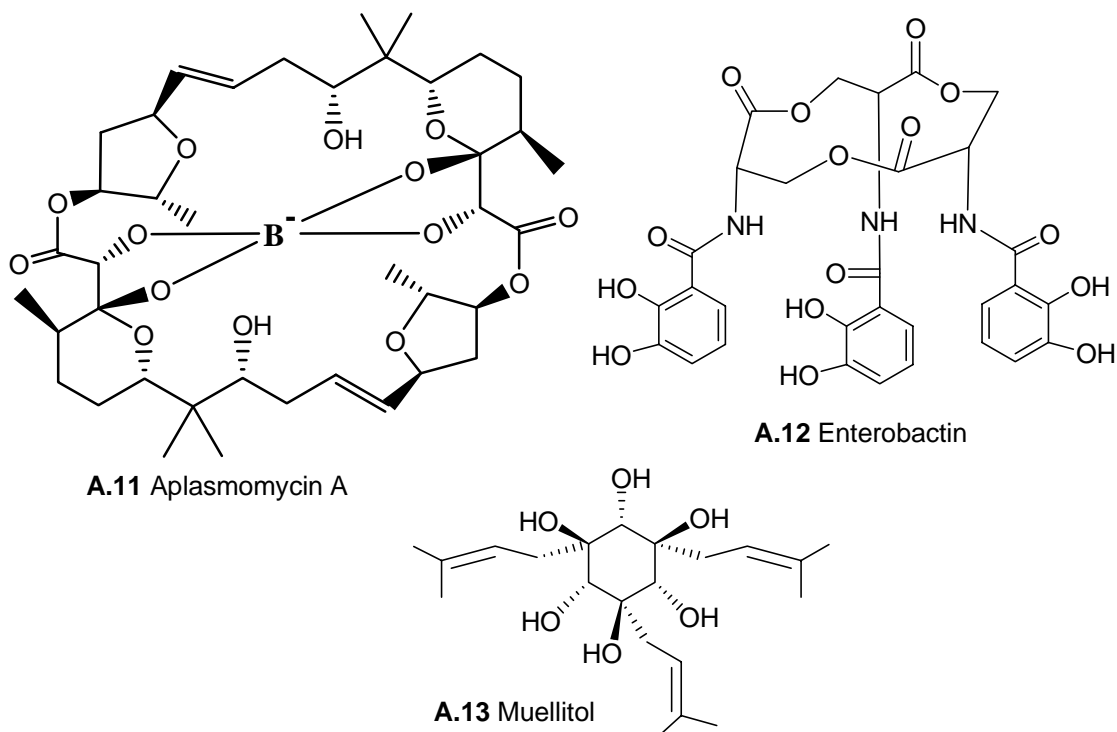


FIGURE A2. Naturally occurring metal complexing agents.

Perhaps knowledge of the existence of metal complexing natural products resulted in extensive investigation of metal complexing agents such as crown ethers, podands, cryptands, calixarenes and the like. Highly selective metal complexing agents have potential for applications in medicine for the treatment of metal intoxication as well as in diagnostic procedures such as magnetic resonance imaging (paramagnetic contrast agents). Recently potential of crown ethers as antitumor agents has also been realized.¹¹ Kinetic and thermodynamic stability of metal complexes is an important consideration for application in diagnostic procedures, while selective complexation is of prime importance in treatment for metal intoxication. The efficiency of metal binding to a ligand or a chelator is dependent on the donor atoms present in the ligand and flexibility of the ligand back bone for accommodation of the metal ion. An understanding of the

interplay of these parameters in a ligand for metal ion binding is essential for the design of selective metal ion binding agents.

In addition to the synthesis of these basic structural entities (as mentioned above), attempts were made to investigate the use of known small organic molecules as scaffolds or back bone for the preparation of metal ion binding agents. These approaches included the introduction of auxiliary groups that could aid / enhance metal ion binding and restrict the relative disposition of atoms coordinating with metal ions.¹² Carbohydrates were also used as core molecules for the construction of crown ethers (e.g., Figure A3. **A.14**, **A.15** from D-glucose; **A.16** from D-mannose; **A.17** from inuline; **A.18**, **A.19** from D-galactose) since a variety of them are available and result in chiral complexing agents with various degrees of flexibility, size of the macrocyclic ring, position and number of free hydroxyl groups. These metal binding agents were tested for their selective metal complexing properties and chiral phase transfer catalysis. It was observed that in general, complexing ability towards simple inorganic cations was dependent on the structure of the core sugar molecule and geometry of the receptor. The topic of carbohydrate derived crown ethers has been reviewed recently¹³ and hence will not be considered for further discussion in the present thesis. The following sections give an account of the metal complexing ability of cyclitols and their derivatives. The interest in the structure and chemistry of cyclitols was revived in the last 2-3 decades due to the realization of the role played by phosphoinositols in various biological phenomena.

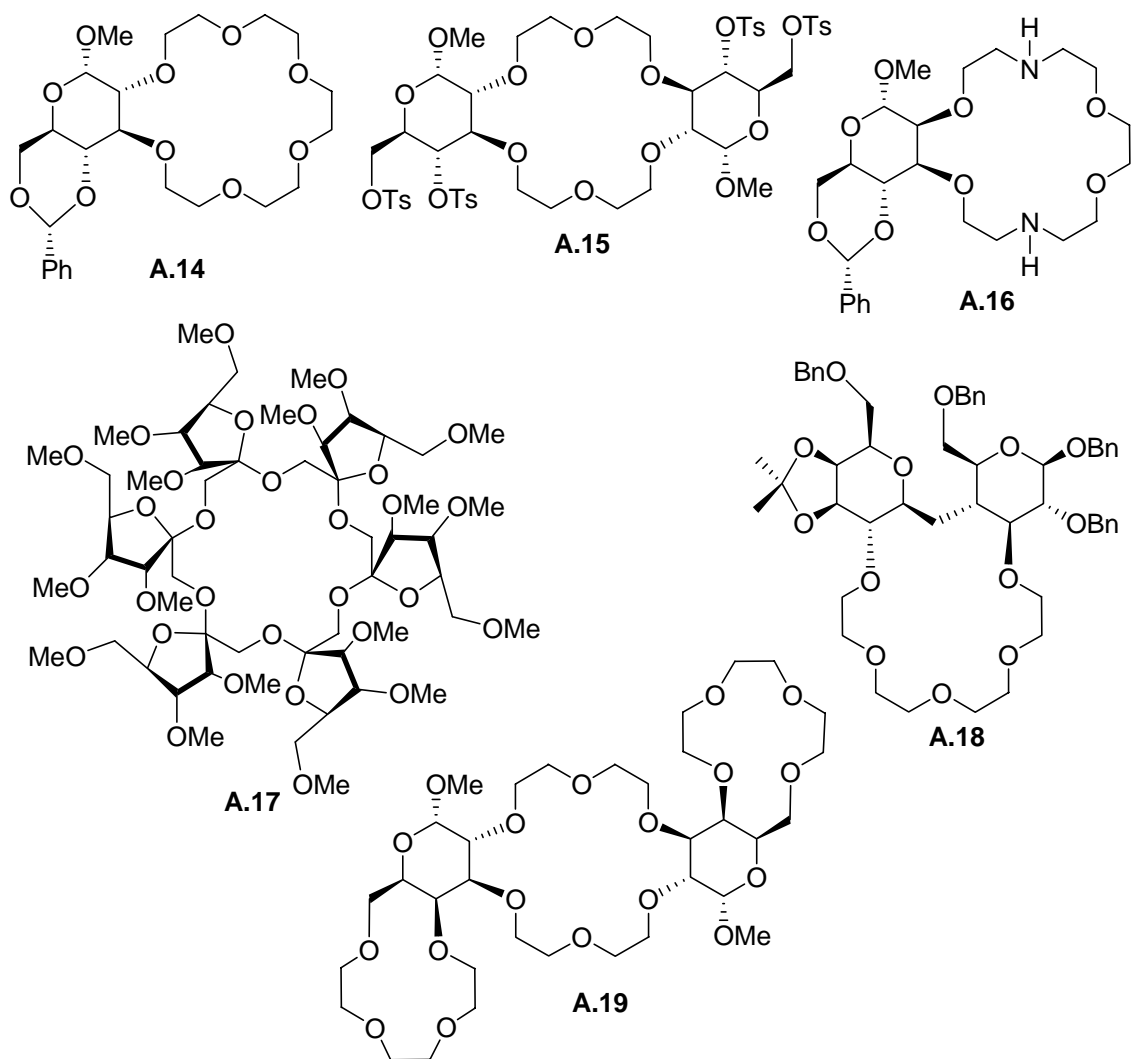


FIGURE A3. Carbohydrate derived crown ethers.

Cell signaling

Cell signaling controls the inner workings of organisms, allowing them to survive, respond and adapt to their surroundings.¹⁴ All living cells (plant or animal) receive and transmit signals in many forms continuously. Hence all cells must have the ability to detect the presence of extracellular molecules and conditions, and must also be able to instigate a range of intracellular responses for their survival. Since different kinds of cell signaling systems are interdependent they must work in concert for the well being of an

organism. Knowledge of the mechanism of cell signaling is also important for the understanding of the growth and activity of an aberrant cell or that of a cell that is combating adverse conditions, since impairment of cell signaling systems could lead to diseases. Cells may signal to each other in different ways, often classified depending on the distance between the signaling cell and the target cell; e.g. electrical, endocrine, paracrine, cell-cell contact, autocrine etc. Cell signaling in multicellular organisms often involve substances such as hormones and neurotransmitters. Lipophilic hormones such as steroids can pass through the lipid bilayer of cell membranes and bind to their target receptors within the cell. Many chemical messengers however are too hydrophilic to cross cell membranes. In order to deliver their message they have to bind to specific receptors on the outside of the cell membrane and activate mechanisms that transmit the signal into the cell. This process is known as *transmembrane signaling* or *signal transduction*.¹⁵ A schematic diagram of the transmembrane cell signaling is shown in Figure A4.

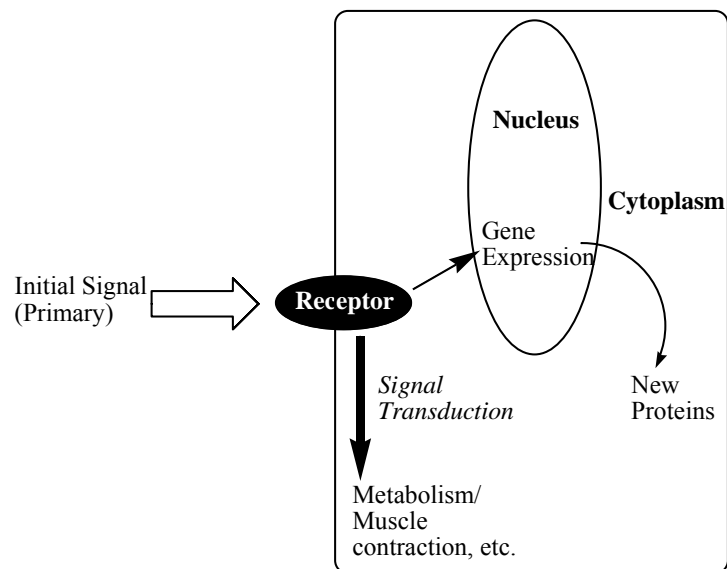
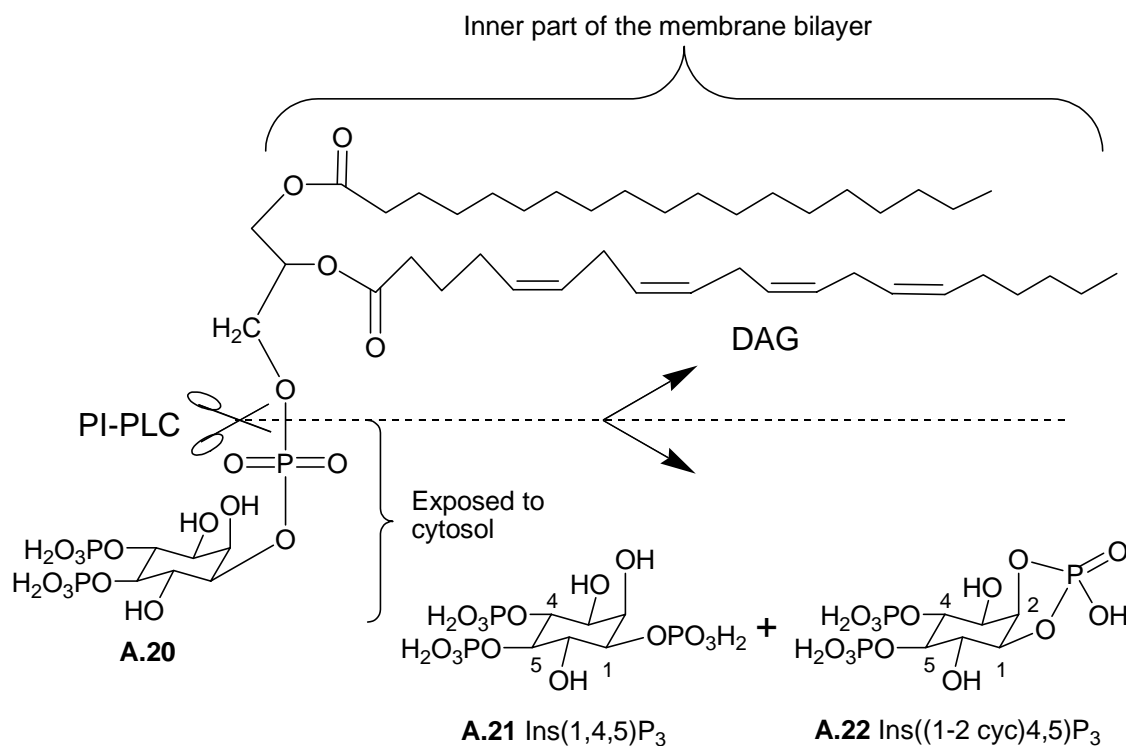


FIGURE A4. Transmembrane cell signaling.

Although, the main event in transmembrane cell signaling may be the arrival of a signal at the cell surface, the following events commonly follow: (i) perception of the signal usually by dedicated proteins referred to as receptors; (ii) transmission of the signal by the receptor into the cell; (iii) passing on the ‘message’ to a series of cell signaling components often known as signaling cascade; (iv) arrival of the message at the final destination in the cell; (v) response by the cell. *D-myio*-Inositol-1,4,5-trisphosphate (Ins(1,4,5)P₃, **A.21**) was recognized as a second messenger in signal transduction pathways in eukaryotic cells.¹⁴ The receptor controlled hydrolysis (Scheme A1) of the membrane bound lipid, phosphatidylinositol-4,5-bisphosphate (PtdIns(4,5)P₂, **A.20**) by phosphatidylinositol-specific phospholipase C (PI-PLC) gives the trisphosphate **A.21**, *D-myio*-inositol-1,2-cyclic-4,5-trisphosphate (Ins((1-2cyc)4,5)P₃, **A.22**) and diacylglycerol (DAG).



SCHEME A1.

On cleavage of the phospholipid **A.20**, hydrophobic DAG- is left in the cell membrane while inositol phosphates, produced are released into the cytoplasm. DAG activates protein kinase C, while **A.21** helps in the release of calcium ions from intracellular stores (endoplasmic reticulum). Both **A.21** and DAG act as secondary messengers in the target cell.¹⁴ **A.21**-induced Ca^{2+} release mediates an abundance of cellular responses as diverse as fertilization, cell growth and differentiation, neuronal signaling, secretion and phototransduction.¹⁶ **A.21** is metabolized eventually to *myo*-inositol via a number of phosphorylation and dephosphorylation reactions. *myo*-Inositol is then reused in the biosynthesis of phosphatidylinositol lipids in endoplasmic reticulum; phospholipids so produced are reincorporated back into the plasma membrane by vesicular transport.¹⁴

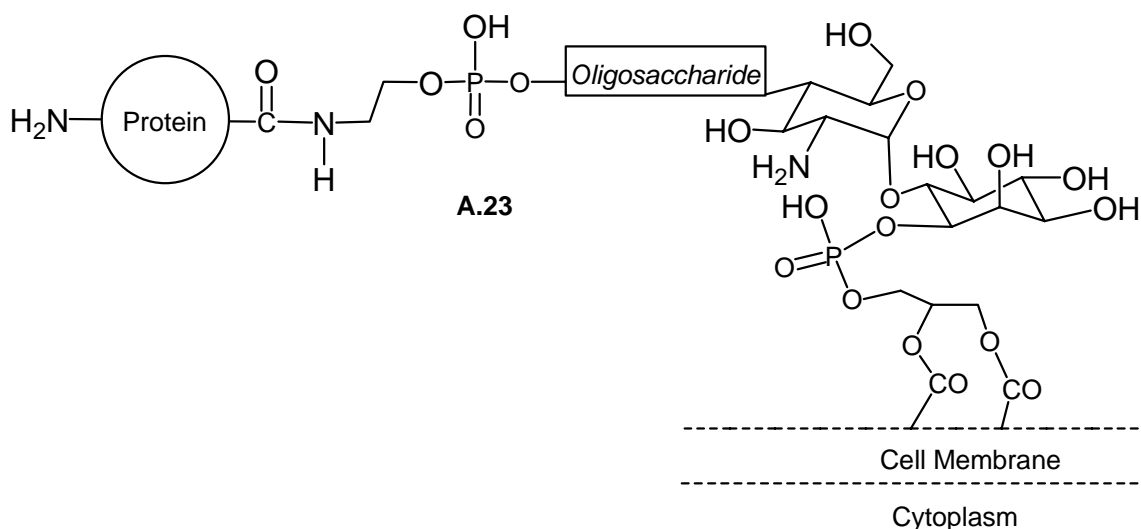


FIGURE A5. Structure of the glycosyl phosphatidylinositol anchor.

myo-Inositol is also a part of the covalent glycosyl phosphatidylinositol (GPI) anchors that attach certain proteins to cell membranes, for example, variant surface glycoprotein of trypanosomes.¹⁷ A typical structure of a GPI anchor (**A23**) is shown in Figure A5; GPI anchors attach proteins to cell membranes via a phosphoethanolamine

unit linked to a trimannose-glucosamine-inositol back bone and a hydrophobic lipid (DAG) that anchors the system to the cell membrane.¹⁸ Lipophosphoglycans and glycoinositol phospholipids, are also thought to play an important role in parasite virulence.^{17b}

Impairment of the *myo*-inositol cycle, which involves several enzymes, could lead to several diseases and hence these pathways in the *myo*-inositol cycle are potential targets for the development of drugs. These developments in biology and medicine revived the chemistry associated with inositols.

Inositol isomers

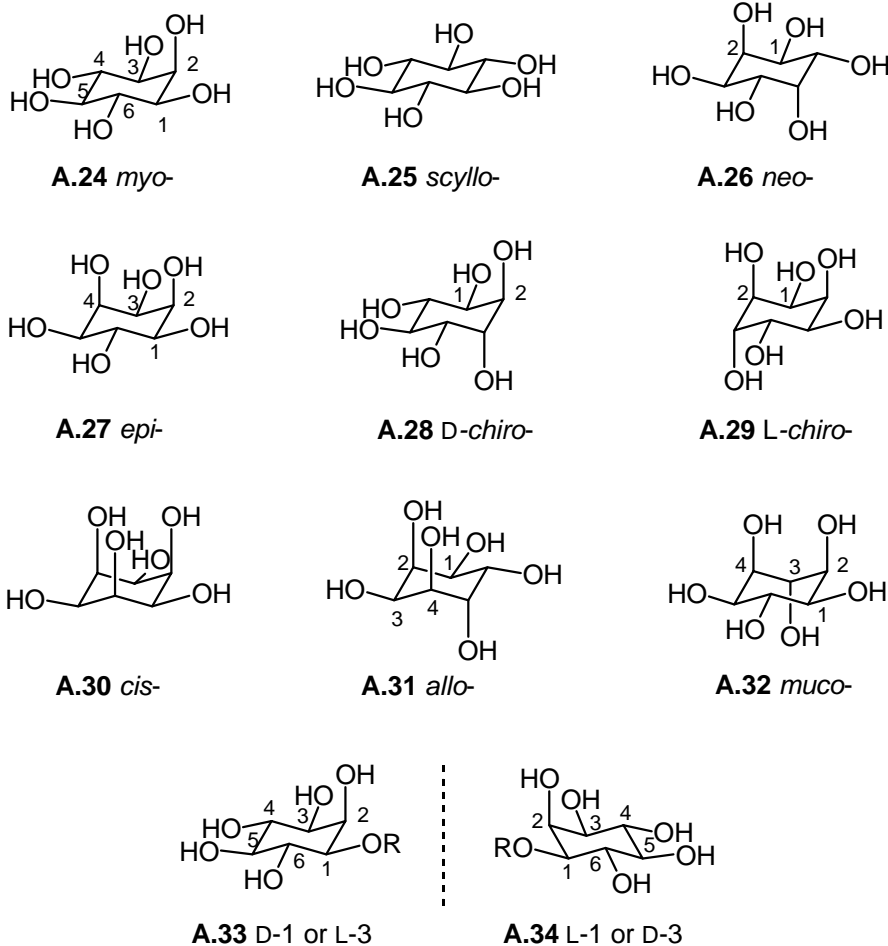


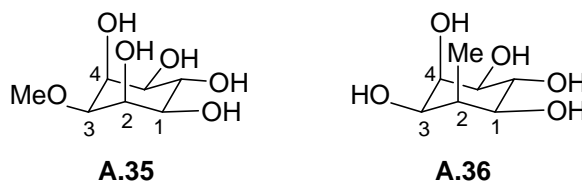
FIGURE A6.

Inositols are cyclohexane hexols; there are eight possible isomers, one of them being an enantiomeric pair (A.28 & A.29) making a total of nine distinct stereoisomers (Figure A6). Among these, *myo*- (A.24), *scyllo*- (A.25) and *chiro*- (A.28 & A.29) inositols or their derivatives occur in nature; *myo*-inositol being the most abundant.¹⁹ *myo*-Inositol is a *meso* isomer with five equatorial hydroxyl groups and an axial hydroxyl group. There is a plane of symmetry passing through C-2 and C-5 atoms. The carbon bearing the axial hydroxyl group is designated as C-2 and the other ring carbons can be numbered from C-1 to C-6 starting from a C-1 atom and proceeding around the ring in clockwise or anticlockwise fashion. According to convention,²⁰ anti-clockwise numbering in unsymmetrically substituted *myo*-inositol leads to the configurational D-prefix and clockwise numbering gives the substituted *myo*-inositol an L-prefix. An IUPAC nomenclature allowing all biologically relevant compounds to be denoted as D-isomers has also been proposed.²¹ Although, many of the unsymmetrically substituted *myo*-inositol derivatives reported in this thesis are racemic, for clarity and simplicity they are represented by only one enantiomer in schemes.

Ability of inositols to complex with metal ions

A comparison of the electrophoretic mobilities of isomeric inositols showed that *cis*-inositol (A.30) was most effective in complexing metal ions such as Ca²⁺, Sr²⁺ and Ba²⁺.²² Complexation of inositols with metal ions was also revealed by changes in the proton chemical shifts in their NMR spectra. It was found²³ that, in the ¹H NMR spectrum of *cis*-inositol (A.30), calcium ions caused the axial-proton signals to shift downfield somewhat more than the equatorial ones. Chemical shifts induced by La³⁺ in the NMR spectrum of *epi*-inositol (A.27) and its derivatives are listed in Table A1.^{24,25}

TABLE A.1: Change in chemical shifts (ppm) in the ^1H NMR spectra of cyclitols on addition of LaCl_3 in D_2O solution.²⁴



Cyclitol	H-1	H-2	H-3	H-4	H-5	H-6	Me
A.27	0.17	0.27	0.55	0.27	0.17	0.07	---
A.35	0.19	0.22	0.43	0.22	0.19	0.08	0.18
A.36	0.23	---	0.58	0.29	0.18	0.12	0.16

The signals in the ^{13}C NMR spectra of polyols were also shifted on complex formation; for example, the limiting shifts of *epi*-inositol (**A.27**) on addition of lanthanum chloride were²⁶: C1, C5 = -0.9, C2, C4 = 0, C3 = +1.3 and C6 = -0.9 ppm. Based on the analysis of the change in chemical shifts the mode of binding of metal ions to *epi*-inositol was postulated to be as shown in **A.37** (Figure A7).^{25,26,27}

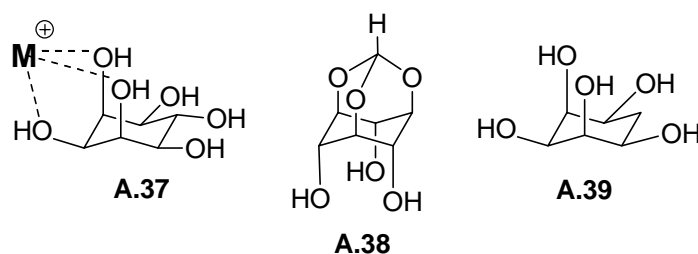


FIGURE A7.

A comparison of the ability of *scyllo*-inositol orthoformate (**A.38**), *cis*-inositol (**A.30**) and *epi*-inositol (**A.27**) to complex with metal ions showed that *syn*-triaxial hydroxyl groups are better for metal ion complexation as compared to an axial-

equatorial-axial arrangement. Similar studies on the complexation of metal ions with the pentols **A.36**²³ and **A.39**²⁴ have also been performed.

Vanadium(IV) complexes of *cis*-inositol (**A.30**) were prepared and their existence in the solid state and solution was demonstrated.²⁸ The formation constants of these complexes were determined by potentiometric titrations and their structure in solution investigated by EPR spectroscopy and cyclic voltammetry. The structures of $[\text{V}(\text{H}_3\text{ino})_2][\text{K}_2(\text{ino})_2]\cdot 4\text{H}_2\text{O}$ (**A.40**, Figure A8) and $[\text{Na}_6\text{V}(\text{H}_3\text{ino})_2](\text{SO}_4)_2\cdot 6\text{H}_2\text{O}$ were determined by single-crystal X-ray analysis. In both the complexes, the inositol molecule is coordinated to the vanadium(IV) center *via* three axial deprotonated oxygen donors.

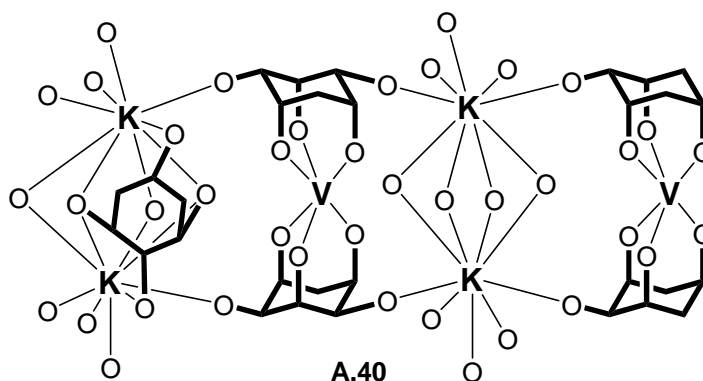


FIGURE A8. Structure of **A.40**, hydrogen atoms and non-coordinating hydroxyl groups are not shown for clarity.

Molecular mechanics²⁹ as well as density functional theory investigations³⁰ to understand the complexation of metal ions by inositols revealed that metal ions of ionic radius $<0.8 \text{ \AA}$ prefer to complex with three (1,3,5) *syn*-axial hydroxyl groups (**A.41**) while those of ionic radius $>0.8 \text{ \AA}$ prefer to complex with one equatorial (C2) and two axial (C1 and C3) hydroxyl groups in *cis*-inositol (**A.42**, Figure A9). These modes of complexation are controlled by the need for large metal ions to maximize the number of

5-membered chelate rings while smaller metal ions need to maximize the number of 6-membered chelate rings. These investigations also suggested that the metal ions of ionic radius $<0.6 \text{ \AA}$ do not coordinate with neutral *cis*-inositol perhaps due to van der Waals repulsion between the donor hydroxyl groups at shorter M-O bond distances.

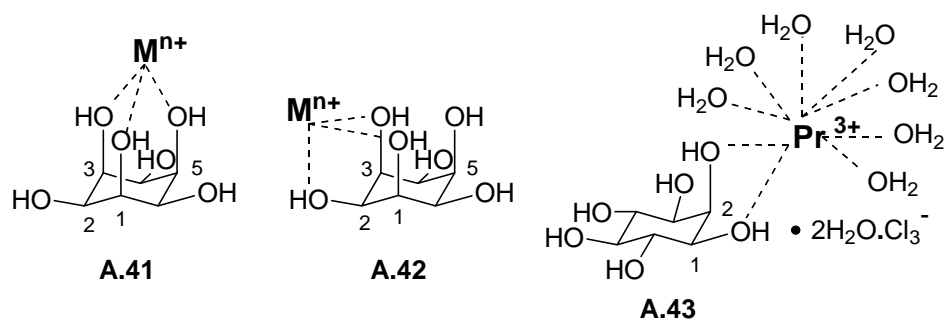


FIGURE A9.

myo-Inositol forms complexes with metal ions, although weakly. Complexes of *myo*-inositol with lanthanide metal salts have been isolated (Figure A9) and the structure of $\text{PrCl}_3 \cdot \text{C}_6\text{H}_{12}\text{O}_6 \cdot 9\text{H}_2\text{O}$ (A.43) solved by X-ray diffraction method.³¹ Two of the inositol oxygen atoms (O1 and O2) are co-ordinated to the metal ion (promethium). These complexes contain a network of hydrogen bonds formed by inositol hydroxyl groups and water molecules. The IR spectra of promethium, neodymium, and samarium inositol complexes were similar, which showed that the three metal ions have similar coordination mode with *myo*-inositol.

Complexation of metal ions by inositol derivatives

myo-Inositol phosphates constitute a class of compounds with profound biological significance and implications in various fields of chemistry, biology and medicine. Since some of the *myo*-inositol phosphates act as second messengers in cellular signal transduction mechanisms and are also involved in mobilization of intracellular calcium,

the complexation behavior of phosphorylated derivatives of inositols (Figure A10) with metal ions including hydrogen ions were investigated.^{32,33}

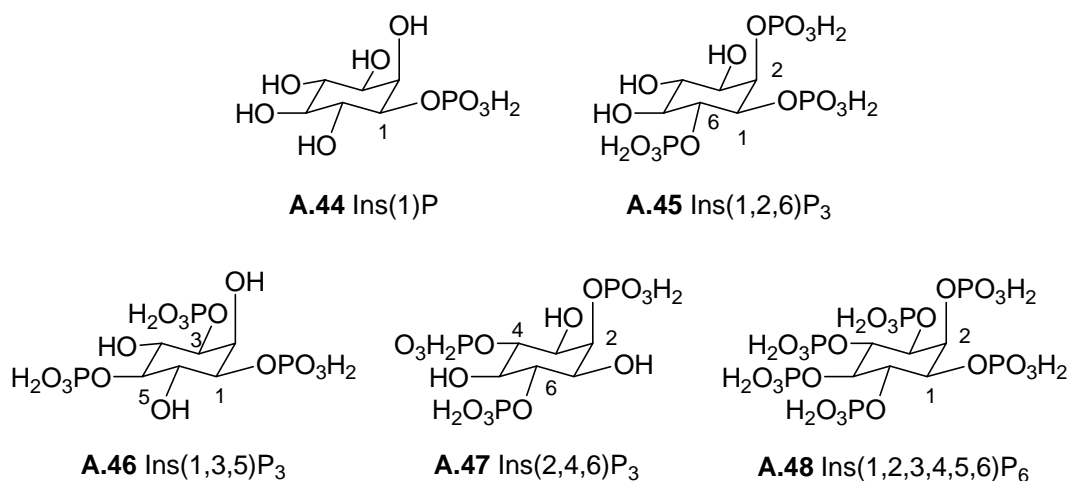


FIGURE A10.

Yet another reason for such investigations could be the fact that lithium salts which are used as agents to control mood swings in manic depressive patients, is known to inhibit the enzyme, *myo*-inositol-1-phosphate phosphatase that hydrolyses *myo*-inositol-1-phosphate (**A44**, Figure A10) to *myo*-inositol. This has been suggested as the cause for the therapeutic effects of lithium.³⁴

The protonation and the complexation properties of the *D*-*myo*-inositol 1,2,6-trisphosphate (Ins(1,2,6)P₃, **A.45**, Figure A10) towards potassium, calcium and magnesium ions were studied in two different media and at different temperatures. Due to several negative charges carried by the ligand over a large pH range, various species which included mononuclear, polynuclear and protonated complexes were found. Comparison of the protonation constants obtained in different media clearly showed the competition between the weak acidic protons of the phosphate groups and potassium ions.³⁵ The complexation properties of the trisphosphate **A.45** towards Li⁺, Na⁺, K⁺, Rb⁺,

and Cs⁺ cations at 25 °C in 0.1M tetra-n-butylammonium bromide medium revealed that the complexes were of high stability and the ligand was nonselective.³⁶ Complexes of **A.45** with cadmium, lead, and mercury displayed higher stabilities than those formed with alkaline-earth cations.³⁷

The stability constants of the complexes formed between Ca²⁺ and Ins(1,4,5)P₃ (**A.21**) in the presence and absence of alkali metal ions suggested that metabolism of **A.21** may be influenced by coordination of either alkali or alkaline-earth cations.³⁸ Investigation of the complexation of **A.21** with aluminum in different media suggested that the intracellular second messenger system involving **A.21** may be disturbed by the presence of the aluminum cations.³⁹ Compound **A.21** also complexes with naturally occurring polyamines such as spermine and spermidine. This perhaps provides a possible simple explanation for the inhibition of **A.21**-induced Ca²⁺ release by spermine. Based on these studies it was speculated that spermine could compete with metallic cations such as Ca²⁺ in the intracellular medium, and consequently might play a regulatory role in the signal transduction pathways mediated by **A.21**.⁴⁰

The protonation and complexation properties of some *myo*-inositol trisphosphates **A.45**, **A.46**, and **A.47** with metal ions Cu²⁺, Zn²⁺, Fe²⁺, and Fe³⁺ using potentiometry and ³¹P NMR spectroscopy has been studied.⁴¹ Investigation of the interaction between metal ions (Cu²⁺, Zn²⁺, Cd²⁺) with inositol phosphates carrying 3-6 phosphate groups (InsP₃-InsP₆) by potentiometric technique showed that the mineral binding capacity per phosphate group was similar irrespective of the number of phosphate groups (>3) present, but the binding strength was lower for the lower inositol phosphates (InsP₃ and InsP₄). The study was performed between pH 3 and 7, which is the

pH range in the upper part of the duodenum, where mineral absorption takes place.⁴² An in vitro study was conducted to investigate the interaction of inositol tris- to pentakisphosphates (InsP₃-InsP₅) with Ca, Zn, and histidine. In general, the solubility of Ca and Zn ions decreased with increasing degree of phosphate substitution on the inositol molecule, i.e., following the order InsP₃ > InsP₄ > InsP₅ > InsP₆. Inositol phosphates showed a greater binding capacity for Zn than for Ca.⁴³

myo-Inositol-1,2,3,4,5,6-hexakisphosphate (Ins(1,2,3,4,5,6)P₆, **A.48**) also known as phytate or phytic acid, is a natural metal chelating agent present in cereals, an important feedstock worldwide. Based on the similarity between the EPR spectra of wheat seeds and that of MnZn₄·**A.48** complex, the manganese storage centers in wheat grains were suggested to be similar heterometallic phytate complexes.⁴⁴

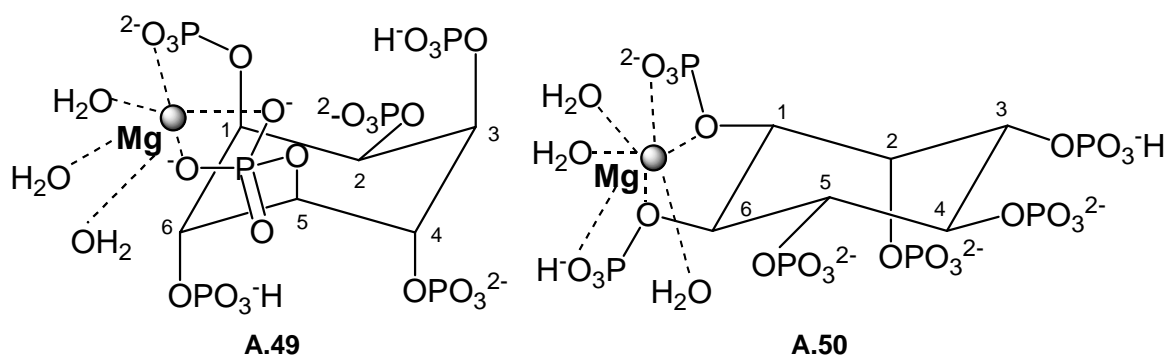


FIGURE A11.

IR and Raman spectroscopic investigation of solid complexes of **A.48** (Figure A11) with alkaline earth cations suggested direct and multidentate phosphate-metal coordination. In $[\text{Mg}(\text{H}_2\text{L})(\text{H}_2\text{O})_3]^{8-}$ (where L is different protonated forms of **A.48**) alternate or vicinal phosphate groups were predicted to chelate Mg^{2+} ions depending on whether **A.48** is in the 5-axial/1-equatorial (**A.49**) or the 1-axial/5-equatorial (**A.50**)

conformation, respectively.⁴⁵ The stability of alkali metal complexes with phytic acid (A.48) follows the trend $\text{Li}^+ \leq \text{Na}^+, \text{K}^+$.⁴⁶

Metal ion complexing ability of inositol phosphates has been exploited for the determination of their mass by HPLC with metal dye detection.⁴⁷ *myo*-Inositol phosphates have been attempted to be used as agents to prevent iron-gall-ink decay in cellulose items.⁴⁸ This property of inositol phosphates is purportedly because the anions occupy all the available coordination sites, thus preventing the reaction of ferrous ions (which brings in the oxidative decay of cellulose) with hydroperoxides. Cellulose paper treated with phytate dodecasodium salt (A.51), phosphates A.52 and A.53 (Figure A12) was about 13, 6 and 15 times respectively more stable than the de-acidified control.

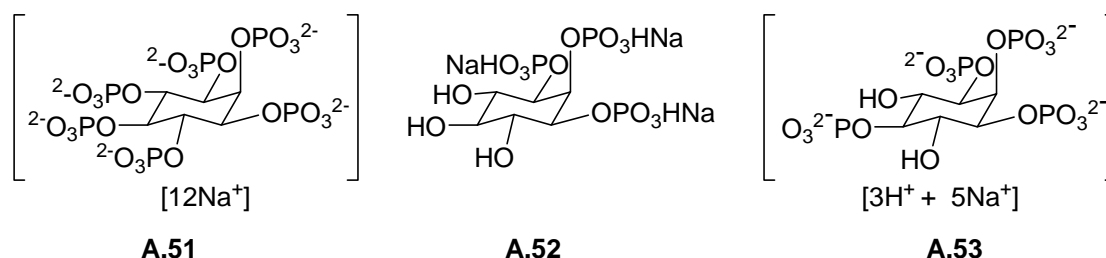


FIGURE A12.

Phosphodiester undergo hydrolysis to phosphomonoesters on complexation with lanthanide metal ions. Phosphatidylinositol was hydrolyzed by rare earth metal chlorides (YCl_3 , LaCl_3 , EuCl_3 , CeCl_3 , and TmCl_3) between pH 7.5 and 8.5 at 30 °C. YCl_3 showed the highest hydrolytic activity. The hydrolytic reaction was specific in that only the P-O bond towards the glycerol moiety was cleaved to generate inositol phosphate and diacyl glycerol. Hence lanthanides appear to mimic the hydrolysis of phosphatidylinositol by the enzyme, phosphatidylinositol-specific phospholipase C (Scheme A1). Non-rare earth metal ions such as Fe(III) , Zn(II) , and Cu(II) were however unable to cleave

phosphatidylinositol.⁴⁹

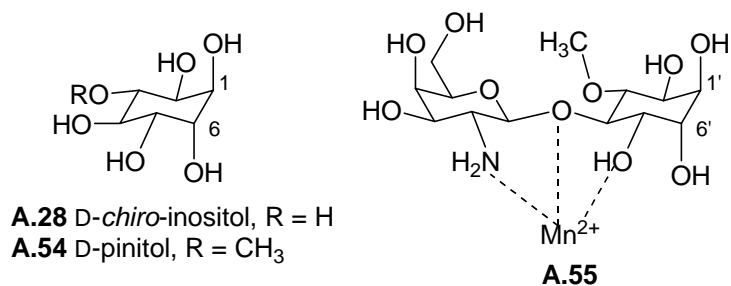


FIGURE A13.

A β -1,4-linked inositol glycan consisting of D-*chiro*-inositol (**A.28**) and galactosamine, (4-O-(2-amino-2-deoxy- β -D-galactopyranosyl)-3-O-methyl-D-*chiro*-inositol) isolated from animal tissue, forms a complex (**A.55**, Figure A13) with manganese. The Mn²⁺ chelate **A.55** activates pyruvate dehydrogenase phosphatase *in vitro* in a dose-dependent manner and hence functions as insulin mimetic. Structure of the glycan **A.55** was determined by chemical degradation and 2D NMR spectroscopy and confirmed by synthesis starting from D-pinitol (**A.54**).⁵⁰

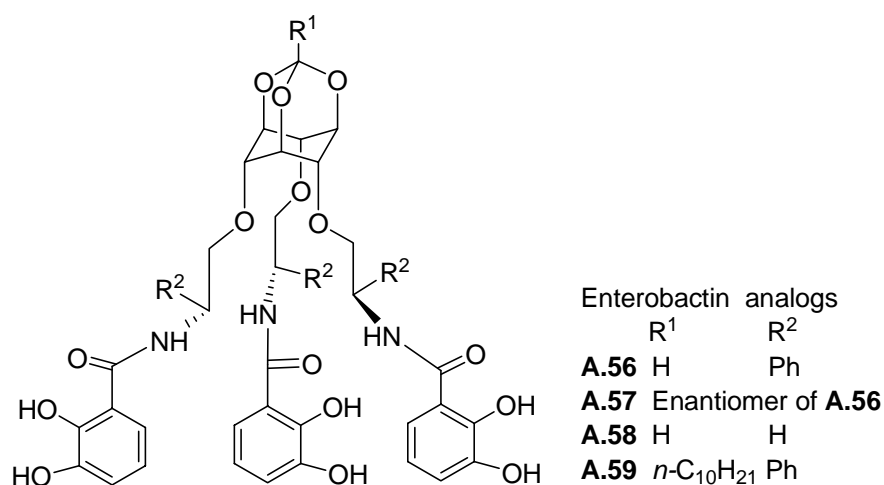


FIGURE A14.

Attempts have been made to incorporate groups onto inositols that aid metal ion binding as well as to synthesize novel structures (using inositols as core molecules) that

could bind to specific metal ions. Kishi synthesized lipophilic enterobactin analogs (Figure A14) using *scyllo*-inositol orthoformate (**A.38**),⁶ as increasing the lipophilicity was expected to affect the tissue distribution of the metal complex; such analogs were thought to have potential medicinal applications.⁵¹ The synthetic chiral analogs of enterobactin exhibited excellent affinity for ferric ions.

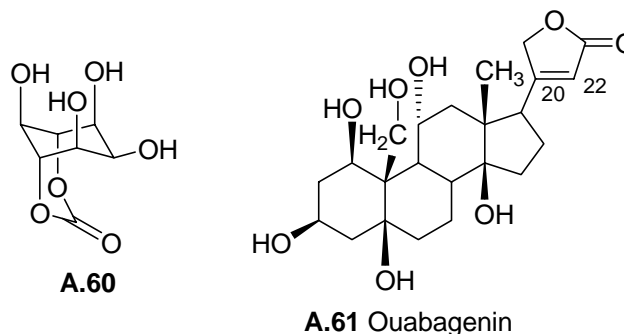
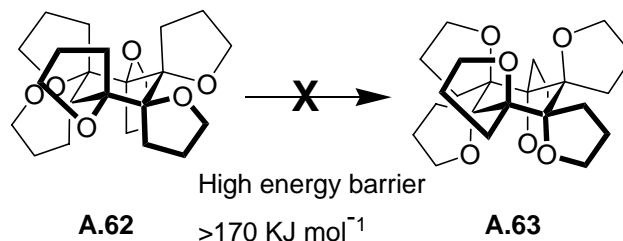


FIGURE A15.

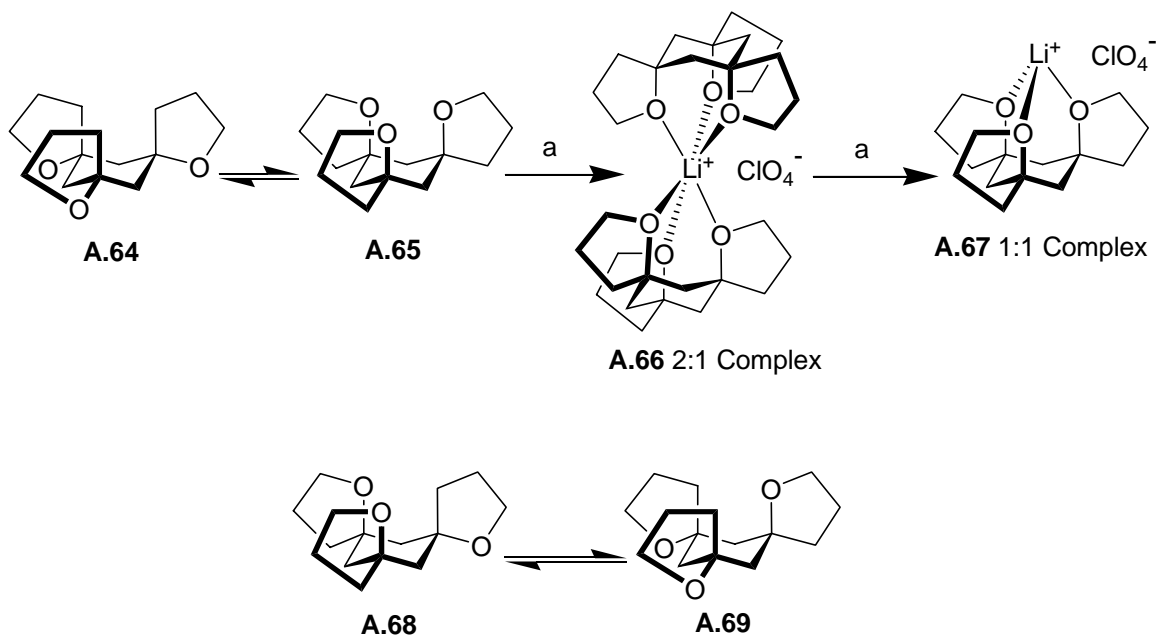
Angyal⁵² synthesized *myo*-inositol 4,6-carbonate (**A.60**, Figure A15) which has three *syn*-axial hydroxyl groups since such compounds were known to complex cations and also since such triols (e.g. ouabagenin - a natural product,⁵³ **A.61**) are scarcely reported in the literature. The ability of **A.60** to complex metal ions was demonstrated by TLC and compared with *cis*-inositol.



SCHEME A2.

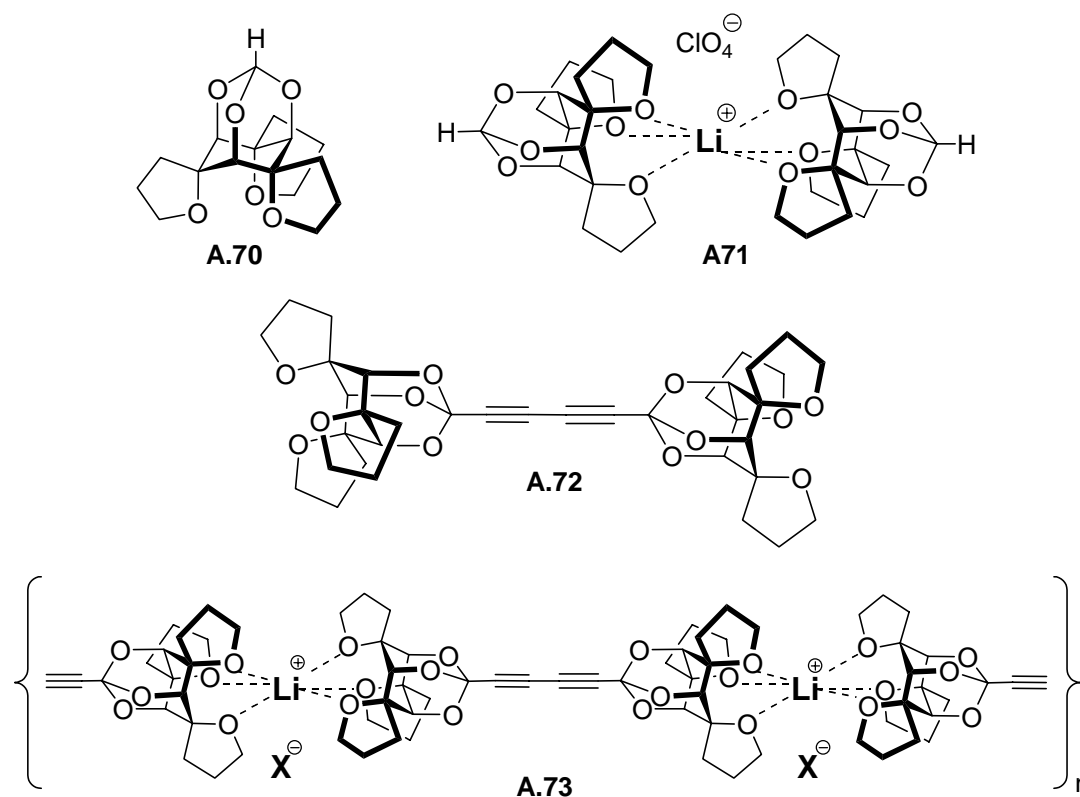
Paquette and co-workers synthesized several rigid inositol based derivatives and investigated their strength and selectivity of complexation with alkali metal ions. The

spiro bifacial ligand **A.62** (Scheme A2) with D_{3d} -symmetry was synthesized and structure established by single crystal X-ray diffraction, which confirmed an equatorial disposition of all six C-O bonds. Contrary to expectations, **A.62** did not form complex with lithium ions.⁵⁴



SCHEME A3. Reagents and conditions: (a) 0.5 eq. LiClO_4 .

Cyclohexane triol based spiro tetrahydrofuranyl derivatives **A.64** and **A.68** (Scheme A3) exhibited contrasting alkali metal binding abilities; although **A.68** showed no measurable tendency to complex with alkali metal ions, **A.64** bound strongly to Li^+ , Na^+ and CH_3NH_3^+ ions. ^{13}C NMR spectroscopic investigation suggested initial formation of a 2:1 complex (**A.66**) which was transformed into a 1:1 complex (**A.67**) upon the addition of more LiClO_4 . However **A.64** only formed a 2:1 complex with sodium ion irrespective of the amount of NaClO_4 added. The complex formation occurred readily although **A.64** existed in the equatorial rich conformation in the solid state and in solution.⁵⁵

**FIGURE A16.**

Introduction of spirotetrahydrofuranyl moieties on inositol orthoesters resulted in selective lithium ion binding agents (Figure A16) which formed rodlike supramolecular ionic polymers. The synthetic protocol for these molecules utilized pre-complexation of intermediates to LiClO₄ for stereocontrol. The metal ion complexation properties of these molecules were similar to that observed with cyclohexane triol derivatives mentioned above. The ligand **A.70** exhibited high selectivity for binding to Li⁺ and formed unique 2:1 sandwich complex (**A.71**).⁵⁶ Also, the ligands **A.70** and **A.72** bound lithium picrate about 1000 times more strongly than sodium and potassium picrates. Compound **A.72** formed rod like polymers (**A.73**) with lithium.⁵⁷

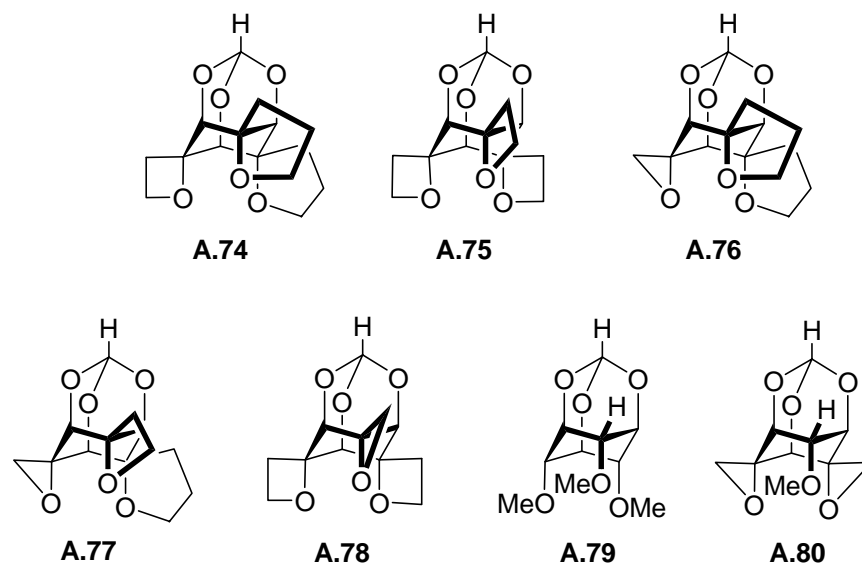


FIGURE A17.

Investigation of solution- and gas-phase alkali metal binding affinities of inositol orthoester derivatives (Figure A17) containing oxirane, oxetane, and THF rings revealed the trend for lithium ion affinity as **A.70** > **A.74** > **A.75** > **A.76** > **A.77** > **A.78** > **A.79** > **A.80**. This order of affinity was correlated with overall size of the ligand (as gauged by nonbonded O...O distances) and the polarizabilities of the oxygen atoms. Although these extensive variations achieved lithium ion selectivity of about 1000 over sodium and potassium, no selectivity was observed between sodium and potassium ions.⁵⁸

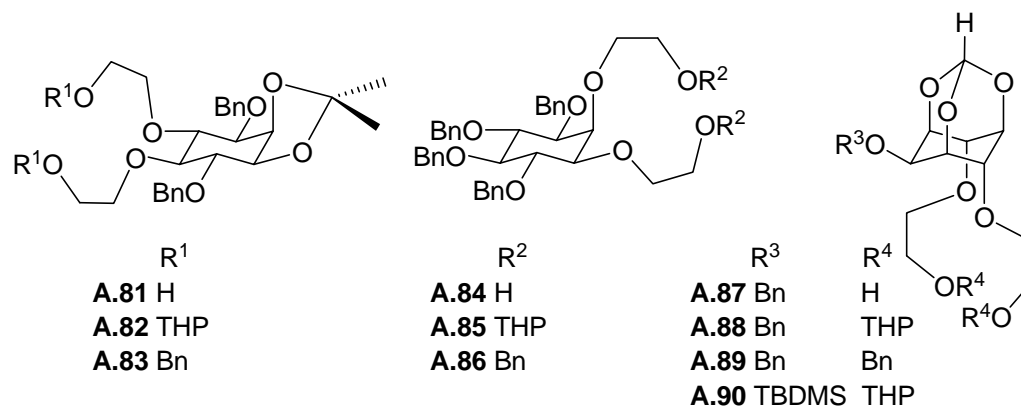


FIGURE A18. *myo*-Inositol derived podands.

myo-Inositol derived podands were synthesized and the extent of their binding with picrates of alkali metals, ammonia and silver were estimated (Figure A18).⁵⁹ These podands bind well with lithium and silver picrates but showed moderate to poor binding toward sodium, potassium, cesium and ammonium picrates. The ion selectivity and the strength of binding appeared to be dependent on the relative orientation of the side-arms (1,2-diequatorial, 1,2-axial – equatorial and 1,3-diaxial) as well as on the nature of the end group present in the podands.

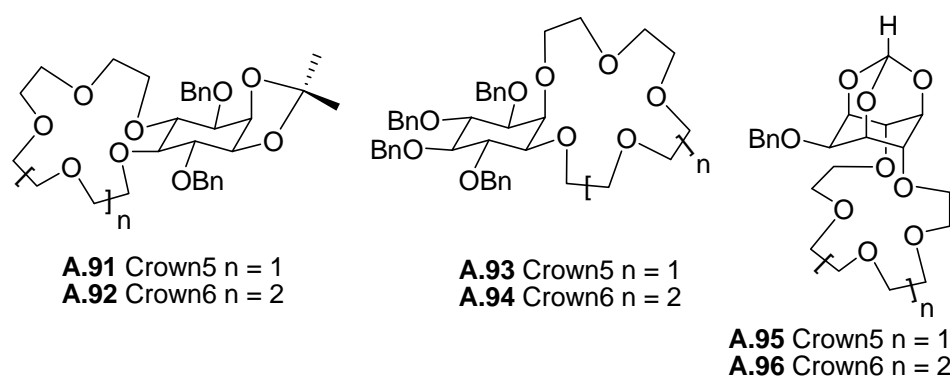
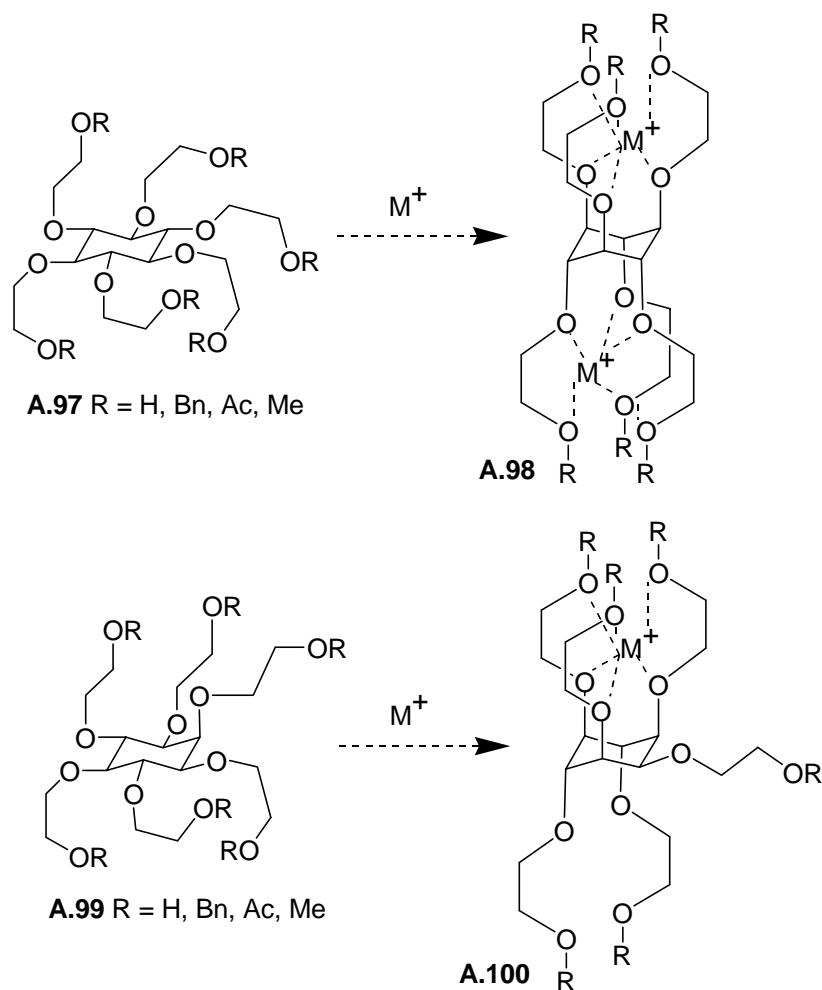


FIGURE A19. *myo*-Inositol-derived crown ethers.

myo-Inositol-derived crown ethers having varying relative orientations (1,2-diequatorial, 1,2-axial – equatorial and 1,3-diaxial) of the oxygen atoms in the ionophoric ring were synthesized and the extent of their binding with picrates of alkali metals, ammonia, and silver were estimated (Figure A19).⁶⁰ These crown ethers bind very well with potassium and silver picrates and showed good to moderate binding toward lithium, sodium, cesium, and ammonium picrates. These *myo*-inositol-derived crown ethers exhibited very strong binding for silver, even though they did not have sulfur or nitrogen coordinating sites in them, which are known to have high affinity for silver. The ratio of binding constants for silver to other ions tested varied from 10^2 to 10^5 . The ion selectivity

and the strength of binding appeared to be dependent on the relative orientation of the oxygen atoms in the ionophoric ring as well as on the size of the macrocyclic ring.



SCHEME A4.

Complexation of hexa *O*-substituted *myo*- and *scyllo*-inositol derivatives (Scheme A4) with alkali metal ions was investigated in order to understand if an equatorial rich system could be coaxed by metal ions into adopting the corresponding axial rich configuration. However, these inositol derivatives did not exhibit high levels of coordination with alkali metal ions.⁶¹

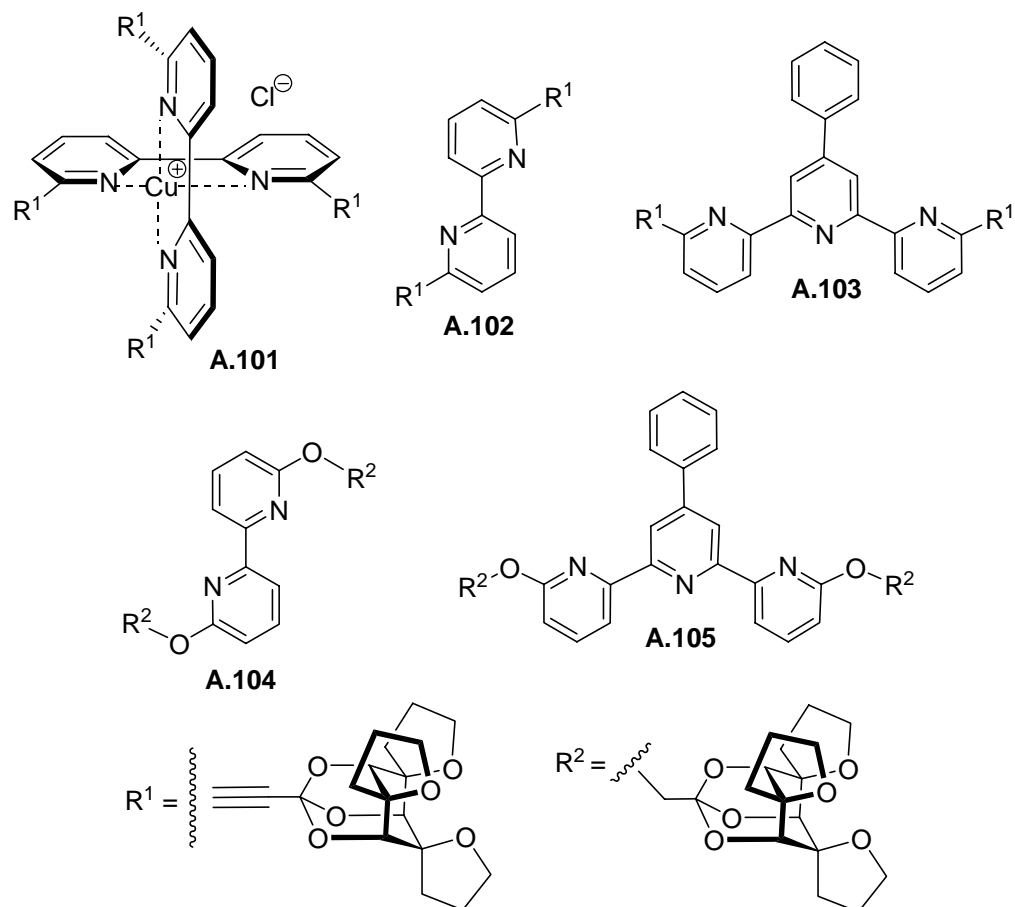
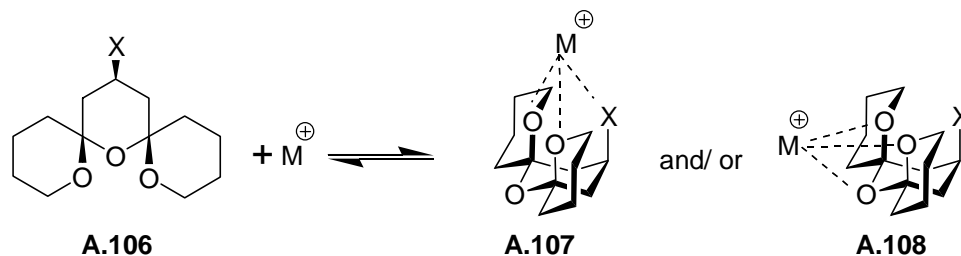


FIGURE A20.

The covalent incorporation of bipyridine and terpyridine ligands to rigid inositol orthoformate derivatives (Figure A20) containing spirotetrahydrofurans resulted in ligands capable of binding Li^+ and transition-metal ions simultaneously.⁶²



SCHEME A5.

Pyran based polyspirocyclic metal ion complexing agents (Scheme A5) were prepared and tested for metal ion binding by picrate extraction method. The compounds having oxygen substituent ($X = \text{OH}$, OMe) did not show appreciable binding to alkali metal picrates but the amino derivative ($X = \text{NHBn}$) exhibited strong binding to alkali metal picrates. Although these molecules possess a framework that offers a 1,3,5-triaxial presentation of ligating centers, it was not clear if indeed these ligands complexed with metal ions in the triaxial conformation.⁶³

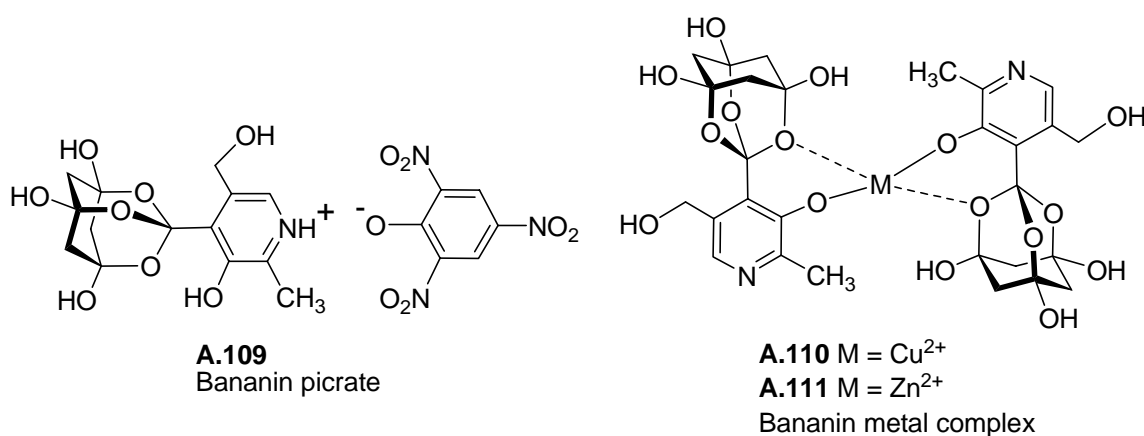
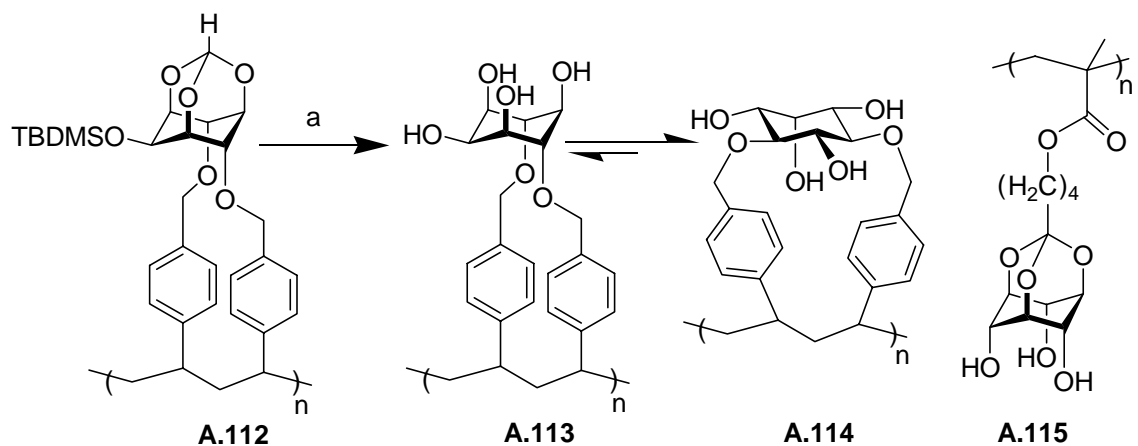


FIGURE A21. Proposed structures of the Cu and Zn complexes.

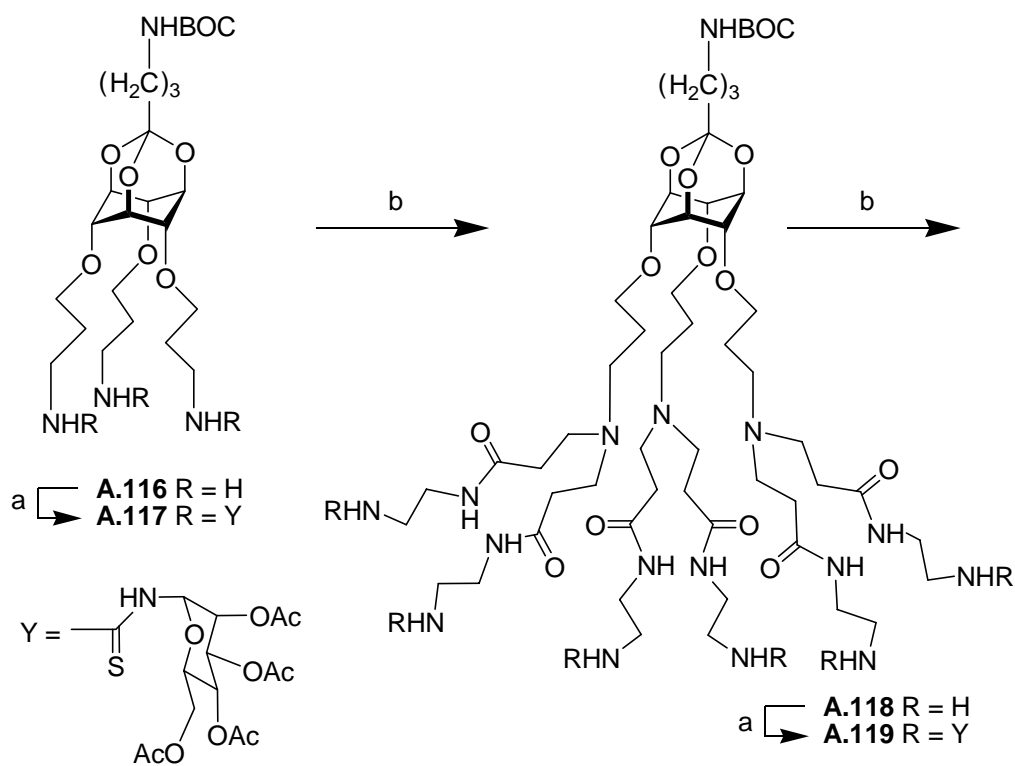
A 1,1,3,3,5,5-hexahydroxycyclohexane derivative, ‘bananin’ (trivial name) structurally similar to inositol orthoester was proposed to chelate with copper and zinc ions (**A.110** and **A.111**, Figure A21). Based on theoretical and structural considerations bananin was proposed to be effective for the inhibition of HIV-1 replication.⁶⁴

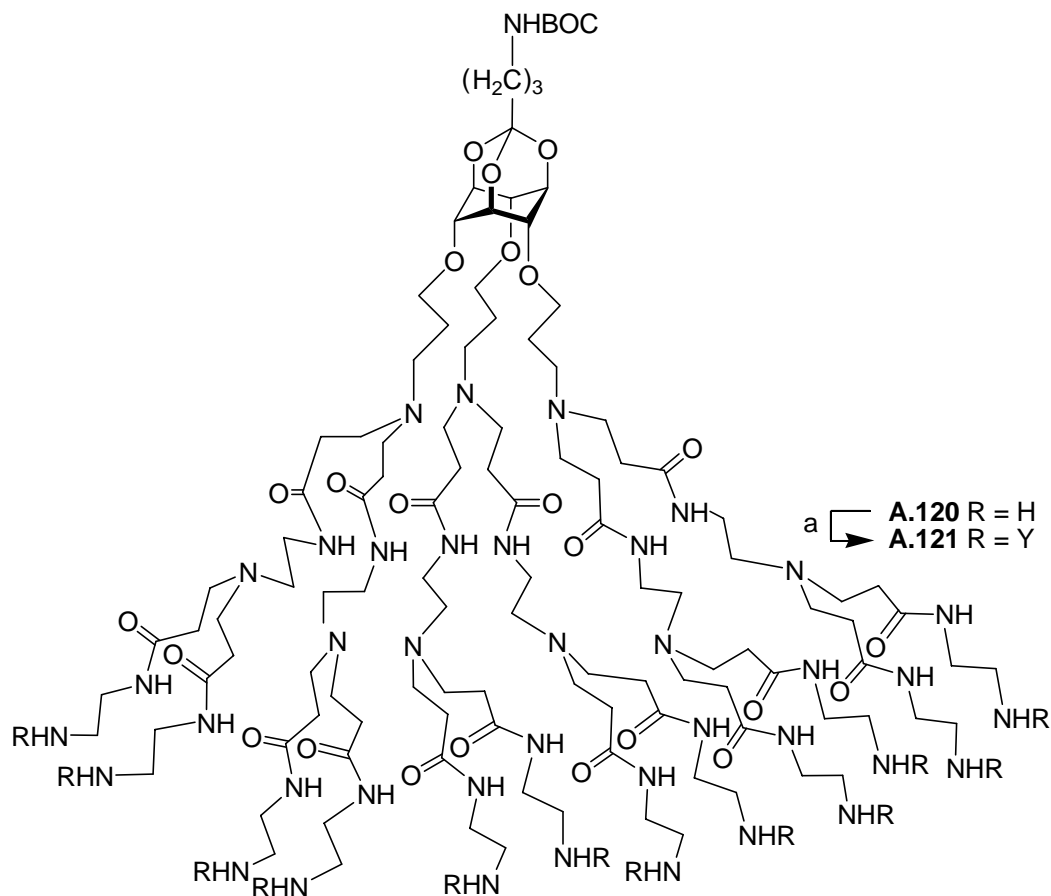
Rigid polymers containing *myo*- or *scyllo*-inositol units were synthesized (Scheme A6) as potential metal chelating agents; however, their ability to complex with metal ions was not tested.⁶⁵



SCHEME A6. Reagents and conditions: (a) TsOH, MeOH, THF.

A *scyllo*-inositol orthoester has been used as a scaffold for the preparation of functionalized glycodendrimers (Scheme A7). These dendrimers were prepared for applications in atomic force-field microscopy (AFM).⁶⁶ Although these compounds appear to have the potential to complex with metal ions, they have not been evaluated as metal complexing agents.⁶⁷





SCHEME A7. *Reagents and conditions:* (a) 2,3,4,6-tetra-O-acetyl- α -D-mannosyl isothiocyanate, DCM, reflux; (b) (i) Methyl acrylate, MeOH, in dark; (ii) ethylenediamine, MeOH.

myo-Inositol has been used as a core molecule and a support for covalent binding of gadolinium chelating agents (Figure A22).⁶⁸ The objective was to increase the sensitivity of magnetic resonance imaging (MRI) contrast agents to study biochemical processes and investigate potential applications in medicine.

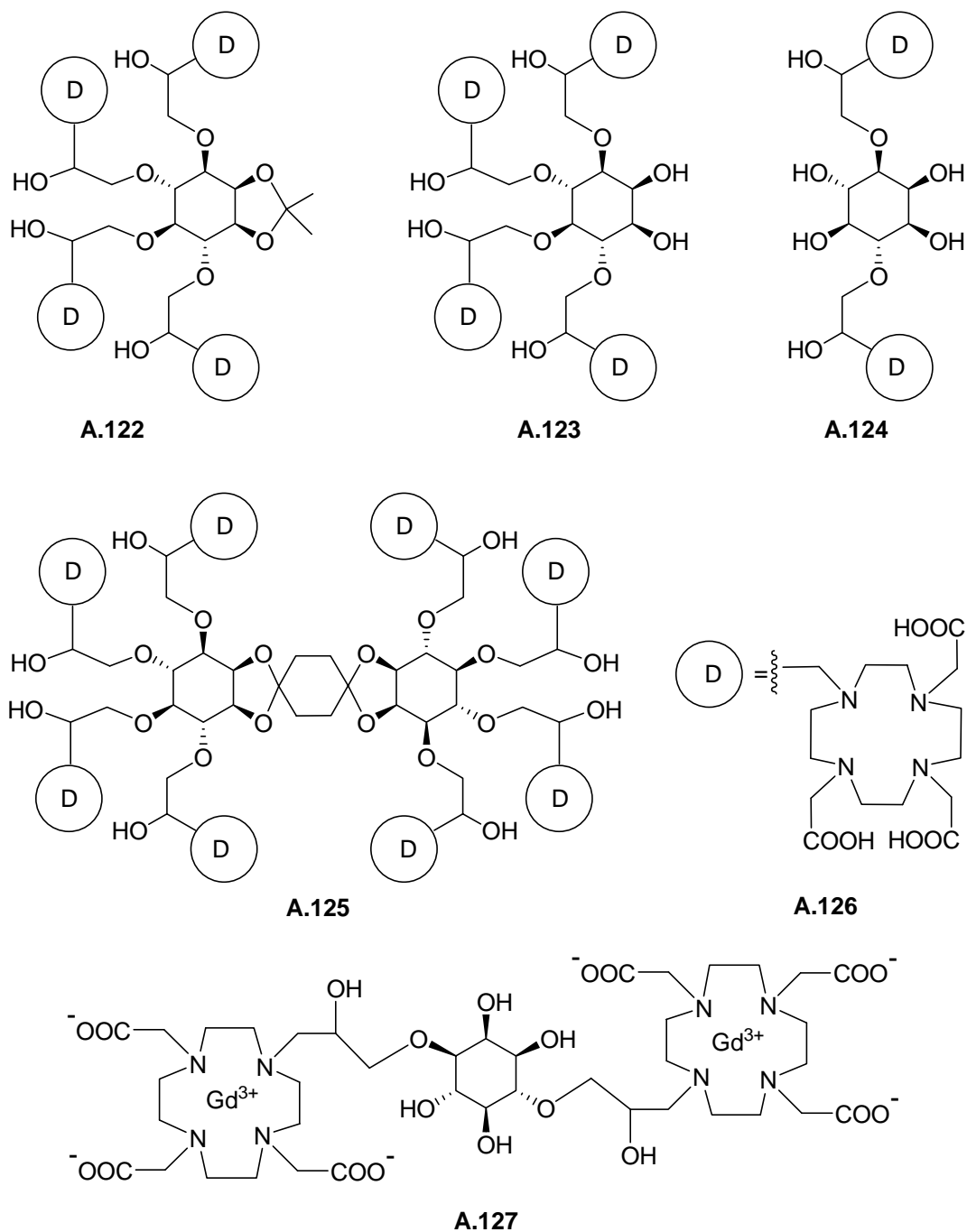


FIGURE A22. *myo*-Inositol based MRI contrast agents.

A *myo*-inositol orthoformate-azacrown ether conjugate (**A.128**, Figure A23) was prepared and its ability to form 1:1 complex with Li⁺ was shown by NMR spectroscopy

and electrospray ionization mass spectrometry. One of the two azacrown ethers was suggested to be responsible for the inclusion of a Li^+ ion.⁶⁹

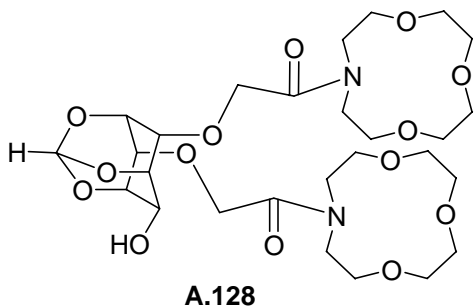
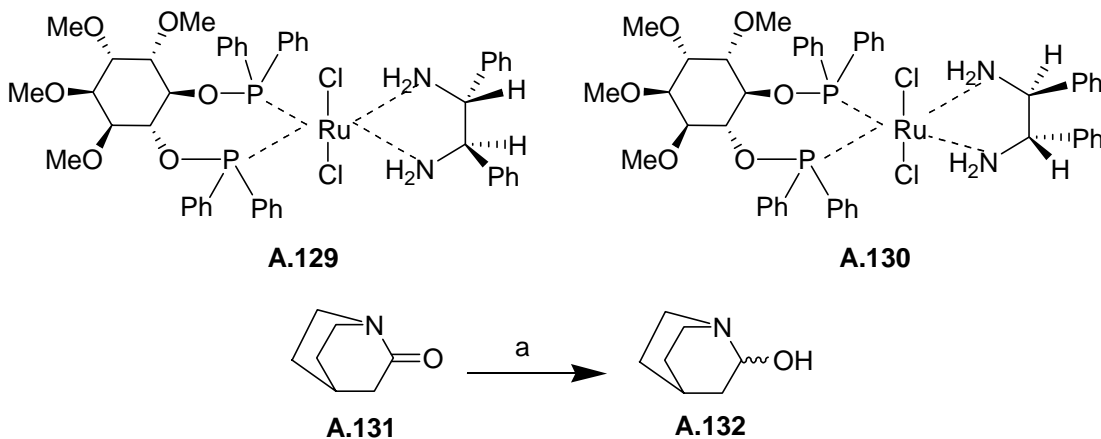


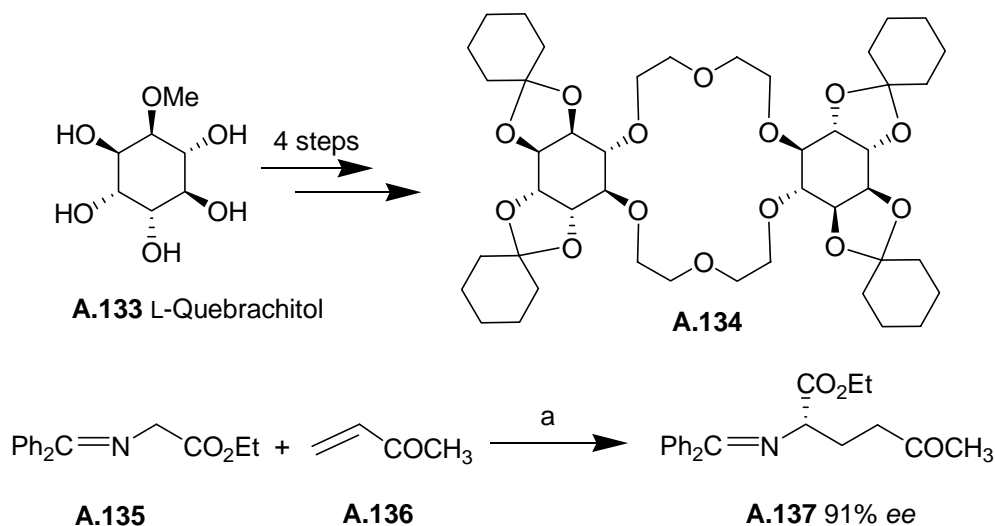
FIGURE A23.

chiro-Inositol derivatives (Scheme A8) have been used for the preparation of a chiral diphosphinite ligand, the ruthenium complexes (**A.129** and **A.130**) of which were effective catalysts for the hydrogenation of carbonyl groups (e.g. **A.131**). Conversions were close to 100%, however the selectivity was low (enantiomeric excess up to 50%).⁷⁰



SCHEME A8. Reagents and conditions: (a) Toluene:*iso*-propanol (1:1), *t*-BuOK, H_2 (1000 psi), 60 °C, 3h, conversion 100% (cat = **A.129**, *ee* = 20%, cat = **A.130**, *ee* = 50%, Substrate:cat = 200:1).

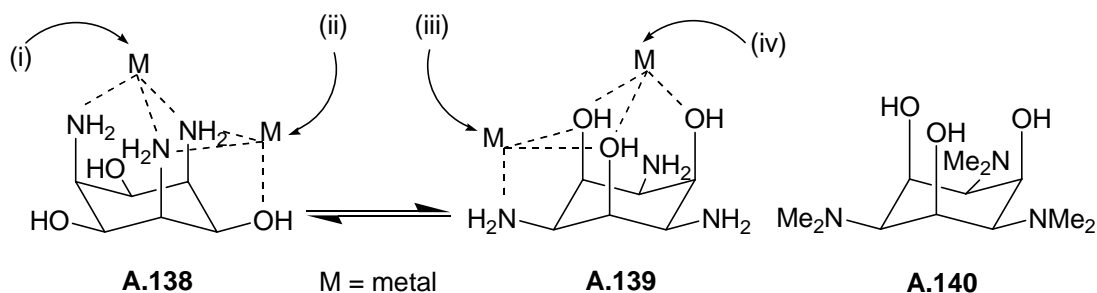
A chiral *chiro*-inositol based crown ether (**A.134**, Scheme A9) was prepared from L-quebrachitol and its catalytic activity in the Michael addition reaction of glycine imine with several Michael acceptors was studied. Its ability to complex with metal ions was however not evaluated.⁷¹



SCHEME A9. Reagents and conditions: (a) **A.134** (0.2 eq.), toluene, t-BuOK (0.2 eq.), -78 °C, 1 h, 32% (*ee* = 91%).

Amino cyclitols are good complexing agents for metal ions since they can coordinate through amino as well as hydroxyl groups. It is generally observed that soft metal cations are preferentially bound to the nitrogen donors. Extensive work on the complexation of about thirty metal ions with 1,3,5-triamino-1,3,5-trideoxy-*cis*-inositol (Scheme A10) revealed four types of metal binding *via* either of the two chair conformations.⁷² Group I and group II metal cations, except Be²⁺ formed mononuclear type (iv) bis complexes;⁷³ divalent transition- and d¹⁰ metal cations generally adopted a bis-type (i) structure;^{74,75,76} lead and bismuth ions co-ordinate with both oxygen and nitrogen in a mixed type (i) and type (iv) complex.^{75,76,77} Homo- and heterodinuclear

metal complexes of N-methylated analog of 1,3,5-triamino-1,3,5-trideoxy-*cis*-inositol (**A.140**, Scheme A10) could cleave phosphodiester of ribonucleoside monophosphates and polyribonucleotides.⁷⁸



SCHEME A10. Curved arrows show potential metal ion sites.

Chiral bis-pyridyl ligands derived from 1,2-diamino-1,2-dideoxy-*myo*-inositol (**A.141**, Figure A24) were prepared for exploring the relationship between chiral ligand structure and enantioselective olefin oxidation catalyzed by their metal complexes.⁷⁹

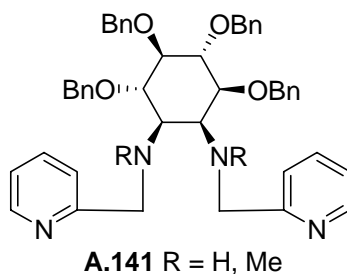
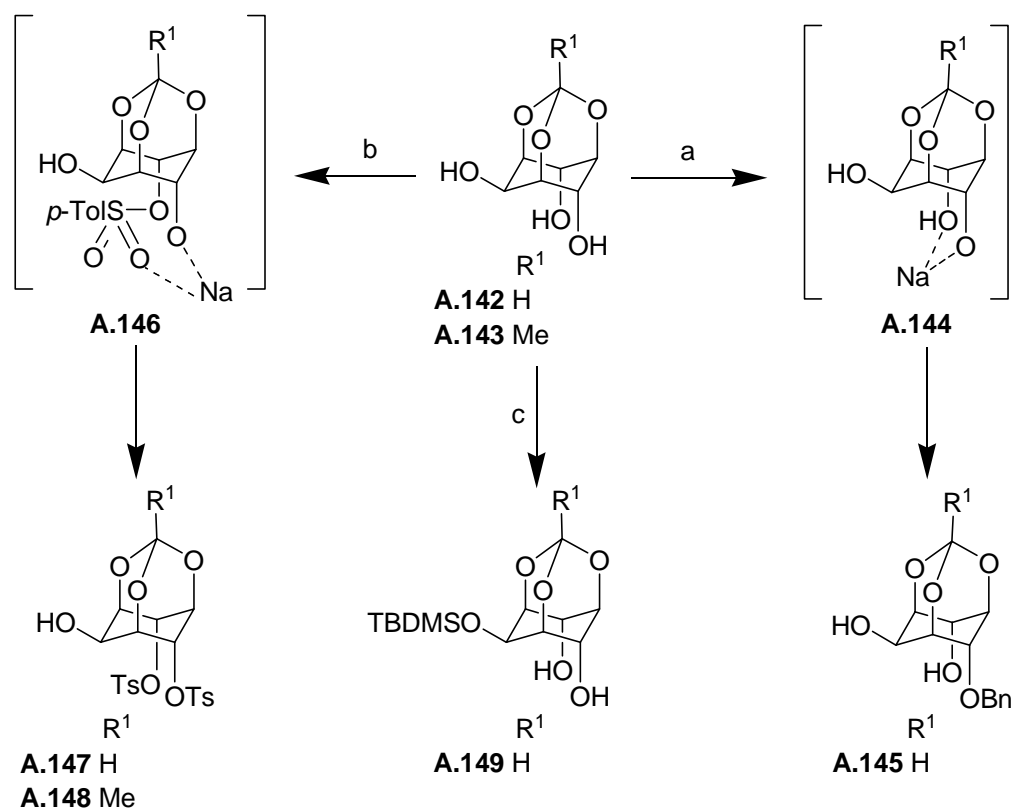


FIGURE A24.

There are several reports on the reactions of inositol derivatives in which chelation with metal ions seems to play a key role in the outcome of the reactions. In most of these reactions, involvement of metal chelates is suggested by circumstantial evidences such as selectivity of product formation, solvent effect, presence or absence of other metal ion binding agents and change in composition of the products with change in metal ions present in the reaction medium. A survey of such reactions reported in the literature is given below.

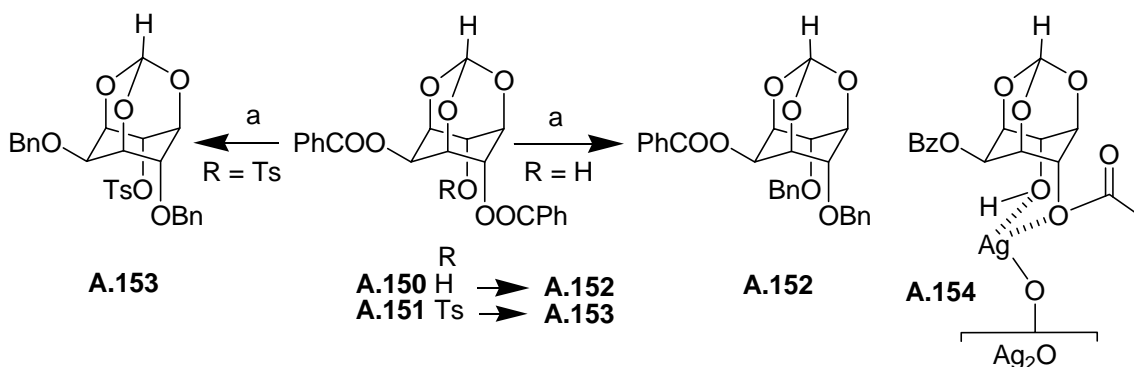
Alkylation,⁸⁰ acylation⁸¹ and sulfonylation⁸² of *myo*-inositol orthoesters (Scheme A11) in the presence of sodium hydride resulted in the exclusive O-substitution at the C4-hydroxyl group. Involvement of a chelate was postulated to explain this regioselective reaction, based on the solvent effects observed for these reactions. Importance of the presence of metal ions for the observed high regioselectivity was also indicated by nature of the product obtained by O-substitution of the triol (**A.142**) in the absence of metal ions⁸³ (formation of **A.149**).



SCHEME A11. Reagents and conditions: (a) NaH, DMF, BnBr (1 eq.); (b) NaH, DMF, TsCl; (c) DMF, imidazole, TBDMSCl.

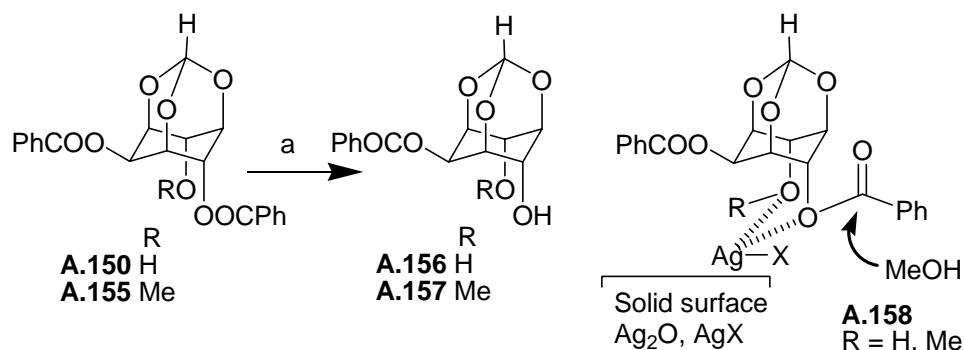
Alkylation of the racemic dibenzoate **A.150** (Scheme A12) in the presence of silver(I) oxide yielded the symmetric dibenzyl ether **A.152**.⁸⁴ Cleavage and *O*-alkylation of the C4-ester group was unexpected; the C2-ester however remained unaffected. The

presence of a sulfonate at the C6-O-position (**A.151**) however resulted in alkylation of both the C2 and the C4-esters (**A.153**).⁸⁵



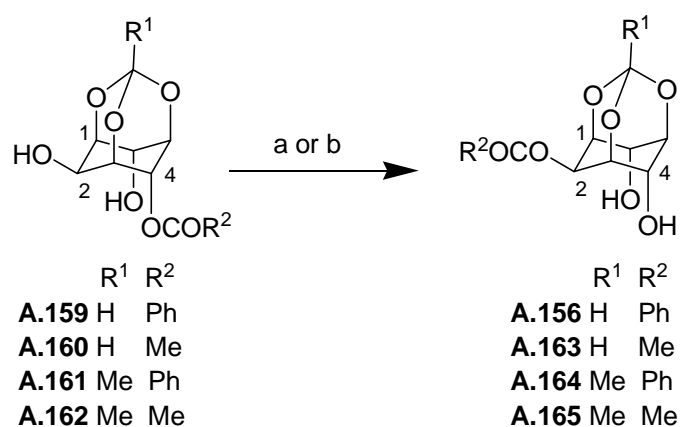
SCHEME A12. Reagents and conditions: (a) DMF, BnBr (excess), Ag₂O.

Reaction of the dibenzoate **A.150** or its methyl ether **A.155** (Scheme A13) with methanol in the presence of silver(I) oxide and a silver halide resulted in exclusive solvolysis of the C4-benzoate to give **A.156** and **A.157** respectively. Catalytic efficiency of the silver halides in bringing about solvolysis of the benzoate decreased in the order AgI > AgBr > AgCl.⁸⁶ These results suggested the involvement of a silver chelate (**A.158**) during the solvolysis reactions.



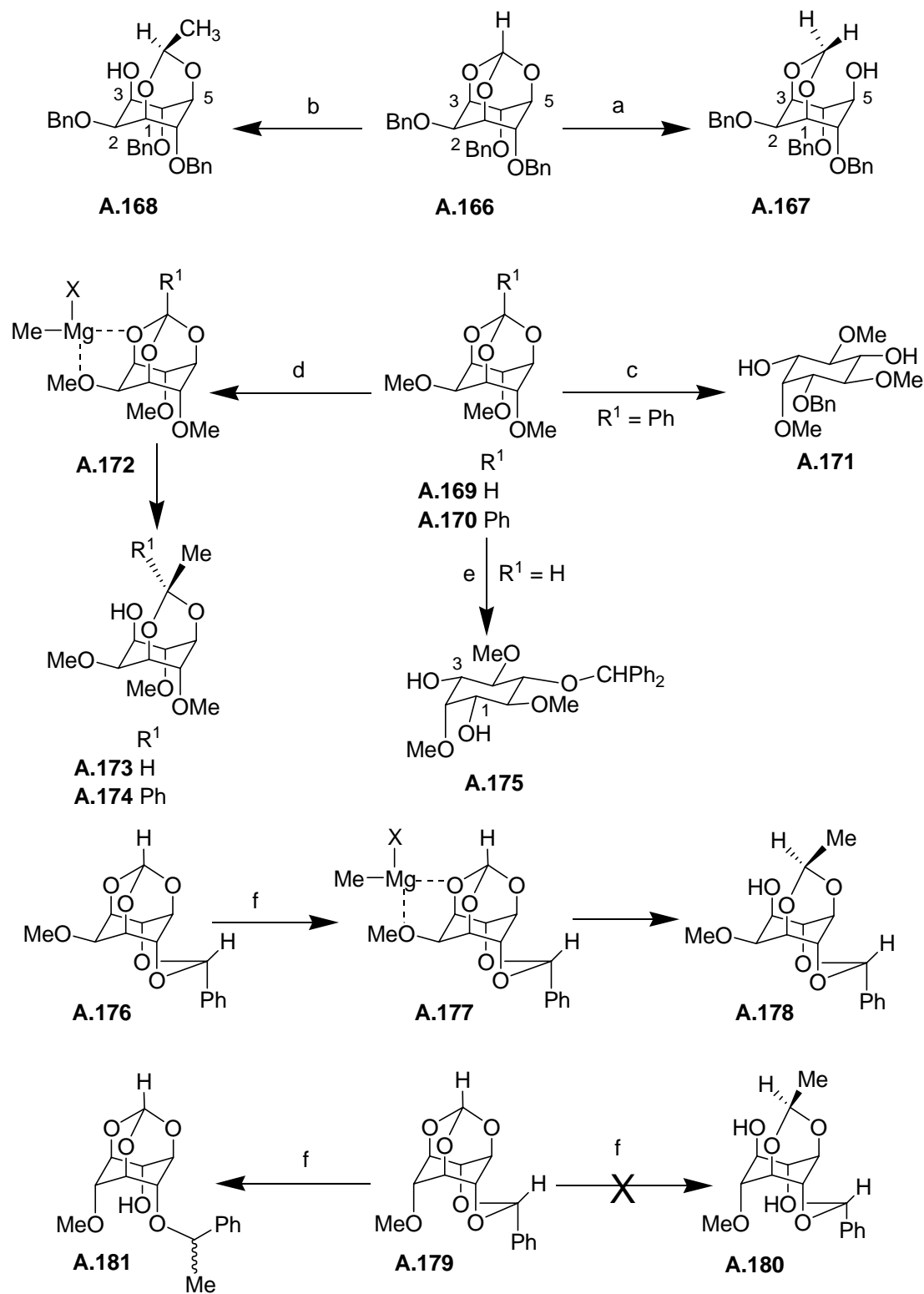
SCHEME A13. Reagents and conditions: (a) DMF-MeOH, Ag₂O, AgX.

Reaction of racemic 4-*O*-acylated *myo*-inositol 1,3,5-orthoesters with strong bases such as sodium hydride or potassium *t*-butoxide resulted in the intramolecular migration of the 4-*O*-acyl group to the 2-*O*-position (Scheme A14). Indication for the involvement of metal chelates during this reaction was suggested by solvent effects and the effect of the presence of a crown-ether in the reaction medium. This isomerization provided an efficient and general method for the preparation of 2-*O*-acylated derivatives of *myo*-inositol 1,3,5-orthoesters.⁸¹



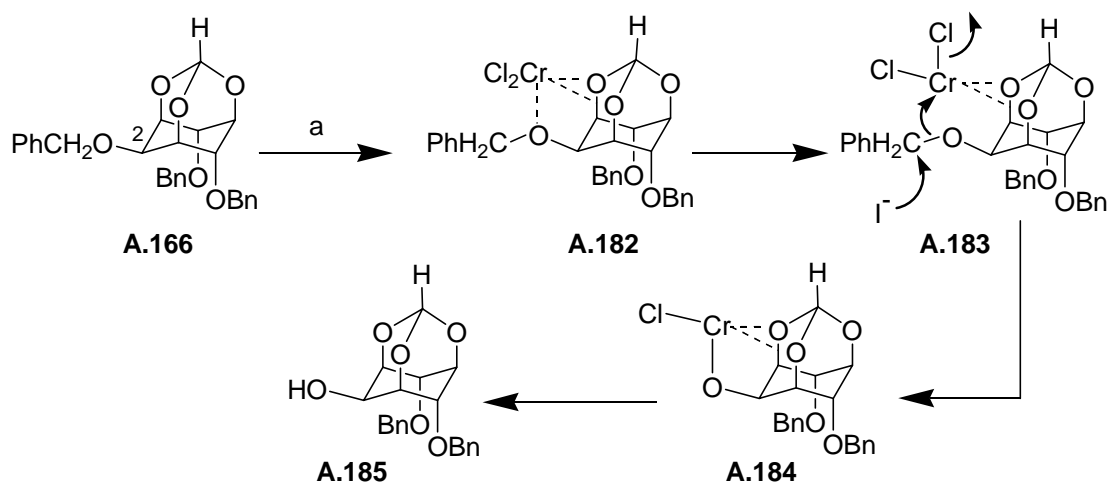
SCHEME A14. Reagents and conditions: (a) DMF, NaH (1 eq.), 5 min; (b) DMF, *t*-BuOK, 5 min.

Regioselective cleavage of *myo*-inositol orthoesters with DIBAL-H,⁸⁷ AlMe₃⁸⁸ and Grignard reagents⁸⁹ can be effected to obtain partially protected *myo*-inositol derivatives as shown in Scheme A15. Reduction of orthoesters with DIBAL-H releases the C5-hydroxyl group (**A.167**) while cleavage with Grignard reagents releases the C1(3)-hydroxyl group (**A.173** and **A.174**). The observed regioselectivity for the cleavage with Grignard reagent was attributed to the presence of the 2-methoxy group which serves as an auxiliary for the chelation of magnesium ion (**A.172**). This suggestion was



SCHEME A15. Reagents and conditions: (a) DIBAL; (b) AlMe_3 ; (c) LiAlH_4 , AlCl_3 , (excess); (d) MeMgBr ; (e) PhMgBr (excess); (f) MeMgI .

based on the fact that Grignard reagents cleaved the orthoester moiety in *myo*-inositol orthoester derivative **A.169** and **A.176**, while benzylidene acetal was cleaved in the *scyllo*-inositol orthoester derivative **A.179** (the orthoester moiety remained unaffected). This was attributed to the relative disposition of the methoxyl group, as cleavage was observed on the same side of the methoxyl group (orthoester in **A.169** or acetal in **A.179**) in the *myo*- and *scyllo*-orthoester derivatives.

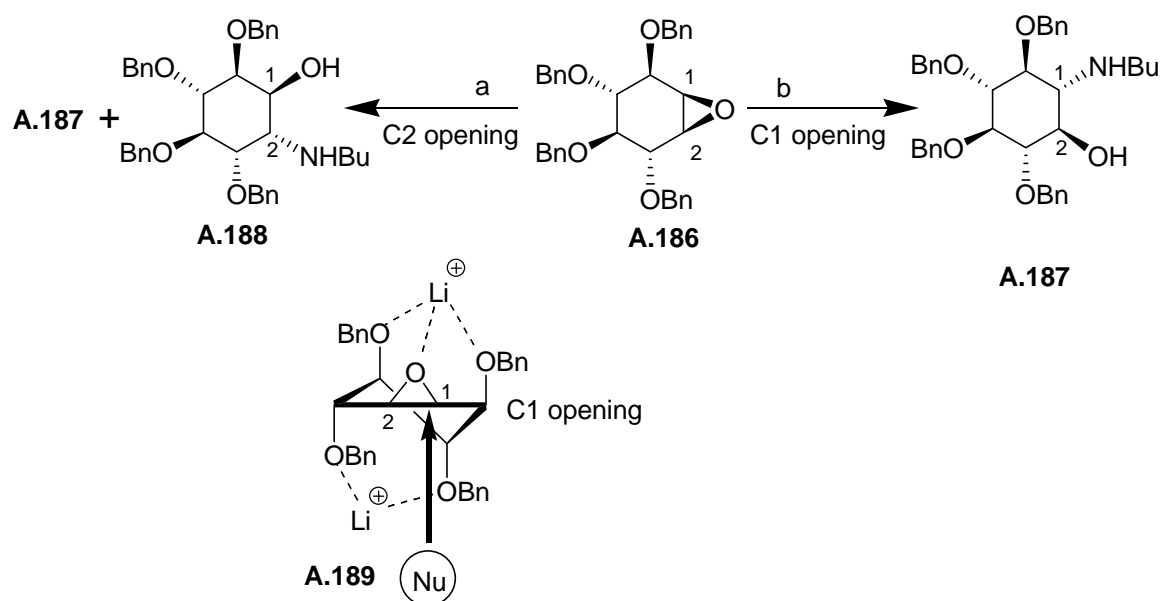


SCHEME A16. Reagents and conditions: (a) CrCl₂, LiI, EtOAc, H₂O.

The C2-benzyl ether in the tribenzyl ether **A.166** could be regioselectively debenzylated using CrCl₂/LiI (Scheme A16) in moist ethyl acetate to give **A.185**. A predictive, three-point coordination model was proposed to explain the observed regioselectivity.⁹⁰

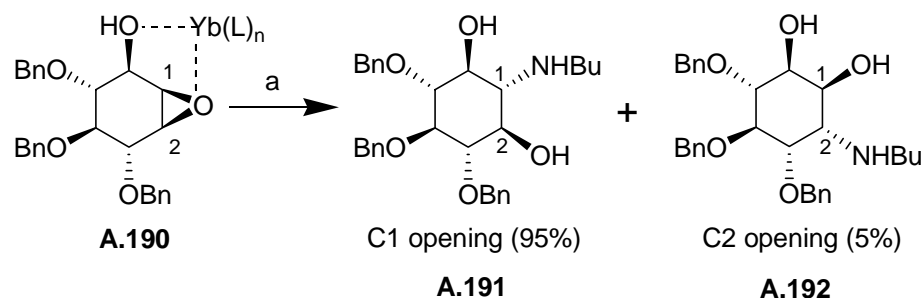
Experimental and theoretical studies on the influence of Li⁺ ions on the regio- and the stereoselectivity in the reaction of cyclitol epoxides with nitrogen nucleophiles (Nu) have been carried out (Scheme A17).⁹¹ Model studies with BuNH₂ as a nucleophile in the absence of Li⁺ ions predicted a mixture of C1 and C2 regio adducts (**A.187** and **A.188**). Inclusion of two Li⁺ ions in the chelate favored the operation of a low populated *all-

axial" conformation (**A.189**) leading ultimately to the C1 adduct (**A.187**). In all the cases, the results could be rationalized by geometric and energetic considerations of the corresponding transition states. Predictions of the theoretical calculations were in good agreement with the experimental results using primary and secondary amines as nucleophiles. In the absence of lithium ion, either the reaction (with BuNH₂) did not proceed or the regio- and the stereoselectivity were poor.



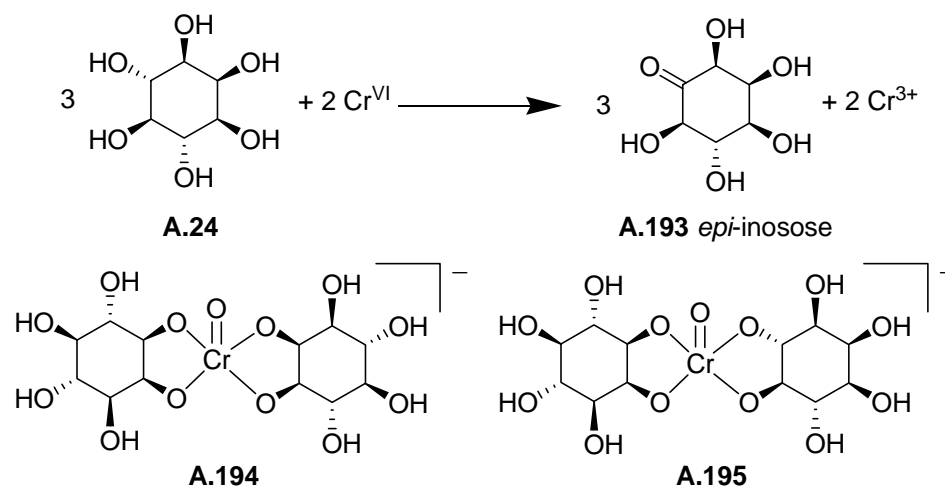
SCHEME A17. Reagents and conditions: (a) CH₃CN, 80 °C, BuNH₂, (**A.187**:**A.188**, 2:3); (b) 2N LiClO₄, CH₃CN, 80 °C, BuNH₂.

Aminolysis and azidolysis of the cyclitol epoxides in the presence of Yb(OTf)₃ (Scheme A18) has been suggested to be chelation-controlled and the free OH group was thought to direct the co-ordination with the lanthanide and bring in efficient regioselective opening of the epoxide.⁹²



SCHEME A18. Reagents and conditions: (a) Yb(OTf)₃, BuNH₂, toluene, 80 °C.

The EPR spectra indicated that five- and six-coordinated oxo-Cr^V intermediates are formed (Scheme A19), with the cyclitol acting as a bidentate ligand during the oxidation of *myo*-inositol (**A.24**) with Cr^{VI} to yield the *epi*-inosose (**A.193**). Kinetic and mechanistic investigations of this oxidation revealed that penta-coordinated oxo-Cr^V species were present at pH > 1, whereas hexa-coordinated species were observed at pH < 1. Oxo-Cr^V bischelates were stable enough to remain for long time in solution.⁹³



SCHEME A19.

The ability of receptors to sense the presence of *D-chiro*-inositol (**A.28**) and not to respond to the presence of *myo*-inositol (**A.24**) utilizing internal photo induced electron

transfer (PET) quenching mechanisms has been suggested to be due to the differences in the modes of chelation to the two inositol isomers (Figure A26).⁹⁴

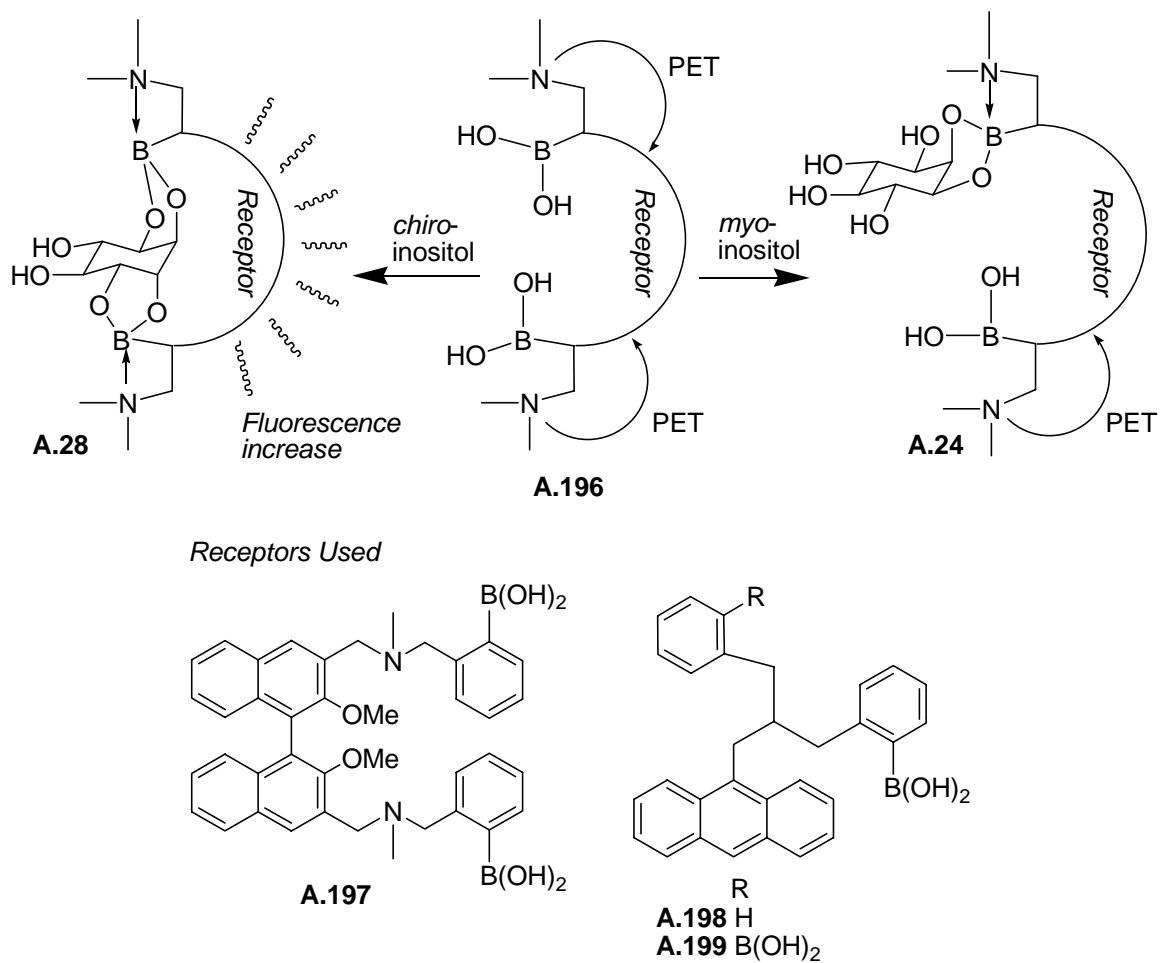


FIGURE A26. Specific receptors to sense the presence of D-*chiro*-inositol.

Conclusions

Various reports on the metal ion complexation behavior of inositols and their derivatives clearly illustrate the potential of inositols as core molecules for building novel metal ion complexing agents. Although phosphoinositols do complex with a variety of metal ions, most of these are co-ordination type of complexes and inositol derived phosphodiester undergo cleavage to the corresponding phosphomono ester. Complexation behavior of inositol derivatives with lithium is of potential interest and applicability due to its known therapeutic applications and inhibitory activity against *myo*-inositol monophosphate phosphatase. Metal ion complexing agents derived from inositols are also of interest due to their applications in catalysis, sequestering of metal ions etc. However, it is evident that there have been very few systematic studies on *myo*-inositol derived crown ethers. The remaining part of this thesis describes an attempt to fill this lacuna.

References

- 1 (a) Moore, C.; Pressman, B. C. *Biochem. Biophys. Res. Commun.* **1964**, *15*, 562-567.
(b) Pressman, B. C. *Proc. Natl. Acad. Sci. USA*, **1965**, *53*, 1076-1083. (c) Chappell, J. B.; Crofts, A. R. *Biochem. J.* **1965**, *95*, 393-402. (d) Graven, S. N.; Lardy, H. A.; Johnson, D.; Rutter, A. *Biochemistry* **1966**, *5*, 1729-1735. (e) Tosteson, D. C.; Andreoli, T. E.; Tieffenberg, M.; Cook, P. J. *Gen. Physiol.* **1968**, *51*, 373-384.
- 2 *Comprehensive Supramolecular Chemistry*, Vol. 1, Gokel, G. W Ed, Pergamon Press, New York, N.Y. **1996**.
- 3 (a) Kilbourn, B. T.; Dunitz, J. D.; Pioda, L. A. R.; Simon, W. *J. Mol. Biol.* **1967**, *30*, 559-563. (b) Dobler, M.; Dunitz, J. D.; Kilbourn, B. T. *Helv. Chim. Acta* **1969**, *52*, 2573-2583.
- 4 Michael, J. P.; Pattenden, G. *Angew. Chem., Int. Ed. Engl.* **1993**, *32*, 1-23.
- 5 Okami, Y. *Pure Appl. Chem.* **1982**, *54*, 1951-1962.
- 6 Tse, B.; Kishi, Y. *J. Am. Chem. Soc.* **1993**, *115*, 7892-7893.
- 7 Fazldeen, H.; Hegarty, M. P.; Lahey, F. N. *Phytochemistry* **1978**, *17*, 1609-1612.
- 8 Angyal, S. J.; Greeves, D.; Littlemore, L. *Aust. J. Chem.* **1985**, *38*, 1561-1566.
- 9 Pollack, J. R.; Neilands, J. B. *Biochem. Biophys. Res. Commun.* **1970**, *38*, 989-992.
- 10 (a) Isied, S. S.; Kuo, G.; Raymond, K. N. *J. Am. Chem. Soc.* **1976**, *98*, 1763-1768.
(b) Loomis, L. D.; Raymond, K. N. *Inorg. Chem.* **1991**, *30*, 906-911. (c) Karpishin, T. B.; Raymond, K. N. *Angew. Chem., Int. Ed. Engl.* **1992**, *31*, 466-468. (d) Stack, T. D. P.; Karpishin, T. B.; Raymond, K. N. *J. Am. Chem. Soc.* **1992**, *114*, 1512-1514.

-
- 11 Marjanović, M.; Kralj, M.; Supek, F.; Frkanec, L.; Piantanida, I.; Šmuc, T.; Tušek-Božić, L. *J. Med. Chem.* **2007**, *50*, 1007-1018.
- 12 (a) *Comprehensive Supramolecular Chemistry*, Ed. Gokel, G. W. Pergamon Press, New York, N.Y. **1996**. For calixarene crown ethers see (b) Bakker, W. I. I.; Verboom, W.; Reinhoudt, D. N. *J. Chem. Soc., Chem. Commun.* **1994**, 71-72. (c) Casnati, A.; Pochini, A.; Ungaro, R.; Ugozzoli, F.; Arnaud, F.; Fanni, S.; Schwing, M.-J.; Egberink, R. J. M.; de Jong, F.; Reinhoudt, D. N. *J. Am. Chem. Soc.* **1995**, *117*, 2767-2777. (d) Casnati, A.; Pochini, A.; Ungaro, R.; Bocchi, C.; Ugozzoli, F.; Egberink, R. J. M.; Struijk, H.; Lutenberg, R.; de Jong, F.; Reinhoudt, D. N. *Chem. Eur. J.* **1996**, *2*, 436-445. (e) Blanda, M. T.; Farmer, D. B.; Brodbelt, J. S.; Goolsby, B. J. *J. Am. Chem. Soc.* **2000**, *122*, 1486-1491. (f) Beer, P. D.; Gale, P. A. *Angew. Chem., Int. Ed.* **2001**, *40*, 486-516. (g) Lee, S. H.; Kim, J. Y.; Ko, J.; Lee, J. Y.; Kim, J. S. *J. Org. Chem.* **2004**, *69*, 2902-2905. (h) Talanova, G. G.; Talanov, V. S.; Hwang, H.-S.; Park, C.; Surowiec, K.; Bartsch, R. A. *Org. Biomol. Chem.* **2004**, *2*, 2585-2592. (i) Tu, C.; Surowiec, K.; Bartsch, R. A. *Tetrahedron Lett.* **2006**, *47*, 3443-3446. For camphor crown ethers see (j) Brisdon, B. J.; England, R.; Mahon, M. F.; Reza, K.; Sainsbury, M. *J. Chem. Soc., Perkin Trans 2* **1995**, 1909-1914. For cage crown ethers see (k) Marchand, A. P.; Kumar, K. A.; McKim, A. S.; Mlinarić-Majerski, K.; Kragol, G. *Tetrahedron* **1997**, *53*, 3467-3474. (l) Marchand, A. P.; Chong, H.-S.; Alihodzic, S. *Tetrahedron* **1999**, *55*, 9687-9696. (m) Marchand, A. P.; Chong, H.-S. *Tetrahedron* **1999**, *55*, 9697-9706. (n) Mlinarić-Majerski, K.; Kragol, G. *Tetrahedron* **2001**, *57*, 449-457. (o) Marchand, A. P.; Hazlewood, A.; Huang, Z.; Vadlakonda, S. K.; Rocha, J.-D. R.; Power, T. D.; Mlinarić-Majerski, K.; Klai,

-
- L.; Kragol, G.; Bryan, J. C. *Struct. Chem.* **2003**, *14*, 279-288. (p) Amendola, V.; Boiocchi, M.; Colasson, B.; Fabbriizzi, L.; Douton, M-J. R.; Ugozzoli, F. *Angew. Chem., Int. Ed.* **2006**, *45*, 6920-6924. For stillbene crown ethers see (q) Futterer, T.; Merz, A.; Lex, J. *Angew. Chem., Int. Ed. Engl.* **1997**, *36*, 611-613.
- 13 Jarosz, S.; Listkowski, A. *Current Org. Chem.* **2006**, *10*, 643-662.
- 14 *Cell Signalling*, Hancock, J. T., Oxford University Press, **2005**.
- 15 Potter, B. V. L.; Lampe, D. *Angew. Chem., Int. Ed. Engl.* **1995**, *34*, 1933-1972.
- 16 *Phosphoinositides: Chemistry, Biochemistry and Biomedical Applications*, Bruzik, K. S. Ed., ACS Symposium Series 718, Washington DC.
- 17 (a) Ferguson, M. A. J.; Low, M.G.; Cross, G. A. M. *J. Biol. Chem.* **1985**, *260*, 14547-14555. (b) Thomas, J. R.; Dwek, R. A.; Rademacher, T. W. *Biochemistry* **1990**, *29*, 5413-5422. (c) Roberts, C.; Madson, R.; Fraser-Reid, B. *J. Am. Chem. Soc.* **1995**, *117*, 1546-1553.
- 18 Sahai, P.; Vishwakarma, R. A. *J. Chem. Soc., Perkin Trans. I* **1997**, 1845-1849.
- 19 Liang, C.; Ewig, C. S.; Stouch, T. R.; Hagler, A. T. *J. Am. Chem. Soc.*, **1994**, *116*, 3904-3911.
- 20 Parthasarathy, R.; Eisenberg, F. *Biochem. J.* **1986**, *235*, 313-322.
- 21 Nomenclature committee – IUB, *Biochem. J.* **1989**, *258*, 1-2.
- 22 Mills, J. A. *Biochem. Biophys. Res. Commun.* **1961-62**, *6*, 418-421.
- 23 Angyal, S. J.; Greeves, D.; Pickles, V. A. *Carbohydr. Res.* **1974**, *35*, 165-173.
- 24 Angyal, S. J.; Hickman, R. J. *Aust. J. Chem.* **1975**, *28*, 1279-1287.
- 25 Angyal, S. J.; Greeves, D. *Aust. J. Chem.* **1976**, *29*, 1223-1230.
- 26 Angyal, S. J.; Littlemore, L.; Gorin, P. A. *J. Aust. J. Chem.* **1985**, *38*, 411-418.

-
- 27 (a) Grasdalen, H.; Anthonsen, T.; Harbitz, O.; Larsen, B.; Smidsroed, O. *Acta Chem. Scand., Ser. A*, **1978**, A32, 31-39, CA on CD 89:43994. (b) Inagaki, F.; Miyazawa, T. *Progr. Nucl. Magn. Reson. Spectrosc.* **1981**, 14, 67-111. (c) Peters, J. A.; Kieboom, A. P. G. *Recl. Trav. Chim. Pays-Bas*, **1983**, 102, 381-392.
- 28 Morgenstern, B.; Kutzky, B.; Neis, C.; Stucky, S.; Hegetschweiler, K.; Garribba, E.; Micera, G. *Inorg. Chem.* **2007**, 46, 3903-3915.
- 29 Hancock, R. D.; Hageitschweiler, K. *J. Chem. Soc., Dalton Trans.* **1993**, (14), 2137-2140.
- 30 Zheng, Y.-J.; Ornstein, R. L.; Leary, J. A. *THEOCHEM*, **1997**, 389, 233-240.
- 31 Yang, L.; Wang, Z.; Zhao, Y.; Tian, W.; Xu, Y.; Weng, S.; Wu, J. *Carbohydr. Res.*, **2000**, 329, 847-853.
- 32 Schlewer, G.; Guedat, P.; Ballereau, S.; Schmitt, L.; Spiess, B. American Chemical Society, *ACS Symp. Ser. 718 (Phosphoinositides)*, **1999**, 255-270.
- 33 Dozol, H.; Blum-Held, C.; Guédât, P.; Maechling, C.; Lanners, S.; Schlewer, G.; Spiess, B. *J. Mol. Str.* **2002**, 643, 171-181.
- 34 (a) Ebstein, R. P.; Lerer, B.; Bennet, E. R.; Shapira, B.; Kindler, S.; Shemesh, Z.; Gerstenhaber, N. *Psychiatry. Res.* **1988**, 24, 45-52. (b) Emilien, G.; Maloteaux, J. M.; Seghers, A.; Charles, G. *Arch. Int. Pharmacodyn. Ther.* **1995**, 330, 251-278. (c) Divish, M. M.; Sheftel, G.; Boyle, A.; Kalasapudi, V. D.; Papolos, D. F.; Lachman, H. M. *J. Neurosci. Res.* **1997**, 28, 40-48. (d) Dixon, J. F. *Proc. Natl. Acad. Sci., USA*, **1997**, 94, 4757-4760.
- 35 Bieth, H.; Schlewer, G.; Spiess, B. *J. Inorg. Biochem.* **1990**, 39, 59-73.
- 36 Bieth, H.; Schlewer, G.; Spiess, B. *J. Inorg. Biochem.* **1991**, 41, 37-44.

-
- 37 Lapp, C.; Spiess, B. *J. Inorg. Biochem.* **1991**, *42*, 257-266.
- 38 Schmitt, L.; Schlewer, G.; Spiess, B. *J. Inorg. Biochem.* **1992**, *45*, 13-19.
- 39 Mernissi-Arifi, K.; Bieth, H.; Schlewer, G.; Spiess, B. *J. Inorg. Biochem.* **1995**, *57*, 127-133.
- 40 Mernissi-Arifi, K.; Imbs, I.; Schlewer, G. Spiess, B. *Biochimica et Biophysica Acta (BBA) - General Subjects.* 1996, *1289*, 404-410.
- 41 Mernissi-Arifi, K.; Wehrer, C.; Schlewer, G.; Spiess, B. *J. Inorg. Biochem.* **1994**, *55*, 263-277.
- 42 Persson, H.; Tüerk, M.; Nyman, M.; Sandberg, A-S. *J. Agric. Food Chem.* **1998**, *46*, 3194-3200.
- 43 Xu, P.; Price, J.; Wise, A.; Aggett, P. J. *J. Inorg. Biochem.* **1992**, *47*, 119-130.
- 44 Rodrigues-Filho, U. P.; Vaz, S. Jr.; Felicissimo, M. P.; Scarpellini, M.; Cardoso, D. R.; Vinhas, R. C.J.; Landers, R.; Schneider, J. F.; McGarvey, B. R.; Andersen, M. L.; Skibsted, L. H. *J. Inorg. Biochem.* **2005**, *99*, 1973-1982.
- 45 Torres, J.; Veiga, N.; Gancheff, J. S.; Domínguez, S.; Mederos, A.; Sundberg, M.; Sánchez, A.; Castiglioni, J.; Díaz, A.; Kremer, C. *J. Mol. Str.* (In press, corrected proof, available online 25 March **2007**) doi:10.1016/j.molstruc.2007.03.035.
- 46 De Stefano, C.; Milea, D.; Pettignano, A.; Sammartano, S. *Anal. Bioanal. Chem.* **2003**, *376*, 1030-1040.
- 47 Mayr, G. W. *Methods Inositide Res.* 83-108. Ed. Irvine, Robin F. Raven: New York, N. Y. **1990**.
- 48 Šala, M.; Kolar, J.; Strlič, M.; Kočevár, M. *Carbohydr. Res.* **2006**, *341*, 897-902.
- 49 Matsumura, K.; Komiyama, M. *J. Inorg. Biochem.* **1994**, *55*, 153-156.

-
- 50 Larner, J.; Price, J. D.; Heimark, D.; Smith, L.; Rule, G.; Piccariello, T.; Fonteles, M. C.; Pontes, C.; Vale, D.; Huang, L. *J. Med. Chem.* **2003**, *46*, 3283-3291.
- 51 (a) Weitzel, F. L.; Raymond, K. N. *J. Org. Chem.* **1981**, *46*, 5234-5237. (b) Kappel, M. J.; Pecoraro, V. L.; Raymond, K. N. *Inorg. Chem.* **1985**, *24*, 2447-2452. (c) Miller, M. J.; Malouin, F. *Acc. Chem. Res.* **1993**, *26*, 241-249.
- 52 Angyal S. J. *Carbohydr. Res.* **2000**, *325*, 313-320.
- 53 Volpp, G.; Tamm, C. *Helv. Chim. Acta* **1957**, *40*, 1860-1865.
- 54 Paquette, L. A.; Tae, J.; Branan, B. M.; Eisenberg, S. W. E.; Hofferberth, J. E. *Angew. Chem., Int. Ed.* **1999**, *38*, 1412-1414.
- 55 Paquette, L. A.; Tae, J.; Hickey, E. R.; Trego, W. E.; Rogers, R. D. *J. Org. Chem.* **2000**, *65*, 9160-9171.
- 56 Tae, J.; Rogers, R. D.; Paquette, L. A. *Org. Lett.* **2000**, *2*, 139-142.
- 57 (a) Paquette, L. A., Tae, J., Gallucci, J. C. *Org. Lett.* **2000**, *2*, 143-146. (b) Paquette, L. A.; Tae, J. *J. Am. Chem. Soc.* **2001**, *123*, 4974-4984.
- 58 Paquette, L. A.; Ra, C. S.; Gallucci, J. C.; Kang, H-J.; Ohmori, N.; Arrington, M. P.; David, W.; Brodbelt, J. S. *J. Org. Chem.* **2001**, *66*, 8629-8639.
- 59 Sureshan, K. M.; Shashidhar, M. S.; Varma, A. J. *J. Chem. Soc., Perkin Trans. 2* **2001**, 2298-2302.
- 60 Sureshan, K. M.; Shashidhar, M. S.; Varma, A. J. *J. Org. Chem.* **2002**, *67*, 6884-6888.
- 61 Paquette, L. A.; Selvaraj, P. R.; Keller, K. M.; Brodbelt, J. S. *Tetrahedron* **2005**, *61*, 231-240.
- 62 Hilmey, D. G.; Paquette, L. A. *J. Org. Chem.* **2004**, *69*, 3262-3270.

-
- 63 McGarvey, G. J.; Stepanian, M. W.; Bressette, A. R.; Sabat, M. *Org. Lett.* **2000**, *2*, 3453–3456.
- 64 Kesel, A. J. *Bioorg. Med. Chem.* **2003**, *11*, 4599-4613.
- 65 Kim, T-H.; Holmes, A. B. *J. Chem. Soc., Perkin Trans. 1* **2001**, 2524-2525.
- 66 (a) Lo, Y.-S.; Zhu, Y.-J.; Beebe, T. P. *Langmuir* **2001**, *17*, 3741–3748. (b) Touhami, A.; Hoffmann, B.; Vasella, A.; Denis, F. A.; Dufrêne, Y. F. *Langmuir* **2003**, *19*, 1745–1751.
- 67 Lee, N-Y.; Jang, W-J.; Yu, S-H.; Im, J.; Chung, S-K. *Tetrahedron Lett.* **2005**, *46*, 6063-6066.
- 68 (a) Ranganathan, R. S.; Fernandez, M. E.; Kang, S. I.; Nunn, A. D.; Ratsep, P. C.; Pillai, K. M. R.; Zhang, X.; Tweedle, M. F. *Investigative Radiology*, **1998**, *33*, 779-797. (b) Caravan, P.; Ellison, J. J.; McMurry, T. J.; Lauffer, R. B. *Chem. Rev.* **1999**, *99*, 2293-2352. (c) Tang, H-A.; Sheng, Y.; Yang, R-D. *Inorg. Chem. Commun.* **2003**, *6*, 1213-1216.
- 69 Hosoda, A.; Kobayashi, S.; Nomura, E.; Miyake, Y.; Nasaka, N.; Kozaki, Y.; Taniguchi, H. Kenkyu Hokoku - Wakayama-ken Kogyo Gijutsu Senta, Volume Date **2001**, 20-22, (Japanese) 2002. CA on CD (**2004**) 140:375390.
- 70 Falshaw, A.; Gainsford, G. J.; Lensink, C.; Slade, A. T.; Wright, L. J. *Polyhedron* **2007**, *26*, 329-337.
- 71 Akiyama, T.; Hara, M.; Fuchibe, K.; Sakamoto, S.; Yamaguchi, K. *Chem. Commun.* **2003**, 1734-1735.
- 72 Hegetschweiler, K. *Chem. Soc. Rev.* **1999**, *28*, 239-249.

-
- 73 Hegetschweiler, K.; Hancock, R. D.; Ghisletta, M.; Kradolfer, T.; Gramlich, V.; Schmalte, H. W. *Inorg. Chem.* **1993**, *32*, 5273-5284.
- 74 Hegetschweiler, K.; Gramlich, V.; Ghisletta, M.; Samaras, H. *Inorg. Chem.* **1992**, *31*, 2341-2346.
- 75 Hegetschweiler, K.; Ghisletta, M.; Faessler, T. F.; Nesper, R.; Schmalte, H. W.; Rihs, G. *Inorg. Chem.* **1993**, *32*, 2032-2041.
- 76 Hegetschweiler, K.; Egli, A.; Herdtweck, E.; Herrmann, W. A.; Alberto, R.; Gramlich, V. *Helv. Chim. Acta* **2005**, *88*, 426-434.
- 77 (a) Ghisletta, M.; Hegetschweiler, K.; Jalett, H-P.; Gerfin, T.; Gramlich, V. *Helv. Chim. Acta* **1992**, *75*, 2233-2242. (b) Kradolfer, T.; Hegetschweiler, K. *Helv. Chim. Acta* **1992**, *75*, 2243-2251. (c) Hegetschweiler, K.; Finn, R. C.; Rarig, R. S., Jr.; Sander, J.; Steinhäuser, S.; Worle, M.; Zubieta, J. *Inorg. Chim. Acta* **2002**, *337*, 39-47.
- 78 Jancsó, A.; Mikkola, S.; Lönnberg, H.; Hegetschweiler, K.; Gajda, T. *Chem. Euro. J.* **2003**, *9*, 5404-5415.
- 79 Azev, V. N.; d'Alarcao, M. *J. Org. Chem.* **2004**, *69*, 4839-4842.
- 80 Billington, D. C.; Baker, R.; Kulagowski, J. J.; Mawer, I. M.; Vacca, J. P.; deSolms, S. J.; Huff, J. R. *J. Chem. Soc., Perkin Trans 1* **1989**, 1423-1429.
- 81 Sureshan, K. M.; Shashidhar, M. S. *Tetrahedron Lett.* **2000**, *41*, 4185-4188.
- 82 Sureshan, K. M.; Shashidhar, M. S. *Tetrahedron Lett.* **2001**, *42*, 3037-3039.
- 83 Lee, H. W.; Kishi, Y. *J. Org. Chem.* **1985**, *50*, 4402-4404.
- 84 Banerjee, T.; Shashidhar M. S. *Tetrahedron Lett.* **1994**, *35*, 8053-8056.

-
- 85 Sureshan, K. M.; Das, T.; Shashidhar, M. S.; Gonnade, R.G.; Bhadbhade, M. M. *Eur. J. Org. Chem.* **2003**, 1035-1041.
- 86 Praveen, T.; Das, T.; Sureshan, K. M.; Shashidhar, M. S.; Samanta, U.; Pal, D.; Chakrabarti, P. *J. Chem. Soc., Perkin Trans. 2* **2002**, 358-365.
- 87 Gilbert, I. H.; Holmes, A. B.; Pestchanker, N. J.; Young, R. C. *Carbohydr. Res.* **1992**, 234, 117-130.
- 88 Gilbert, I. H.; Holmes, A. B.; Young, R. C. *Tetrahedron Lett.* **1990**, 31, 2633-2634.
- 89 Yeh, S-M.; Lee, G. H.; Wang, Y.; Luh, T-Y. *J. Org. Chem.* **1997**, 62, 8315-8318.
- 90 Falck, J. R.; Barma, D. K.; Venkataraman, S. K.; Baati, R.; Mioskowski, C. *Tetrahedron Lett.* **2002**, 43, 963-966.
- 91 Serrano, P.; Llebaria, A.; Vázquez, J.; de Pablo, J.; Anglada, J. M.; Delgado, A. *Chem. Eur. J.* **2005**, 11, 4465-4472.
- 92 An Serrano, P.; Llebaria, A.; Delgado, A. *J. Org. Chem.* **2002**, 67, 7165-7167.
- 93 Santoro, M.; Caffaratti, E.; Salas-Peregrin, J. M.; Korecz, L.; Rockenbauer, A.; Sala, L. F.; Signorella, S. *Polyhedron* **2007**, 169-177.
- 94 Jr. Gray, C. W.; Johnson, L. L.; Walker, B. T.; Sleevi, M. C.; Campbell, A. S.; Plourde R.; Houston, T. A. *Bioorg. Med. Chem. Lett.* **2005**, 15, 5416-5418.

PART-B

Chapter 1

Synthesis and metal ion binding studies of *myo*-inositol derived crown ethers.

Section 1: Metal ion binding studies with *myo*-inositol derived crown-4-ethers.

Once you start a working on something, don't be afraid of failure and don't abandon it.

People who work sincerely are the happiest.

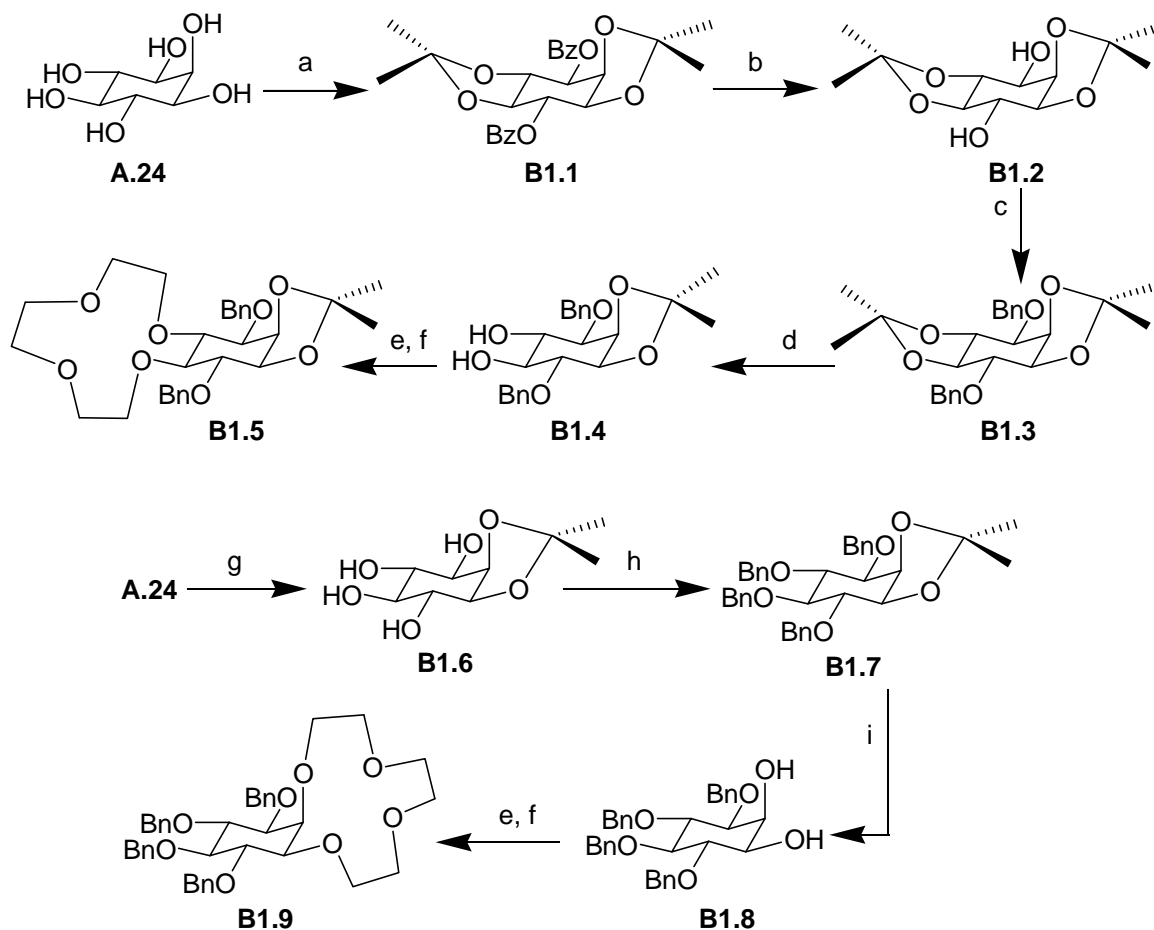
-Chanakya (Indian politician, strategist and writer, 350 BC-275 BC)

1.1 Introduction

As evident from the discussion presented in Part A of this thesis, there are very few reports on systematic studies involving *myo*-inositol derived neutral metal complexing agents. Earlier work in our laboratory had shown that some *myo*-inositol based podands¹ and crown ethers² bind silver ions preferentially. Most of these complexing agents contained five or six oxygen atoms capable of ligating metal ions and some of these ligands bound lithium picrate moderately well. In view of the contemporary interest in studies related to neutral complexing agents specific for lithium ions,³ we undertook the preparation of *myo*-inositol derived crown-4 ethers and evaluation of their ability to bind with metal picrates. Also, the fact that different regioselectivities are observed during *O*-alkylation,^{4,5} *O*-acylation,⁶ *O*-sulfonylation,⁷ and transesterification⁶ reactions of *myo*-inositol 1,3,5-orthoformate and its derivatives, on using reagents containing sodium and lithium ions, as well as the ability of lithium to inhibit the activity of *myo*-inositol-1-phosphate phosphatase⁸ which has been implicated for the therapeutic effect of lithium in its use as a drug for manic depression,⁹ prompted us to prepare *myo*-inositol derived crown ethers and investigate their binding to lithium. Accordingly the present section deals with the preparation and metal ion binding study of *myo*-inositol derived crown-4-ethers. Simple crown-4 ethers and their analogs have been tested earlier for their specificity for binding to lithium ions¹⁰ and it is well known that lithium ions bind better to crown-4 ethers as compared to larger crown ethers.

1.2 Results and discussion

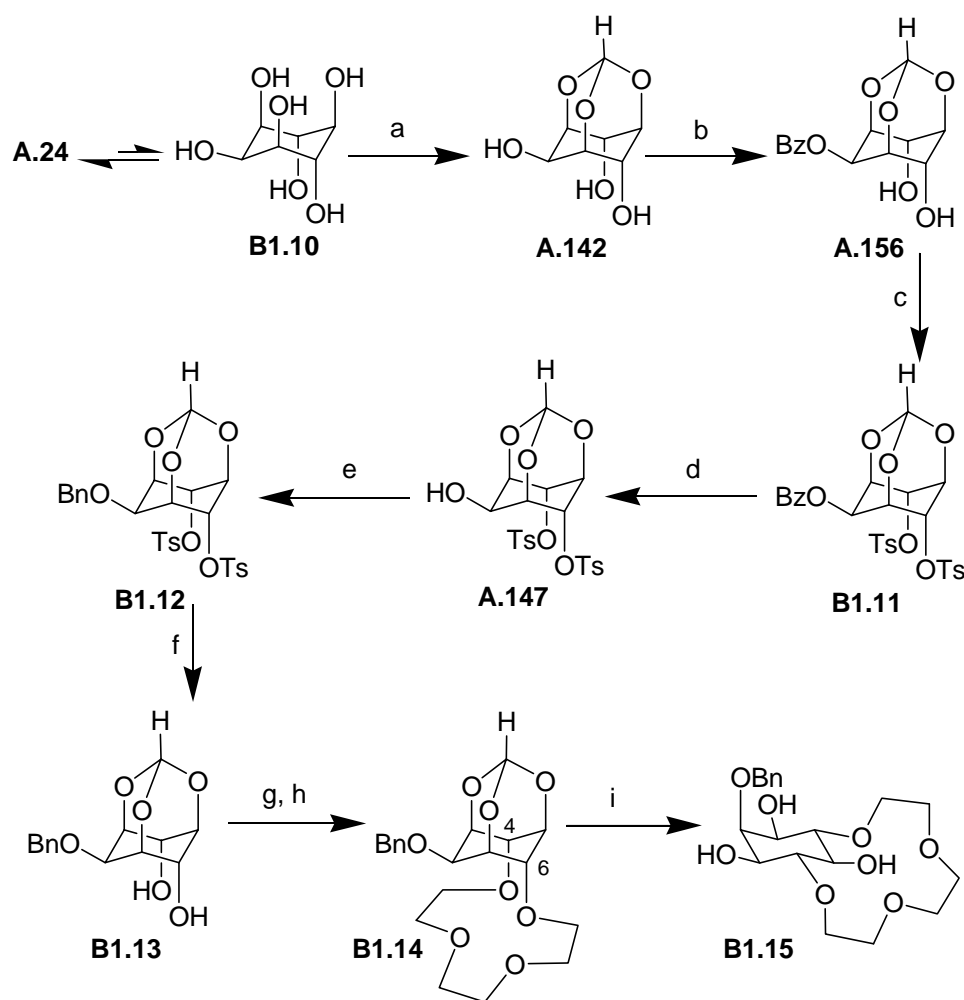
The *myo*-inositol-derived crown ethers¹¹ (**B1.5**, **B1.9**, **B1.14**, Scheme B1.1 and B1.2) were prepared by the reaction of the diols **B1.4**, **B1.8** and **B1.13** with



SCHEME B1.1. *Reagents and Conditions:* (a) (i) DMF, 2,2'-dimethoxypropane, TsOH, 100 °C, 2 h, Et₃N; (ii) pyridine, BzCl, 2 h, 32%; (b) MeOH, NaOH, reflux, 30 min, 2% HCL, 90%; (c) DMF, NaH, BnBr, 0 °C to rt, 15 min, 96%; (d) acetone:water (40:1), TsOH (cat), 45 min, rt, 52%; (e) THF, NaH, TsO(CH₂CH₂O)₃Ts, reflux, 24 h; (f) MeOH, NaOMe, reflux, 8 h, 36% (for **B1.5**), 28% (for **B1.9**); (g) DMSO, 2,2'-dimethoxypropane, TsOH, 110 °C, 4 h, 70%; (h) DMF, NaH, BnBr, 0 °C to rt, 20 h, 75%; (i) acetic acid:water (4:1), 100 °C, 3 h, 73%.

triethyleneglycol ditosylate, in the presence of sodium hydride. The diols **B1.4**¹², **B1.8**¹³ and **B1.13**⁷ were prepared from commercially available *myo*-inositol (**A.24**), by methods reported in the literature. The crown ethers **B1.5**, **B1.9** and **B1.14** could not be easily

separated from unreacted triethyleneglycol ditosylate by column chromatography. Hence the crude product obtained was refluxed with sodium methoxide in methanol to convert the unreacted triethyleneglycol ditosylate to the corresponding dimethyl ether, from which the required crown ethers were separable. Yield of the crown-4-ethers (from the respective diol) was in the range 24-36%; this is lower than the yields reported² for *myo*-inositol derived crown-5 and crown-6 ethers (63-98%). Yields ranging from 1% to 99% for the preparation of crown-4 ethers have been reported in the literature.^{10g,10h,14}



SCHEME B1.2. Reagents and Conditions: (a) DMF, triethylorthoformate, TsOH, 100 °C, 3 h; (b) pyridine, BzCl, 12 h, 94%; (c) pyridine, TsCl, 80 °C, 24 h, 97%; (d) *i*-BuNH₂,

MeOH, reflux, 6 h. 98%; (e) DMF, BnBr, NaH, 0 °C to rt, 10 min, 86%; (f) Mg turnings, THF: MeOH (1:3), rt, 12 h, 91%; (g) THF, NaH, TsO(CH₂CH₂O)₃Ts, reflux, 24 h; (h) MeOH, NaOMe, reflux, 8 h. 24%; (i) TFA: H₂O (3:2, 8 mL), rt, 5 h, 87%.

We also attempted to use lithium hydride as a base for the preparation of the crown-4 ether **B1.14** to see if the use of lithium ions during the reaction of an inositol derived diol with triethyleneglycol ditosylate would improve the yield of the crown-4 ethers. Reaction of **B1.13** with triethyleneglycol ditosylate in the presence of lithium hydride in THF failed to give the crown ether **B1.14**. The same reaction however could be carried out in DMF at room temperature to obtain **B1.14** (30%), but the yield did not improve. Crystals of the crown-4-ether **B1.14**, suitable for single crystal X-ray diffraction (Figure B1.1), could be obtained on slow evaporation of a cold (5-10 °C) methanol solution over several weeks. From X-ray structure of **B1.14** cavity size of the ionophoric ring could be estimated.^{10e} Our attempts to obtain crystals of **B1.5** and **B1.9** failed.

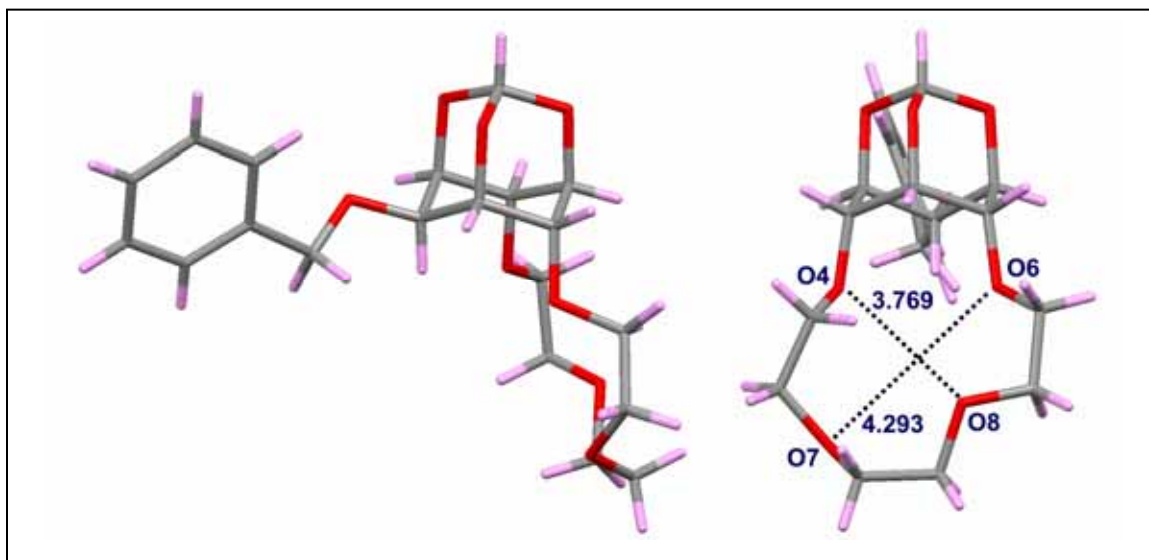


FIGURE B1.1. Views of a molecule of **B1.14** in its crystals showing the cavity (0.729 Å × 1.253 Å, van der Waals radius for O is 1.52 Å) in the crown ether.

We also obtained the crown-4-ether triol (**B1.15**, Scheme B1.2) by cleavage of the orthoformate in the crown-4 ether **B1.14**. We were able to obtain good quality crystals of **B1.15** for single crystal X-ray diffraction studies (Figure B1.2) by the slow evaporation of a methanol solution at ambient temperature.

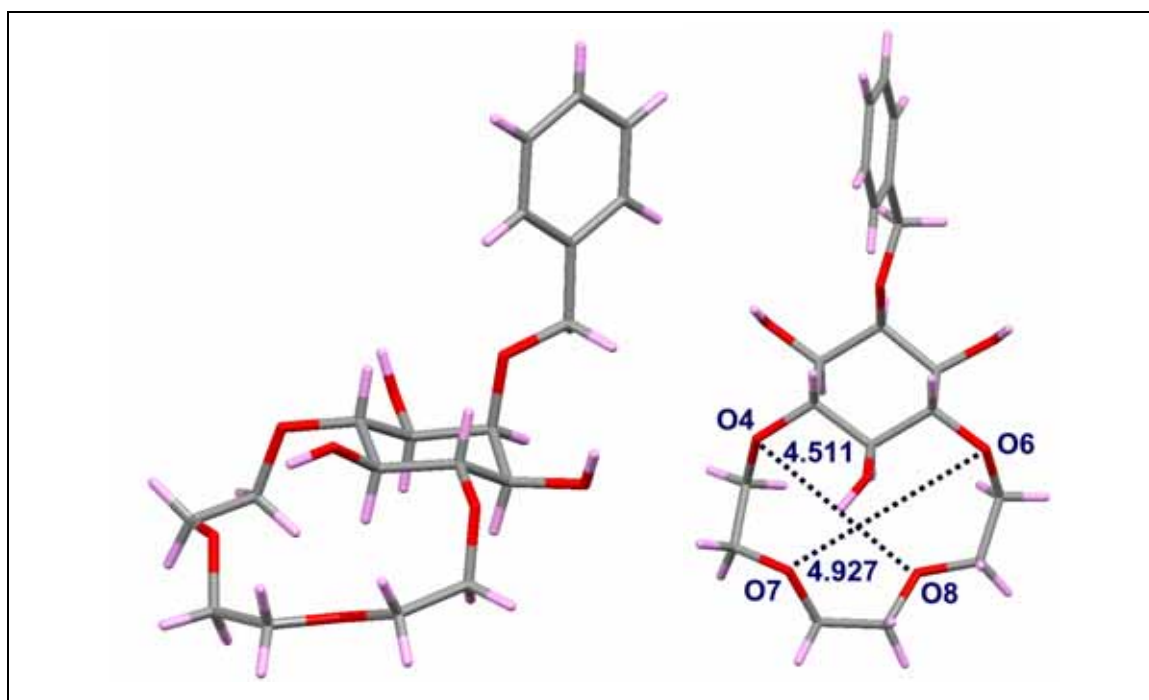
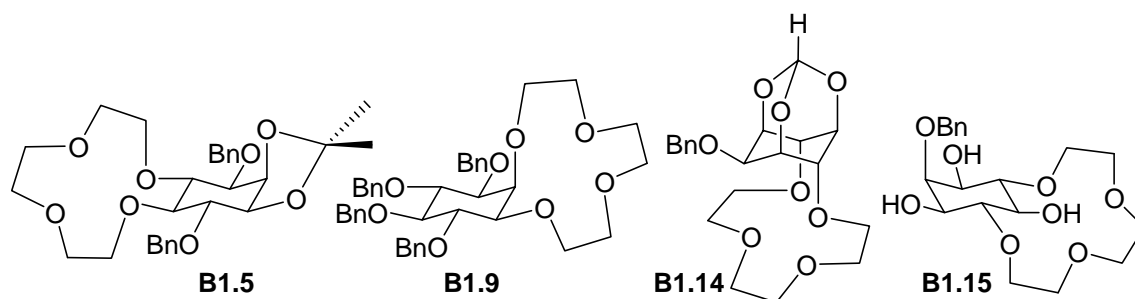


FIGURE B1.2. Views of a molecule of **B1.15** in its crystals showing the cavity ($1.471 \text{ \AA} \times 1.887 \text{ \AA}$, van der Waals radii for O is 1.52 \AA) in the crown ether.

In crown-4-ethers **B1.5**, **B1.9** and **B1.14**, two of the oxygen atoms in the ionophoric ring have varying relative orientations (1,2-diequatorial in **B1.5**, 1,2-axial-equatorial in **B1.9**, 1,3-diaxial in **B1.14**), as they are part of the *myo*-inositol ring. Furthermore, while **B1.5** and **B1.9** are 12-crown-4 systems, **B1.14** can be considered as a 13-crown-4 system or a 15-crown-4 system, since the crown ether is part of a cage like system. Although the rings are larger, the distance between the two axial oxygen atoms

(C4- and C6-) in the crown ether **B1.14** is less than that between any two oxygen atoms in the crown ethers **B1.5** and **B1.9**. The association constants (Table B1.1) of crown-4 ethers **B1.5**, **B1.9**, **B1.14** and **B1.15** with alkali metal picrates as well as ammonium and silver picrates, were evaluated by Cram's picrate method.¹⁵ For the calculation of the association constants shown in Table B1.1 we have assumed the formation of 1:1 complexes with all cations.

TABLE B1.1: Association constants ($K_a \times 10^{-4} \text{ dm}^3 \text{ mol}^{-1}$) in CDCl_3 for the binding of crown-4-ethers **B1.5**, **B1.9**, **B1.14** and **B1.15** with metal picrates at 27 °C.



Crown ether	Li^+	Na^+	K^+	Cs^+	NH_4^+	Ag^+
B1.5	100	25.4	6.27	20.2	2.96	14.4
B1.9	19.9	3.95	0.97	2.12	3.97	15.9
B1.14	27.2	2.96	0.69	0.62	0.21	0.9
B1.15	35.62	2.09	1.30	5.83	1.82	2.87

From the Table B1.1, it is seen that all the four *myo*-inositol derived crown-4-ethers exhibit the highest binding constant for lithium picrate (among the picrates tested) as expected. Among the four crown ethers, the crown ether **B1.5** derived from the

diequatorial diol **B1.4** binds lithium picrate best. Lithium picrate binds better to inositol based crown-4-ethers when compared to 12-crown-4-ether ($K_a = 1.6 \times 10^4$).¹⁶

TABLE B1.2: Ratio of association constants: lithium picrate to other picrates for *myo*-inositol derived crown-4-ethers.

Ratio	Li ⁺ /Na ⁺	Li ⁺ /K ⁺	Li ⁺ /Cs ⁺	Li ⁺ /NH ₄ ⁺	Li ⁺ /Ag ⁺
B1.5	4	16	5	34	7
B1.9	5	20	9	5	1
B1.14	9	40	44	130	30
B1.15	17	27	6	20	12

The magnitude of the preference of individual crown ethers for binding to a metal ion (M₁) among a group of 'n' metal ions can be estimated by the ratio of association constants (K_{M_1} / K_{M_n}), for binding to the same crown ether. The ratio of the binding constants for lithium picrate to that of other metal picrates (Table B1.2) shows that the crown ether **B1.14**, having 1,3-diaxial orientation exhibits the highest selectivity for lithium as compared to other metal picrates, (except between lithium and sodium, for which the selectivity is better for **B1.15**). It is pertinent to note that although all the crown ethers have four oxygen atoms in the ionophoric ring, in the di-equatorial (**B1.5**) and axial-equatorial (**B1.9**) crown ethers all the oxygen atoms are separated by two carbon atoms, whereas, in the di-axial crown ether (**B1.14**), oxygen atoms attached to the inositol ring (at C-4 and C-6) are separated by three carbon atoms, but are closer to each other

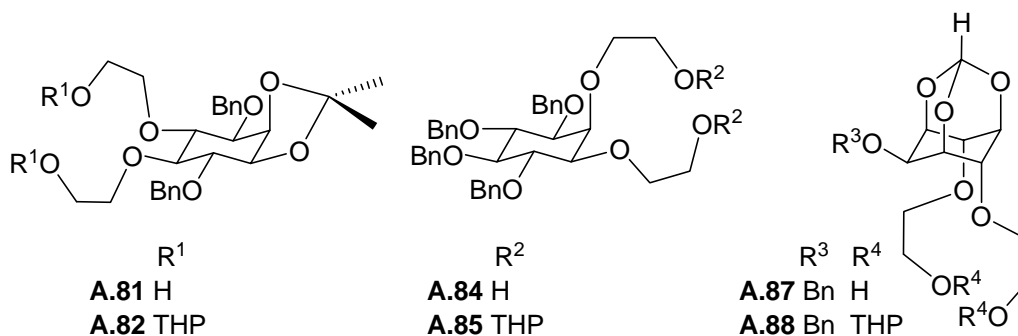
due to their di-axial disposition. Interestingly, these differences lead to better selectivity for binding to lithium picrate.

TABLE B1.3: Ratio of association constants between crown-4-ethers having different stereochemistry.

Ratio	Li ⁺	Na ⁺	K ⁺	Cs ⁺	NH ₄ ⁺	Ag ⁺
B1.5/ B1.9	5	6	6	10	0.7	0.9
B1.5/ B1.14	4	9	9	33	14	16
B1.5/ B1.15	3	12	5	3	2	5
B1.9/ B1.14	0.7	1	1	3	19	18
B1.15/ B1.14	1	0.7	2	9	9	3

A comparison of the ratio of association constants between crown-4-ethers having different relative orientations (Table B1.3) of the two of the oxygen atoms (attached to the inositol ring) reveals that this difference matters most for the binding of cesium ions ($K_{a(B1.5)} / K_{a(B1.14)} = 33$).

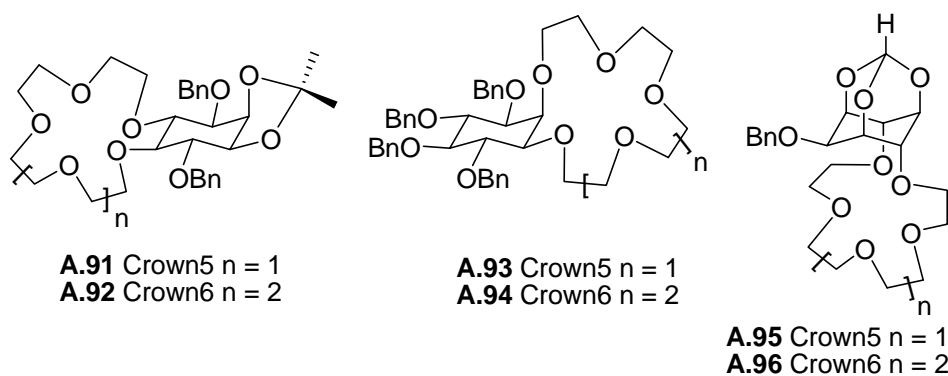
The metal picrate binding characteristics of a few *myo*-inositol-derived podands (Table B1.4), which are open chain analogs of crown-4-ethers have earlier been reported.¹ Table B1.4 shows the ratio of binding constants between the *myo*-inositol derived crown-4-ethers and the corresponding podands. An increase in the value of the association constants on going from podands to crown ethers indicates the contribution of the ionophoric ring towards the binding of metal picrates.

TABLE B1.4: Ratio of association constants between crown-4-ethers and podands.¹

Ratio	Li^+	Na^+	K^+	Cs^+	NH_4^+	Ag^+
B1.5/ A.81^a	42.79	----	20.16	375	19.47	3.56
B1.5/ A.82	4.79	14.86	12.93	77.7	5.14	1.96
B1.9/ A.84	3.77	12.19	2.22	13.93	21.81	1.41
B1.9/ A.85	0.90	7.88	1.55	3.77	23.63	1.39
B1.14/ A.87	11.67	42.28	---	---	26.25	0.71
B1.14/ A.88	1.32	1.99	1.21	4.08	0.73	0.63

^a For association constants of podands **A.81**, **A.82**, **A.84**, **A.85**, **A.87** and **A.88** with metal picrates see Table B1.13, Section 3, page 118.

The metal picrate extraction ability of crown-4 ethers is not very different from those of podands with a THP ether end group. This is perhaps because the THP ether podands contain six oxygen atoms (two more than the crown-4 ethers) capable of ligation to the metal ions, which could augment binding of metal ions.

TABLE B1.5: Ratio of association constants between the *myo*-inositol derived crown ethers.²

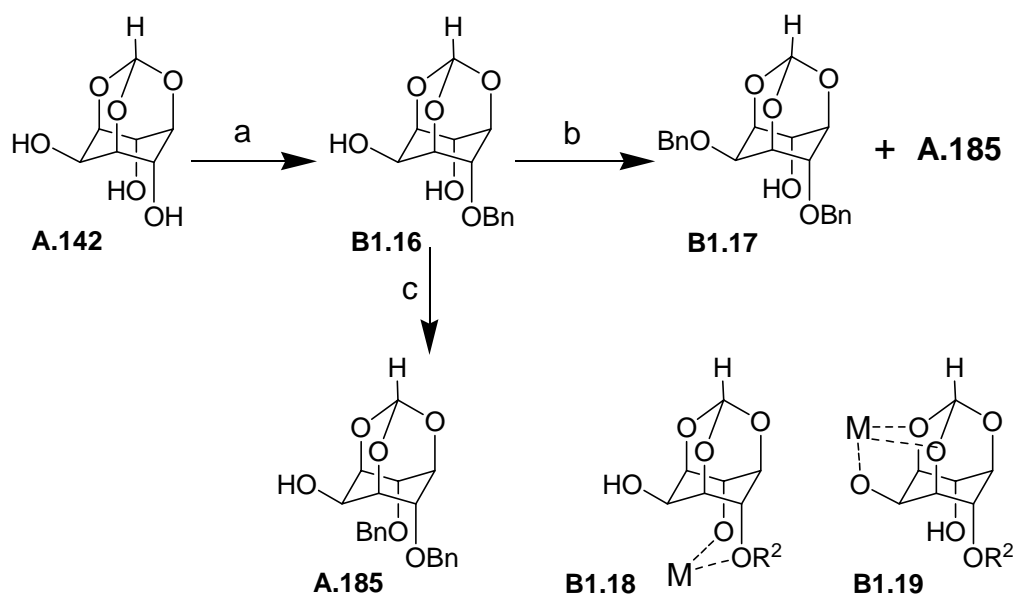
Stereochemistry	Ratio	Li ⁺
1,2-diequatorial	B1.5/ A.91^a	10
	B1.5/ A.92	21
1,2-axial-equatorial	B1.9/ A.93	2
	B1.9/ A.94	1
1,3-diaxial	B1.14/ A.95	2
	B1.14/ A.96	3

^aFor association constants of crown ethers **A.91** - **A.96** with metal picrates see Table B1.14, Section 3, page 119.

It is pertinent to compare the lithium picrate binding ability of crown-4 ethers with *myo*-inositol-derived crown-5 and crown-6 ethers (Table B1.5), which were earlier reported from our laboratory.² Table B1.5 shows the ratio of binding constants between the crown-4 ethers and the corresponding crown-5 ethers and crown-6 ethers. All the crown ethers being compared have the same relative stereochemistry of the crown ether

ring and the other hydroxyl protecting groups. This comparison reveals that the effect of the crown ether ring size for the binding of lithium picrate matters most in the case of the crown ethers (**B1.5**, **A.91**, and **A.92**) derived from the diequatorial diol **B1.4**. In the case of crown ethers derived from axial-equatorial diols (**B1.9**, **A.93**, and **A.94**) and di-axial diols (**B1.14**, **A.95**, and **A.96**), the size of the crown ether does not seem to matter for the binding of lithium picrate.

The observed trend in the extraction of the metal picrates by inositol-derived crown-4-ethers, especially for lithium, is interesting with regard to the experimentally observed regioselectivity for the sodium hydride and butyllithium (Scheme B1.3) assisted *O*-alkylation of *myo*-inositol orthoesters.¹⁷



SCHEME B1.3. Reagents and Conditions: (a) DMF, NaH (1 eq.), BnBr (1 eq.); (b) DMF, NaH (2 eq.), BnBr (2 eq.); (c) DMF, LiH or BuLi, BnBr.

Reaction of the triol (**A.142**) with alkyl halides⁹ in the presence of one equivalent of sodium hydride is known to result in exclusive reaction at the C4(6)-*O*-position to yield the monobenzyl ether **B1.16**; further reaction of the diol **B1.16** with alkyl halides in

the presence of sodium hydride results in the formation of a mixture of isomeric ethers **B1.17** and **A.185**⁴ (benzylation is shown as an example in Scheme B1.3). Alkylation of other *myo*-inositol orthoesters follows the same trend. However, benzylation of the diol **B1.16** using butyllithium or lithium hydride¹⁷ as the base instead of sodium hydride, resulted in the exclusive formation of the symmetrical dibenzyl ether **A.185**. *O*-alkylation of the monoether **B1.16** in the absence of metal ions is known to provide the unsymmetrical diether **B1.17** as the major product.¹⁸ The fact that the reaction assisted by lithium hydride or butyllithium gave the diether **A.185** as the major product was attributed to better chelation of lithium ions (as compared to sodium ions) by the 4,6-diaxial oxygen atoms resulting in relatively higher stability of the chelate **B1.18** (as compared to **B1.19**, also see Part A, page 47). The observed metal ion selectivity in picrate extraction studies (Table B1.2) i.e. better selectivity for the binding of lithium exhibited by the 1,3-diaxial crown-4 ether **B1.14** as compared to crown-4 ethers with other relative orientations strongly compliments the observed regioselectivity and supports the involvement and importance of chelates during *O*-alkylation of *myo*-inositol orthoesters.

1.3 Conclusions

myo-Inositol derived crown-4-ethers in which two of the oxygen atoms in the crown ether moiety had different relative orientations were prepared. Metal picrate binding studies revealed that the crown ether having 1,3-diaxial orientation shows the highest selectivity for binding to lithium although the crown ether having 1,2-diequatorial orientation exhibited the highest binding constant for lithium picrate. These results imply that relative binding affinity of metal ions to crown ethers can be tuned by varying the relative orientation of crown ether oxygen atoms. A comparison of the metal picrate binding characteristics of inositol derived crown-4-ethers shows that although the strength of binding of metal picrates to these crown ethers could depend on various factors, the selectivity of binding of metal ions can be modulated by reducing the flexibility of the crown ether oxygen atoms and the distance between them. The results presented in this section also complement the observed variation in regioselectivity for the *O*-substitution reactions of *myo*-inositol 1,3,5-orthoesters in the presence of different metal ions and support the involvement of chelates during these reactions.

**Section 2: Inositol derived crown ethers: effect of
auxiliary protecting groups on their metal ion binding
ability.**

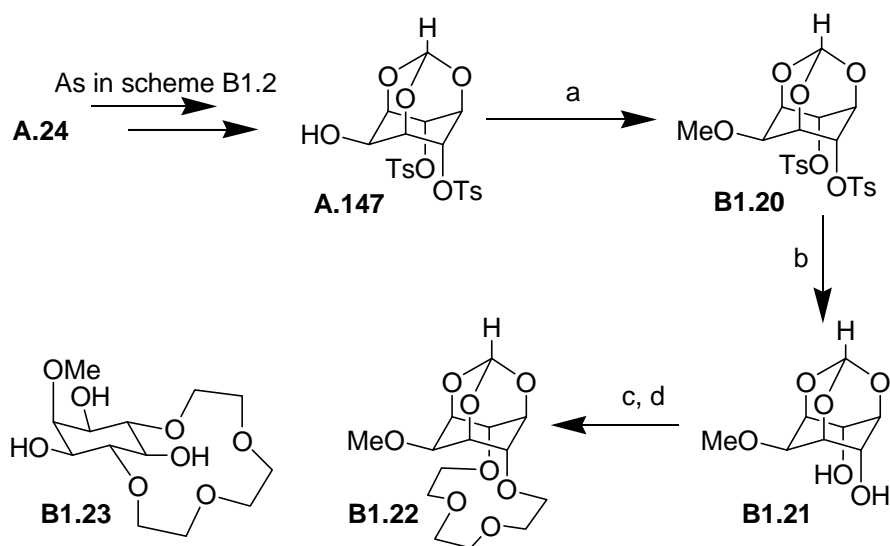
1.4 Introduction

The work carried out previously in our laboratory had shown that *myo*-inositol based podands and crown ethers (See Table B1.4 and B1.5 in Section 1, page 75 and 76 respectively), which were designed and synthesized taking cue from the unusual and selective reactions exhibited by inositol derivatives, (see Part A, pages 47-50) exhibited preferential binding to lithium (previous section), potassium and silver ions.^{1,2,19} In particular, the relative orientation of the crown-ether oxygen atoms in *myo*-inositol derived crown ethers appeared to play a significant role in their binding to metal picrates.^{2,19} These results indicated that six secondary hydroxyl groups of inositols could be used for the construction of isomeric crown ethers having different relative orientations of oxygen atoms which influence their preference for binding to metal ions. However, it was not clear whether the observed preferences were solely due to the variation in the relative stereo disposition of the oxygen atoms in the crown ether and whether the pendant groups attached to other oxygen atoms on the inositol ring also played a role in the binding of metal ions. This was because all the crown ethers investigated had only benzyl ether groups on the carbocyclic ring and metal ion binding characteristics of different crown ethers could not be compared since they had varying number of benzyl groups. Hence it was interesting to see the effect of hydroxyl protecting groups on metal ion binding to inositol derived crown ethers and whether a simple approach of changing these pendant groups could be used to tune the binding of a particular metal ion to crown ethers derived from inositols. The continued interest in the tuning of metal ion binding ability of neutral complexing agents is mainly because of the various applications that they find in different areas of chemistry,²⁰ biology²¹ and

medicine.²² As mentioned in Part A of this thesis, various approaches^{1,2,3b,3d,3f,14d,19,23} for improving the complexation and transport of cations have earlier been attempted, with varying degrees of success. This section presents results of a systematic study that reveals the effect of auxiliary hydroxyl-protecting groups (methyl vs. benzyl) for the binding of metal ions to inositol derived crown ethers. This investigation is also of interest in the context of the *picrate effect*²⁴—preferential extraction of alkali metal picrates due to the presence of aromatic rings in crown ethers that has been observed earlier.

1.5 Results and Discussion

myo-Inositol derived crown ethers (**B1.22**, **B1.25**, **B1.31**, **B1.34** and **B1.37**)¹¹ having different relative orientation of the crown ether oxygen atoms and containing auxiliary methyl and benzyl ethers were prepared from *myo*-inositol (**A.24**). Scheme B1.4 shows preparation of the crown-4 ether **B1.22**; the precursor, diol **B1.21**, was prepared as reported earlier.^{25,26} We also observed that the orthoformate moiety in **B1.22** was susceptible to hydrolysis since we were able to obtain a small amount of the orthoester cleaved crown-4 ether (**B1.23**) from the recovered **B1.22** (after picrate extraction experiments). Good quality single crystals of **B1.23** suitable for X-ray diffraction studies were obtained on storing the recovered **B1.22** in a refrigerator for several weeks. An ORTEP diagram of **B1.23** is shown in Figure B1.3. Crown ether cavity size in **B1.23** was $1.509 \text{ \AA} \times 1.914 \text{ \AA}$ which is slightly larger than the cavity ($1.471 \text{ \AA} \times 1.887 \text{ \AA}$) in the analogous crown ether **B1.15** containing a benzyl group (see Figure B1.2).



SCHEME B1.4. *Reagents and Conditions:* (a) DMF, MeI, NaH, 0 °C to rt, 95-100%; (b) Mg/ THF:MeOH (1:3), rt, 24 h. 94%; (c) THF, NaH, TsO(CH₂CH₂O)₃Ts, reflux, 24 h; (d) MeOH, NaOMe, reflux, 12 h. 37% (for two steps).

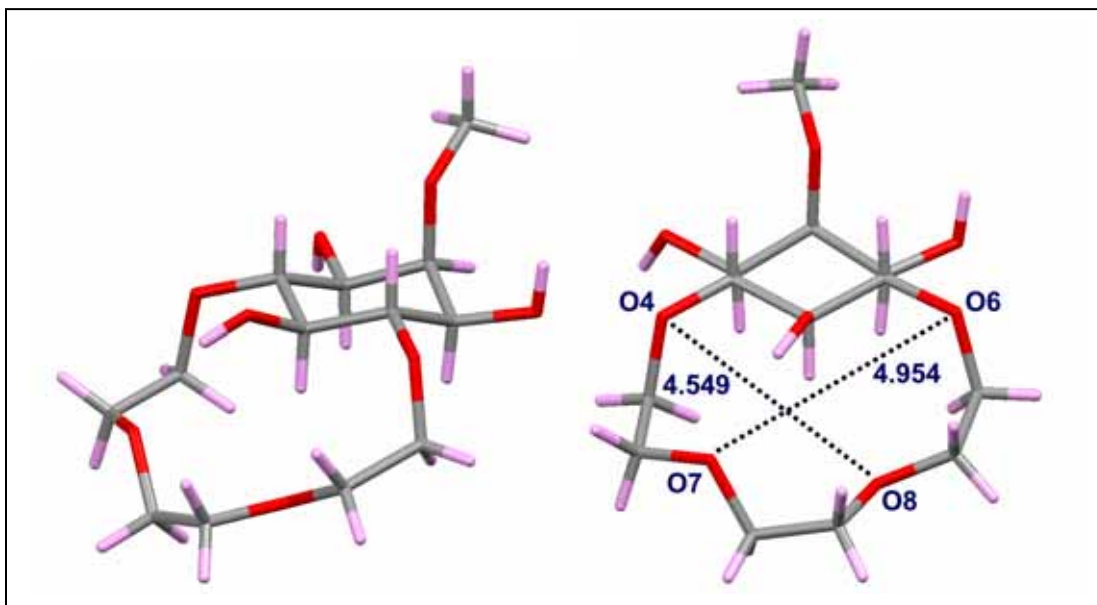
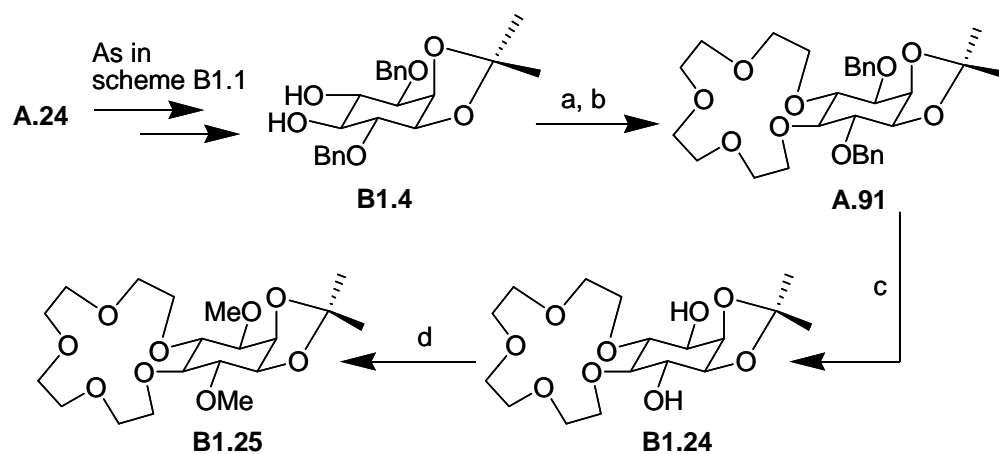


FIGURE B1.3. A view of a molecule of **B1.23** in its crystal showing the crown ether cavity (1.509 Å × 1.914 Å, van der Waals radius for O is 1.52 Å).

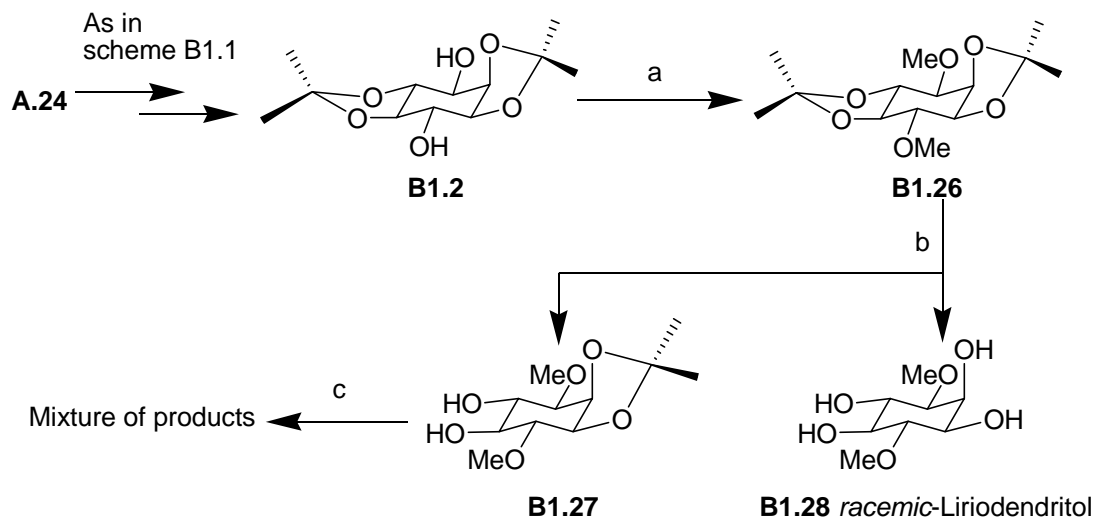
The crown-5 ether **B1.25** (Scheme B1.5) was prepared from the known crown ether **A.91**² by the sequential hydrogenolysis of the benzyl groups followed by *O*-

methylation (of **B1.24**); overall yield of **B1.25** was 4.6% (from *myo*-inositol). This procedure was much more convenient than the route where the methyl ethers were introduced prior to crown ether formation (see Scheme B1.6).



SCHEME B1.5. *Reagents and Conditions:* (a) THF, NaH, TsO(CH₂CH₂O)₄Ts, reflux, 24 h; (b) MeOH, NaOMe, reflux, 12 h, 38% (for two steps); (c) MeOH, 10% Pd/C, H₂, rt, 3 h, 95%; (d) DMF, NaH, MeI, 0 °C to rt, 1 h, 52%.

We first attempted to prepare the crown-5 ether **B1.25** from a reaction of the diol **B1.27** (Scheme B1.6) with tetraethyleneglycol ditosylate, but the yield was too low to be of practical value since a complex mixture of products resulted (as revealed by TLC). Also, the selective cleavage of the *trans* acetonide (in the dimethyl ether **B1.26**) without disturbing the *cis* acetonide was not as selective, by procedures reported for the dibenzyl ether **B1.3** (Scheme B1.1).¹² Various reaction conditions and the corresponding yield of the diol **B1.27** and tetrol **B1.28** (racemic liriodendritol, a natural product²⁷) obtained on cleavage of the acetonides in **B1.26** are shown in Table B1.6. Best yield of the desired diol **B1.27** was obtained by carrying out the solvolysis using catalytic amount of camphor sulphonic acid, in a mixture of dichloromethane: methanol (2:1).



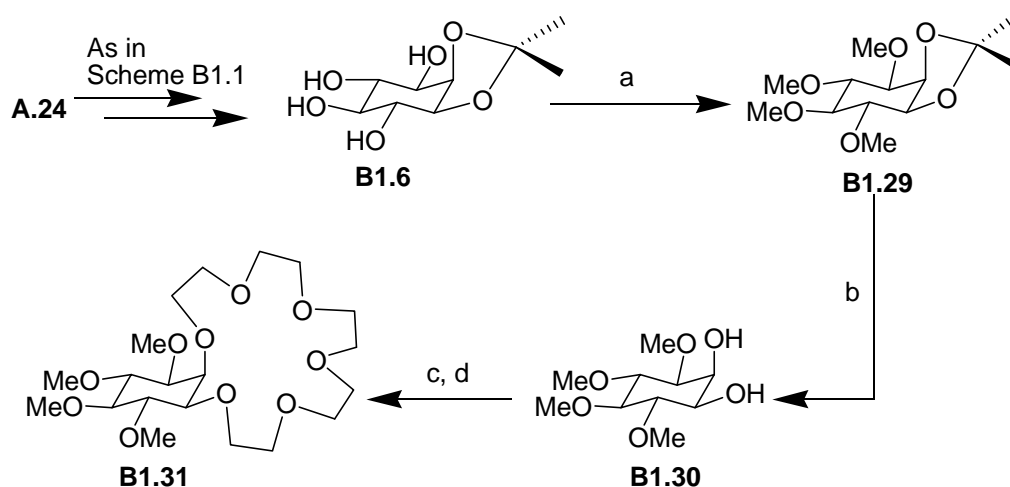
SCHEME B1.6. *Reagents and Conditions:* (a) DMF, NaH, MeI, 0 °C to rt, 61%; (b) see Table B1.6, 87%; (c) THF, NaH, TsO(CH₂CH₂O)₅Ts, reflux, 24 h.

TABLE B1.6: Selective deprotection of *trans* acetonide in **B1.26**.

Entry	Reaction Conditions	% Yield	
		B1.27	B1.28
1	TsOH, acetone:H ₂ O (40:1 v/v), 15 min. ¹²	---	~100
2	CHCl ₃ :MeOH (2:1 v/v), amberlite 120 (H ⁺), 20 min. ²⁸	---	~100
3	TsOH, DCM:MeOH (40:1 v/v), 0 °C, 30 min. ²⁹	43	46
4	CH ₃ COCl, DCM:MeOH (2:1 v/v), rt, 22 h. ³⁰	70	15
5	Camphorsulfonic acid (cat), DCM:MeOH (2:1 v/v), rt, 3 h. ²⁵	87	---

The racemic crown-6 ether **B1.31** was prepared as shown in Scheme B1.7. The diol **B1.30** was prepared as reported,³¹ (yield 48%) except that, methylation of the tetrol

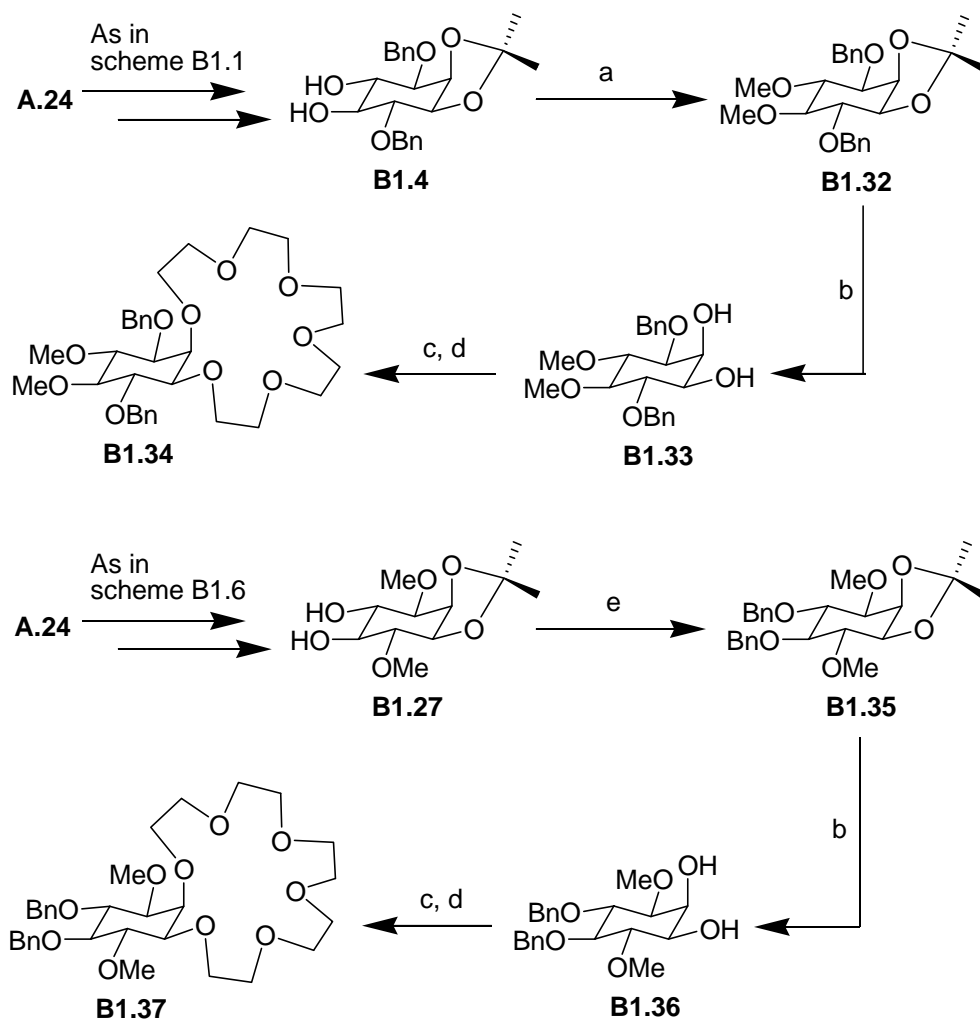
B1.6 was carried out using sodium hydride and methyl iodide instead of silver(I) oxide and methyl iodide. Use of sodium hydride was much more convenient in terms of work-up procedure and also the yield was higher (70%).²⁵



SCHEME B 1.7. *Reagents and Conditions:* (a) DMF, NaH, MeI, 0 °C to rt, 18 h, 70%; (b) acetic acid:water (4:1), 100 °C, 30 min, 77%; (c) THF, NaH, TsO(CH₂CH₂O)₅Ts, reflux, 24 h; (d) MeOH, NaOMe, reflux, 12 h. 37% (for two steps).

The crown ethers **B1.34** and **B1.37** (Scheme B1.8) were prepared from the diols **B1.4**¹² and **B1.27** respectively. The crown ethers **B1.34** and **B1.37** were prepared to investigate the effect of the relative position of the benzyl groups on the binding of metal ions to *myo*-inositol derived crown ethers.

As observed during the preparation of *myo*-inositol derived crown ethers earlier in Section 1, in most of the experiments the respective oligoethyleneglycol ditosylate could not be separated from crown ethers by column chromatography. Hence, crude crown ethers were refluxed with sodium methoxide in methanol to convert the un-reacted oligoethyleneglycol ditosylate to the corresponding dimethyl ether, from which crown ethers could be separated.

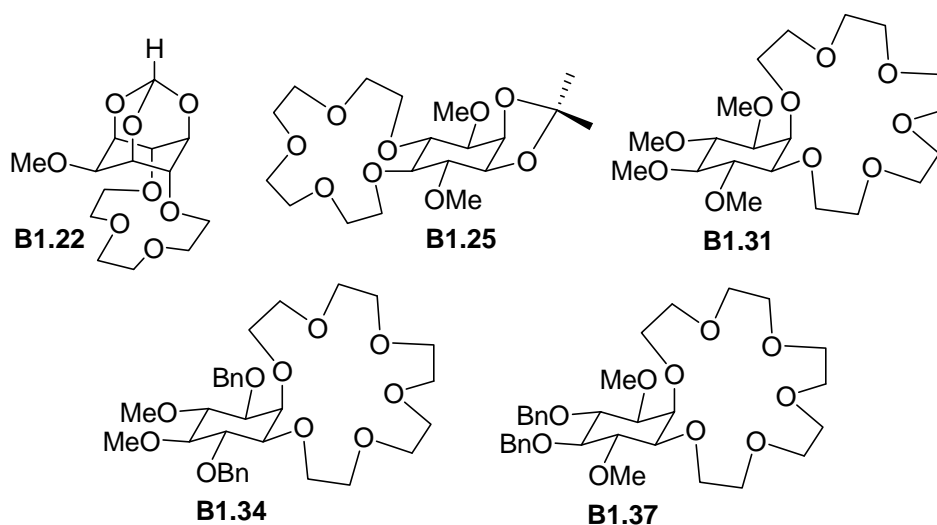


SCHEME B1.8. *Reagents and Conditions:* (a) DMF, NaH, MeI, 0 °C to rt, 20 h, 87%; (b) acetic acid:water (4:1), 100 °C, 3 h, 82% (for **B1.33**), 77% (for **B1.36**); (c) THF, NaH, TsO(CH₂CH₂O)₅Ts, reflux, 24 h; (d) MeOH, NaOMe, reflux, 8-10 h, 68% (for **B1.34**), 74% (for **B1.37**); (e) DMF, NaH, BnBr, 0 °C to rt, 1 h, 53%.

The yield of crown-5 ethers and crown-6 ethers were in the range 37-74% which is comparable to the yield of *myo*-inositol derived crown ethers reported previously² from our laboratory and for other crown ethers reported in the literature.^{10a,14a-14c,32,33,34} The

yield of crown-5 and crown-6 ethers is much higher than the yields reported for *myo*-inositol derived crown-4 ethers (Section 1), as expected.

TABLE B1.7. Association constants ($K_a \times 10^{-4} \text{ dm}^3 \text{ mol}^{-1}$) of *myo*-inositol derived crown ethers with metal picrates in CDCl_3 at 27 °C.



Picrate	Li^+	Na^+	K^+	Cs^+	NH_4^+	Ag^+
B1.22	15.6	2.39	0.67	0.29	0.11	0.17
B1.25	294.5	2.91	2.20	0.82	0.61	4.63
B1.31	1.75	6.51	48	1.31	22.2	63.1
B1.34	9.67	21.78	555.6	11.48	139.31	286.27
B1.37	7.97	28.39	460.35	37.56	933.88	348.59

The metal picrate binding constants for the newly synthesized crown ethers are listed in Table B1.7. The crown-6-ethers **B1.31** and **B1.34** showed better binding to potassium and silver picrate as expected while the crown-6-ether **B1.37** exhibited highest

binding to ammonium picrate. The dimethyl crown-5-ether **B1.25** exhibited highest binding constant for lithium picrate among the newly synthesized crown ethers.

Table B1.8: Selected ratio^a of association constants for crown ethers in Table B1.7.

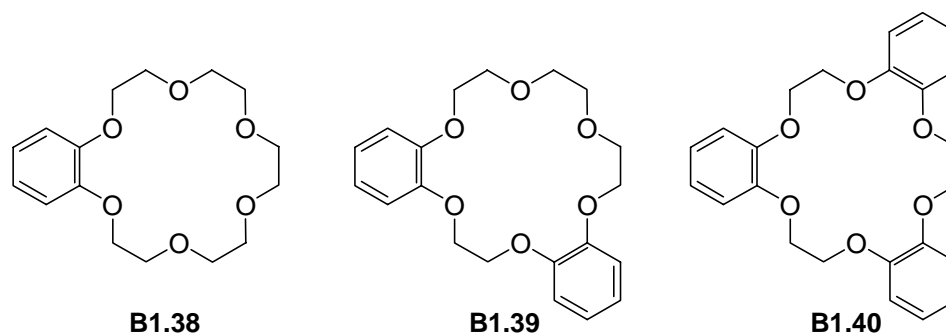
Crown ether	Li^+/Na^+	Li^+/K^+	Li^+/Cs^+	$\text{Li}^+/\text{NH}_4^+$	Li^+/Ag^+
B1.22	6.5	23.3	53.8	141.8	91.8
B1.25	101.19	133.85	359.12	482.8	63.60
	Ag^+/Li^+	Ag^+/Na^+	Ag^+/K^+	Ag^+/Cs^+	$\text{Ag}^+/\text{NH}_4^+$
B1.31	36	9.7	1.3	48.2	2.8
	K^+/Li^+	K^+/Na^+	K^+/Cs^+	K^+/NH_4^+	K^+/Ag^+
B1.34	57.4	25.5	48.4	4	2
B1.37	57.8	16.2	12.2	0.5	1.3
	$\text{NH}_4^+/\text{Li}^+$	$\text{NH}_4^+/\text{Na}^+$	NH_4^+/K^+	$\text{NH}_4^+/\text{Cs}^+$	$\text{NH}_4^+/\text{Ag}^+$
B1.37	117.2	32.9	2	24.9	2.7

^a For complete listing of ratios see Table B1.15, Section 3, page 120.

Calculation of the ratio of association constants between different metal picrates (which reveals the magnitude of the preference of a crown ether for the binding to a particular metal ion) for binding to the same crown ether shows that highest selectivity is exhibited by the crown ether **B1.25** (Table B1.8) for the binding of lithium picrate ($K_{a(\text{Li}^+)}/K_{a(\text{NH}_4^+)} \approx 482.8$) and the lowest selectivity is exhibited by the crown ether **B1.37** for the binding of potassium ($K_{a(\text{K}^+)}/K_{a(\text{Ag}^+)} \approx 1.3$) and ammonium ($K_{a(\text{NH}_4^+)}/K_{a(\text{K}^+)} \approx 2$)

picrates. It is interesting to note that the crown-5 ether **B1.25** exhibits better binding and selectivity for lithium as compared to the crown-4 ether **B1.22**. The crown-6 ethers **B1.31**, **B1.34** and **B1.37** show good binding and selectivity for silver, potassium and ammonium picrates respectively. However selectivity between any two of potassium, ammonium and silver picrates, exhibited by **B1.34** and **B1.37** is marginal. These results support the earlier findings^{2,19} that binding and selectivity of *myo*-inositol derived crown ethers to metal picrates depend on (a) the size of the crown ether; (b) relative orientation of the crown ether oxygen atoms; and in addition, these results also suggest that the auxiliary groups present on the *myo*-inositol ring affect the binding of metal ions to crown ethers (Also see Table B1.10). The narrow range of selectivity exhibited by the crown ethers **B1.34** and **B1.37** (for the binding of metal picrates tested) as compared to the crown ether **B1.25** (most selective for lithium) may be attributed to the presence of benzyl ether groups in the former two crown ethers. Presence of aromatic rings in crown ethers is reported to influence their selectivity towards the binding of metal picrates (*picrate effect*²⁴). Selected examples from the literature are shown in Table B1.9.

TABLE B1.9: Separation factors for competitive alkali metal picrate extraction from aqueous solution into CHCl_3 by crown ethers **B1.38**, **B1.39** and **B1.40**.²⁴

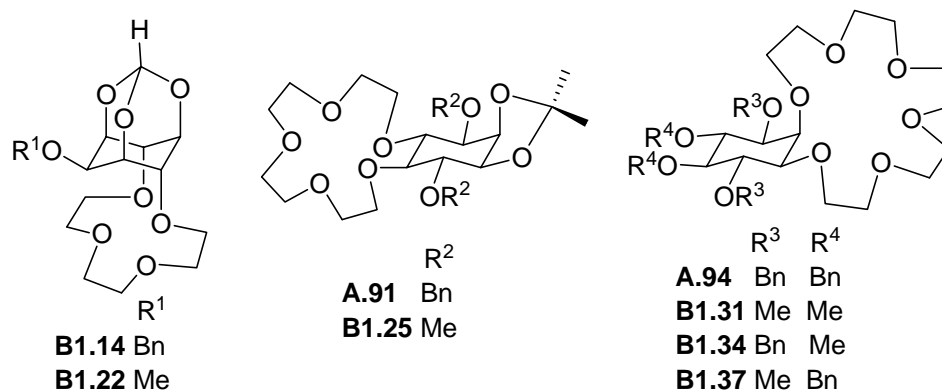


Crown ether	$\alpha_{\text{K,Na}}$	$\alpha_{\text{K,Rb}}$	$\alpha_{\text{K,Cs}}$
B1.38	66.3	4.0	16.5
B1.39	27.0	3.85	8.50
B1.40	12.1	4.48	11.0

A comparison of the metal picrate extraction constants of the tetramethyl crown ether **B1.31** with the corresponding dibenzyl crown ethers **B1.34** and **B1.37** (Table B1.7) shows that the latter two crown ethers exhibit better binding of potassium, ammonium and silver picrates. The extent of selectivity for these picrates is in general better in the case of dibenzyl crown ethers **B1.34** and **B1.37** than the selectivity exhibited by the tetramethyl crown ether **B1.31**. Furthermore, it is interesting to note that picrates of silver, potassium and ammonia bind better to the crown ethers **B1.31**, **B1.34** and **B1.37** respectively (compared to other picrates tested for the given crown ether). If benzyl ethers were merely contributing to the binding of picrates due to *picrate effect*²⁴ these

dibenzyl ethers **B1.34** and **B1.37** should have exhibited worse selectivity for potassium and silver picrates as compared to the corresponding tetramethyl crown ether **B1.31**.

Table B1.10: Ratio of association constants for the binding of metal picrates to *myo*-inositol derived crown ethers having same stereochemistry but different protecting groups.



Crown ether	Li ⁺	Na ⁺	K ⁺	Cs ⁺	NH ₄ ⁺	Ag ⁺
B1.14 [#] / B1.22	1.7	1.2	1	2.1	1.9	5.3
A.91 ² / B1.25	0.03	1.5	1.2	1.6	1.3	7.4
A.94 ² / B1.31	9.3	7	733.3	9	26.4	78447
B1.34 / B1.31	5.5	3.3	11.6	8.8	6.3	4.5
B1.37 / B1.31	4.6	4.4	9.6	28.7	41.9	5.5
A.94 ² / B1.34	1.7	2.1	63.3	1	4.2	17291
A.94 ² / B1.37	2	1.6	76.5	0.3	0.6	14200
B1.37 / B1.34	0.8	1.3	0.8	3.3	6.7	1.2

[#] for the binding constant of **B1.14** see Table B1.1, Section 1, page 72.

² For the calculation of ratio of binding constants, values for **A.91** and **A.94**, were taken from reference 2 (reproduced in Table B1.14, Section 3, page 119).

These results clearly show that selective binding of metal picrates can be tuned by changing the protecting groups (methyl to benzyl) on inositol hydroxyl groups. Hence we compared (Table B1.10) the metal picrate extraction characteristics of the crown ethers reported in the present study (having methyl groups) with those containing only benzyl groups on the *myo*-inositol ring.^{2,19}

A comparison of the ratios of picrate extraction constants between crown ethers with methyl groups (**B1.22**, **B1.25**, **B1.31**) and the corresponding crown ether with benzyl groups (**B1.14**, **A.91**, **A.94**) showed that presence of benzyl ethers contributes significantly to the binding of potassium and silver picrates, especially in the crown-6-ether **A.94**. It is known that olefinic^{35,36} and aromatic^{37,38} π -electron systems contribute significantly towards the formation of silver complexes and, binding of potassium to calixarene^{39,40} derived crown ethers is enhanced by the presence of aromatic groups, near the crown ether moiety. Figure B1.4 shows a few compounds containing aromatic rings which bind silver and potassium preferentially.

Although all the *myo*-inositol derived crown ethers containing benzyl groups bind metal picrates better than the corresponding crown ethers containing methyl ethers, unusually high ratio of association constants (Table B1.10) is exhibited for the binding of silver picrate ($K_{a(A.94)}/K_{a(B1.31)} \approx 78447$), followed by potassium picrate ($K_{a(A.94)}/K_{a(B1.31)} \approx 733.3$). If the contribution of benzyl ethers for the binding of metal picrates was only due to *picrate effect*,²⁴ then the ratio of binding constants for silver (and potassium) picrate between the crown ethers (as above) should have been comparable to that of other picrates.

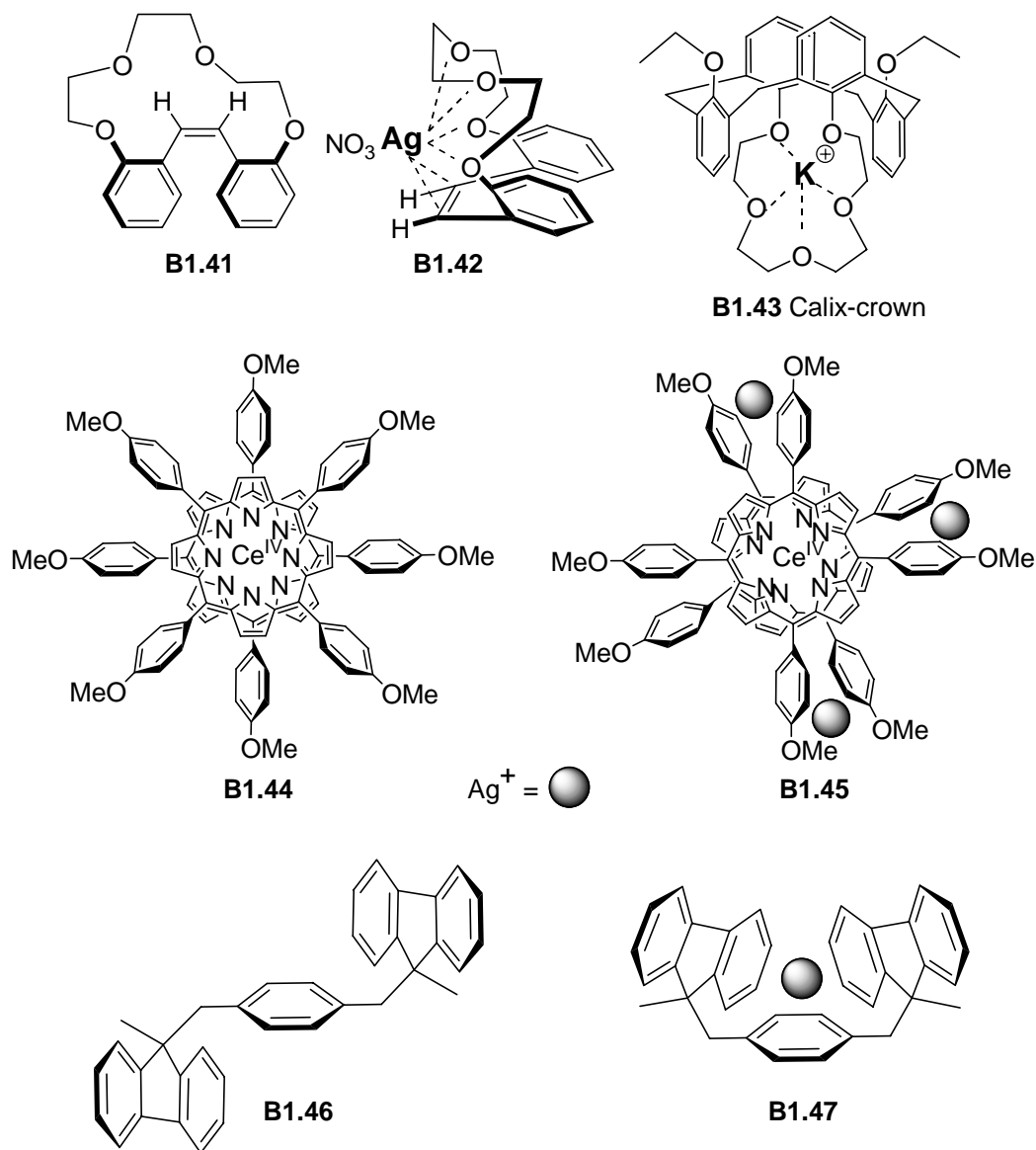
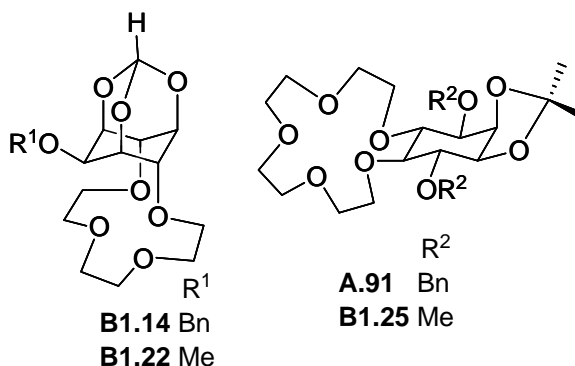


FIGURE B1.4. Silver and potassium ion complexing compounds.

We also calculated the ratio of extraction constants between lithium picrate and other picrates for crown-4 and crown-5-ethers (Table B1.11) and similar ratios for the extraction of potassium and silver picrates for crown-6-ethers (Table B1.12), since these crown ethers exhibited highest binding constants for lithium, potassium and silver picrates. A comparison of these values for a given crown ether containing methyl/ benzyl protecting groups was interesting.

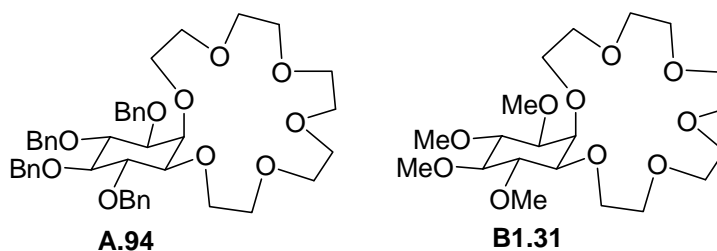
Table B1.11: Ratio of Association Constants: Lithium picrate to other picrates.

Crown ether	Li^+/Na^+	Li^+/K^+	Li^+/Cs^+	$\text{Li}^+/\text{NH}_4^+$	Li^+/Ag^+
B1.14	9	40	44	130	30
B1.22	7	23	54	142	92
A.91 ²	2	4	7	12	0.27
B1.25	101	134	359	483	64

² For the calculation of ratio of binding constants value for **A.91** was taken from reference 2 (reproduced in Table B1.14, Section 3, page 119).

The extent of picrate effect was revealed by the selectivity of metal picrate binding exhibited by methyl crown ethers as compared to benzyl crown ethers. For example, the selectivity for the binding of lithium picrate to the methyl crown-4-ether **B1.22** was $K_{a(\text{Li}^+)}/K_{a(\text{NH}_4^+)} \approx 142$, while the corresponding value for the benzyl crown **B1.14** was $K_{a(\text{Li}^+)}/K_{a(\text{NH}_4^+)} \approx 130$. Similarly, the highest selectivity for the binding of lithium picrate to the methyl crown-5-ether **B1.25** observed was $K_{a(\text{Li}^+)}/K_{a(\text{NH}_4^+)} \approx 483$, while the corresponding value for the benzyl crown **A.91** was $K_{a(\text{Li}^+)}/K_{a(\text{NH}_4^+)} \approx 12$ (Table B1.11).

Table B1.12: Ratio of Association Constants: potassium and silver picrates to other picrates.



Crown ether	K^+/Li^+	K^+/Na^+	K^+/Cs^+	K^+/NH_4^+	K^+/Ag^+
B1.31	24.42	7.37	36.64	2.16	0.76
A.94 ²	2160	774	2983	60	0.007
	Ag^+/Li^+	Ag^+/Na^+	Ag^+/K^+	Ag^+/Cs^+	Ag^+/NH_4^+
B1.31	36	9.7	1.3	48.2	2.8
A.94 ²	3×10^5	1.1×10^5	140.6	4.2×10^5	8447

² For the calculation of ratio of binding constants value for **A.94** was taken from reference 2 (reproduced in Table B1.14, Section 3, page 119).

In contrast, the selectivity for the binding of potassium and silver picrates (Table B1.12) to the methyl crown-6-ether **B1.31** were $Ka_{(K^+)}/Ka_{(Cs^+)} = 36.6$ and $Ka_{(Ag^+)}/Ka_{(Cs^+)} = 48.2$ respectively, while the corresponding values for the benzyl crown-6-ether **A.94** were $Ka_{(K^+)}/Ka_{(Cs^+)} = 2983$ and $Ka_{(Ag^+)}/Ka_{(Cs^+)} = 4.2 \times 10^5$. In the former crown ethers (**B1.22** vs. **B1.14** and **B1.25** vs. **A.91**, Table B1.11) this result is in accordance with the *picrate effect*²⁴ (reduction in selectivity due to the presence of aromatic groups in crown ethers) reducing the selectivity among metal picrates. However for the crown 6-ethers (**B1.31** vs. **A.94**, Table B1.12) the selectivity pattern is the opposite of that expected due

to *picrate effect*.²⁴ Hence these results also reveal that the selectivity for the binding of metal ions to *myo*-inositol derived crown ethers can be tuned by varying the auxiliary groups on the inositol ring. These results clearly show that the benzyl groups in *myo*-inositol derived crown-6-ether **A.94** are indeed necessary for the binding of K^+ and Ag^+ ions.

A comparison of the binding constants for the isomeric crown ethers **B1.34** and **B1.37** with metal picrates (Table B1.7) reveals that relative position of the benzyl groups in crown-6-ethers do not have much bearing on their metal picrate binding abilities. However, ratio of metal picrate binding constants for dibenzyl crown ethers (**B1.34**, **B1.37**) and tetramethyl crown ether **B1.31** shows that the presence of two benzyl groups in the former increases their binding to metal picrates. Similarly ratio of the binding constants for tetrabenzyl crown ether **A.94** to the corresponding dibenzyl crown ethers (**B1.34**, **B1.37**, Table B1.10) show that binding of potassium and silver picrates increase dramatically due to the presence of two additional benzyl groups ($K_{a(A.94)} / K_{a(B1.34)} \approx 17291$ and $K_{a(A.94)} / K_{a(B1.37)} \approx 14200$ for the binding of silver picrate). These results suggest that benzyl protecting groups in *myo*-inositol derived crown ethers interact with cations³⁶⁻⁴¹ rather than enhancing the binding of metal picrates by merely interacting with picrate anions. It is likely that the unusually large binding of tetra-benzyl crown ether **A.94** with silver picrate observed could be due to the co-operative binding between silver picrate and crown ethers rather than formation of 1:1 complexes. This is schematically represented in Figure B1.5. Our attempts to obtain single crystals of *myo*-inositol derived crown ethers with metal picrates (the structure of which could have revealed the nature of metal binding to crown ethers) were not successful.

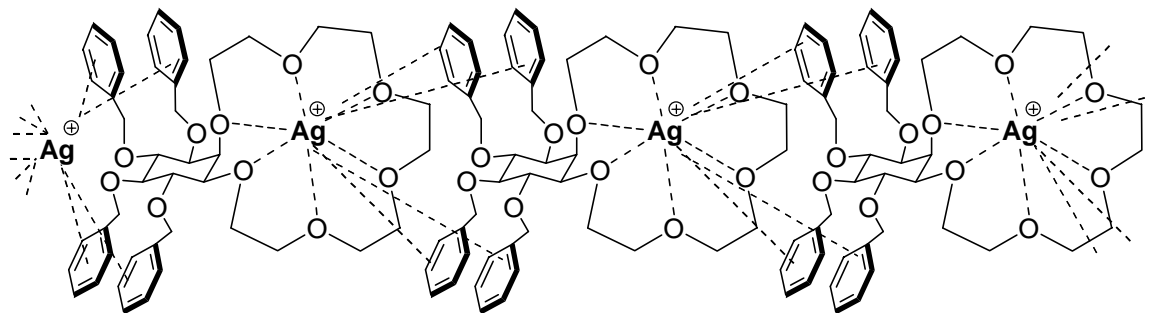


FIGURE B1.5. Co-operative binding between silver picrate and *myo*-inositol derived crown ethers containing benzyl groups.

1.6 Conclusions

Synthesis and evaluation of picrate extraction constants for inositol derived crown ethers and inositol orthoformate derived crown ethers having different substitutions on the inositol oxygen atoms (not involved in crown ether formation) showed that the efficiency of metal picrate binding is influenced by these O-substituents. Consequently, these results indicate that the extent of metal ion binding to the crown ethers can be tuned by changing the auxiliary protecting groups on the inositol hydroxyl groups. A comparison of the crown ethers containing benzyl groups at different relative positions and containing different number of benzyl groups on the inositol ring show that although the relative position of the benzyl groups with respect to the crown ethers do not have much bearing on their binding and selectivity to metal ions, the number of benzyl groups have a profound effect on the binding to metal ions. Hence binding of inositol-based crown ethers to potassium and silver can be enhanced by the introduction of benzyl ethers on the inositol ring. The results also suggest that the enhanced binding of potassium and silver picrates could be due to cooperative binding between crown ether molecules and metal ions resulting in the formation of aggregates rather than the formation of individual 1:1 complexes.

Section 3

1.7 Experimental Section

General methods. All the solvents used were purified according to literature procedures.⁴¹ Sodium hydride used in experiments was 60% suspension in mineral oil. All air or moisture sensitive reactions were conducted under argon or nitrogen atmosphere. Thin layer chromatography was performed on E Merck pre-coated 60 F₂₅₄ plates and the spots were rendered visible either by shining UV light or by charring the plates with chromic acid. Flash column chromatography was carried out on silica gel (230-400 mesh). Compounds previously reported in the literature were characterized by comparison of their melting point and / or ¹H NMR spectra with the reported data. IR spectra were recorded in CHCl₃ solution or as thin film (neat) on a Shimadzu FTIR-8400 spectrophotometer. NMR spectra were recorded in CDCl₃ solution on Bruker AV200 spectrometer, unless otherwise mentioned and chemical shifts (δ) reported are referred to TMS as an internal standard. Microanalytical data were obtained using a Carlo-Erba CHNS-0 EA 1108 elemental analyzer. All the melting points were recorded on a Büchi B-540 electro-thermal melting point apparatus and are uncorrected. Yields refer to chromatographically and spectroscopically pure compounds. Procedure for the preparation of crown ethers and estimation of their binding constants were as reported earlier.^{2,19} Alkali metal and ammonium picrates^{42,43,44} silver picrate,⁴⁵ tetra(ethylene glycol) ditosylate⁴⁶ and penta(ethylene glycol) ditosylate⁴⁶ were prepared as reported in the literature. Metal picrates were dried under reduced pressure, at room temperature and stored in the dark. Picrate extraction studies were done by equilibrating a solution of the

compound in CDCl_3 and metal picrate in water. The association constant K_a was calculated by Cram's procedure.¹⁵

Single crystal X-ray analysis. For single crystal X-ray diffraction analysis, good quality crystals were selected using Leica Polarizing microscope. X-ray intensity data were collected on a Bruker SMART APEX CCD diffractometer with graphite monochromatized ($\text{Mo K}\alpha = 0.71073 \text{ \AA}$) radiation at room temperature. All the data were corrected for Lorentzian, polarization and absorption effects using Bruker's SAINT and SADABS programs. SHELX-97⁴⁷ was used for structure solution and full matrix least squares refinement on F^2 . Hydrogen atoms were included in the refinement as per the riding model. Crystal data and details of data collection, structure solution and refinements, ORTEP⁴⁸ plots and packing diagrams for individual compounds are given in the appendix.

Synthesis of crown ethers. General procedure. A solution of oligoethyleneglycol ditosylate (1.2-1.3 mmol) in dry THF (50 mL) was added drop-wise over 2 h to a refluxing solution of the required *myo*-inositol derived diol (1 mmol) and sodium hydride (4 mmol) in dry THF (100 mL), in an atmosphere of nitrogen/ argon. Refluxing was continued for another 24 h, after which the reaction mixture was cooled to ambient temperature and the solvent was evaporated under reduced pressure. The residue was extracted with chloroform and washed successively with water and brine. The organic layer was dried over anhydrous sodium sulfate and evaporated under reduced pressure to give a gum. The crude product was dissolved in dry methanol (7-10 mL) and heated under reflux with sodium methoxide (5-10 mmol) for 8-12 h. Methanol was evaporated under reduced pressure to get a gum, which was purified by column

chromatography on silica gel using ethyl acetate and light petroleum (gradient elution) as eluent to obtain the crown ether.

Racemic 1,2-O-isopropylidene-3,6-di-O-benzyl-4,5-(12-crown-4)-myo-inositol (B1.5).

The diol **B1.4**¹² (0.4 g, 1 mmol), sodium hydride (0.160 g, 4 mmol) and triethyleneglycol ditosylate (0.596 g, 1.3 mmol) were used to obtain the crown ether **B1.5** (as mentioned in the general procedure, page 101) and was isolated as a gum (0.188 g, 36%).

IR (neat): $\tilde{\nu} = 3350\text{-}3570\text{ cm}^{-1}$ (H₂O).

¹H NMR (200 MHz; CDCl₃): $\delta = 1.33$ (s, 3H; CH₃), 1.48 (s, 3H; CH₃), 3.16 (t, $J = 9$ Hz, 1H, Ins-H), 3.55-4.10 (m, 16H; OCH₂CH₂O, 4Ins-H), 4.18 (t, $J = 4.4$ Hz, 1H; InsC2-H), 4.50-5.0 (m, 4H; CH₂Ph), 7.15-7.60 (m, 10H; Ar-H).

¹³C NMR (50.3 MHz; CDCl₃): $\delta = 25.9$ (CH₃), 27.8 (CH₃), 70.7 (CH₂), 71.0 (CH₂), 72.3 (CH₂), 72.5 (CH₂), 73.3 (CH₂), 74.0 (CH₂), 74.6 (Ins-C), 79.1 (Ins-C), 81.2 (Ins-C), 82.5 (Ins-C), 82.7 (Ins-C), 109.7 (CMe₂), 127.4 (Ar-C), 127.7 (Ar-C), 127.9 (Ar-C), 128.2 (Ar-C), 128.4 (Ar-C), 138.4 (Ar-C), 138.7 (Ar-C).

Elemental analysis: Anal. Calcd. for C₂₉H₃₈O₈·2H₂O (550.66): C, 63.25; H, 7.68. Found: C, 63.69; H, 7.41%.

Note: As revealed by spectroscopy and analytical data, the crown-ether **B1.5** always contained water and was not stable either as gum or in solution for long periods of time (few weeks). We suspect that some of the benzylic methylene groups undergo oxidation on storage. This was indicated by the infrared and ¹H NMR spectra of samples stored over long periods of time.

Racemic 1,2-(12-crown-4)-3,4,5,6-tetra-O-benzyl-myoinositol (B1.9). The diol **B1.8**¹³ (0.541 g, 1 mmol), sodium hydride (0.160 g, 4 mmol) and triethyleneglycol ditosylate

(0.550 g, 1.2 mmol) were used to obtain the crown ether **B1.9** (as mentioned in the general procedure, page 101) and was isolated as a gum (0.185 g, 28%).

IR (neat): $\tilde{\nu} = 3200\text{-}3600\text{ cm}^{-1}$ (H_2O).

^1H NMR (200 MHz; CDCl_3): $\delta = 3.16$ (d, $J = 10$ Hz, 1H; Ins-H), 3.30-3.45 (m, 2H, $\text{OCH}_2\text{CH}_2\text{O}$), 3.55-3.85 (m, 10H; $\text{OCH}_2\text{CH}_2\text{O}$), 3.90-4.20 (m, 5H; Ins-H), 4.55-5.0 (m, 8H; CH_2Ph), 7.15-7.50 (m, 20H; Ar-H).

^{13}C NMR (50.3 MHz; CDCl_3): $\delta = 70.5$ (CH_2), 70.7 (CH_2), 71.9 (CH_2), 72.3 (CH_2), 72.5 (CH_2), 72.6 (CH_2), 72.8 (CH_2), 75.6 (CH_2), 80.6 (Ins-C), 80.7 (Ins-C), 81.2 (Ins-C), 81.6 (Ins-C), 83.5 (Ins-C), 127.2 (Ar-C), 127.5 (Ar-C), 127.6 (Ar-C), 127.8 (Ar-C), 128.1 (Ar-C), 129.7 (Ar-C), 138.4 (Ar-C), 138.9 (Ar-C).

Elemental analysis: Anal. Calcd. for $\text{C}_{40}\text{H}_{46}\text{O}_8 \cdot 2\text{H}_2\text{O}$ (690.84): C, 69.54; H, 7.29. Found: C, 69.33; H, 6.92%.

Note: As revealed by spectroscopy and analytical data, the crown-ether **B1.9**, always contained water and was not stable either as gum or in solution for long periods of time (few weeks). We suspect that some of the benzylic methylene groups undergo oxidation on storage. This was indicated by the infrared and ^1H NMR spectra of samples stored over long periods of time.

2-O-Benzyl-4,6-(13-crown-4)-myo-inositol 1,3,5-orthoformate (B1.14). The diol **B1.13**⁷ (0.280 g, 1 mmol), sodium hydride (0.160 g, 4 mmol) and triethyleneglycol ditosylate (0.596 g, 1.3 mmol) were used to prepare the crown ether **B1.14** (as mentioned in the general procedure, page 101) and was isolated as a gum (0.094 g, 24%).

IR (neat): $\tilde{\nu} = 3200\text{-}3600\text{ cm}^{-1}$ (H_2O).

^1H NMR (200 MHz; CDCl_3): δ = 3.35-3.90 (m, 12H; $\text{OCH}_2\text{CH}_2\text{O}$), 3.99 (d, J = 1 Hz, 1H; Ins-H), 4.15-4.25 (m, 2H; Ins-H), 4.25-4.35 (m, 2H; Ins-H), 4.51 (m, 1H; Ins-H), 4.75 (s, 2H; CH_2Ph), 5.55 (d, J = 1 Hz, 1H; HCO_3), 7.25-7.50 (m, 5H; Ar-H).

^{13}C NMR (50.3 MHz; CDCl_3): δ = 66.9 (Ins-C), 67.6 (Ins-C), 69.7 (CH_2), 70.3 (CH_2), 70.4 (Ins-C), 71.2 (CH_2), 71.3 (CH_2), 74.4 (Ins-C), 103.2 (HCO_3), 127.8 (Ar-C), 128.1 (Ar-C), 128.4 (Ar-C), 137.9 (Ar-C).

Elemental analysis: Anal. Calcd. for $\text{C}_{20}\text{H}_{26}\text{O}_8 \cdot \text{H}_2\text{O}$ (412.43): C, 58.24; H, 6.84. Found: C, 58.60; H, 7.14%.

Note: As revealed by spectroscopy and analytical data, the crown-ether **B1.14**, always contained water and was not stable either as gum or in solution for long periods of time (few weeks). We suspect that some of the benzylic methylene groups undergo oxidation on storage. This was indicated by the infrared and ^1H NMR spectra of samples stored over long periods of time.

2-O-Benzyl-4,6-(13-crown-4)-myo-inositol (B1.15). Crown ether **B1.14** (0.200 g, 0.507 mmol) was stirred with trifluoro acetic acid: water (3:1, 8 mL) at room temperature for 5 h. Solvents were evaporated under reduced pressure to get a brownish gum. Gum was dissolved in methanol (30 mL) and boiled with activated charcoal and filtered. The colorless filtrate was concentrated and allowed to evaporate at room temperature; good crystals of the crown ether **B1.15** (0.170 g, 87.63%) were obtained after 3 days.

IR (neat): $\tilde{\nu}$ = 3205-3562 cm^{-1} .

^1H NMR (200 MHz; CDCl_3): δ = 2.49 (bs, 3H; OH, D_2O exchangeable), 3.50-3.85 (m, 14H; $\text{OCH}_2\text{CH}_2\text{O}$, 2Ins-H), 3.09-4.10 (m, 3H; Ins-H), 4.32 (t, J = 3 Hz, 1H; C2-H), 4.70-4.96 (m, 2H; CH_2Ph), 7.25-7.46 (m, 5H; Ar-H).

^{13}C NMR (50.3 MHz; CDCl_3): δ = 67.5 (CH_2), 70.1 (Ins-C), 71.0 (CH_2), 71.8 (CH_2), 73.0 (CH_2), 81.5 (Ins-C), 127.6 (Ar-C), 127.7 (Ar-C), 128.3 (Ar-C), 138.3 (Ar-C).

Elemental analysis: Anal. Calcd. for $\text{C}_{19}\text{H}_{28}\text{O}_8 \cdot \text{H}_2\text{O}$ (402.45): C, 56.70; H, 7.54. Found: C, 56.49; H, 7.54%.

2-O-methyl-4,6-(13-crown-4)-myo-inositol 1,3,5-orthoformate (B1.22). The diol **B1.21**^{25,26} (0.204 g, 1 mmol), sodium hydride (0.160 g, 4 mmol), triethyleneglycol ditosylate (0.596 g, 1.3 mmol) and dry THF (100 mL) were used to prepare the crown ether **B1.22** (as mentioned in the general procedure, page 101) and was isolated as a gum (0.108 g, 37%) by column chromatography (eluent 35% ethyl acetate in light petroleum).

IR (Neat): $\tilde{\nu}$ = 3390-3640 cm^{-1} (H_2O).

^1H NMR (200 MHz; CDCl_3): δ = 3.53 (s, 3H; OCH_3), 3.58-3.81 (m, 12H; $\text{OCH}_2\text{CH}_2\text{O}$), 3.85 (dd, J_1 = 7 Hz, J_2 = 2 Hz, 1H; Ins-H), 4.25 (t, J = 4 Hz, 2H; Ins-H), 4.31-4.41 (m, 2H; Ins-H), 4.49-4.60 (m, 1H; Ins-H), 5.52 (s, 1H; HCO_3).

^{13}C NMR (50.3 MHz; CDCl_3): δ = 56.4 (OCH_3), 67.4 (Ins-C), 69.1 (Ins-C), 69.5 (CH_2), 69.6 (Ins-C), 70.2 (CH_2), 70.7 (CH_2), 74.4 (Ins-C), 103 (HCO_3).

Elemental Analysis: Anal. Calcd. for $\text{C}_{14}\text{H}_{22}\text{O}_8 \cdot 2\text{H}_2\text{O}$ (354.36): C, 47.45; H, 7.39. Found: C, 47.85; H, 7.13%.

Racemic 1,2-O-isopropylidene-4,5-(15-crown-5)-myo-inositol (B1.24). A mixture of racemic crown ether **A.91**² (0.136 g, 0.2 mmol) and 10% Pd/C (0.040 g) in methanol (7 mL) was stirred at room temperature, under hydrogen atmosphere for 3 h. The reaction mixture was filtered and the filtrate was concentrated on rotary evaporator to get the diol **B1.24** as a gum (0.087 g, 95%). This experiment was repeated to get more of the diol.

IR (Neat): $\tilde{\nu}$ = 3417, 3425, 3442 cm^{-1} .

Elemental Analysis: Anal. Calcd. For C₁₇H₃₀O₉ (378.42): C, 53.95; H, 7.99. Found: C, 53.56; H, 7.63%.

Racemic 1,2-*O*-isopropylidene-3,6-di-*O*-methyl-4,5-(15-crown-5)-*myo*-inositol (B1.25). A mixture of the diol **B1.24** (0.188 g, 0.5 mmol) obtained above, sodium hydride (0.048 g, 2.0 mmol) and DMF (4 mL) was stirred for 10 min at 0-5 °C and then a solution of methyl iodide (0.31 mL, 5.0 mmol) in DMF (1 mL) was added drop-wise. The reaction mixture was allowed to come to room temperature and stirred for further 1 h. Excess sodium hydride was destroyed by adding methanol (1 mL) and the reaction mixture was concentrated under reduced pressure to a semi-solid. This was dissolved in chloroform (80 mL), washed with water (20 mL × 3) followed by brine, and the organic layer was dried over anhydrous sodium sulfate and the solvent was removed under reduced pressure to obtain a gum. This was purified by flash column chromatography (eluent 35% ethyl acetate in light petroleum) to get the crown ether **B1.25** as a gum (0.1047 g, 52%), which turned to a solid on storing in a refrigerator.

m.p: 57 °C.

IR (Neat): $\tilde{\nu} = 3400\text{-}3600\text{ cm}^{-1}$ (H₂O).

¹H NMR (200 MHz; CDCl₃): $\delta = 1.36$ (s, 3H; CH₃), 1.53 (s, 3H; CH₃), 3.10 (t, $J = 9$ Hz, 1H; Ins-H), 3.33-3.43 (m, 2H; Ins-H), 3.54 (s, 3H; OCH₃), 3.57 (s, 3H; OCH₃), 3.60-4.03 (m, 18H; 2 Ins-H and OCH₂CH₂O), 4.39 (dd, $J_1 = 5$ Hz, $J_2 = 4$ Hz, 1H; Ins-H).

¹³C NMR (50.3 MHz; CDCl₃): $\delta = 25.8$ (CH₃), 27.7 (CH₃), 59.0 (OCH₃), 60.1 (OCH₃), 70.3 (CH₂), 70.4 (CH₂), 70.6 (CH₂), 71.09 (CH₂), 71.11 (CH₂), 72.2 (CH₂), 72.3 (CH₂), 73.6 (Ins-C), 78.6 (Ins-C), 79.5 (Ins-C), 80.8 (Ins-C), 82.5 (Ins-C), 84.4 (Ins-C), 109.7 (CMe₂).

Elemental Analysis: Anal. Calcd. for $C_{19}H_{34}O_9 \cdot 0.75H_2O$ (419.985): C, 54.33; H, 8.52. Found: C, 54.39; H, 8.27%.

A small amount (0.07 g, 38%) of 1,4-di-*O*-methyl-5,6-(15-crown-5)-*myo*-inositol was also obtained.

1H NMR (200 MHz; $CDCl_3$): δ = 2.95-3.20 (m, 2H; Ins-H), 3.36-3.49 (m, 5H; Me, 2 OH), 3.50-4.16 (m, 26H; Me, OCH_2CH_2O , 3 Ins-H), 4.19 (t, J = 2.4 Hz, 1H; InsC2-H).

Racemic 1,2:4,5-diisopropylidene-3,6-di-*O*-methyl-*myo*-inositol (B1.26). A mixture of racemic 1,2:4,5-diisopropylidene-*myo*-inositol⁴⁹ (**B1.2**, 3.161 g, 12.1 mmol), sodium hydride (1.944 g, 48.6 mmol), and DMF (28 mL) was stirred at 0-5 °C for 10 min under nitrogen atmosphere; then methyl iodide (3 mL, 48.6 mmol) was added. The reaction mixture was allowed to come to room temperature and stirred for 30 min. Excess sodium hydride was destroyed by adding methanol (0.5 mL) and the solvent was evaporated under reduced pressure to obtain a solid. The solid was dissolved in dichloromethane (200 mL), washed with water (50 mL \times 3), and brine. The organic layer was dried over anhydrous sodium sulfate, and the solvent was removed under reduced pressure to obtain the crude dimethyl ether **B1.26**. This on filtration through a column of silica gel (eluent 20% ethyl acetate in light petroleum) gave **B1.26** as a white solid (2.136 g, 61%).

m.p: 81-83 °C. Crystallization from dichloromethane:light petroleum, gave rocky crystals. mp 83 °C.

IR ($CHCl_3$): $\tilde{\nu}$ = 3480-3550 cm^{-1} (H_2O).

1H NMR (200 MHz; $CDCl_3$): δ = 1.33 (s, 3H; CH_3), 1.39 (s, 3H; CH_3), 1.41 (s, 3H; CH_3), 1.52 (s, 3H; CH_3), 3.27 (dd, J_1 = 10 Hz, J_2 = 9 Hz, 1H; Ins-H), 3.40-3.50 (m, 1H; Ins-H),

3.52 (s, 6H; OCH₃), 3.59 (dd, $J_1 = 10$ Hz, $J_2 = 4$ Hz, 1H; Ins-H), 3.80-3.95 (m, 1H; Ins-H), 4.00-4.13 (m, 1H; Ins-H), 4.50 (t, $J = 5$ Hz, 1H; Ins-H).

¹³C NMR (50.3 MHz; CDCl₃): $\delta = 25.3$ (CH₃), 26.4 (CH₃), 27.5 (CH₃), 57.4 (OCH₃), 58.2 (OCH₃), 75.1 (Ins-C), 76.2 (Ins-C), 77.7 (Ins-C), 80.7 (Ins-C), 82.3 (Ins-C), 109.3 (CMe₂), 111.5 (CMe₂).

Elemental Analysis: Anal. Calcd. for C₁₄H₂₄O₆·0.2H₂O (291.944): C, 57.59; H, 8.42. Found: C, 57.77; H, 8.54%.

Racemic 1,2-*O*-isopropylidene-3,6-di-*O*-methyl-*myo*-inositol (B1.27). Procedure A.

The racemic dimethyl ether **B1.26** (0.050 g, 0.173 mmol) and *p*-toluenesulfonic acid (0.005 g, 0.029 mmol) were dissolved in acetone:water (40:1, 1.2 mL) mixture at room temperature and stirred for a few minutes (5-10 min.). Reaction was quenched by adding dry triethylamine (0.5 mL), and concentrated under vacuum to get white solid which on filtration type column (10% methanol in chloroform) gave liri dendritol (**B1.28**, 0.041 g, 95%). m.p 201 °C. Lit. m.p.²⁷ 203 °C.

Procedure B. The racemic dimethyl ether **B1.26** (0.144 g, 0.5 mmol), was dissolved in dry chloroform:methanol (2:1, 10 mL) and stirred with Amberlite 120 (H⁺) (0.144 g) for 30-40 min. Reaction was quenched by adding dry triethylamine (4 mL) and concentrated under reduced pressure to get solid. This was dissolved in methanol and filtered, which on concentration gave liri dendritol (**B1.28**, 0.120 g, 96%) m.p. 201 °C. Lit. m.p.²⁷ 203 °C.

Procedure C. The racemic dimethyl ether **B1.26** (0.100 g, 0.347 mmol) and *p*-toluenesulfonic acid (0.005 g, 0.029 mmol) were dissolved in dichloromethane: methanol (40:1, 1.2 mL) and stirred at 0 °C for 2 h. 45 min. Reaction was quenched by adding dry

triethylamine (2 mL) and concentrated under reduced pressure to obtain a solid. Column chromatography (10% methanol in chloroform) of the solid gave the diol **B1.27** (0.037 g, 43%) and liriiodendritol (**B1.28**, 0.033 g, 46%).

Data for B1.27:

m.p: 143-144 °C.

IR (CHCl₃): $\tilde{\nu} = 3400\text{-}3600\text{ cm}^{-1}$ (OH).

¹H NMR (200 MHz; CDCl₃): $\delta = 1.39$ (s, 3H; CH₃), 1.56 (s, 3H; CH₃), 2.98 (broad s, 2H; OH, D₂O exchangeable), 3.25-3.45 (m, 3H; Ins-H), 3.57 (s, 3H; OCH₃), 3.60 (s, 3H; OCH₃), 3.88 (t, $J = 9$ Hz, 1H; Ins-H), 4.00-4.15 (m, 1H; Ins-H), 4.52 (dd, $J_1 = 5$ Hz, $J_2 = 4$ Hz, 1H; Ins-H).

¹³C NMR (50.3 MHz; CDCl₃): $\delta = 25.9$ (CH₃), 28.0 (CH₃), 58.0 (OCH₃), 59.6 (OCH₃), 71.4 (Ins-C), 72.8 (Ins-C), 79.0 (Ins-C), 79.1 (Ins-C), 84.0 (Ins-C), 109.9 (CMe₂).

Elemental Analysis: Anal. Calcd. for C₁₁H₂₀O₆ (248.28): C, 53.21; H, 8.11. Found: C, 53.22; H, 8.35%.

Procedure D. The racemic dimethyl ether **B1.26** (0.600 g, 2.083 mmol) and acetyl chloride (0.22 mL, 0.003 mmol) were dissolved in dichloromethane: methanol (2:1, 12 mL) and stirred at 0 °C for 22 h. Analysis of the reaction mixture by TLC indicated the appearance of liriiodendritol and hence the reaction was quenched by adding dry triethylamine (2 mL). The reaction mixture was concentrated and the crude product was purified by column chromatography to get the diol **B1.27** (0.360 g, 70%), starting material **B1.26** (0.069 g, 13%) and liriiodendritol (**B1.28**, 0.062 g, 14%).

Procedure E. The racemic dimethyl ether **B1.26** (0.576 g, 2 mmol) and camphorsulfonic acid (0.002 g, 0.008 mmol) were dissolved in dry dichloromethane:methanol (2:1, 15

mL) and stirred for 2.5 h at room temperature under nitrogen atmosphere. The reaction was quenched by the addition of triethylamine (2 mL). The solvents were evaporated under reduced pressure to give a white solid. This crude product was purified over a column of silica gel (ethyl acetate-light petroleum, gradient elution) to obtain **B1.27** as a white solid (0.435 g, 87%). Crystallization from ethyl acetate: light petroleum gave colorless crystals.

Racemic 1,2-isopropylidene-3,4,5,6-tetra-O-methyl-myoinositol (B1.29). A mixture of the tetrol **B1.6** (2.0 g, 9.1 mmol), sodium hydride (3.636 g, 90.9 mmol), and THF (50 mL) was stirred for 10 min at 0-5 °C and then methyl iodide (11.5 mL, 185 mmol) was added drop-wise, and the reaction mixture was allowed to come to room temperature. After 30 min, DMF (15 mL) was added and stirring continued for 24 h. The reaction mixture was diluted with chloroform (100 mL), washed with water (20 mL × 3) followed by brine, and the organic layer was dried over anhydrous sodium sulfate. The solvent was removed under reduced pressure, and the residue was purified by flash column chromatography (eluent 15% ethyl acetate in light petroleum) to get **B1.29** as an oil (1.767 g, 70%).⁵⁰

¹H NMR (200 MHz; CDCl₃): δ = 1.35 (s, 3H; CH₃), 1.53 (s, 3H; CH₃), 3.00 (dd, $J_1 = 9$ Hz, $J_2 = 8$ Hz, 1H; Ins-H), 3.34-3.48 (m, 3H; Ins-H), 3.54 (s, 3H; OCH₃), 3.55 (s, 3H; OCH₃), 3.56 (s, 3H; OCH₃), 3.57 (s, 3H; OCH₃), 4.03 (t, $J = 6$ Hz, 1H; Ins-H), 4.40 (dd, $J_1 = 6$ Hz, $J_2 = 4$ Hz, 1H; Ins-H).

¹³C NMR (50.3 MHz; CDCl₃): δ = 25.2 (CH₃), 27.1 (CH₃), 58.7 (OCH₃), 59.5 (OCH₃), 59.7 (OCH₃), 73.4 (Ins-C), 78.0 (Ins-C), 78.7 (Ins-C), 82.0 (Ins-C), 83.3 (Ins-C), 83.8 (Ins-C), 109.4 (CMe₂).

Racemic 1,4,5,6-tetra-*O*-methyl-*myo*-inositol (B1.30). The tetramethyl ether **B1.29** (1.4 g, 5.1 mmol) obtained above was dissolved in acetic acid: water (4:1, 5 mL) and stirred at 100 °C for 3 h. The solution obtained was cooled to ambient temperature and evaporated under reduced pressure to get a solid. The product was purified by column chromatography to get the diol **B1.30** as a white solid (0.916 g, 77%). Crystallization from ethyl acetate: light petroleum, gave colorless needles.

m.p: 105-106 °C. Lit³¹ m.p. 102-104 °C.

IR (CHCl₃): $\tilde{\nu} = 3210\text{-}3600\text{ cm}^{-1}$ (OH).

¹H NMR (200 MHz; CDCl₃): $\delta = 2.56$ (s, 1H; OH, D₂O exchangeable), 2.68 (s, 1H; OH, D₂O exchangeable), 3.0 (t, $J = 9$ Hz, 1H; Ins-H), 3.05 (dd, $J_1 = 7$ Hz, $J_2 = 3$ Hz, 1H; Ins-H), 3.34-3.42 (m, 2H; Ins-H), 3.45 (t, $J = 9$ Hz, 1H; Ins-H), 3.50 (s, 3H; OCH₃), 3.61 (s, 3H; OCH₃), 3.62 (s, 3H; OCH₃), 3.65 (s, 3H; OCH₃), 4.22 (m, 1H; Ins-H).

¹³C NMR (50.3 MHz; CDCl₃): $\delta = 58.1$ (OCH₃), 60.5 (OCH₃), 60.8 (OCH₃), 68.4 (Ins-C), 71.2 (Ins-C), 81.6 (Ins-C), 82.6 (Ins-C), 82.8 (Ins-C), 85.1 (Ins-C).

Racemic 1,2-(18-crown-6)-3,4,5,6-tetra-*O*-methyl-*myo*-inositol (B1.31). The diol **B1.30** (0.236 g, 1 mmol), sodium hydride (0.160 g, 4 mmol), pentaerythritol ditosylate (0.710 g, 1.3 mmol) and dry THF (100 mL) were used to prepare the crown ether **B1.31** (as mentioned in the general procedure, page 101) which was isolated as a gum (0.163 g, 37%) after flash column chromatography (eluent 3% methanol in dichloromethane).

IR (Neat): $\tilde{\nu} = 3200\text{-}3650\text{ cm}^{-1}$ (H₂O).

¹H NMR (200 MHz; CDCl₃): δ = 2.85-2.98 (m, 2H; Ins-H), 3.05 (dd, $J_1 = 10$ Hz, $J_2 = 2$ Hz, 1H; Ins-H), 3.35-3.85 (m, 32H; OCH₃, OCH₂CH₂O), 3.97 (t, $J = 6$ Hz, 2H; Ins-H), 4.07 (t, $J = 3$ Hz, 1H; Ins-H).

¹³C NMR (50.3 MHz; CDCl₃): δ = 57.9 (OCH₃), 58.7 (OCH₃), 60.5 (OCH₃), 70.2 (CH₂), 70.6 (CH₂), 71.4 (CH₂), 71.6 (CH₂), 74.1 (Ins-C), 81.2 (Ins-C), 82.0 (Ins-C), 82.6 (Ins-C), 82.7 (Ins-C), 85.3 (Ins-C).

Elemental Analysis: Anal. Calcd. for C₂₀H₃₈O₁₀·H₂O (456.53): C, 52.61; H, 8.83. Found: C, 52.66; H, 8.73%.

Racemic 1,2-*O*-isopropylidene-3,6-di-*O*-benzyl-4,5-di-*O*-methyl-*myo*-inositol (B1.32).

Racemic 1,2-*O*-isopropylidene-3,6-di-*O*-benzyl-*myo*-inositol⁴⁰ (**B1.4**, 0.8 g, 2.0 mmol), sodium hydride (0.320 g, 8.0 mmol), and DMF (8 mL) were stirred at 0-5°C under nitrogen atmosphere for a few minutes. Then methyl iodide (0.74 mL, 12.0 mmol) was added drop-wise. The reaction mixture was allowed to come to room temperature and stirred for 20 h. The reaction was quenched by the addition of methanol (0.5 mL); DMF was removed under reduced pressure to obtain crude compound as a solid. This crude compound was dissolved in dichloromethane (200 mL), washed with water (50 mL × 3) followed by brine and the organic layer dried over anhydrous sodium sulfate. The solvent was evaporated under reduced pressure; the residue was purified by column chromatography (eluent 15% ethyl acetate in light petroleum) to get the dimethyl ether **B1.32** as a gum (0.753 g, 87%).

IR (Neat): $\tilde{\nu} = 3380-3540$ cm⁻¹(OH).

¹H NMR (200 MHz; CDCl₃): δ = 1.35 (s, 3H; CH₃), 1.50 (s, 3H; CH₃), 3.01-3.14 (m, 1H; Ins-H), 3.51-3.58 (m, 2H; Ins-H), 3.59 (s, 3H; OCH₃), 3.62 (s, 3H; OCH₃), 3.68 (dd, $J_1 =$

2 Hz, $J_2 = 1$ Hz, 1H; Ins-H), 4.07 (t, $J = 6$ Hz, 1H; Ins-H), 4.24 (dd, $J_1 = 6$ Hz, $J_2 = 3$ Hz, 1H; Ins-H), 4.70-4.90 (m, 4H; CH₂Ph), 7.30-7.50 (m, 10H; Ar-H).

¹³C NMR (50.3 MHz; CDCl₃): $\delta = 25.4$ (CH₃), 27.3 (CH₃), 60.1 (OCH₃), 72.9 (CH₂Ph), 73.4 (CH₂Ph), 74.3 (Ins-C), 76.3 (Ins-C), 78.4 (Ins-C), 81.6 (Ins-C), 82.3 (Ins-C), 83.9 (Ins-C), 109.4 (CMe₂) 127.2 (Ar-C), 127.5 (Ar-C), 127.6 (Ar-C), 128.0 (Ar-C), 128.1 (Ar-C), 138.1 (Ar-C), 138.3 (Ar-C).

Elemental Analysis: Anal. Calcd. for C₂₅H₃₂O₆·0.2H₂O (432.13): C, 69.48; H, 7.55; found: C, 69.43; H, 7.74%.

Racemic 1,4-di-O-benzyl-5,6-di-O-methyl-myo-inositol (B1.33). The dimethyl ether **B1.32** (0.720 g, 1.7 mmol) obtained above was dissolved in acetic acid: water (4:1, 10 mL) and stirred at 100 °C for 3 h. The solution obtained was cooled to ambient temperature and evaporated at reduced pressure to obtain a gum. Co-evaporation of the gum with dry benzene (10 mL × 3) gave **B1.33** as a white solid (0.538 g, 82%).

m.p.: 109-111 °C; crystallization from dichloromethane: light petroleum gave colorless needles, mp 111-112 °C.

IR (CHCl₃): $\tilde{\nu} = 3220$ -3568 cm⁻¹ (OH).

¹H NMR (200 MHz; CDCl₃): $\delta = 2.51$ (broad s, 2H; OH, D₂O exchangeable), 3.09 (t, $J = 9$ Hz, 1H; Ins-H), 3.31 (dd, $J_1 = 10$ Hz, $J_2 = 3$ Hz, 1H; Ins-H), 3.41 (dd, $J_1 = 10$ Hz, $J_2 = 3$ Hz, 1H; Ins-H), 3.58 (t, $J = 9$ Hz, 1H; Ins-H), 3.67 (s, 3H; OCH₃), 3.68 (s, 3H; OCH₃), 3.69-3.76 (m, 1H; Ins-H), 4.16 (t, $J = 3$ Hz, 1H; Ins-H), 4.65-5.10 (m, 4H; CH₂Ph), 7.25-7.45 (m, 10H; Ar-H).

¹³C NMR (50.3 MHz; CDCl₃): $\delta = 60.9$ (OCH₃), 61.1 (OCH₃), 69.3 (Ins-C), 71.4 (Ins-C), 72.5 (CH₂Ph), 75.2 (CH₂Ph), 79.5 (Ins-C), 81.1 (Ins-C), 83.4 (Ins-C), 85.2 (Ins-C), 127.6

(Ar-C), 127.7 (Ar-C), 127.9 (Ar-C), 128.37 (Ar-C), 128.39 (Ar-C), 137.9 (Ar-C), 138.6 (Ar-C).

Elemental Analysis: Anal. Calcd. for $C_{22}H_{28}O_6$ (388.46): C, 68.02; H, 7.26. Found: C, 68.16; H, 7.27%.

Racemic 1,2-(18-crown-6)-3,6-di-O-benzyl-4,5-di-O-methyl-myoinositol (B1.34). The racemic diol **B1.33** (0.200 g, 0.5 mmol), sodium hydride (0.124 g, 3.1 mmol), pentaerythritol ditosylate (0.365 g, 0.7 mmol) and dry THF (75 mL) were used to prepare the crown ether **B1.34** (as mentioned in the general procedure, page 101) which was isolated as a gum (0.207 g, 68%) after column chromatography (eluent 30% ethyl acetate in light petroleum).

IR ($CHCl_3$): $\tilde{\nu} = 3300-3500\text{ cm}^{-1}$ (H_2O).

1H NMR (200 MHz; $CDCl_3$): $\delta = 3.04$ (t, $J = 9$ Hz, 1H; Ins-H), 3.12 (dd, $J_1 = 10$ Hz, $J_2 = 2$ Hz, 1H; Ins-H), 3.19 (dd, $J_1 = 10$ Hz, $J_2 = 2$ Hz, 1H; Ins-H), 3.50-3.85 (m, 26H; OCH_3 , OCH_2CH_2O), 3.92 (t, $J = 5$ Hz, 1H; Ins-H), 4.00 (dd, $J_1 = 5$ Hz, $J_2 = 4$ Hz, 1H; Ins-H), 4.06 (t, $J = 2$ Hz, 1H; Ins-H), 4.55-4.95 (m, 4H; CH_2Ph), 7.25-7.45 (m, 10H; Ar-H).

^{13}C NMR (50.3 MHz; $CDCl_3$): $\delta = 60.8$ (OCH_3), 60.9 (OCH_3), 70.31 (CH_2), 70.37 (CH_2), 70.38 (CH_2), 70.42 (CH_2), 70.43 (CH_2), 70.55 (CH_2), 70.61 (CH_2), 70.63 (CH_2), 70.66 (CH_2), 71.8 (CH_2), 72.4 (CH_2), 75.28 (Ins-C), 75.3 (CH_2), 80.2 (Ins-C), 81.2 (Ins-C), 83.2 (Ins-C), 85.4 (Ins-C), 127.2 (Ar-C), 127.3 (Ar-C), 127.8 (Ar-C), 128.0 (Ar-C), 128.1 (Ar-C), 138.4 (Ar-C), 139.0 (Ar-C).

Elemental Analysis: Anal. Calcd. for $C_{32}H_{46}O_{10} \cdot H_2O$ (608.72): C, 63.14; H, 7.94. Found: C, 63.35; H, 8.03%.

Racemic 1,2-*O*-isopropylidene-3,6-di-*O*-methyl-4,5-di-*O*-benzyl-*myo*-inositol (B1.35).

A mixture of racemic **B1.27** (1.045 g, 4.2 mmol), sodium hydride (2.524 g, 63.1 mmol) and DMF (10 mL) was stirred at 0-5 °C under nitrogen atmosphere and then benzyl bromide (5 mL, 42 mmol) was added drop-wise. The reaction mixture was allowed to attain room temperature and stirred for 1 h. Excess sodium hydride was destroyed by adding methanol (0.5 mL) and the mixture concentrated under reduced pressure to get a semi-solid. It was dissolved in chloroform (200 mL), washed with water (30 mL × 4) followed by brine and dried over anhydrous sodium sulfate. The solvent was evaporated under reduced pressure to get crude **B1.35** as an oily liquid. The crude product was purified by column chromatography (eluent 10% ethyl acetate in light petroleum) to obtain the dibenzyl ether **B1.35** as a gum (0.965 g, 53%).

¹H NMR (200 MHz; CDCl₃): δ = 1.41 (s, 3H; CH₃), 1.59 (s, 3H; CH₃), 3.37 (t, *J* = 9 Hz, 1H; Ins-H), 3.45-3.56 (m, 2H; Ins-H), 3.60 (s, 3H; OCH₃), 3.63 (s, 3H; OCH₃), 3.89 (t, *J* = 9 Hz, 1H; Ins-H), 4.12 (dd, *J*₁ = 7 Hz, *J*₂ = 6 Hz, 1H; Ins-H), 4.48 (dd, *J*₁ = 5 Hz, *J*₂ = 4 Hz, 1H; Ins-H), 4.70-4.95 (m, 4H; CH₂Ph), 7.30-7.55 (m, 10H; Ar-H).

¹³C NMR (50.3 MHz; CDCl₃): δ = 25.6 (CH₃), 27.6 (CH₃), 59.0 (OCH₃), 60.0 (OCH₃), 73.5 (Ins-C), 74.94 (CH₂Ph), 74.98 (CH₂Ph), 78.6 (Ins-C), 79.5 (Ins-C), 80.5 (Ins-C), 82.0 (Ins-C), 84.3 (Ins-C), 109.7 (CMe₂), 127.5 (Ar-C), 127.8 (Ar-C), 128.2 (Ar-C), 138.5 (Ar-C).

Elemental Analysis: Anal. Calcd. for C₂₅H₃₂O₆ (428.53): C, 70.07; H, 7.52. Found: C, 69.63; H, 7.33%.

Racemic 1,4-di-*O*-methyl-5,6-di-*O*-benzyl-*myo*-inositol (B1.36). A mixture of racemic **B1.35** (0.924 g, 2.1 mmol), acetic acid: water (4:1, 10 mL) was stirred at 100 °C for 3 h.

The reaction mixture was cooled to ambient temperature and concentrated under reduced pressure to obtain a gum. Co-evaporation of the residue with dry benzene (7 mL \times 3) gave a white solid. It was purified by column chromatography (eluent 50% ethyl acetate in light petroleum) to obtain the diol **B1.36** as a white solid (0.647 g, 77%).

m.p: 112-114 °C.

IR (CHCl₃): $\tilde{\nu}$ = 3270-3585 cm⁻¹ (OH).

¹H NMR (400 MHz; CDCl₃): δ = 2.62 (broad s, 1H; OH, D₂O exchangeable), 2.69 (broad s, 1H; OH, D₂O exchangeable) 3.20 (dd, J_1 = 9 Hz, J_2 = 3 Hz, 1H; Ins-H), 3.39 (t, J = 9 Hz, 1H; Ins-H), 3.45 (dd, J_1 = 10 Hz, J_2 = 3 Hz, 1H; Ins-H), 3.53 (s, 3H; OCH₃), 3.54-3.59 (m, 1H; Ins-H), 3.66 (s, 3H; OCH₃), 3.85 (t, J = 9 Hz, 1H; Ins-H), 4.26 (t, J = 3 Hz, 1H; Ins-H), 4.75-4.90 (m, 4H; CH₂Ph), 7.25-7.40 (m, 10H; Ar-H).

¹³C NMR (50.3 MHz; CDCl₃): δ = 58.3 (OCH₃), 61.3 (OCH₃), 68.5 (Ins-C), 71.6 (Ins-C), 75.4 (CH₂Ph), 75.6 (CH₂Ph), 81.4 (Ins-C), 82.1 (Ins-C), 82.9 (Ins-C), 83.0 (Ins-C), 127.4 (Ar-C), 127.7 (Ar-C), 127.8 (Ar-C), 128.2 (Ar-C), 138.4 (Ar-C), 138.6 (Ar-C).

Elemental Analysis: Anal. Calcd. for C₂₂H₂₈O₆ (388.46): C, 68.02; H, 7.26. Found: C, 67.62; H, 7.31.

Racemic 1,2-(18-crown-6)-3,6-di-O-methyl-4,5-di-O-benzyl-myo-inositol (B1.37).

Racemic **B1.36** (0.200 g, 0.5 mmol), sodium hydride (0.074 g, 3.1 mmol), pentaerythritol ditosylate (0.365 g, 0.7 mmol) and dry THF (75 mL) were used to prepare the crown ether **B1.37** (as mentioned in the general procedure, page 101) which was isolated as a gum (0.222 g, 74%) after column chromatography (eluent 25% ethyl acetate in light petroleum).

IR (Neat): $\tilde{\nu}$ = 3481-3587 cm⁻¹ (H₂O).

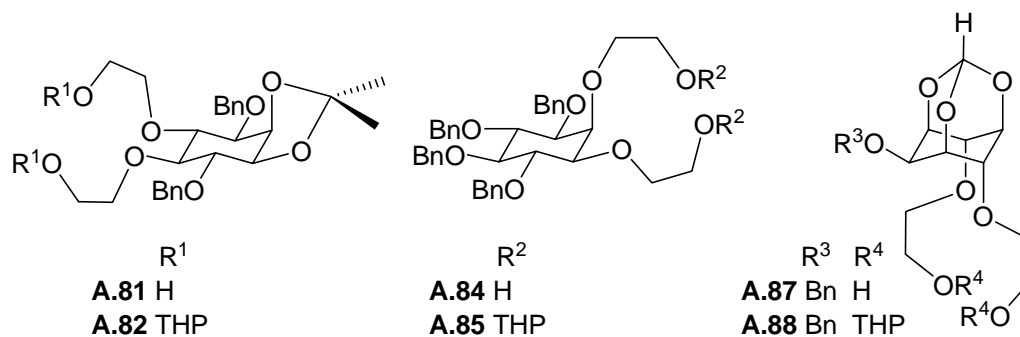
¹H NMR (200 MHz; CDCl₃): δ = 3.00-3.19 (m, 2H; Ins-H), 3.31 (t, *J* = 9 Hz, 1H; Ins-H), 3.50 (s, 3H; OCH₃), 3.61-3.82 (m, 23H; OCH₃, OCH₂CH₂O), 3.99 (t, *J* = 6 Hz, 2H; Ins-H), 4.12 (t, *J* = 2 Hz, 1H; Ins-H), 4.55-5.05 (m, 4H; CH₂Ph), 7.25-7.45 (m, 10H; Ar-H).

¹³C NMR (50.3 MHz; CDCl₃): δ = 58.2 (OCH₃), 61.0 (OCH₃), 70.38 (CH₂), 70.43 (CH₂), 70.5 (CH₂), 70.7 (CH₂), 70.8 (CH₂), 70.9 (CH₂), 71.7 (CH₂), 71.8 (CH₂), 74.3 (Ins-C), 75.6 (CH₂Ph), 75.7 (CH₂Ph), 81.4 (Ins-C), 81.6 (Ins-C), 82.7 (Ins-C), 83.1 (Ins-C), 83.5 (Ins-C), 127.3 (Ar-C), 127.4 (Ar-C), 127.8 (Ar-C), 128.2 (Ar-C), 138.8 (Ar-C), 138.9 (Ar-C).

Elemental Analysis: Anal. Calcd. for C₃₂H₄₆O₁₀·H₂O (608.72): C, 63.14; H, 7.94. Found: C, 63.34; H, 7.81%.

TABLE B1.13: Association constants ($K_a \times 10^{-4} \text{ dm}^3 \text{ mol}^{-1}$) in CDCl_3 for the binding of podands¹ **A.81**, **A.82**, **A.84**, **A.85**, **A.87** and **A.88** with metal picrates at 25 °C.

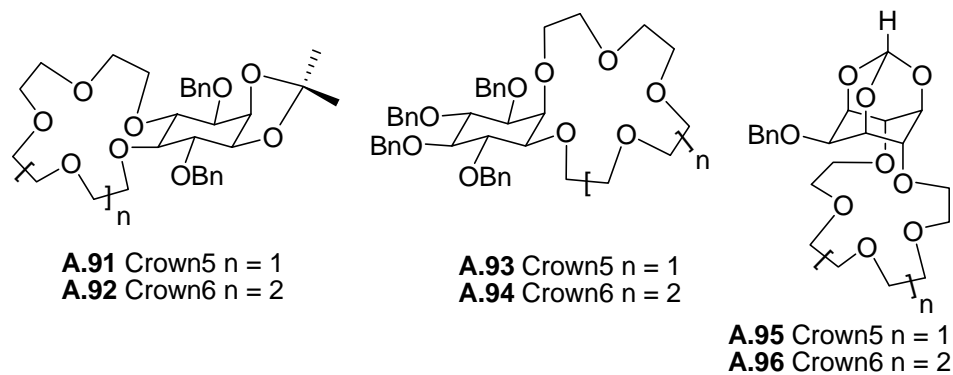
Reproduced from reference 1.



Podand	Li^+	Na^+	K^+	Cs^+	NH_4^+	Ag^+
A.81	2.337	— ^a	0.311	0.054	0.152	4.04
A.82	20.887	1.709	0.485	0.26	0.576	7.355
A.84	5.275	0.324	0.436	0.152	0.182	11.281
A.85	22.14	0.501	0.627	0.562	0.168	11.4
A.87	2.331	0.07	— ^a	— ^a	0.008	1.262
A.88	20.55	1.488	0.568	0.152	0.287	1.423

^a No detectable amount of picrate was present.

TABLE B1.14: Association constants ($K_a \times 10^{-4} \text{ dm}^3 \text{ mol}^{-1}$) in CDCl_3 for the binding of crown ethers² **A.91-A.96** with lithium picrate at 25°C . Reproduced from reference 2.



Crown ether	Li^+	Na^+	K^+	Cs^+	NH_4^+	Ag^+
A.91	9.57	4.43	2.59	1.31	0.81	34.2
A.92	4.87	4.66	32.6	1.93	7.87	186
A.93	12.9	64.7	6.7	1.33	1.83	2.76×10^4
A.94	16.3	45.5	35.2×10^4	11.8	586	4.95×10^6
A.95	12.0	38.6	2.47	0.49	1.02	590
A.96	9.71	6.28	757	1.11	171	89.1

Table B1.15: Ratio of association constants between metal picrates for a given *myo*-inositol derived crown ether.

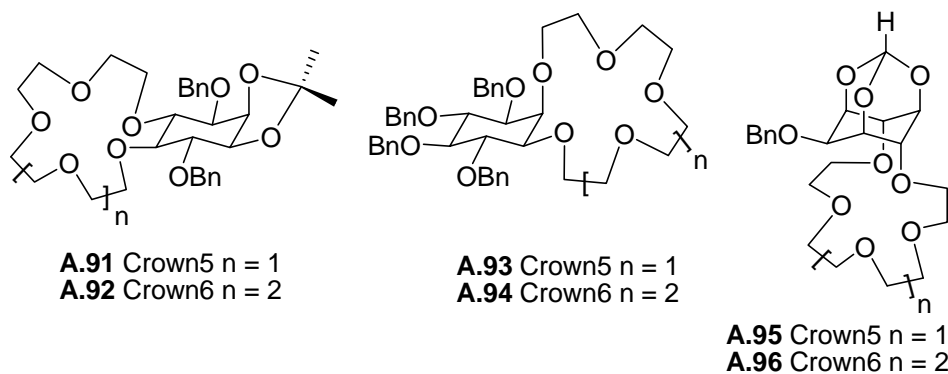
Crown ether	Li^+/Na^+	Li^+/K^+	Li^+/Cs^+	$\text{Li}^+/\text{NH}_4^+$	Li^+/Ag^+
B1.14	9.2	39.4	43.9	129.5	30.2
A.91 ²	2.2	3.7	7.3	11.8	0.3
A.94 ²	0.358	4.63×10^{-4}	1.38	0.027	3.29×10^{-6}
B1.22	6.5	23.3	53.8	141.8	91.8
B1.25	101.2	133.9	359.1	482.8	63.6
B1.31	0.3	0.04	1.3	0.08	0.03
B1.34	0.4	0.02	0.8	0.07	0.03
B1.37	0.3	0.02	0.2	8×10^{-3}	0.02
	Na^+/Li^+	Na^+/K^+	Na^+/Cs^+	$\text{Na}^+/\text{NH}_4^+$	Na^+/Ag^+
B1.14	0.108	4.28	4.77	14.09	3.28
A.91 ²	0.462	1.71	3.38	5.46	0.129
A.94 ²	2.79	1.29×10^{-3}	3.85	0.077	9.19×10^{-6}
B1.22	0.153	3.56	8.24	21.72	14.05
B1.25	9.8×10^{-3}	1.32	3.54	4.77	0.628
B1.31	3.72	0.135	4.96	0.293	0.103
B1.34	2.252	0.039	1.897	0.156	0.076
B1.37	3.562	0.061	0.755	0.03	0.081
	K^+/Li^+	K^+/Na^+	K^+/Cs^+	K^+/NH_4^+	K^+/Ag^+

B1.14	0.02	0.2	1.1	3.3	0.8
A.91²	0.3	0.6	2	3.2	0.07
A.94²	2159	773.6	2983	60	7×10^{-3}
B1.22	0.04	0.3	2.3	6.1	3.9
B1.25	7×10^{-3}	0.8	2.7	3.6	0.5
B1.31	27.4	7.4	36.6	2.2	0.8
B1.34	57.4	25.5	48.4	4	2
B1.37	57.8	16.2	12.2	0.5	1.3
	Cs⁺/Li⁺	Cs⁺/Na⁺	Cs⁺/K⁺	Cs⁺/NH₄⁺	Cs⁺/Ag⁺
B1.14	0.022	0.209	0.898	2.95	0.688
A.91²	0.136	0.295	0.505	1.61	0.038
A.94²	0.733	0.259	3.35×10^{-3}	0.02	2.38×10^{-6}
B1.22	6.52	23.28	53.79	141.81	91.76
B1.25	2.78×10^{-3}	0.281	0.372	1.344	0.177
B1.31	0.748	0.201	0.207	0.59	0.02
B1.34	1.187	0.527	0.02	0.082	0.04
B1.37	4.712	1.323	0.081	0.04	0.107
	NH₄⁺/Li⁺	NH₄⁺/Na⁺	NH₄⁺/K⁺	NH₄⁺/Cs⁺	NH₄⁺/Ag⁺
B1.14	7.7×10^{-3}	0.07	0.304	0.338	0.233
A.91²	0.084	0.182	0.312	0.618	0.023
A.94²	35.95	12.87	0.016	49.66	1.183

B1.22	7×10^{-3}	0.05	0.2	0.4	0.6
B1.25	2×10^{-3}	0.2	0.3	0.7	0.1
B1.31	14.4	6.4	0.2	12.1	0.5
B1.34	117.2	32.9	2	24.9	2.7
	Ag⁺/Li⁺	Ag⁺/Na⁺	Ag⁺/K⁺	Ag⁺/Cs⁺	Ag⁺/NH₄⁺
B1.14	0.03	0.3	1.3	1.4	4.3
A.91²	3.6	7.7	13.2	26.1	42.2
A.94²	3×10^5	1.1×10^5	140.6	4.2×10^5	8447
B1.22	0.01	0.07	0.2	0.6	1.5
B1.25	0.01	1.6	2.1	5.6	7.6
B1.31	36	9.7	1.3	48.2	2.8
B1.34	29.6	13.1	0.5	24.9	2
B1.37	43.7	12.3	0.8	9.3	0.4

For the calculation of ratio of binding constants, K_a values for **A.91** and **A.94**, were obtained from reference 2.

TABLE B1.16: Ratio of association constants: lithium picrate to other picrates for crown-5 and crown-6-ethers.²



Ratio	Li^+/Na^+	Li^+/K^+	Li^+/Cs^+	$\text{Li}^+/\text{NH}_4^+$	Li^+/Ag^+
A.92	1.04	0.149	2.52	0.618	0.026
A.93	0.199	1.92	9.69	7.04	4.67×10^{-4}
A.95	0.31	4.85	24.48	11.76	0.02
A.96	1.54	0.012	8.77	0.056	0.108

1.8 References

- 1 Sureshan, K. M.; Shashidhar, M. S.; Varma, A. J. *J. Chem. Soc., Perkin Trans. 2* **2001**, 2298-2302.
- 2 Sureshan, K. M.; Shashidhar, M. S.; Varma, A. J. *J. Org. Chem.* **2002**, *67*, 6884-6888.
- 3 (a) Paquette, L. A.; Tae, J.; Hickey, E. R.; Rogers, R. D. *Angew. Chem., Int. Ed.* **1999**, *38*, 1409-1411. (b) Paquette, L. A.; Tae, J.; Gallucci, J. C. *Org. Lett.* **2000**, *2*, 143-146. (c) Paquette, L. A.; Tae, J.; Hickey, E. R.; Trego, W. E.; Rogers, R. D. *J. Org. Chem.* **2000**, *65*, 9160-9171. (d) Paquette, L. A.; Tae, J. *J. Am. Chem. Soc.* **2001**, *123*, 4974-4984. (e) Paquette, L. A.; Ra, C. S.; Gallucci, J. C.; Kang, H.-J.; Ohmori, N.; Arrington, M. P.; David, W.; Brodbelt, J. S. *J. Org. Chem.* **2001**, *66*, 8629-8639. (f) Hilmey, D. G.; Paquette, L. A. *J. Org. Chem.* **2004**, *69*, 3262-3270. (g) Paquette, L. A.; Selvaraj, P. R.; Keller, K. M.; Brodbelt, J. S. *Tetrahedron*, **2005**, *61*, 231-240.
- 4 Billington, D. C.; Baker, R.; Kulagowski, J. J.; Mawer, I. M.; Vacca, J. P.; deSolms, S. J.; Huff, J. R. *J. Chem. Soc., Perkin Trans. 1* **1989**, 1423-1429.
- 5 Das, T.; Shashidhar, M. S. *Carbohydr. Res.* **1997**, *297*, 243-249.
- 6 Sureshan, K. M.; Shashidhar, M. S. *Tetrahedron Lett.* **2000**, *41*, 4185-4188.
- 7 Sureshan, K. M.; Shashidhar, M. S. *Tetrahedron Lett.* **2001**, *42*, 3037-3039.
- 8 (a) Ebstein, R. P.; Lerer, B.; Bennett, E. R.; Shapira, B.; Kindler, S.; Shemesh, Z.; Gerstenhaber, N. *Psychiatry Res.* **1988**, *24*, 45-52. (b) Miller, D. J.; Surfraz, M. B.-U.; Akhtar, M.; Gani, D.; Allemann, R. K. *Org. Biomol. Chem.* **2004**, *2*, 671-688.

-
- (c) Surfraz, M. B-U.; Miller, D. J.; Gani, D.; Allemann, R. K. *Tetrahedron Lett.* **2003**, *44*, 7677-7679.
- 9 (a) Emilien, G.; Maloteaux, J. M.; Seghers, A.; Charles, G. *Arch. Int. Pharmacodyn. Ther.* **1995**, *330*, 251-278. (b) Divish, M. M.; Sheftel, G.; Boyle, A.; Kalasapudi, V. D.; Papolos, D. F.; Lachman, H. M. *J. Neurosci. Res.* **1997**, *28*, 40-48. (c) Dixon, J. F. *Proc. Natl. Acad. Sci., USA*, **1997**, *94*, 4757-4760.
- 10 (a) Pedersen, C. J. *J. Am. Chem. Soc.* **1967**, *89*, 2495-2496. (b) Pedersen, C. J. *J. Am. Chem. Soc.* **1967**, *89*, 7017-7036. (c) Pedersen, C. J. in *Synthetic Multidentate Macrocyclic Compounds*, Eds. Izatt, R. M.; Christensen, J. J., Academic Press, New York, **1978**. (d) Olsher, U. *J. Am. Chem. Soc.* **1982**, *104*, 4006-4007. (e) Shoham, G.; Lipscomb, W. N.; Olsher, U. *J. Chem. Soc., Chem. Commun.* **1983**, 208-209. (f) Shoham, G.; Christianson, D. W.; Bartsch, R. A.; Heo, G. S.; Olsher, U.; Lipscomb, W. N. *J. Am. Chem. Soc.* **1984**, *106*, 1280-1285. (g) Kitazawa, S.; Kimura, K.; Yano, H.; Shono, T. *J. Am. Chem. Soc.* **1984**, *106*, 6978-6983. (h) Czech, B. P.; Babb, D.A.; Son, B.; Bartsch, R. A. *J. Org. Chem.* **1984**, *49*, 4805-4810. (i) Bartsch, R. A.; Czech, B. P.; Kang, S. I.; Stuart, L. E.; Walkowiak, W.; Charewicz, G. S. H.; Son, B. *J. Am. Chem. Soc.* **1985**, *107*, 4997-4998. (j) Kimura, K.; Yano, H. Kitazawa, S.; Shono, T. *J. Chem. Soc., Perkin Trans 2* **1986**, 1945-1951. (k) Kimura, K.; Tanaka, M.; Iketani, S-I.; Shono, T. *J. Org. Chem.* **1987**, *52*, 836-844. (l) Pedersen, C. J. *J. Inclusion Phenom.* **1988**, *6*, 337-350. (m) Olsher, U.; Bartsch, R. A.; Pugia, M. J.; Shoham, G. *J. Am. Chem. Soc.* **1989**, *111*, 9217-9222. (n) Bartsch, R. A. *Solvent Extr. Ion Exch.* **1989**, *7*, 829-854. (o) Katky, R.; Nicholson, P. E.; Parker, D. *J. Chem. Soc., Perkin Trans. 2* **1990**, 321-327. (p) Olsher, U.;

-
- Frolow, F.; Dalley, N. K.; Weiming, J.; Yu, Z-Y.; Knobeloch, J. M.; Bartsch, R. A. *J. Am. Chem. Soc.* **1991**, *113*, 6570-6574. (q) Dalley, N. K.; Jiang, W. M.; Olsher, U. *J. Incl. Phenom. Mol. Recogn.* **1992**, *12*, 305-312. (r) Suzuki, K.; Yamada, H.; Sato, K.; Watanabe, K.; Hisamoto, H.; Tobe, Y.; Kobiro, K. *Anal. Chem.* **1993**, *65*, 3404-3410. (s) Inoue, Y.; Hakushi, T.; Liu, Y.; Tong, L. H. *J. Org. Chem.* **1993**, *58*, 5411-5413.
- 11 Compounds reported in this thesis are either *racemic* or have *meso* configuration. However, for racemic compounds, one of the enantiomers is shown in schemes for brevity and simplicity. Accordingly, numbering of inositol ring carbons may be clockwise or anti-clockwise.
- 12 Gigg, J.; Gigg, R.; Payne, S.; Conant, R. *J. Chem. Soc., Perkin Trans. 1* **1987**, 423-429.
- 13 Gigg, R.; Warren, C. D. *J. Chem. Soc. (C)*, **1969**, 2367-2371.
- 14 (a) Pedersen, C. J.; Frensdroff, H. K. *Angew. Chem. Int. Ed.* **1972**, *11*, 16-25. (b) Christensen, J. J.; Eatough, D. J.; Izatt, R. M. *Chem. Rev.* **1974**, *74*, 351-384. (c) Izatt, R. M.; Bradshaw, J. S.; Nielsen, S. A.; Lamb, J. D.; Christensen, J. J. *Chem. Rev.* **1985**, *85*, 271-339. (d) Inokuma, S.; Takezawa, M.; Satoh, H.; Nakamura, Y.; Sasaki, T.; Nishimura, J. *J. Org. Chem.* **1998**, *63*, 5791-5796.
- 15 Moore, S. S.; Tarnowski, T. L.; Newcomb, M.; Cram, D. J. *J. Am. Chem. Soc.* **1977**, *99*, 6398-6405.
- 16 Iimori, T.; Erickson, S. D.; Rheingold, A. L.; Still, W. C. *Tetrahedron Lett.* **1989**, *30*, 6947-6950.
- 17 Devaraj, S.; Shashidhar, M. S.; Dixit, S. S. *Tetrahedron* **2005**, *61*, 529-536.

-
- 18 Baudin, G.; Glänzer, B. I.; Swaminathan, K. S.; Vasella, A. *Helv. Chim. Acta* **1988**, *71*, 1367-1378.
- 19 Dixit, S. S.; Shashidhar, M. S.; Devaraj, S. *Tetrahedron* **2006**, *62*, 4360-4363.
- 20 (a) Jedlinski, Z. *Pure. Appl. Chem.* **1993**, *65*, 483-488. (b) Botti, P.; Ball, H. L.; Rizzi, E.; Lucietto, P.; Pinori, M.; Mascagni, P. *Tetrahedron* **1995**, *51*, 5447-5458. (c) van Nostrum, C. F.; Picken, S. J.; Schouten, A.-J.; Nolte, R. J. M. *J. Am. Chem. Soc.* **1995**, *117*, 9957-9965. (d) *Comprehensive Supramolecular Chemistry Vol. 1, Molecular Recognition: Receptors for Cationic Guests*, Ed. Gokel, G. W. Pergamon Press, New York, N.Y. **1996**. (e) Itoh, T.; Takagi, Y.; Murakami, T.; Hiyama, Y.; Tsukube, H. *J. Org. Chem.* **1996**, *61*, 2158-2163. (f) Shephard, D. S.; Johnson, B. F. G.; Matters, J.; Simon, P. *J. Chem. Soc., Dalton Trans*, **1998**, 2289-2292.
- 21 (a) Otda, K.; Kimura, S.; Imanishi, Y. *J. Chem. Soc., Perkin Trans 1* **1993**, 3011-3016. (b) Reetz, M. T.; Huff, J.; Rudolph, J.; Toellner, K.; Deege, A.; Goddard, R. *J. Am. Chem. Soc.* **1994**, *116*, 11588-11589.
- 22 (a) *Crown Compounds*, Cooper, S. R. Ed. VCH, New York, N. Y. **1992**. (b) Dumont, B.; Joly, J.-P.; Chapleur, Y.; Marsura, A. *Bioorg. Med. Chem. Lett.* **1994**, *4*, 1123-1126.
- 23 (a) Hegetschweiler, K. *Chem. Soc. Rev.* **1999**, *28*, 239-249 and references cited therein. (b) Angyal, S. J. *Carbohydr. Res.* **2000**, *325*, 313-320. (c) Grote, Z.; Lehaire, M.-L.; Scopelliti, R.; Severin, K. *J. Am. Chem. Soc.* **2003**, *125*, 13638-13639.
- 24 Talanova, G. G.; Elkarim, N. S. A.; Talanov, V. S.; Hanes, Jr. R. E.; Hwang, H.-S.; Bartsch, R. A.; Rogers, R. D. *J. Am. Chem. Soc.* **1999**, *121*, 11281-11290.

-
- 25 Dixit, S. S.; Shashidhar, M. S. *Tetrahedron* **2007** (Accepted).
 - 26 Sarmah, M. P. PhD. Thesis, April **2005**, University of Pune.
 - 27 Angyal, S. J.; Bender, V. J. *Chem. Soc.* **1961**, 4718-4720.
 - 28 Ravikumar, K. S.; Farquhar, D. *Tetrahedron Lett.* **2002**, *43*, 1367-1368.
 - 29 Gauthier, D. R.; Bender, S. L. *Tetrahedron Lett.* **1996**, *37*, 13-16.
 - 30 Kozikowski, A. P.; Fauq, A. H. *J. Am. Chem. Soc.* **1990**, *112*, 7403-7404.
 - 31 Angyal, S. J.; Melrose, G. J. H. *J. Chem. Soc.* **1965**, 6494-6500.
 - 32 Jarosz, S.; Listkowski, A. *Current Org. Chem.* **2006**, *10*, 643-662 and references cited therein.
 - 33 Yamato, K.; Fernandez, F. A.; Vogel, H. F.; Bartsch, R. A.; Dietz, M. L. *Tetrahedron Lett.* **2002**, *43*, 5229-5232.
 - 34 Costero, A. M.; Villarroya, J. P.; Gil, S.; Aurell, M. J.; Ramirez de Arellano, M. C. *Tetrahedron* **2002**, *58*, 6729-6734.
 - 35 Futterer, T.; Merz, A.; Lex, J. *Angew. Chem., Int. Ed. Engl.* **1997**, *36*, 611-613.
 - 36 Kim, H. S.; Ryu, J. H.; Kim, H.; Ahn, B. S.; Kang, Y.S. *Chem. Commun.* **2000**, 1261-1262.
 - 37 Ikeda, M.; Tanida, T.; Takeuchi, M.; Shinkai, S. *Org. Lett.* **2000**, *2*, 1803-1805.
 - 38 Bakker, W. I. I.; Verboom, W.; Reinhoudt, D. N. *J. Chem. Soc., Chem. Commun.* **1994**, 71-72.
 - 39 Casnati, A.; Pochini, A.; Ungaro, R.; Bocchi, C.; Ugozzoli, F.; Egberink, R. J. M.; Struijk, H.; Lutenberg, R.; de Jong, F.; Reinhoudt, D. N. *Chem. Eur. J.* **1996**, *2*, 436-445.

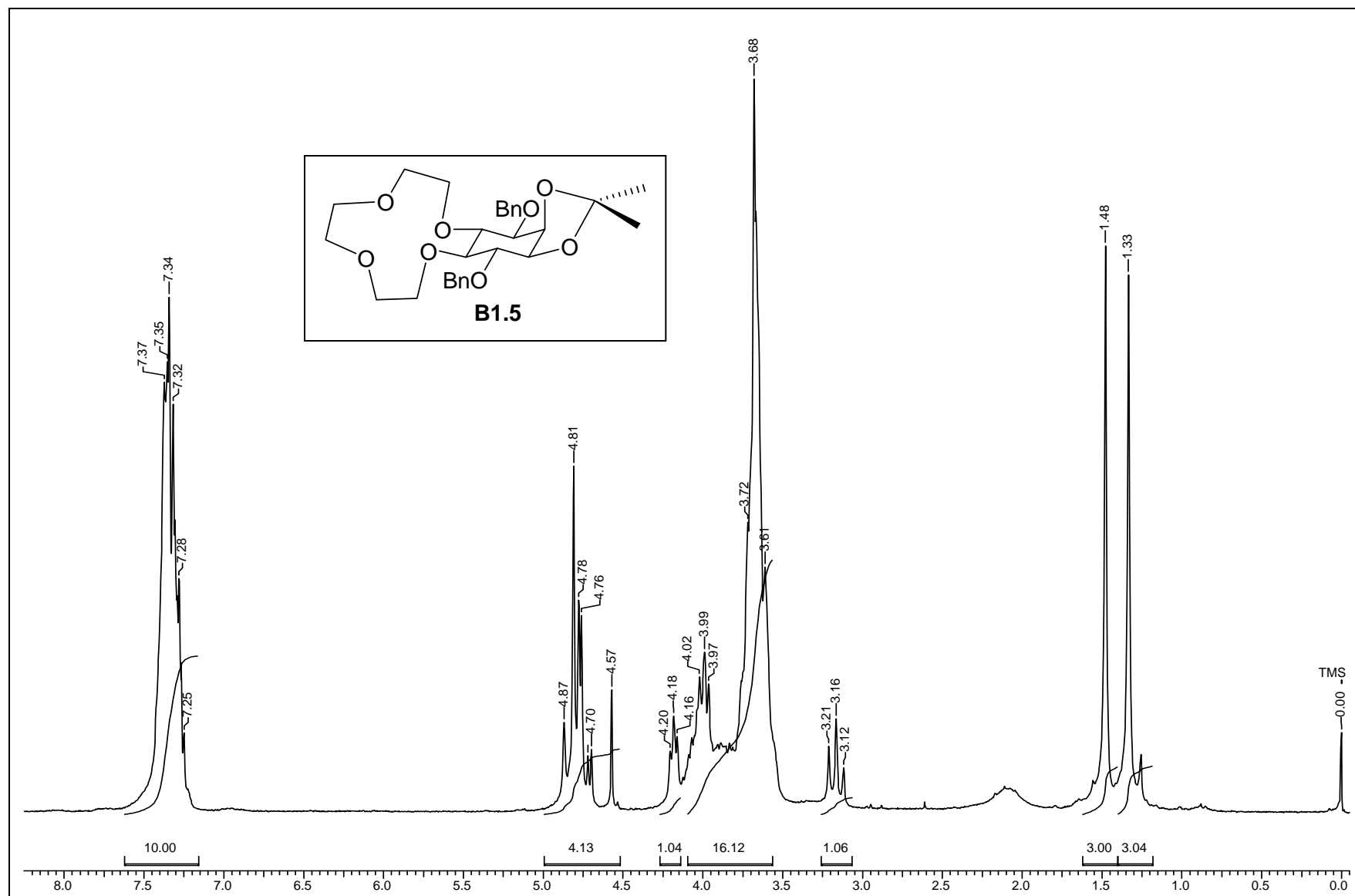
- 40 Ghidini, E.; Ugozzoli, F.; Ungaro, R.; Harkema, S.; El-Fadl, A. A.; Reinhoudt, D. N. *J. Am. Chem. Soc.* **1990**, *112*, 6979-6985.
- 41 Armarego, W. L. F.; Perrin, D. D. *Purification of Laboratory Chemicals*, Butterworth-Heinemann, Oxford, **1996**.
- 42 Copland, M. A.; Fuoss, R. M. *J. Phys. Chem.* **1964**, *68*, 1177-1180.
- 43 Silberrad, O.; Phillips, H. A. *J. Chem. Soc.* **1908**, *93*, 474-489.
- 44 Brown, R.; Jones, W. E. *J. Chem. Soc.* **1946**, 781-782.
- 45 Inoue, Y.; Ouchi, M.; Hakushi, T. *Bull. Chem. Soc. Jpn.* **1985**, *58*, 525-530.
- 46 Ouchi, M.; Inoue, Y.; Kanzaki, T.; Hakushi, T. *J. Org. Chem.* **1984**, *49*, 1408-1412.
- 47 SHELX-97, Sheldrick, G. M. SHELX97, Program for crystal structure solution and refinement, University of Göttingen, Germany, 1997
- 48 Burnett, M. N.; Johnson, C. K. ORTEP III, report ORNL- 6895, Oak Ridge National Laboratory, Tennessee, U.S.A., 1996
- 49 Gigg, J.; Gigg, R.; Payne, S.; Conant, R. *Carbohydr. Res.* **1985**, *142*, 132-134.
- 50 Gent, P. A.; Gigg, R. *J. Chem. Soc. (C)*, **1970**, *16*, 2253-2255.

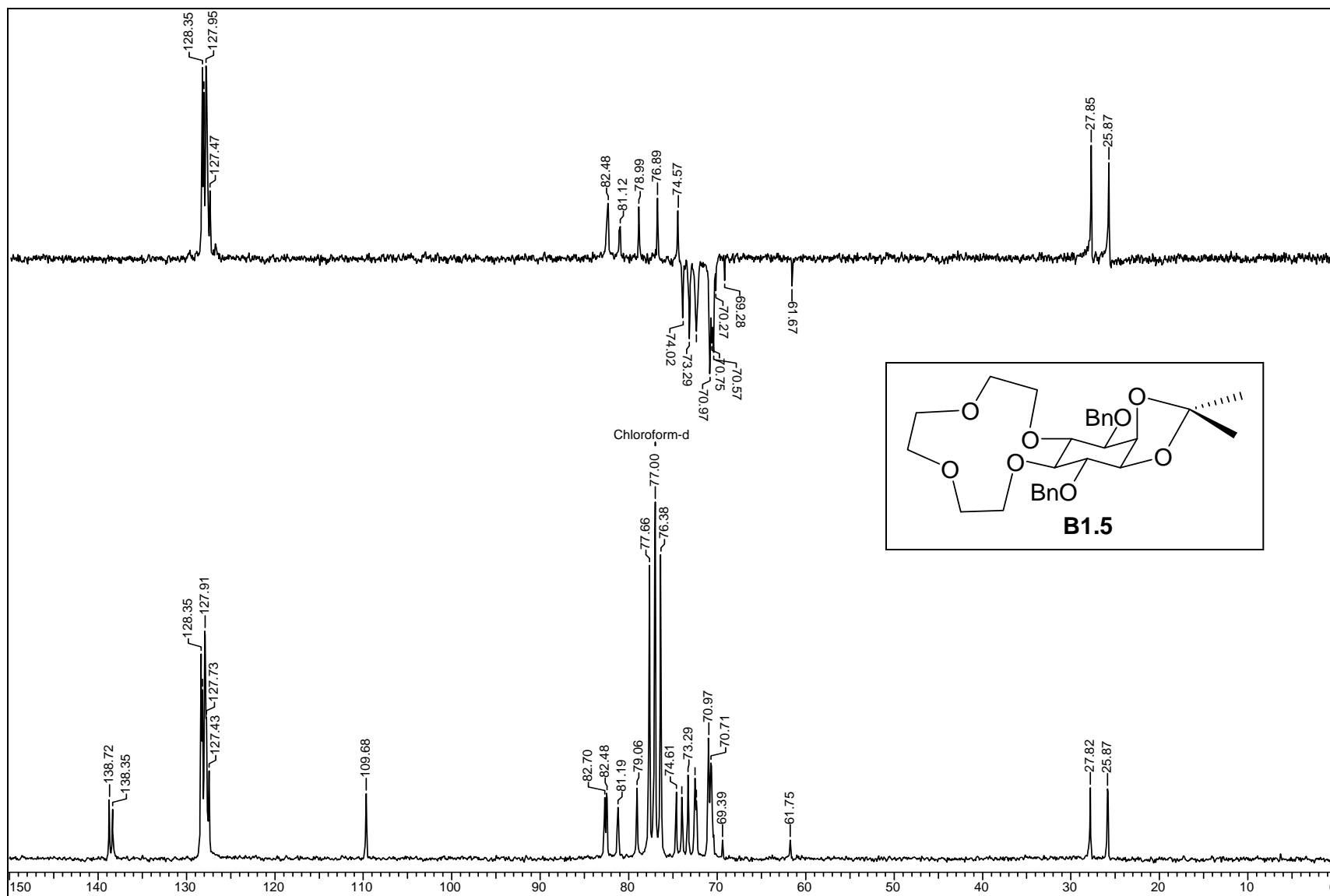
1.9 Appendix

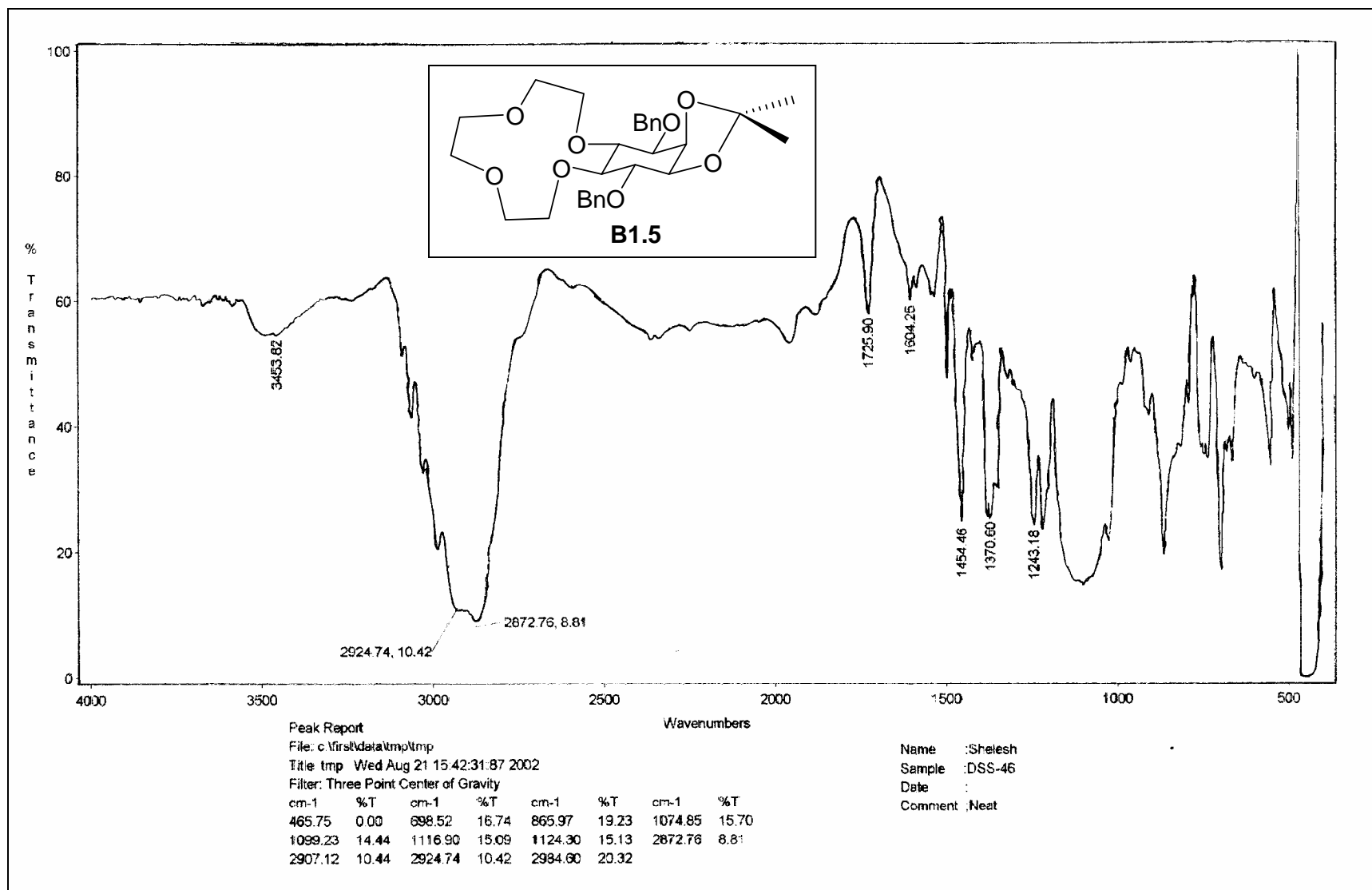
Sr. No	Index	Page No.
1	^1H spectrum of B1.5	133
2	^{13}C and DEPT NMR spectrum of B1.5	134
3	IR spectrum of B1.5	135
4	^1H spectrum of B1.9	136
5	^{13}C and DEPT NMR spectrum of B1.9	137
6	IR spectrum of B1.9	138
7	^1H spectrum of B1.14	139
8	^{13}C and DEPT NMR spectrum of B1.14	140
9	IR spectrum of B1.14	141
10	ORTEP, packing diagram and crystal data table of B1.14	142
11	^1H spectrum of B1.15	143
12	D_2O exchange spectrum of B1.15	144
13	^{13}C and DEPT NMR spectrum of B1.15	145
14	IR spectrum of B1.15	146
15	ORTEP, packing diagram and crystal data table of B1.15	147
16	^1H spectrum of B1.22	148
17	^{13}C and DEPT NMR spectrum of B1.22	149
18	IR spectrum of B1.22	150
19	ORTEP, packing diagram and crystal data table of B1.23	151
20	^1H spectrum of B1.25	152
21	^{13}C and DEPT NMR spectrum of B1.25	153
22	IR spectrum of B1.25	154
23	^1H spectrum of B1.26	155
24	^{13}C NMR spectrum of B1.26	156
25	DEPT NMR spectrum of B1.26	157
26	IR spectrum of B1.26	158
27	ORTEP, packing diagram and crystal data table of B1.26	159

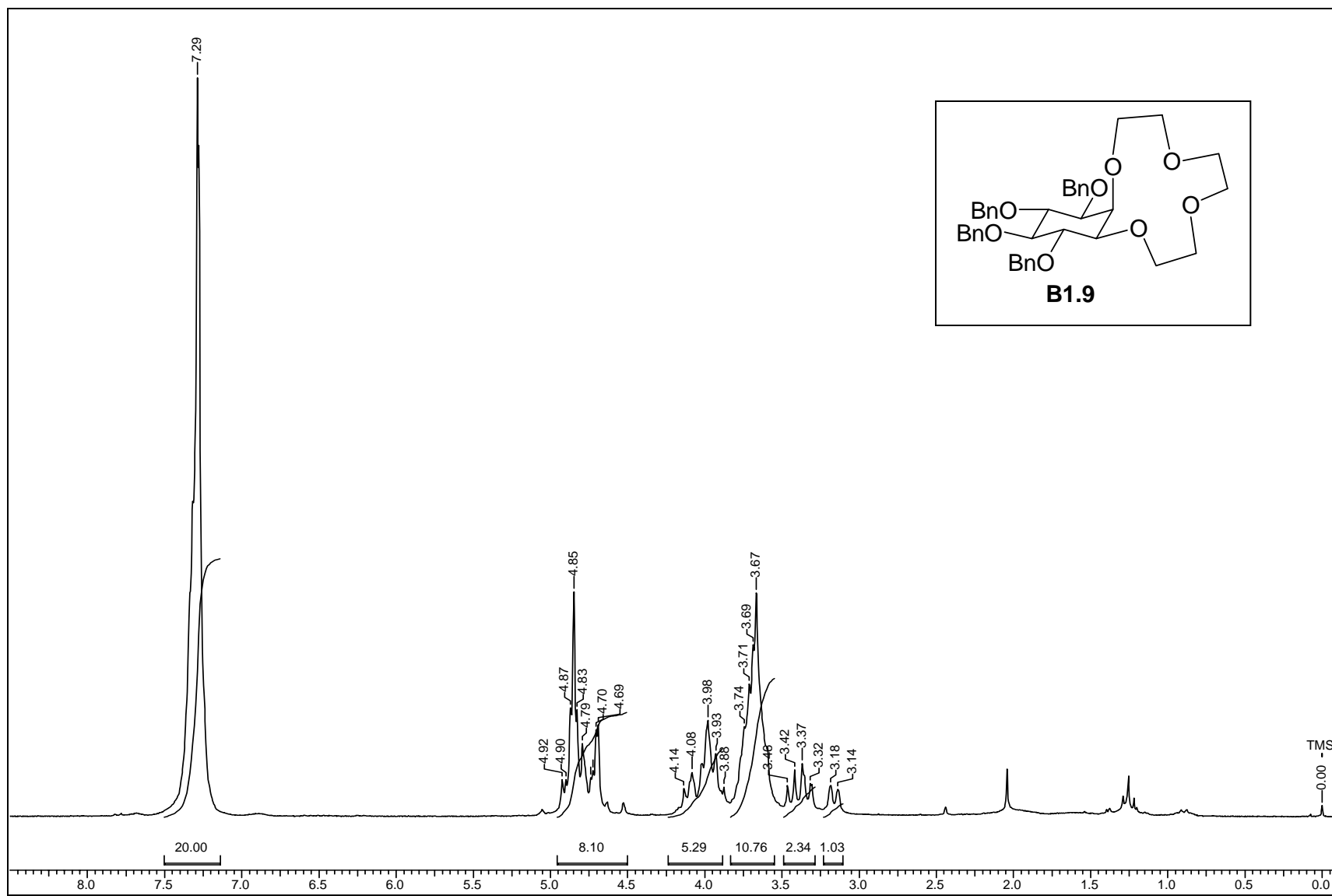
28	^1H spectrum of B1.27	160
29	D ₂ O exchange spectrum of B1.27	161
30	^{13}C and DEPT NMR spectrum of B1.27	162
31	IR spectrum of B1.27	163
32	ORTEP, packing diagram and crystal data table of B1.27	164
33	^1H spectrum of B1.29	165
34	^{13}C and DEPT NMR spectrum of B1.29	166
35	IR spectrum of B1.29	167
36	^1H spectrum of B1.30	168
37	D ₂ O exchange spectrum of B1.30	169
38	^{13}C and DEPT NMR spectrum of B1.30	170
39	IR spectrum of B1.30	171
40	ORTEP, packing diagram and crystal data table of B1.30	172
41	^1H spectrum of B1.31	173
42	^{13}C and DEPT NMR spectrum of B1.31	174
43	IR spectrum of B1.31	175
44	^1H spectrum of B1.32	176
45	^{13}C and DEPT NMR spectrum of B1.32	177
46	IR spectrum of B1.32	178
47	^1H spectrum of B1.33	179
48	D ₂ O exchange spectrum of B1.33	180
49	^{13}C and DEPT NMR spectrum of B1.33	181
50	IR spectrum of B1.33	182
51	ORTEP, packing diagram and crystal data table of B1.33	183
52	^1H spectrum of B1.34	184
53	^{13}C and DEPT NMR spectrum of B1.34	185
54	IR spectrum of B1.34	186
55	^1H spectrum of B1.35	187
56	^{13}C and DEPT NMR spectrum of B1.35	188

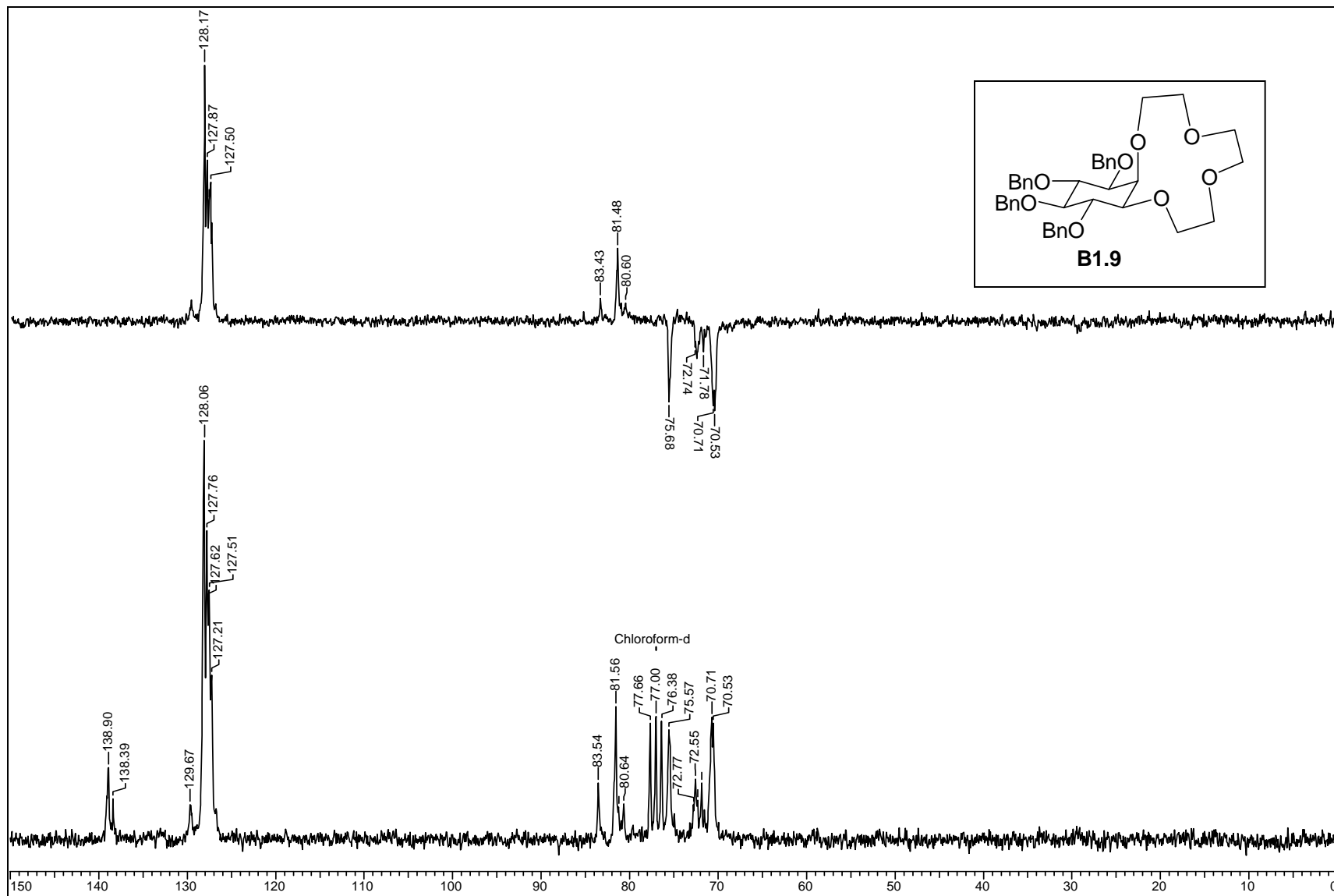
57	IR spectrum of B1.35	189
58	¹ H spectrum of B1.36	190
59	D ₂ O exchange spectrum of B1.36	191
60	¹³ C and DEPT NMR spectrum of B1.36	192
61	IR spectrum of B1.36	193
62	¹ H spectrum of B1.37	194
63	¹³ C and DEPT NMR spectrum of B1.37	195
64	IR spectrum of B1.37	196

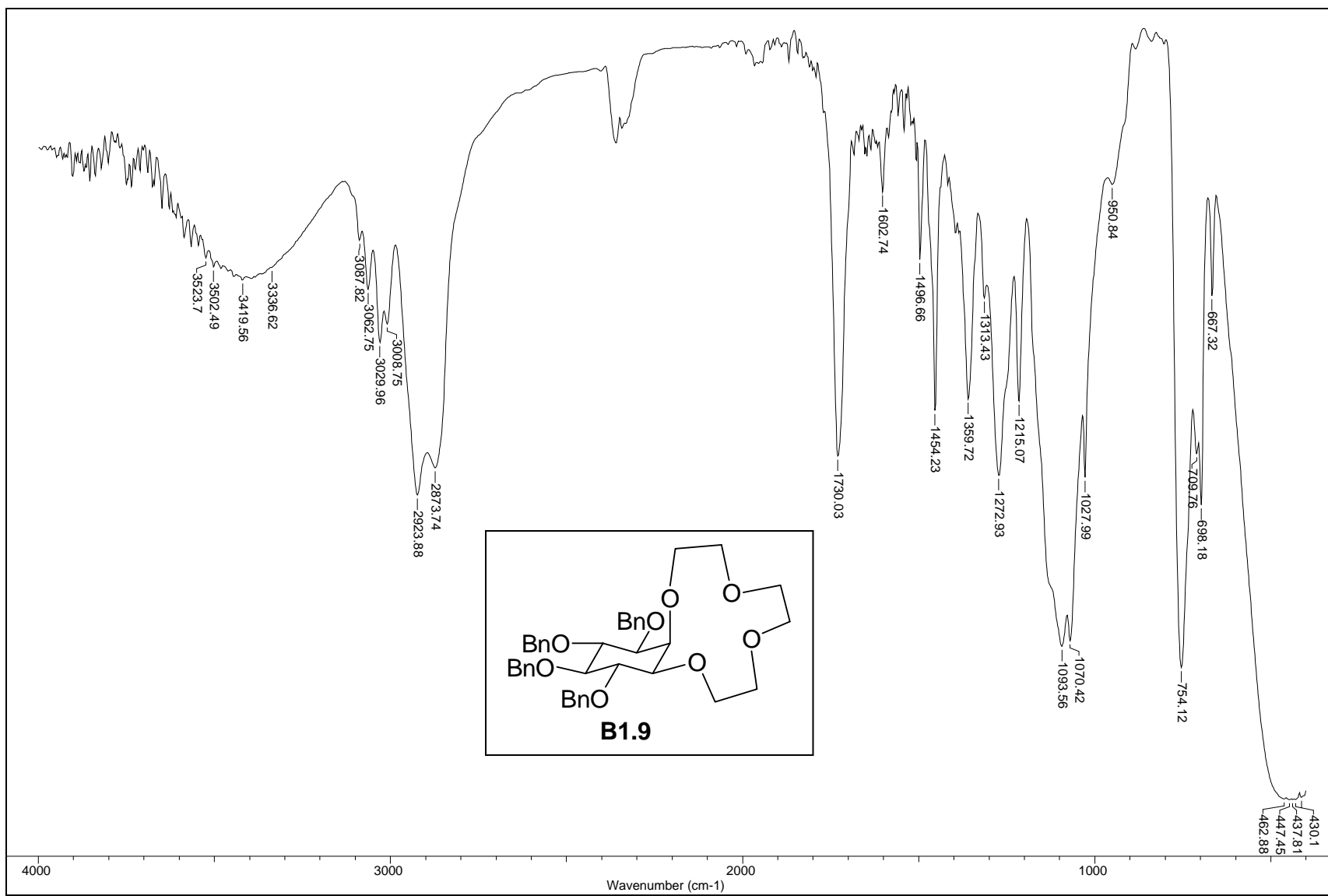


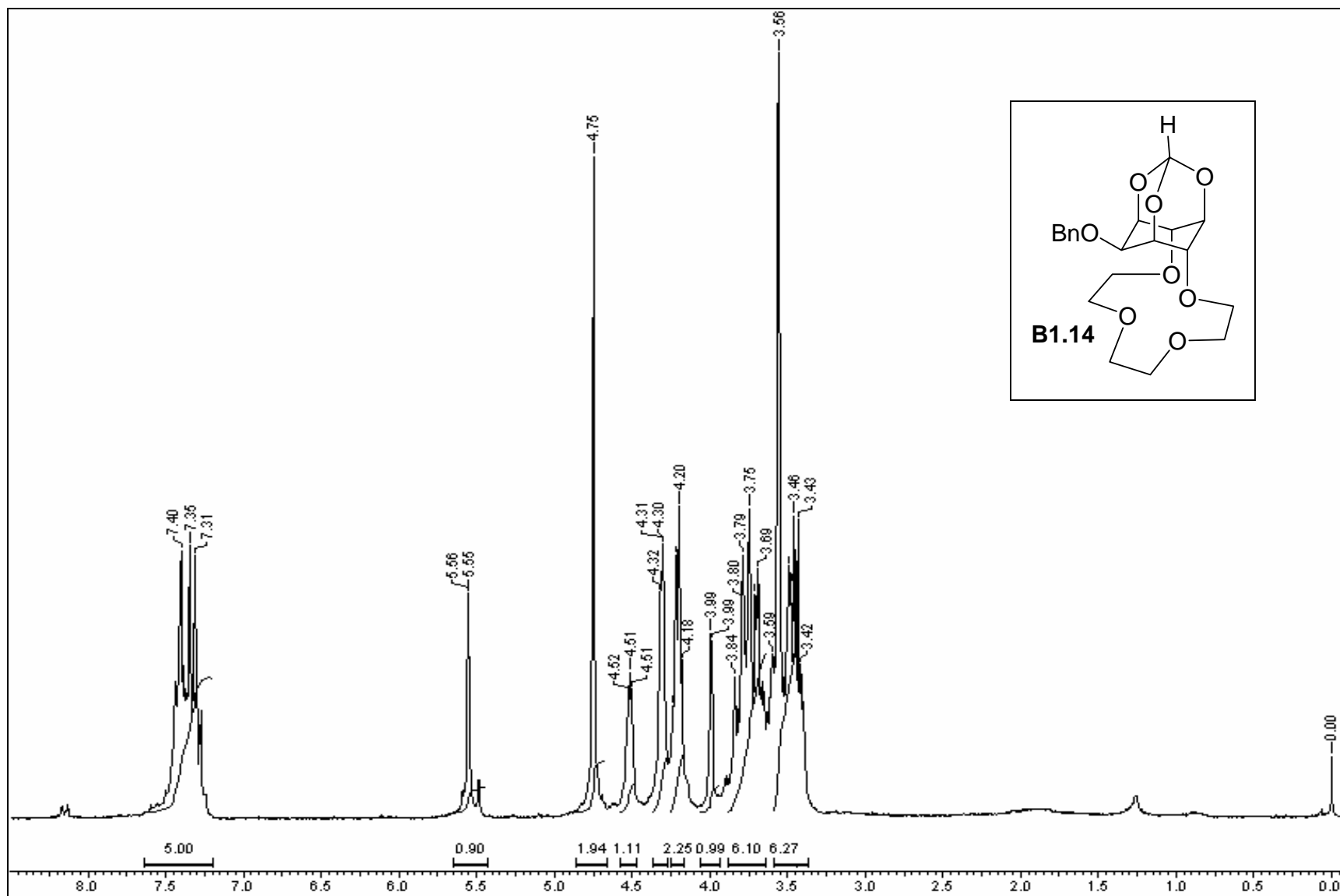


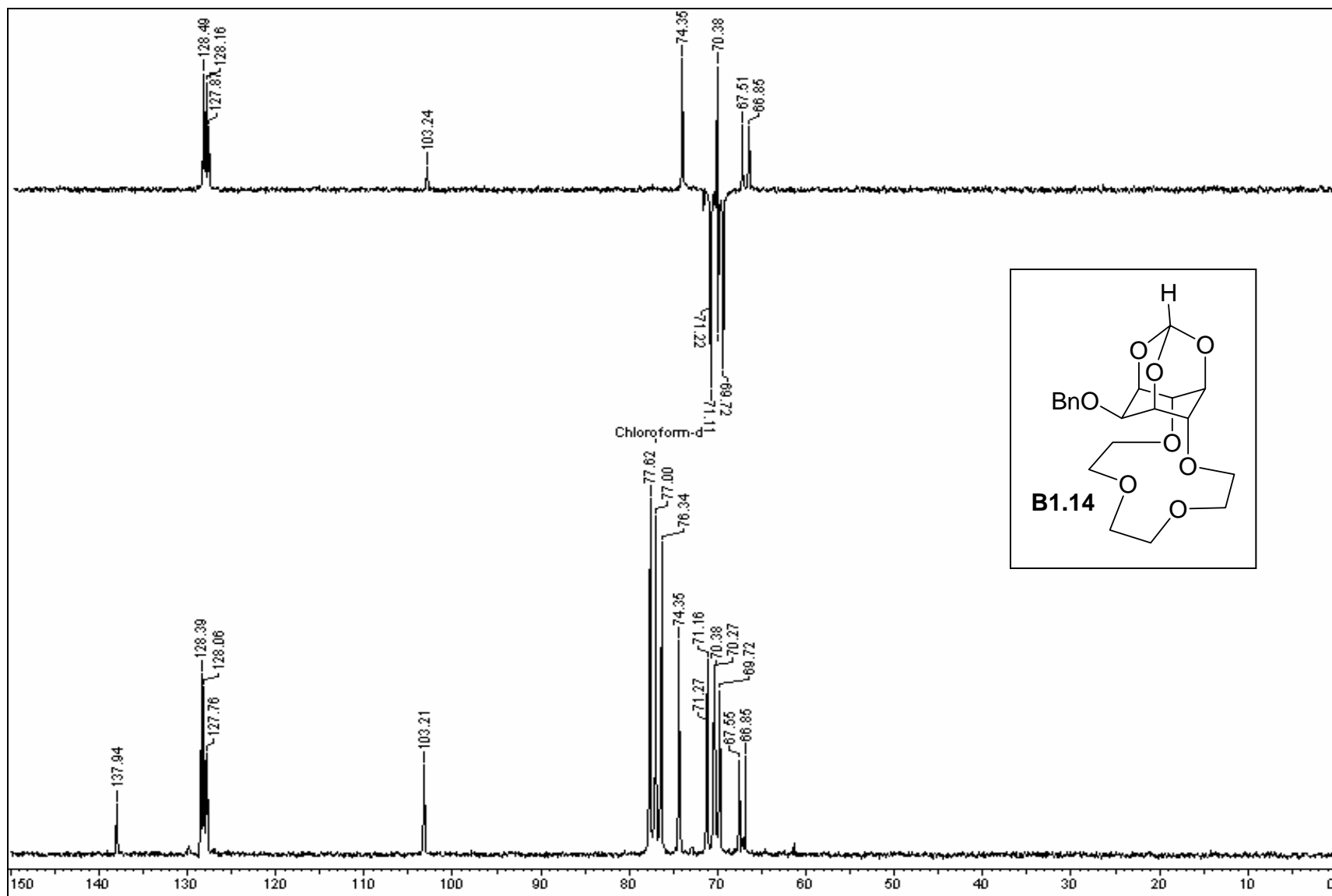


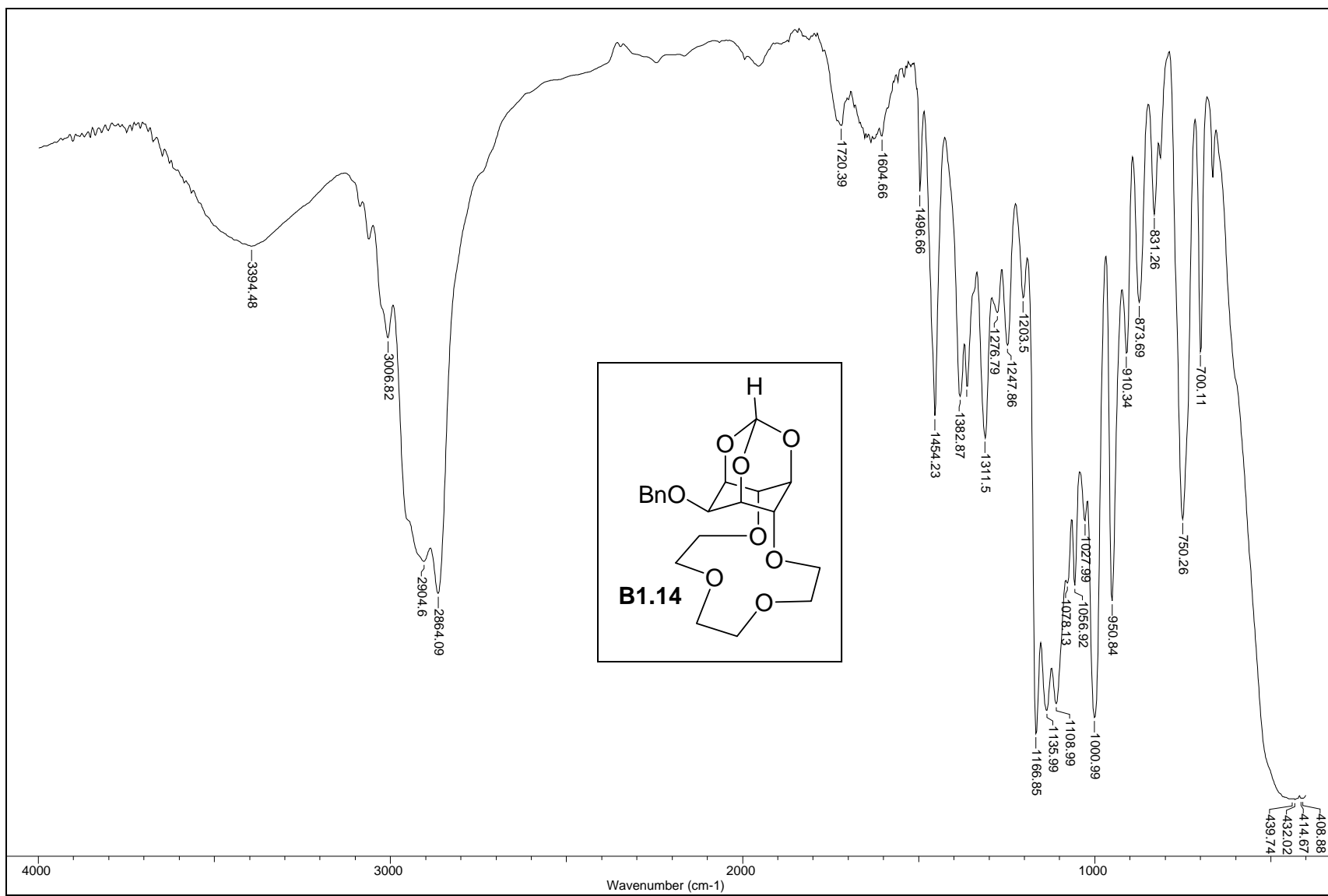


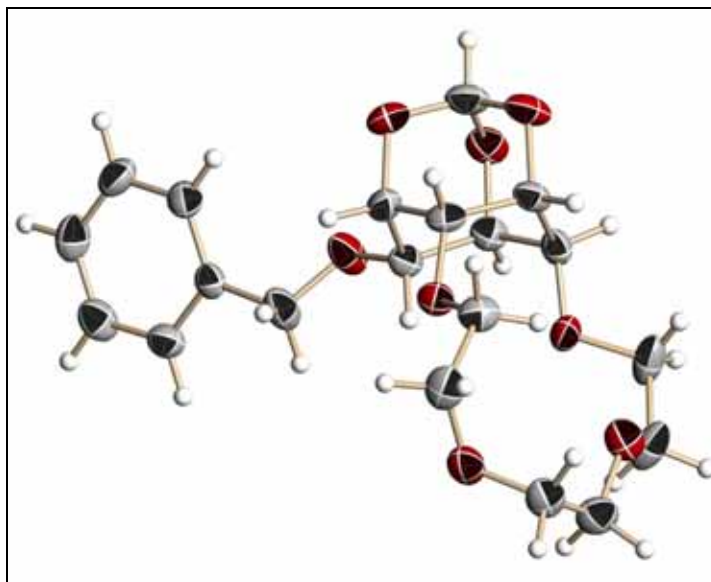




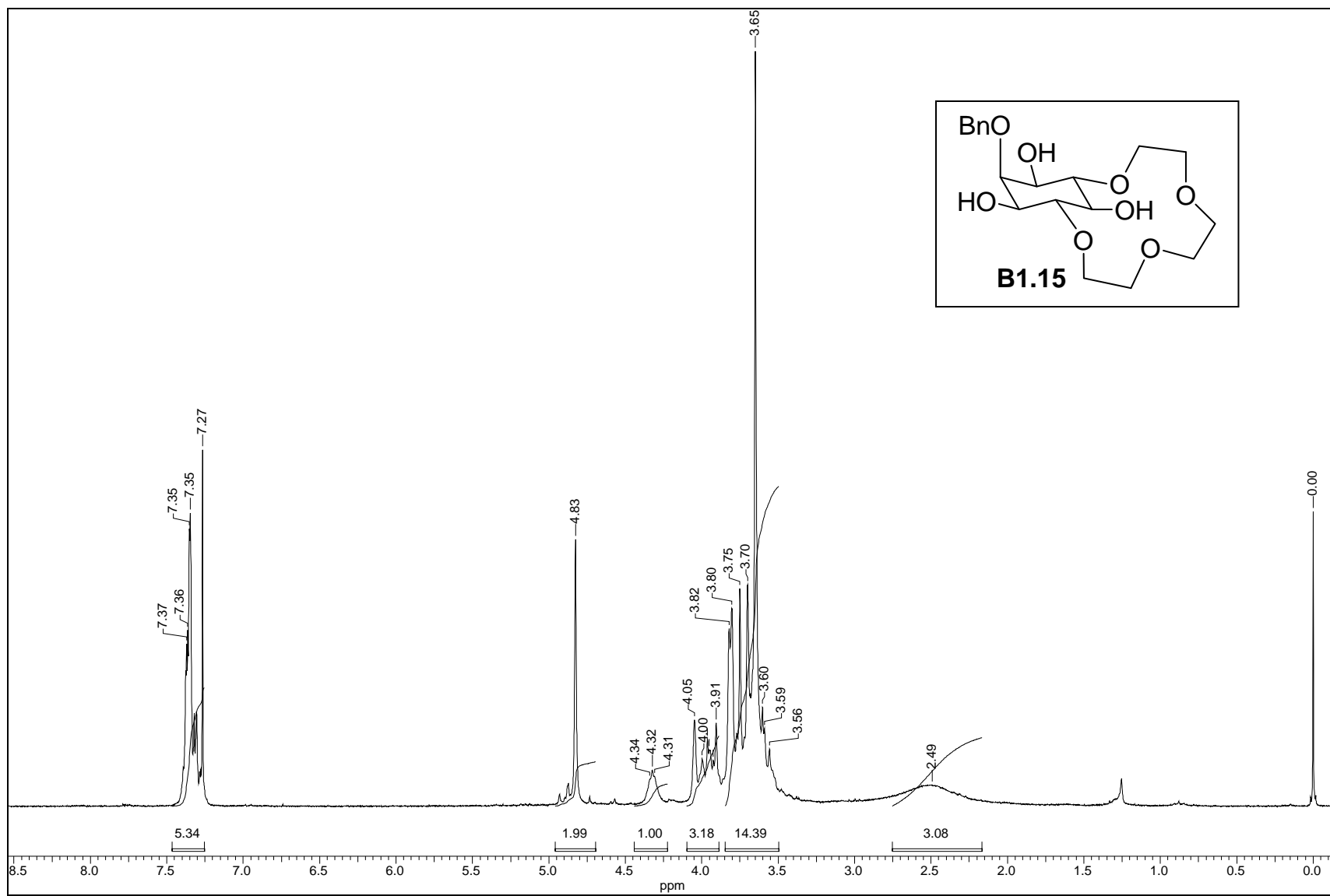


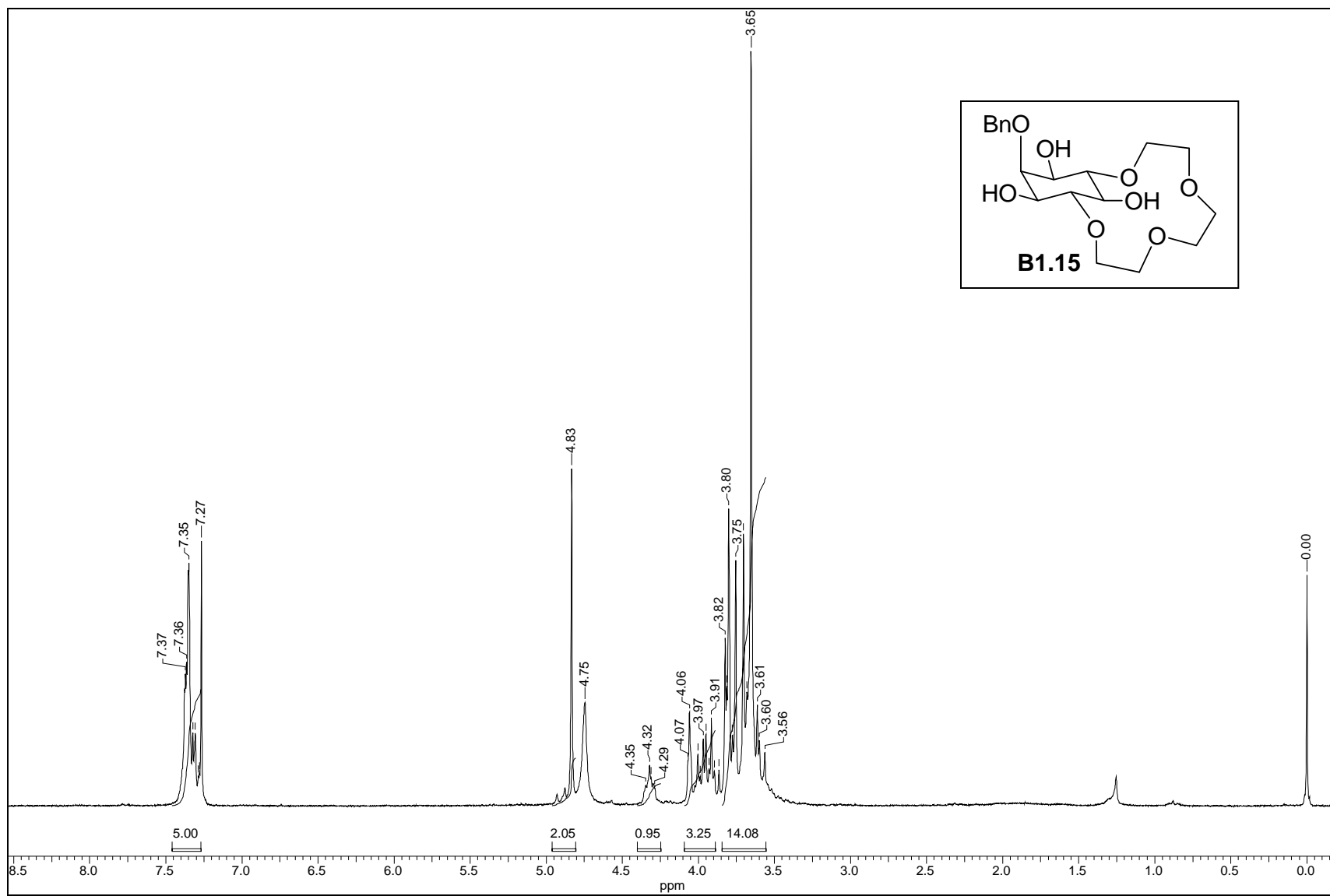


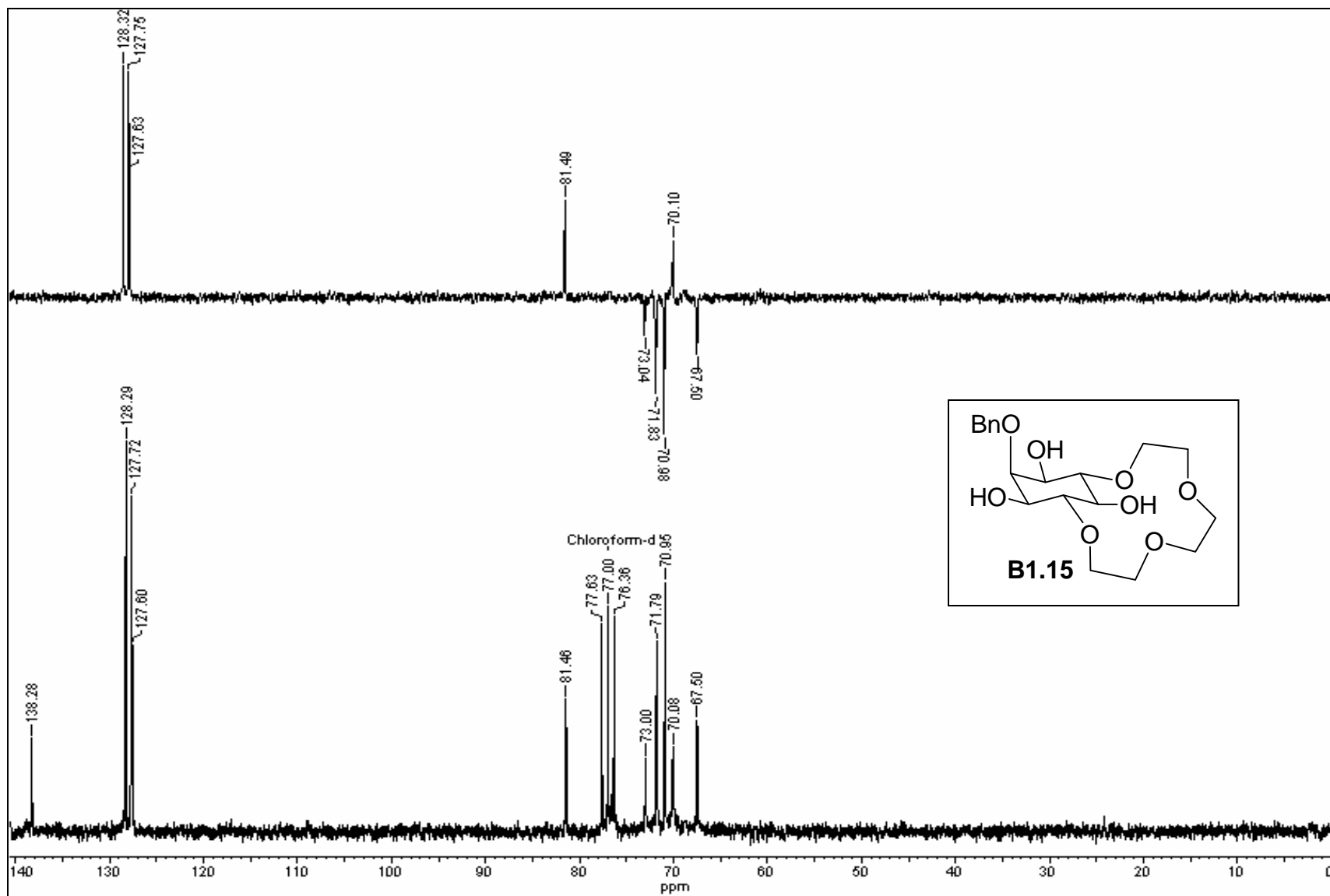


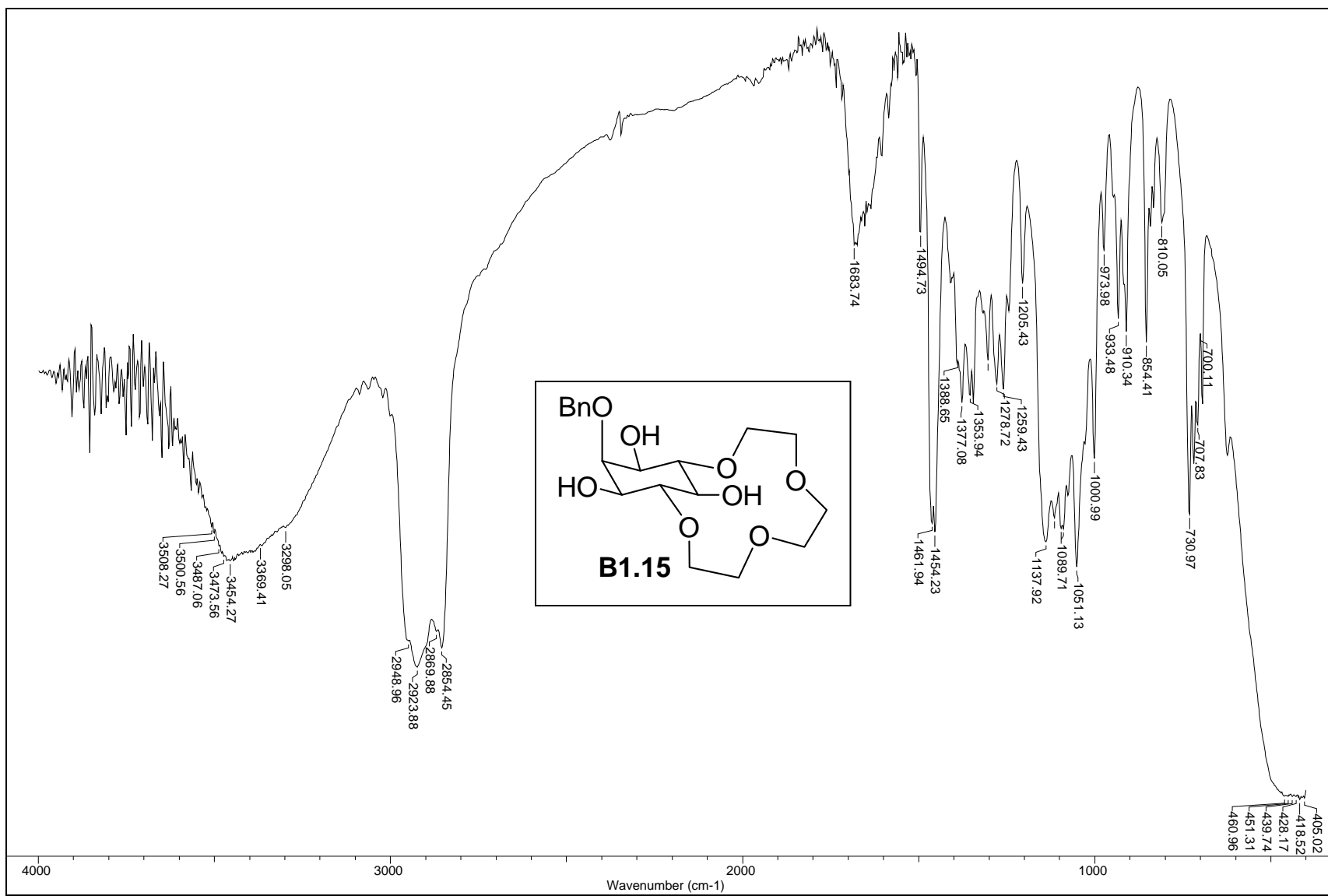
ORTEP diagram of **B1.14**Crystal data table of **B1.14**

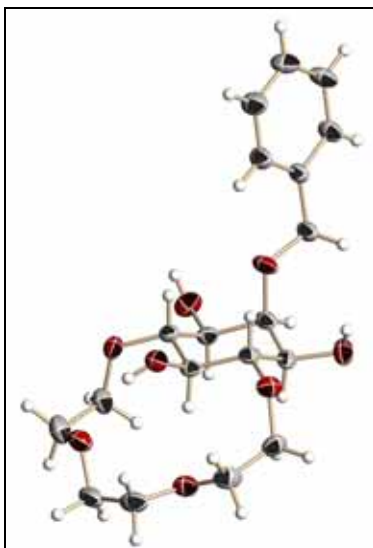
Identification code	B1.14 (crystallized from MeOH)
Empirical formula	C ₂₀ H ₂₆ O ₈
Formula weight	394.41
Temperature	297(2) K
Wavelength	0.71073 Å
Crystal system, space group	Triclinic, P -1
Unit cell dimensions	a = 9.178(4) Å, α = 106.796(7)° b = 10.153(4) Å, β = 96.430(7)° c = 12.314(5) Å, γ = 114.920(7)°
Volume	959.4(7) Å ³
Z, Calculated density	2, 1.365 Mg/m ³
Absorption coefficient	0.106 mm ⁻¹
F(000)	420
Crystal size	0.26 x 0.17 x 0.08 mm
θ range for data collection	2.38 to 25.00°
Limiting indices	-10 ≤ h ≤ 10, -12 ≤ k ≤ 12, -14 ≤ l ≤ 14
Reflections collected / unique	9301 / 3364 [R(int) = 0.0228]
Completeness to θ = 25.00	99.7 %
Absorption correction	Semi-empirical from equivalents
Max. and min. transmission	0.9916 and 0.9731
Refinement method	Full-matrix least-squares on F ²
Data / restraints / parameters	3364 / 0 / 253
Goodness-of-fit on F ²	1.043
Final R indices [I > 2σ (I)]	R1 = 0.0692, wR2 = 0.1700
R indices (all data)	R1 = 0.0889, wR2 = 0.1848
Largest diff. peak and hole (ρ _{max} & ρ _{min})	0.758 and -0.275 e. Å ⁻³



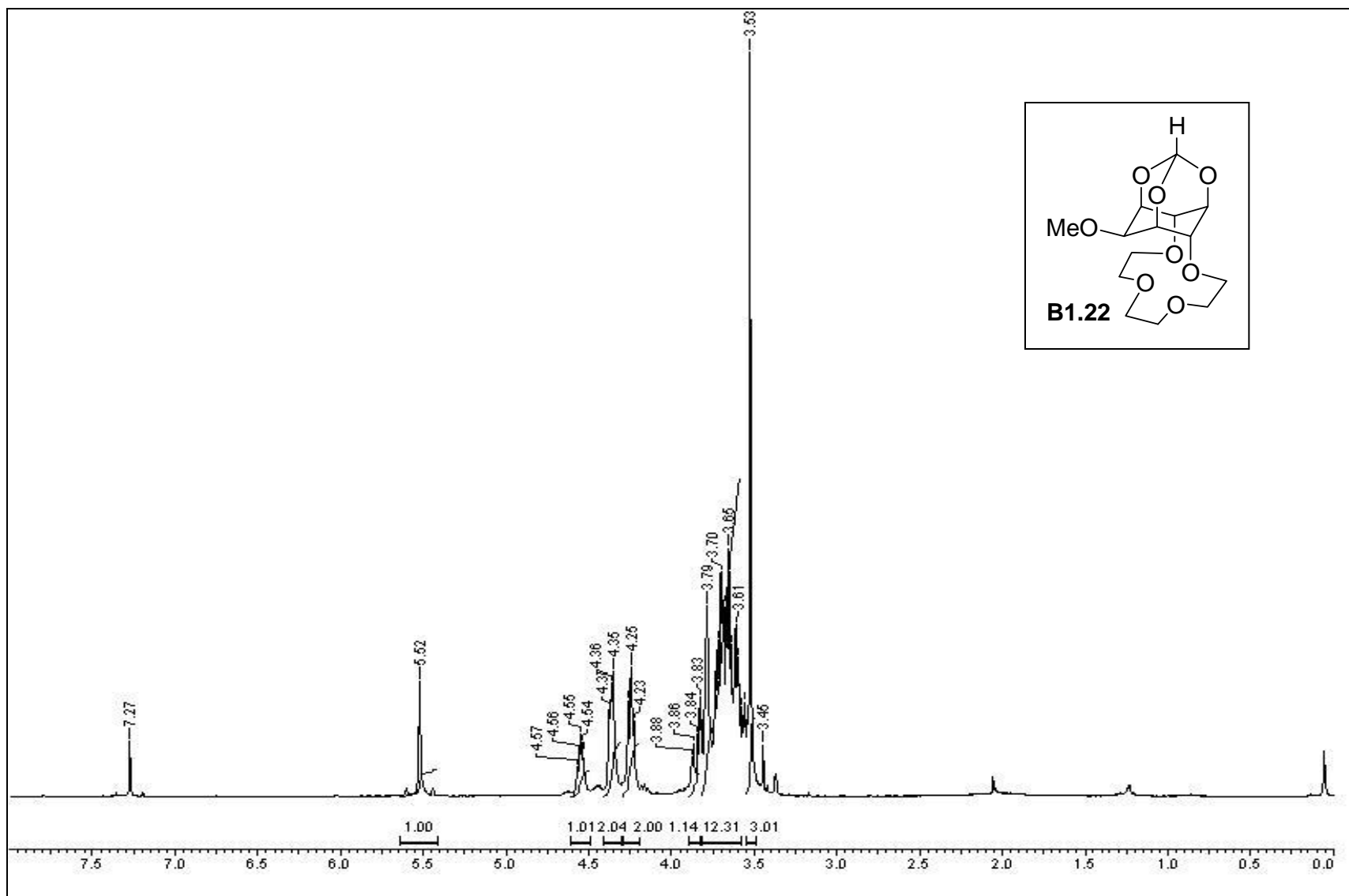


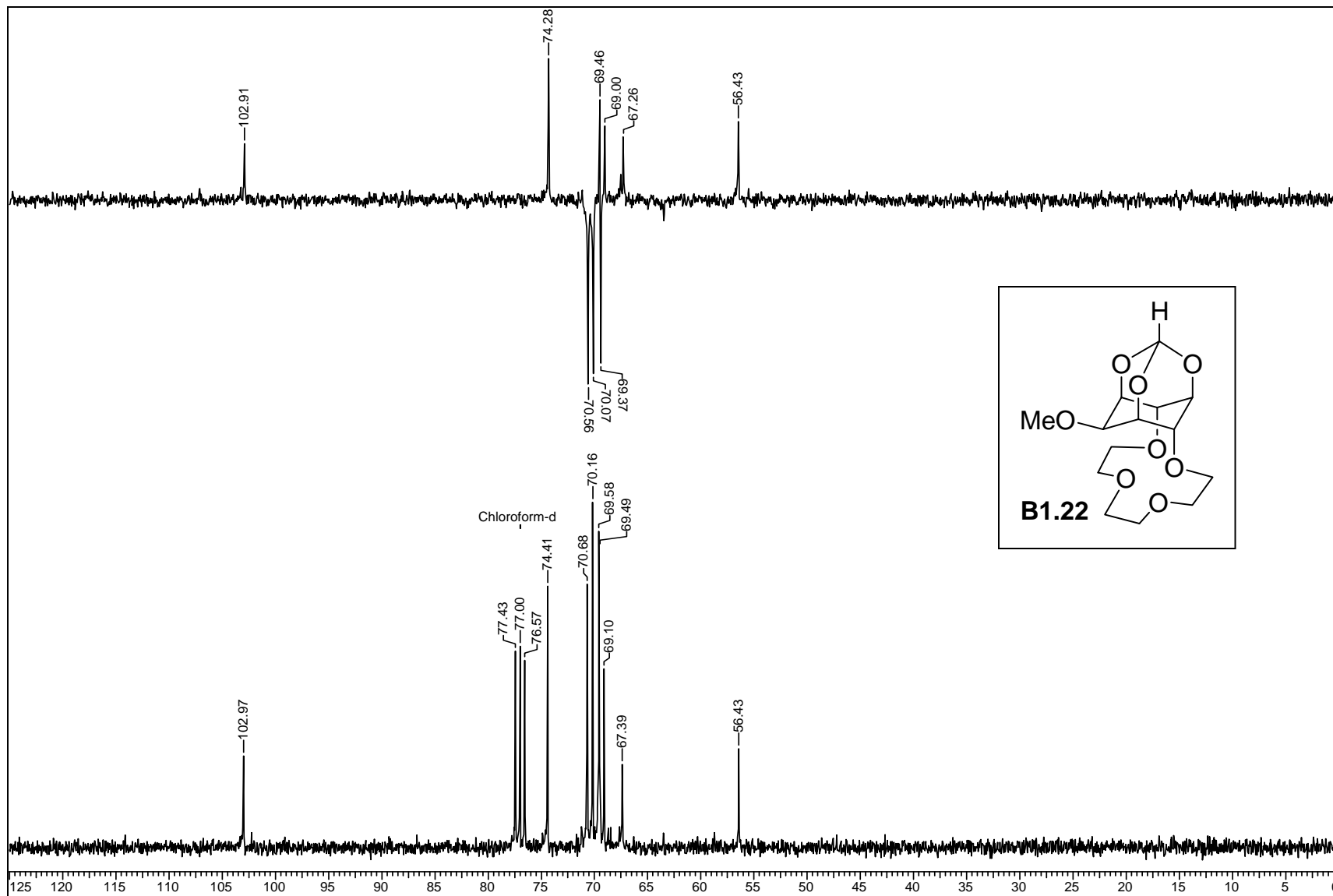


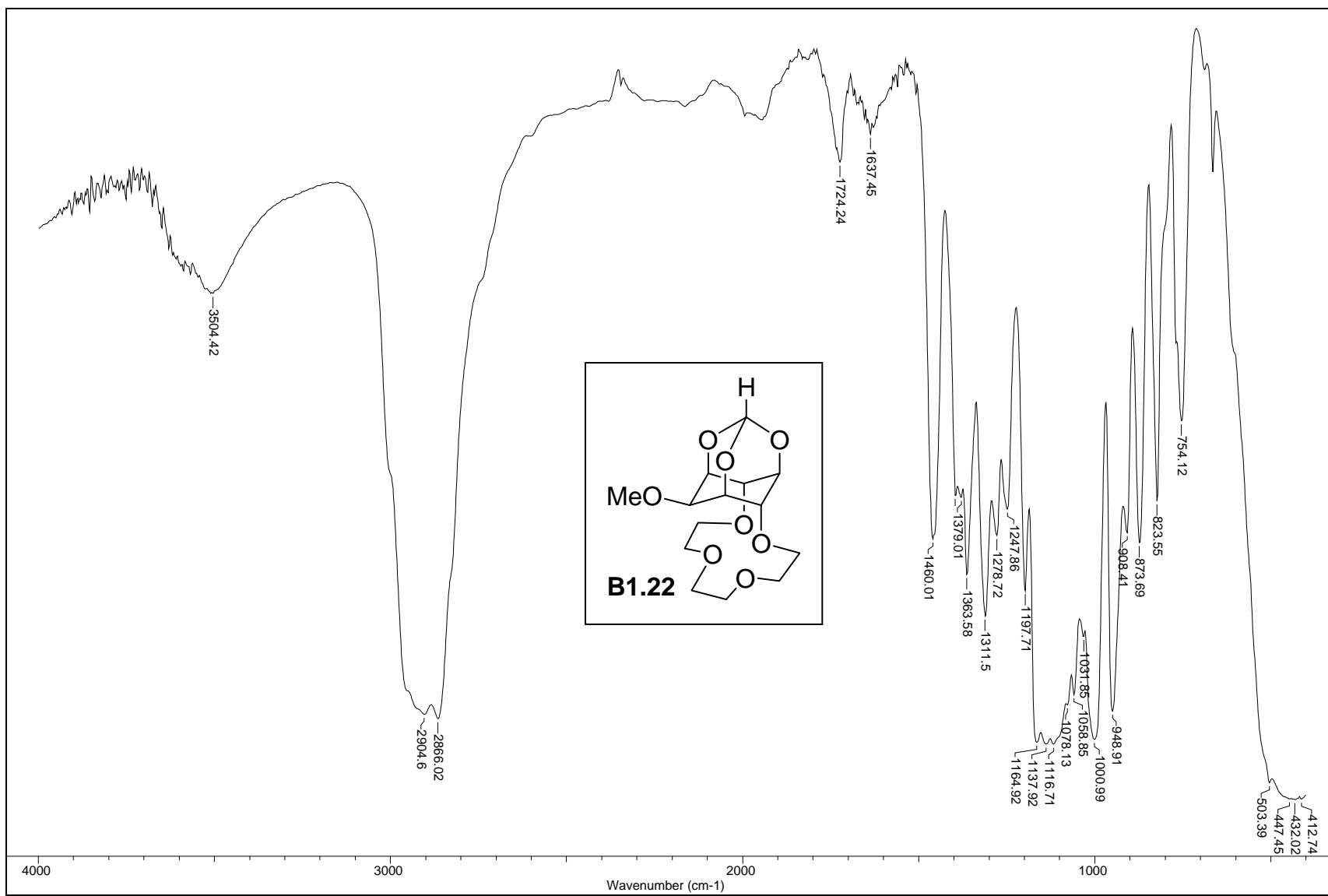


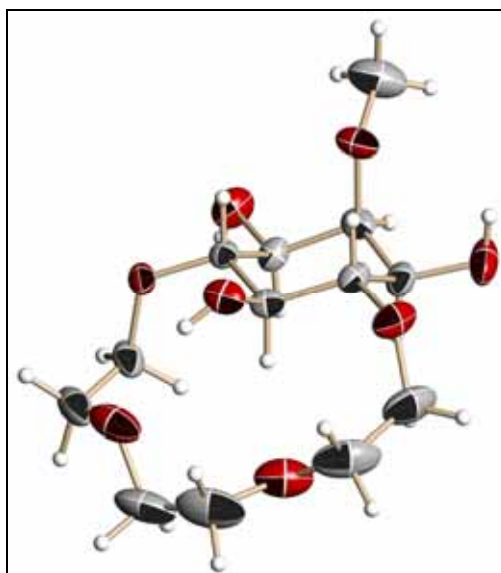
ORTEP diagram of **B1.15**Crystal data table of **B1.15**

Identification code	B1.15 (crystallized from MeOH)
Empirical formula	C ₁₉ H ₂₈ O ₈
Formula weight	384.41
Temperature	297(2) K
Wavelength	0.71073 Å
Crystal system, space group	Triclinic, P-1
Unit cell dimensions	a = 9.525(3) Å α = 92.274(4)° b = 10.616(3) Å β = 103.997(4)° c = 10.864(3) Å γ = 115.784(4)°
Volume	946.5(4) Å ³
Z, Calculated density	2, 1.349 Mg/m ³
Absorption coefficient	0.105 mm ⁻¹
F(000)	412
Crystal size	0.78 x 0.65 x 0.61 mm
θ range for data collection	2.43 to 25.00°
Limiting indices	-11 ≤ h ≤ 11, -12 ≤ k ≤ 12, -12 ≤ l ≤ 12
Reflections collected / unique	9137 / 3319 [R(int) = 0.0203]
Completeness to θ = 25.00	99.4 %
Absorption correction	Semi-empirical from equivalents
Max. and min. transmission	0.9388 and 0.9227
Refinement method	Full-matrix least-squares on F ²
Data / restraints / parameters	3319 / 0 / 247
Goodness-of-fit on F ²	1.032
Final R indices [I > 2σ (I)]	R1 = 0.0385, wR2 = 0.1019
R indices (all data)	R1 = 0.0426, wR2 = 0.1057
Largest diff. peak and hole (ρ _{max} & ρ _{min})	0.253 and -0.230 e. Å ⁻³

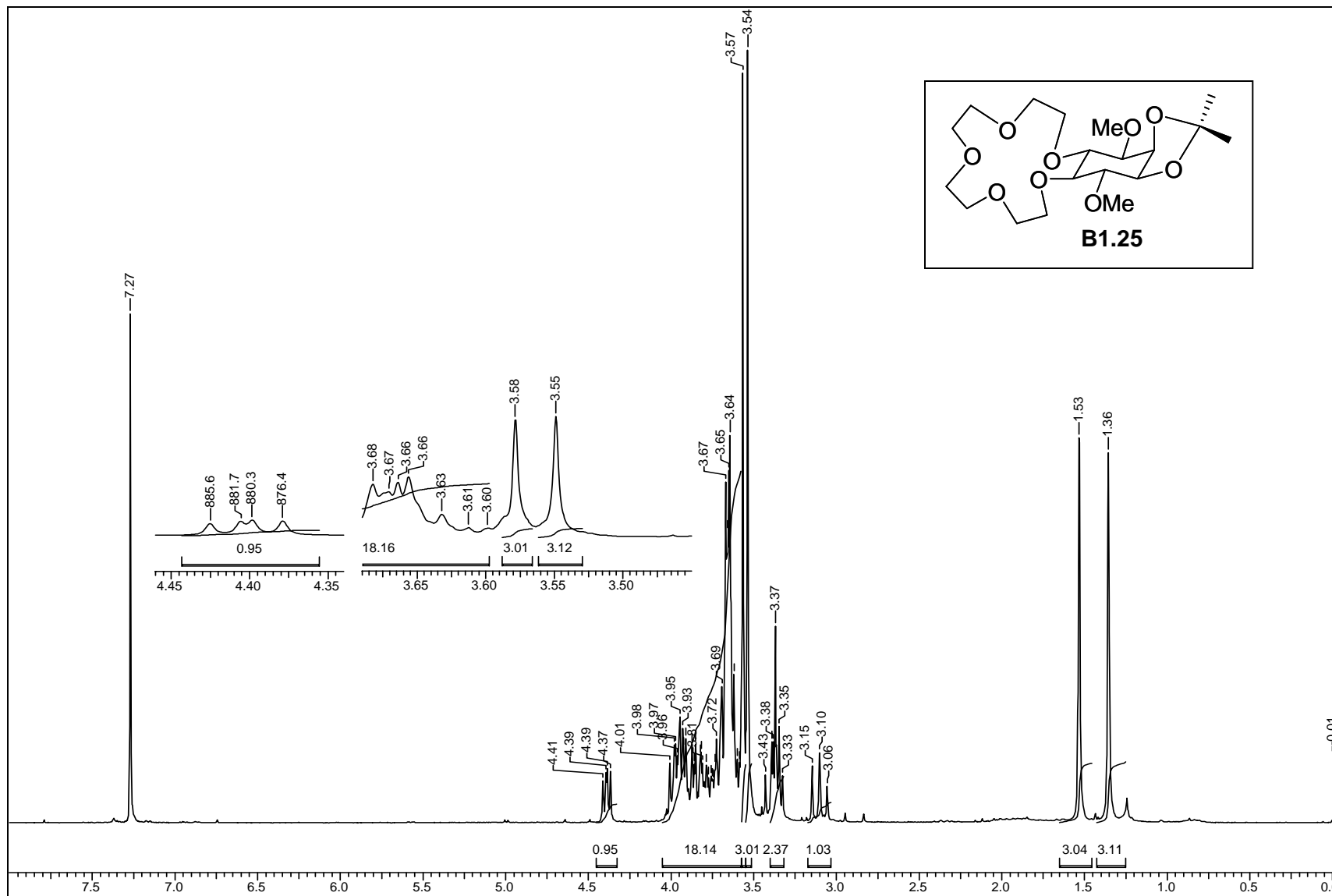


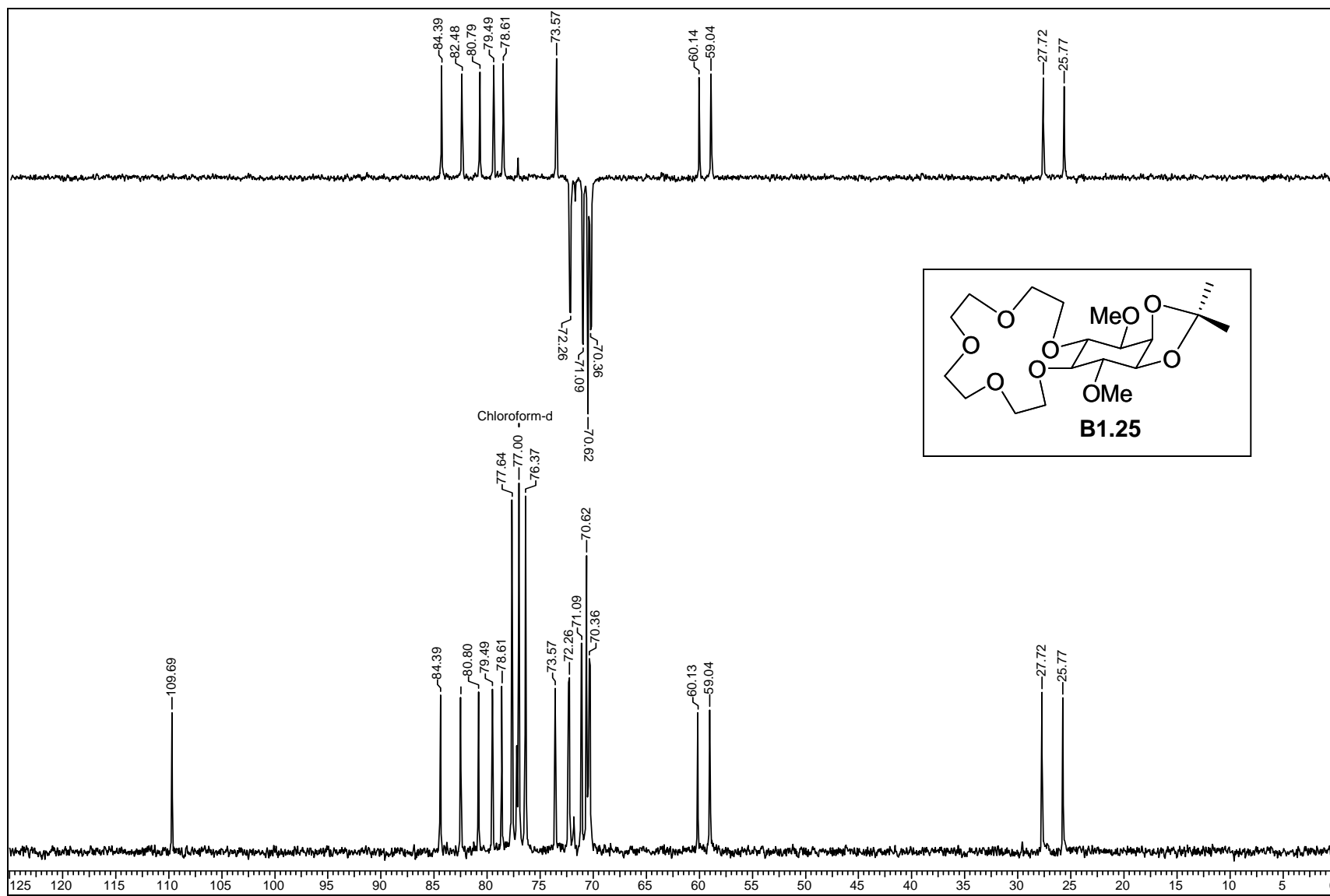


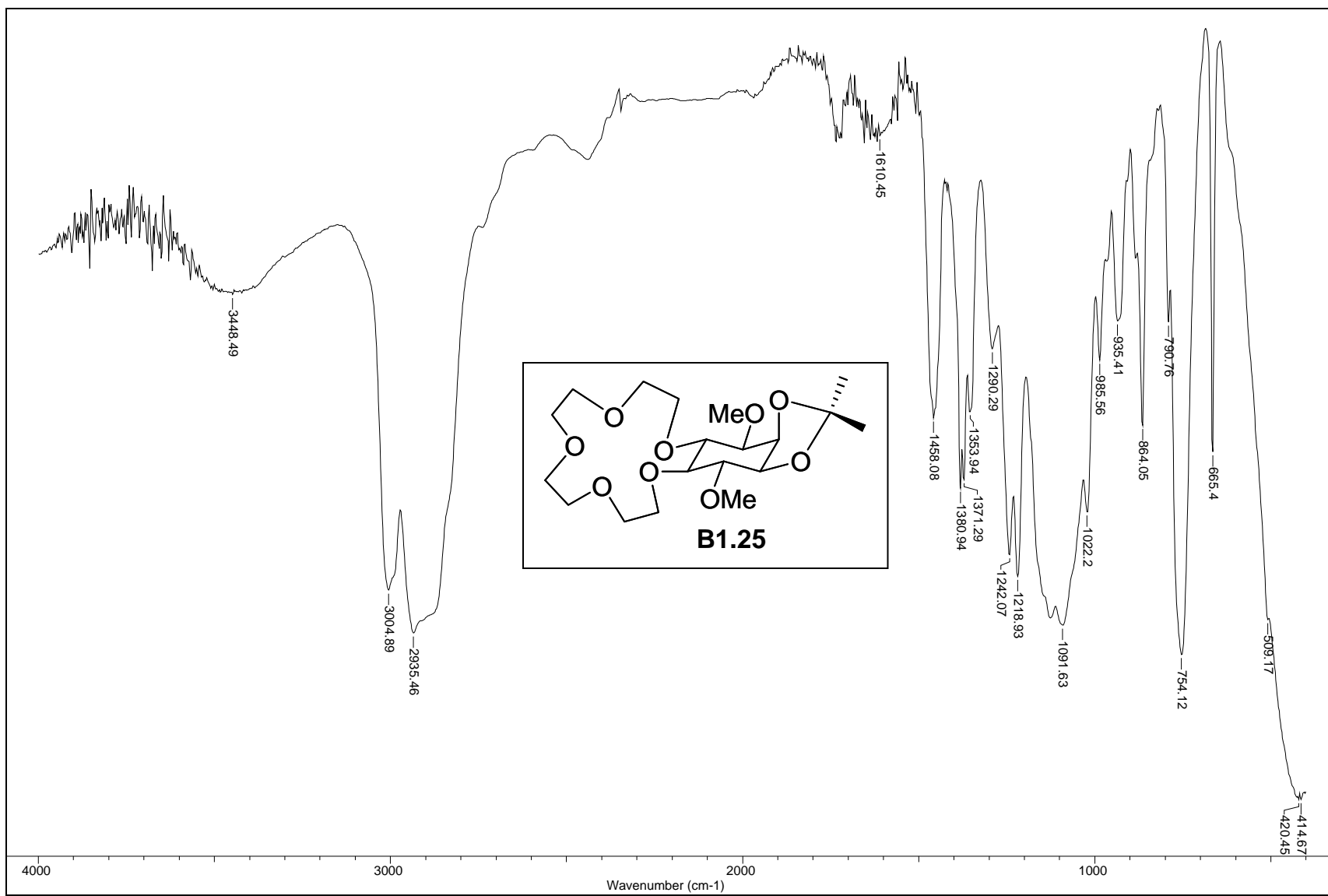


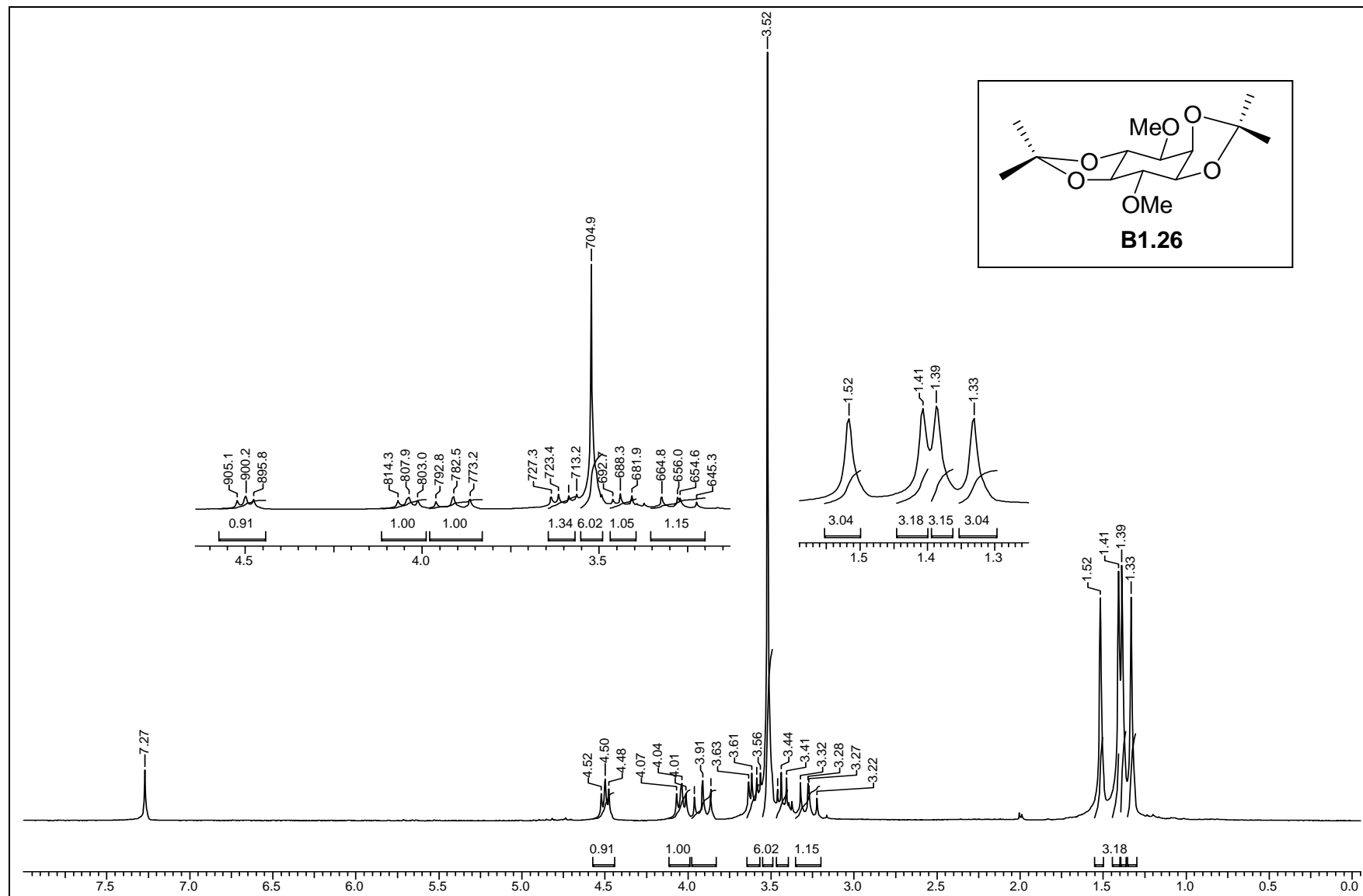
ORTEP diagram of **B1.23**Crystal data table of **B1.23**

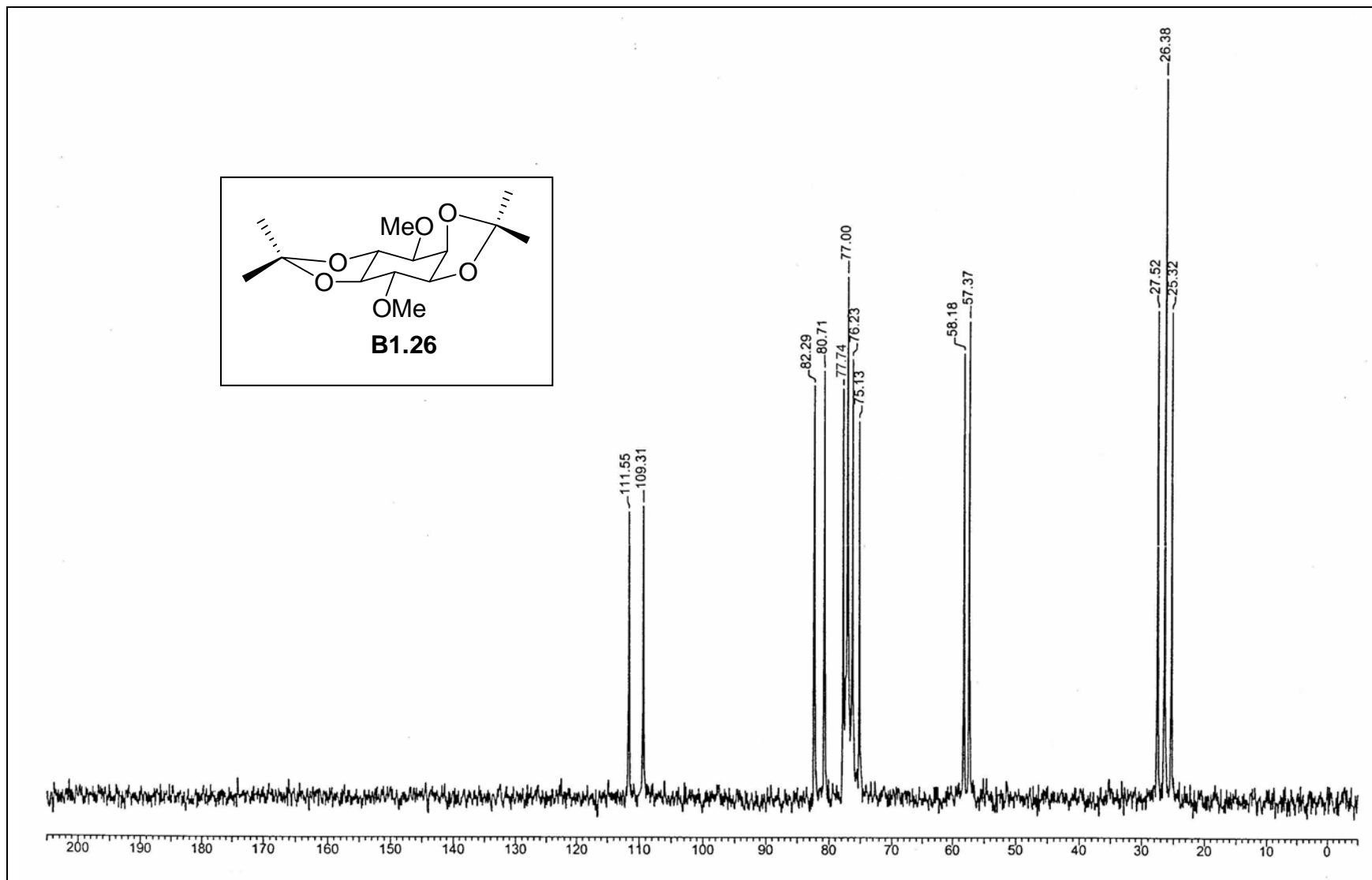
Identification code	B1.23
Empirical formula	$C_{13} H_{24} O_8$
Formula weight	308.32
Temperature	297(2) K
Wavelength	0.71073 Å
Crystal system, space group	Monoclinic, $C 2/c$
Unit cell dimensions	$a = 18.232(8) \text{ \AA}$, $\alpha = 90^\circ$ $b = 17.753(8) \text{ \AA}$, $\beta = 92.958(8)^\circ$ $c = 9.602(4) \text{ \AA}$, $\gamma = 90^\circ$
Volume	$3104(2) \text{ \AA}^3$
Z, Calculated density	8, 1.320 Mg/m^3
Absorption coefficient	0.109 mm^{-1}
F(000)	1328
Crystal size	0.33 x 0.04 x 0.02 mm
θ range for data collection	1.60 to 25.00°
Limiting indices	$-21 \leq h \leq 21$, $-18 \leq k \leq 21$, $-8 \leq l \leq 11$
Reflections collected / unique	9243 / 2734 [R(int) = 0.1172]
Completeness to $\theta = 24.99$	100.0 %
Absorption correction	Semi-empirical from equivalents
Max. and min. transmission	0.9978 and 0.9648
Refinement method	Full-matrix least-squares on F^2
Data / restraints / parameters	2734 / 0 / 194
Goodness-of-fit on F^2	1.044
Final R indices [$I > 2\sigma(I)$]	$R1 = 0.0937$, $wR2 = 0.1333$
R indices (all data)	$R1 = 0.2309$, $wR2 = 0.1700$
Largest diff. peak and hole (ρ_{\max} & ρ_{\min})	0.189 and $-0.155 \text{ e. \AA}^{-3}$

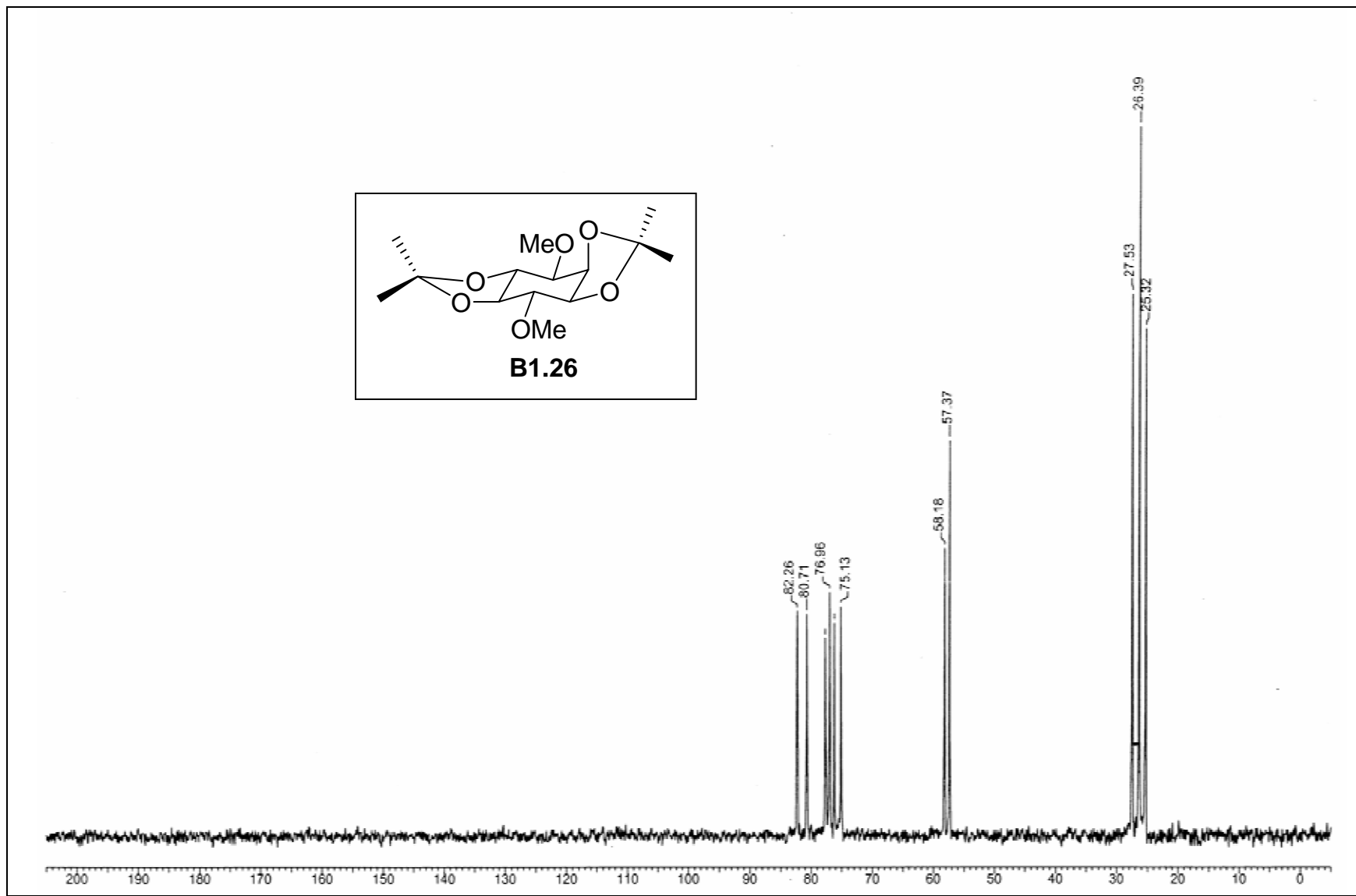
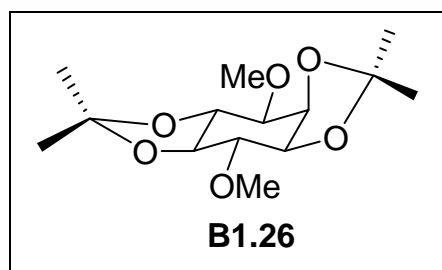


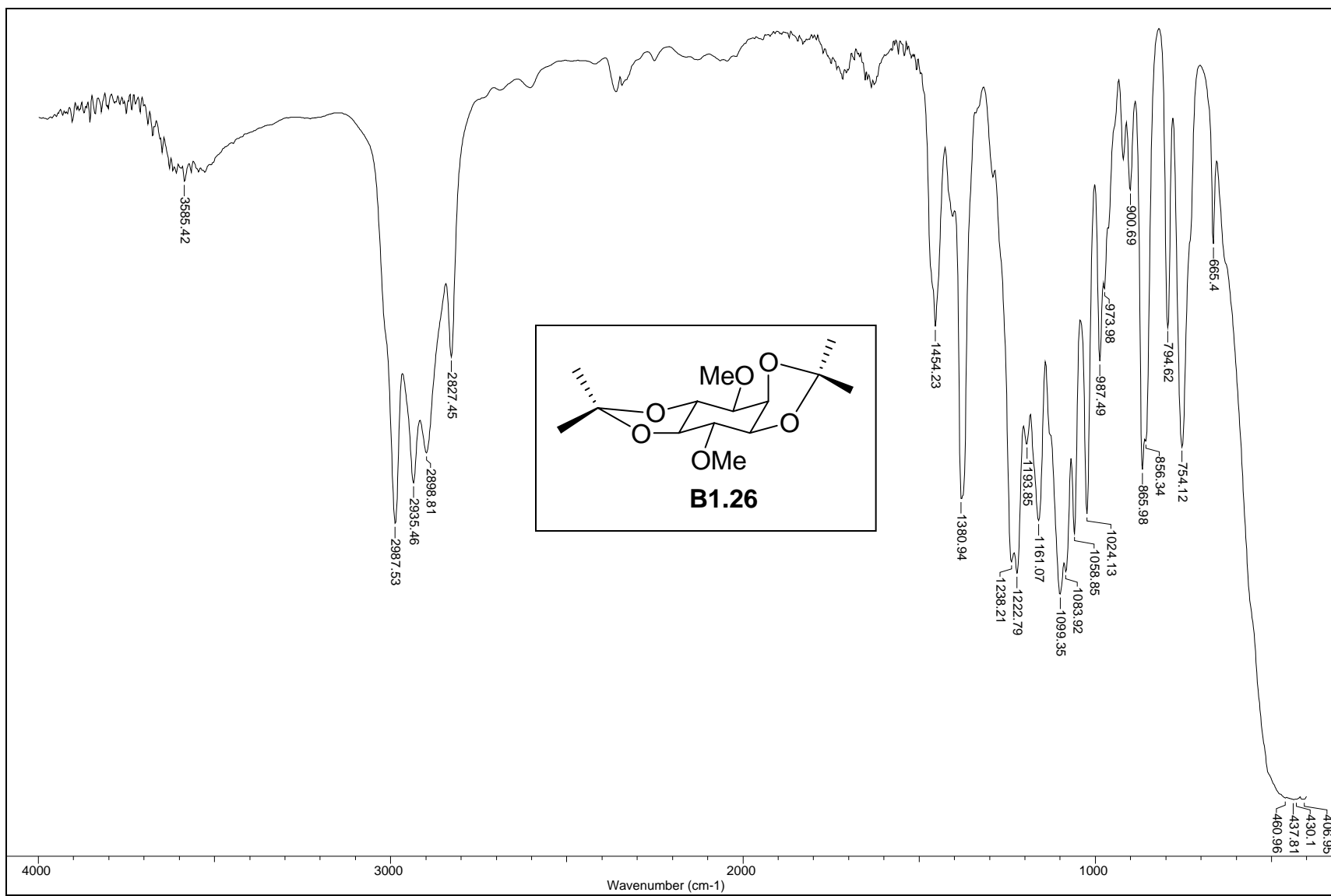


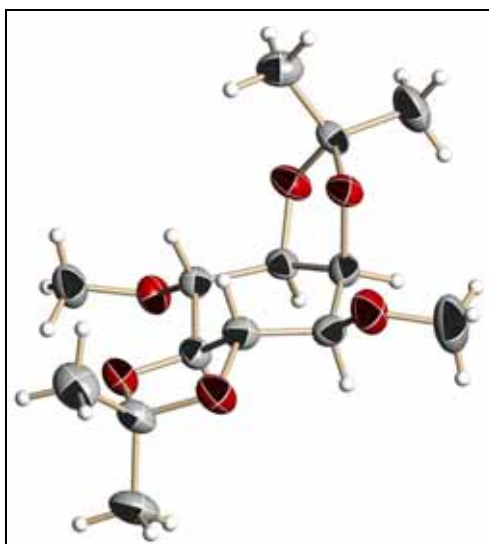




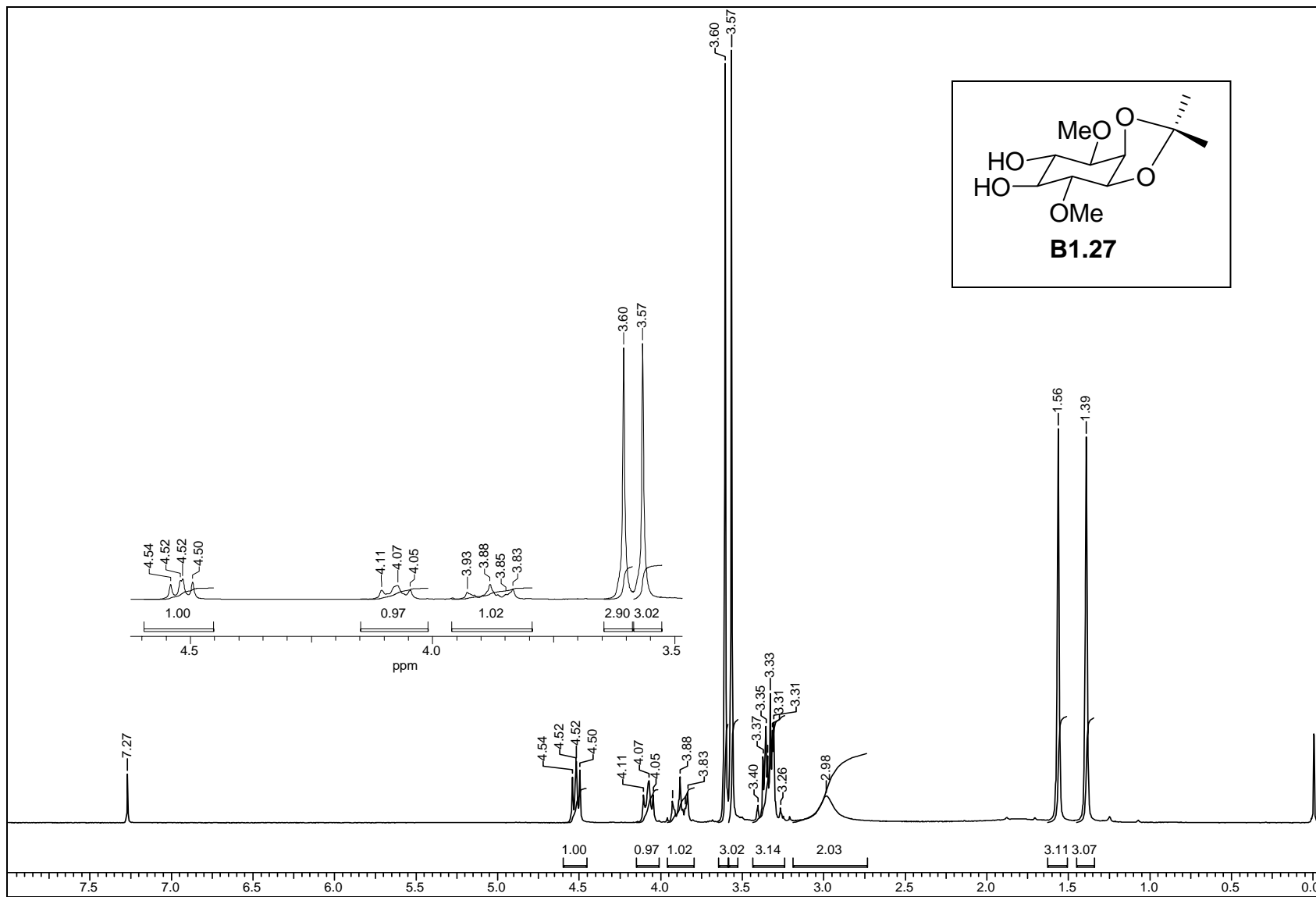


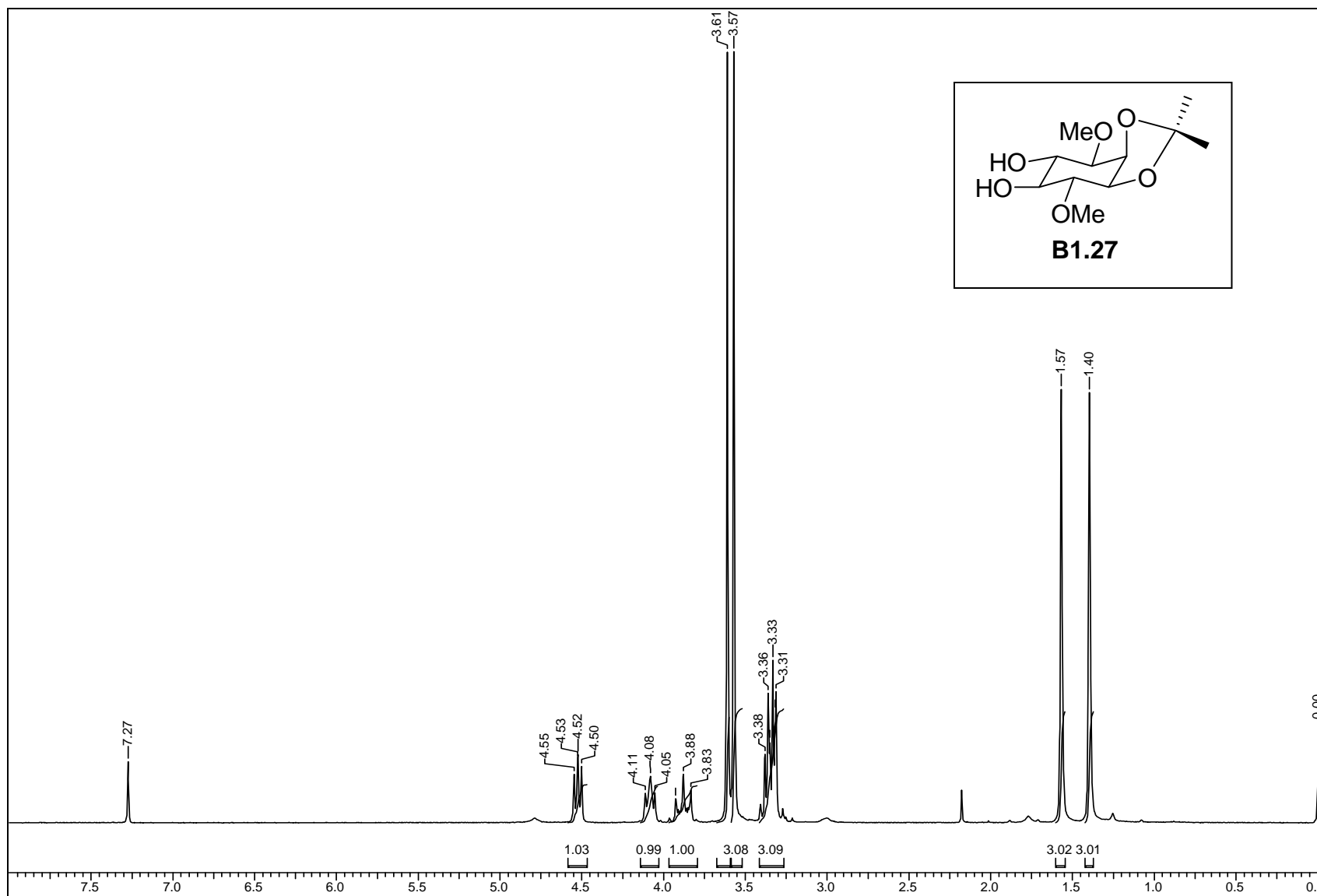


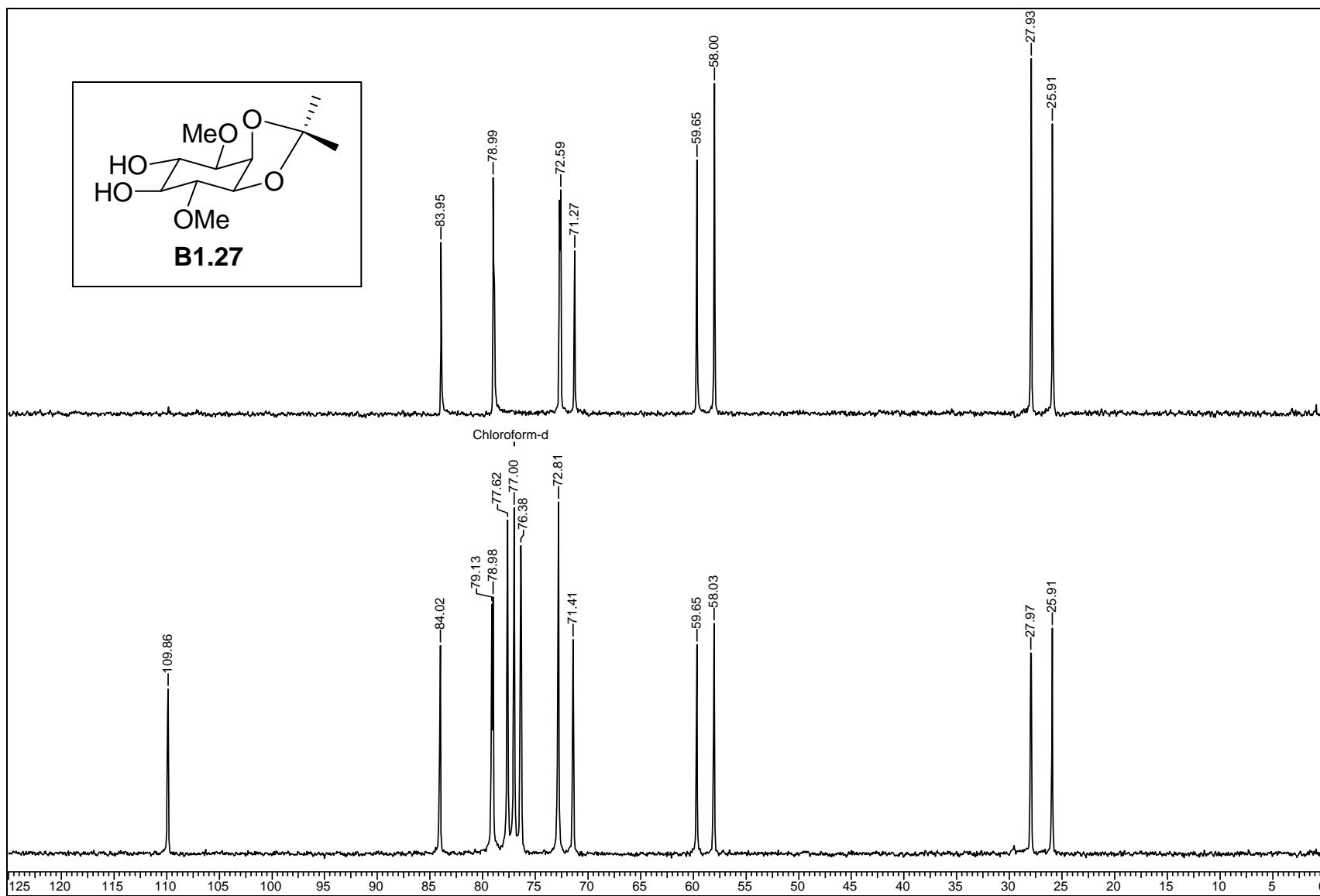


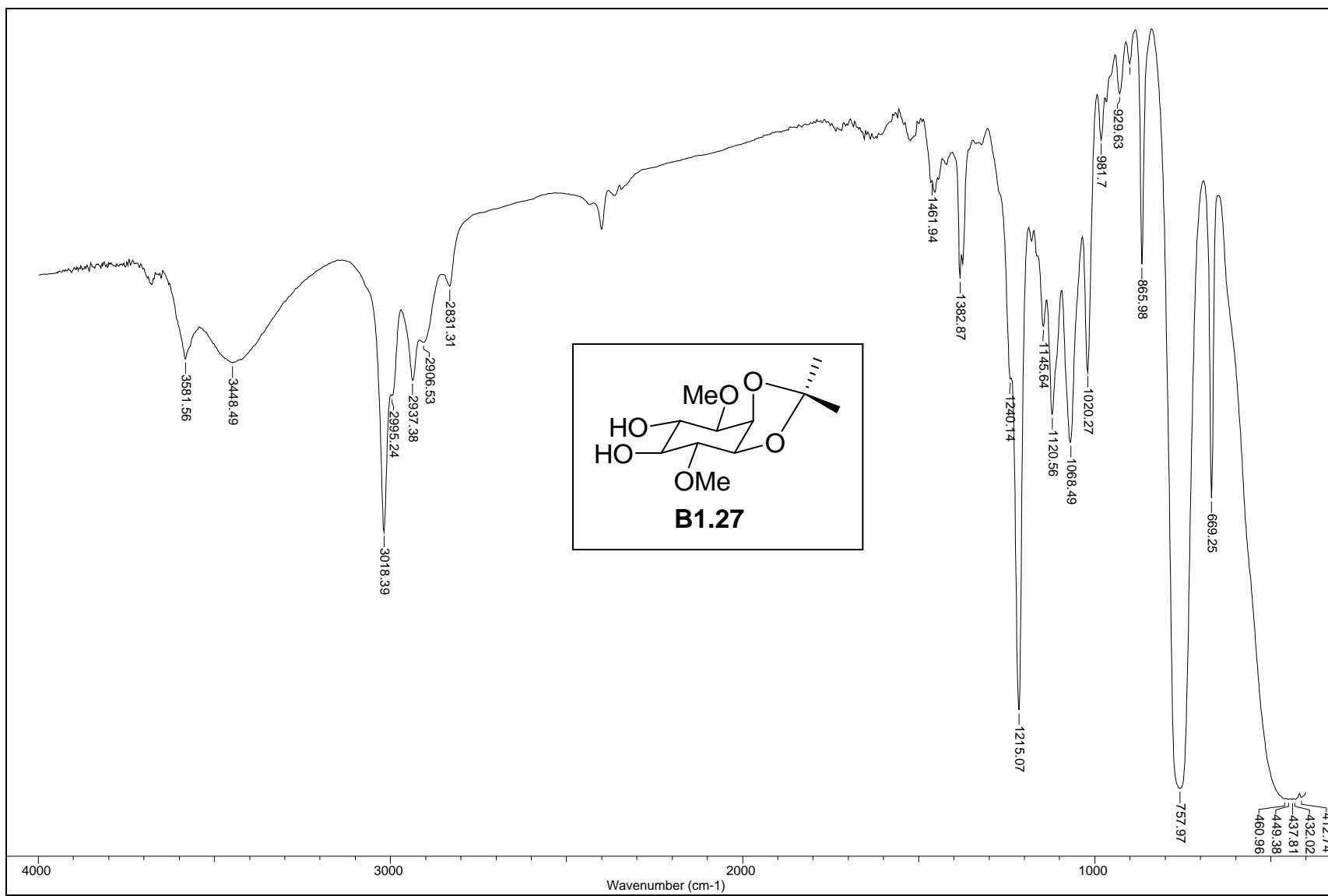
ORTEP diagram of **B1.26**Crystal data table of **B1.26**

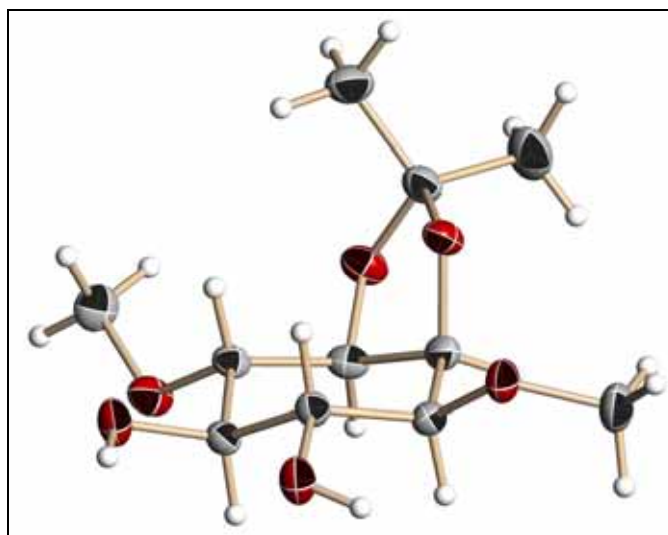
Identification code	B1.26 (crystallized from DCM, light petroleum)
Empirical formula	C ₁₄ H ₂₄ O ₆
Formula weight	288.33
Temperature	297(2) K
Wavelength	0.71073 Å
Crystal system, space group	Triclinic, P-1
Unit cell dimensions	a = 5.3884(10) Å α = 77.783(3)° b = 9.8355(17) Å β = 81.279(3)° c = 15.532(3) Å γ = 80.173(3)°
Volume	787.0(2) Å ³
Z, Calculated density	2, 1.217 Mg/m ³
Absorption coefficient	0.094 mm ⁻¹
F(000)	312
Crystal size	0.75 x 0.72 x 0.36 mm
θ range for data collection	1.35 to 25.00°
Limiting indices	-6 ≤ h ≤ 6, -11 ≤ k ≤ 11, -18 ≤ l ≤ 18
Reflections collected / unique	5601 / 2764 [R(int) = 0.0359]
Completeness to θ = 25.00	99.2 %
Absorption correction	Semi-empirical from equivalents
Max. and min. transmission	0.9669 and 0.9327
Refinement method	Full-matrix least-squares on F ²
Data / restraints / parameters	2764 / 0 / 187
Goodness-of-fit on F ²	1.057
Final R indices [I > 2σ (I)]	R1 = 0.0837, wR2 = 0.2122
R indices (all data)	R1 = 0.1033, wR2 = 0.2281
Largest diff. peak and hole (ρ _{max} & ρ _{min})	0.424 and -0.181 e. Å ⁻³



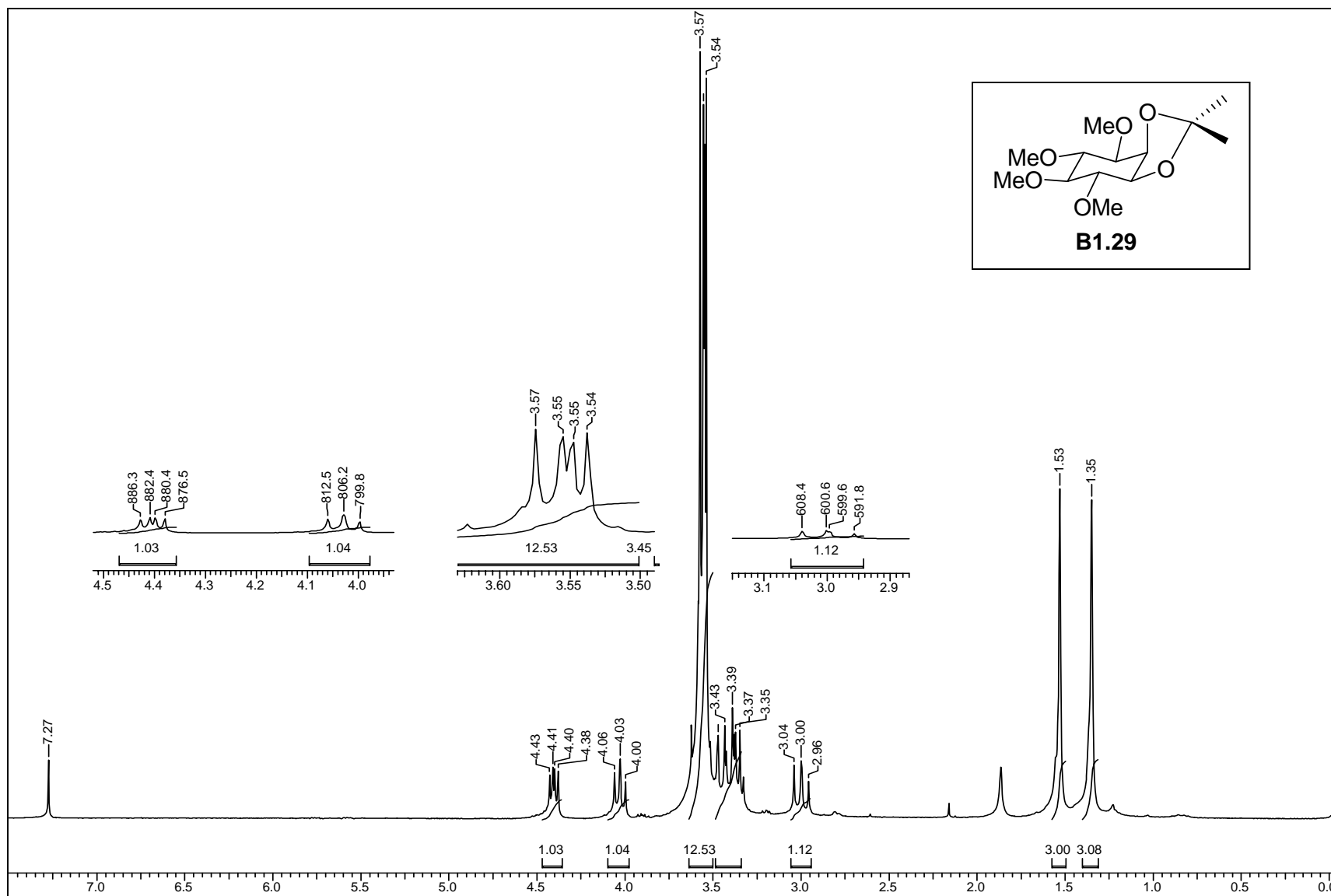


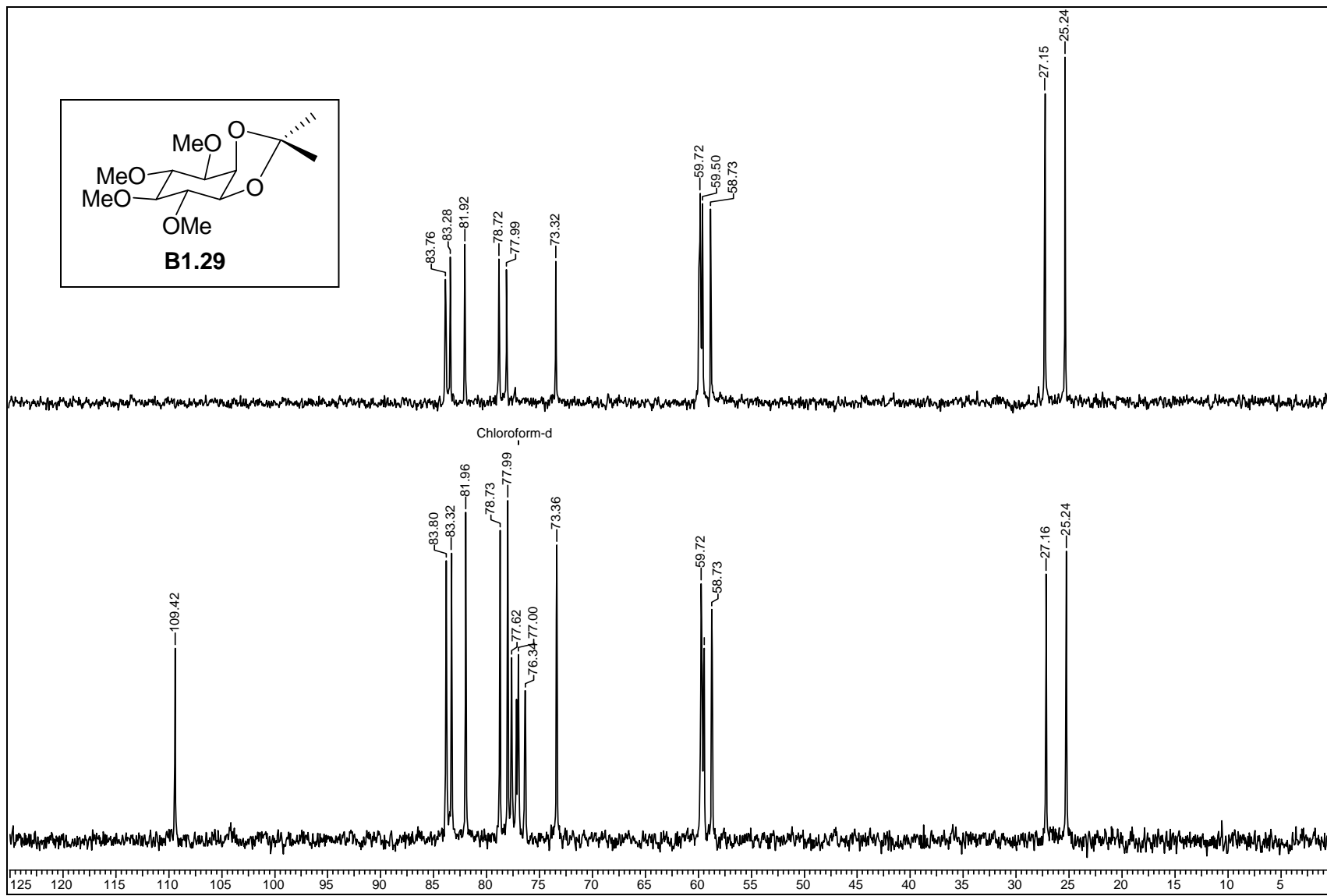


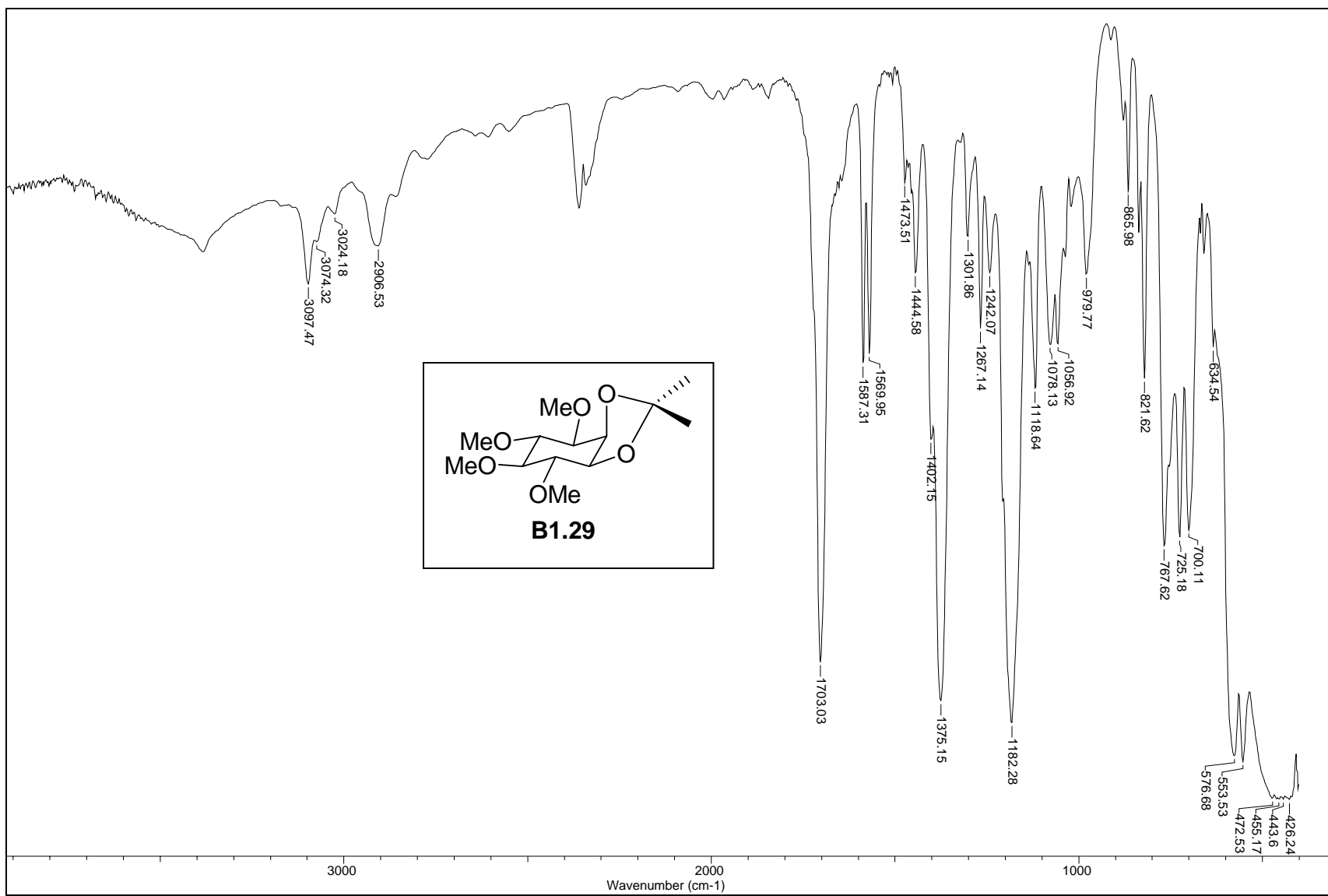


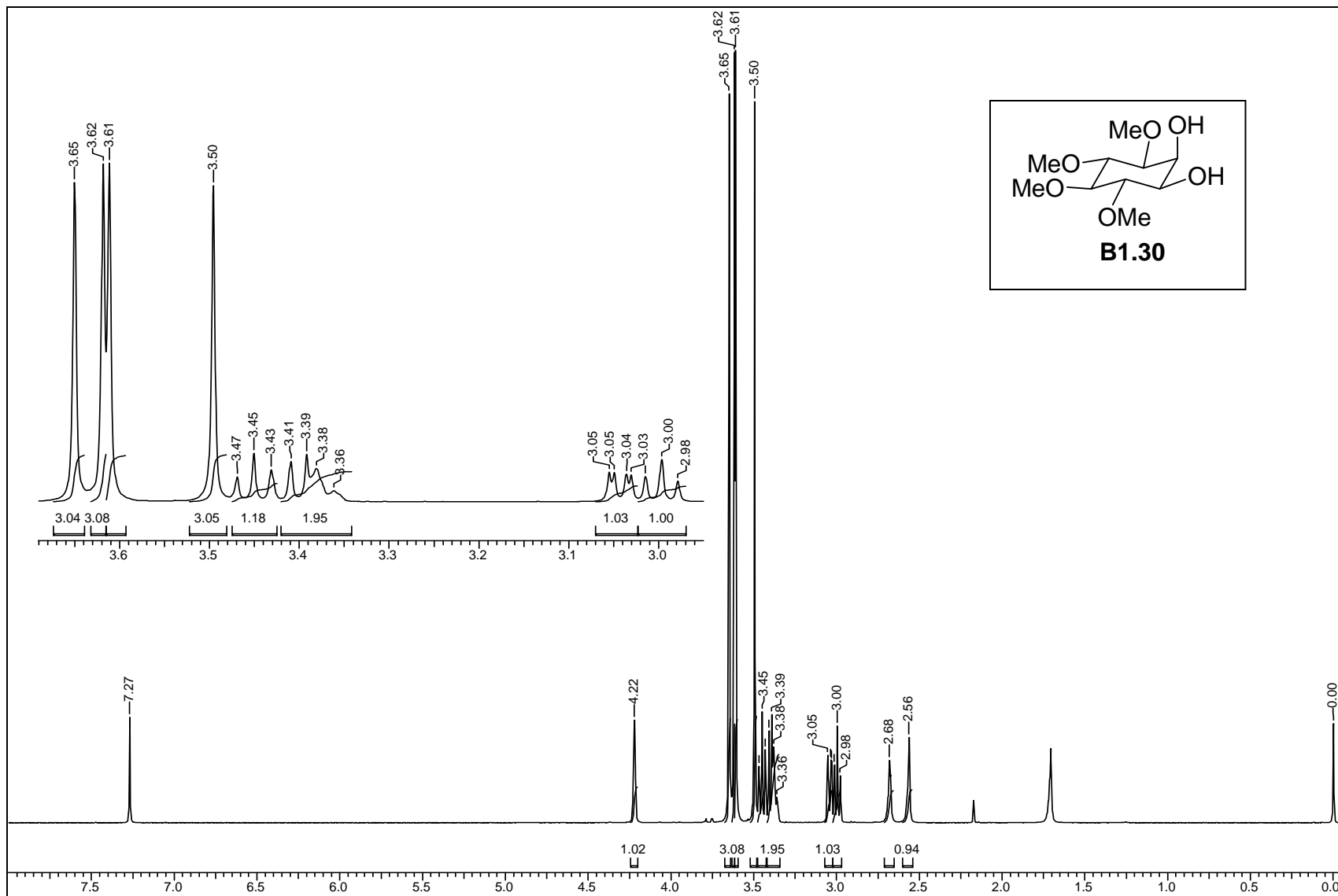
ORTEP diagram of **B1.27**Crystal data table of **B1.27**

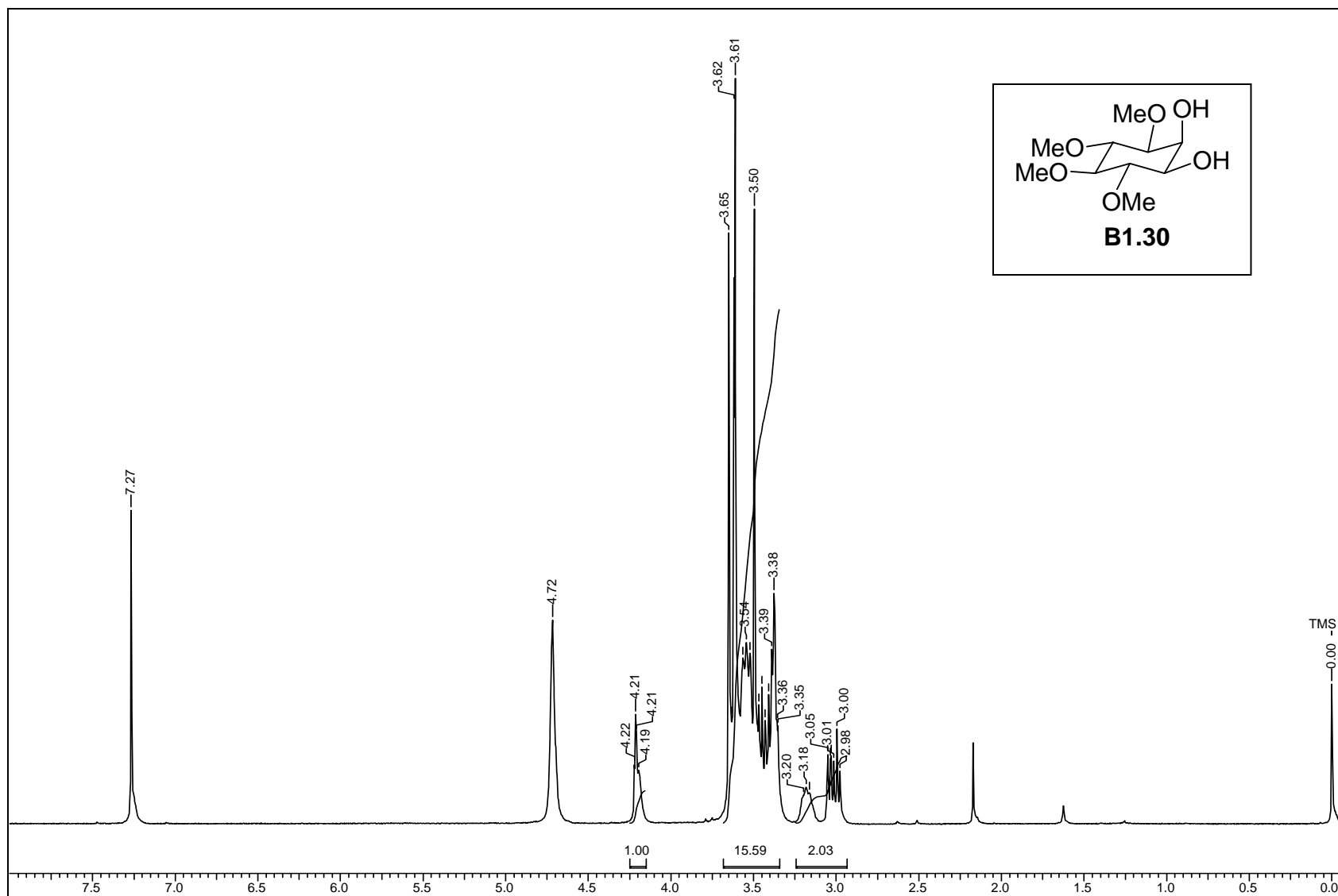
Identification code	B1.27 (crystallized from EtOAc, light petroleum)
Empirical formula	C ₁₁ H ₂₀ O ₆
Formula weight	248.27
Temperature	297(2) K
Wavelength	0.71073 Å
Crystal system, space group	Monoclinic, P 21/n
Unit cell dimensions	a = 6.304(3) Å α = 90° b = 23.230(12) Å β = 98.634(8)° c = 8.412(4) Å γ = 90°
Volume	1217.9(11) Å ³
Z, Calculated density	4, 1.354 Mg/m ³
Absorption coefficient	0.110 mm ⁻¹
F(000)	536
Crystal size	0.62 x 0.54 x 0.37 mm
θ range for data collection	2.60 to 24.99°
Limiting indices	-7 ≤ h ≤ 7, -27 ≤ k ≤ 27, -10 ≤ l ≤ 10
Reflections collected / unique	10492 / 2139 [R(int) = 0.0195]
Completeness to θ = 24.99	99.9 %
Absorption correction	Semi-empirical from equivalents
Max. and min. transmission	0.9605 and 0.9351
Refinement method	Full-matrix least-squares on F ²
Data / restraints / parameters	2139 / 0 / 234
Goodness-of-fit on F ²	1.052
Final R indices [I > 2σ (I)]	R1 = 0.0350, wR2 = 0.0900
R indices (all data)	R1 = 0.0367, wR2 = 0.0914
Largest diff. peak and hole (ρ _{max} & ρ _{min})	0.201 and -0.189 e. Å ⁻³

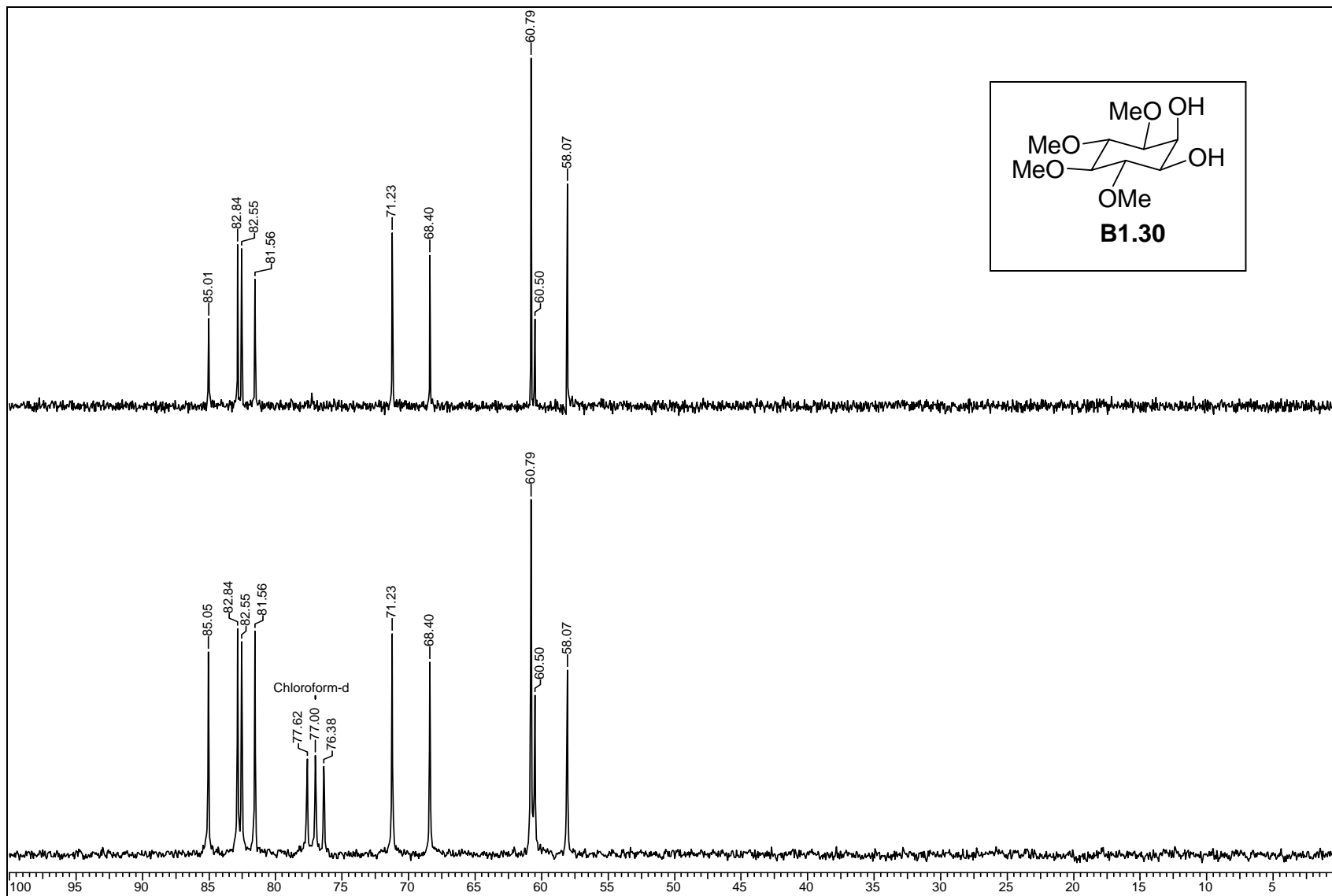


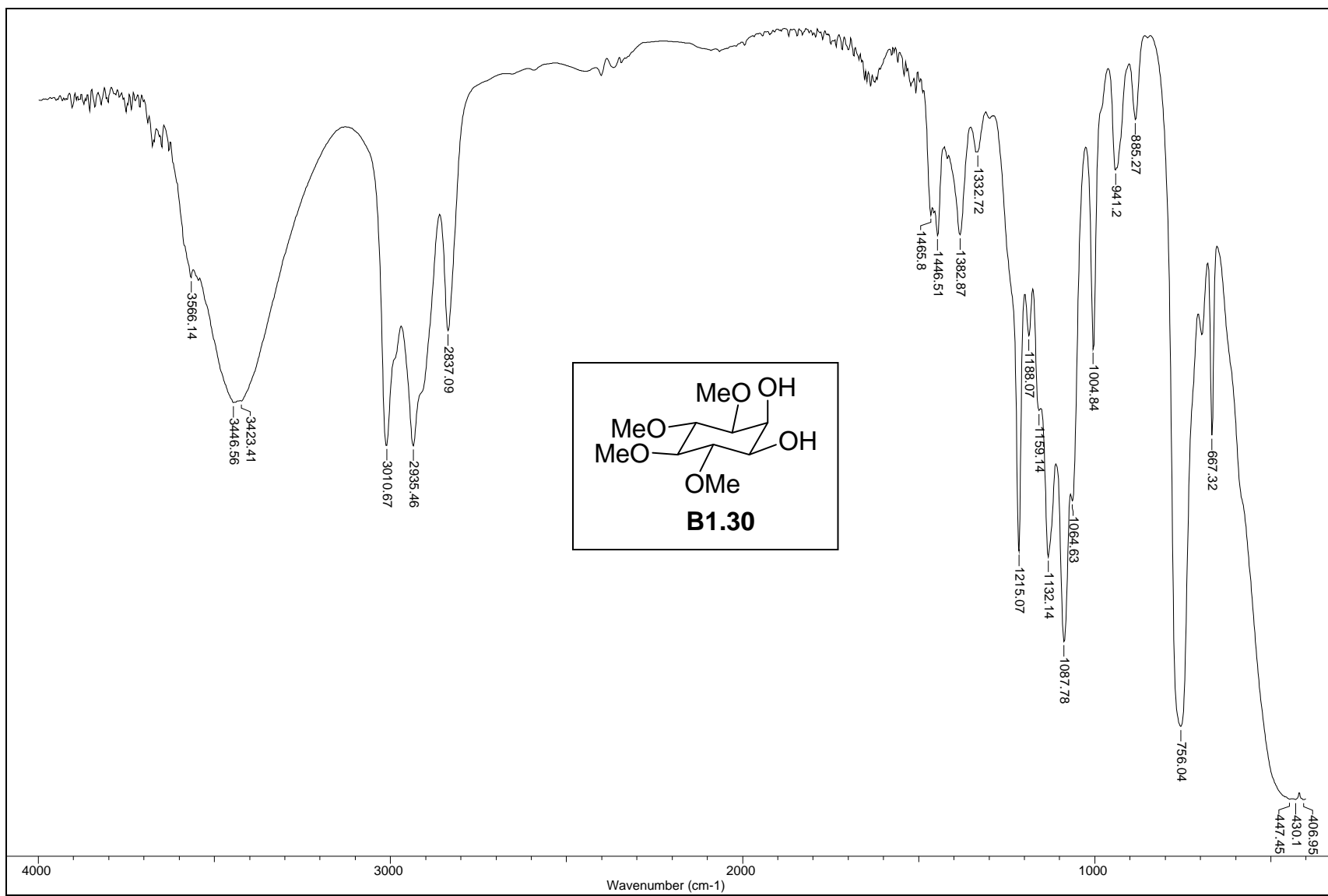


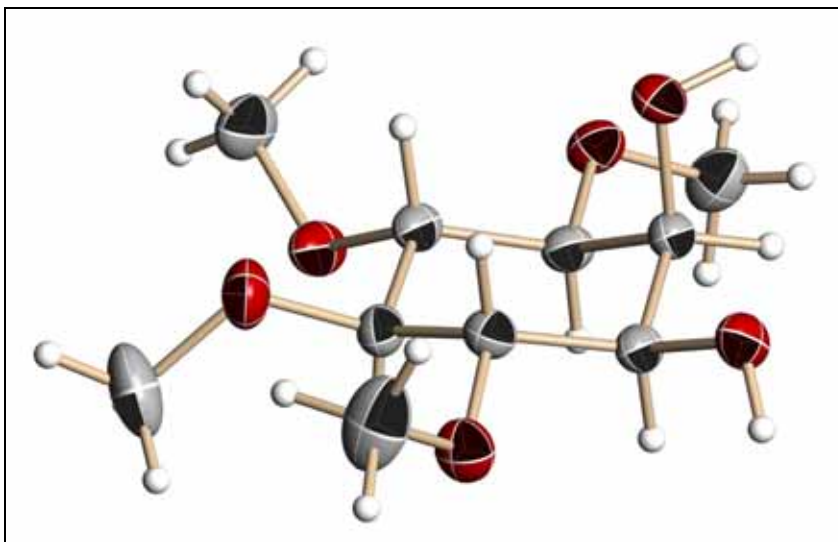




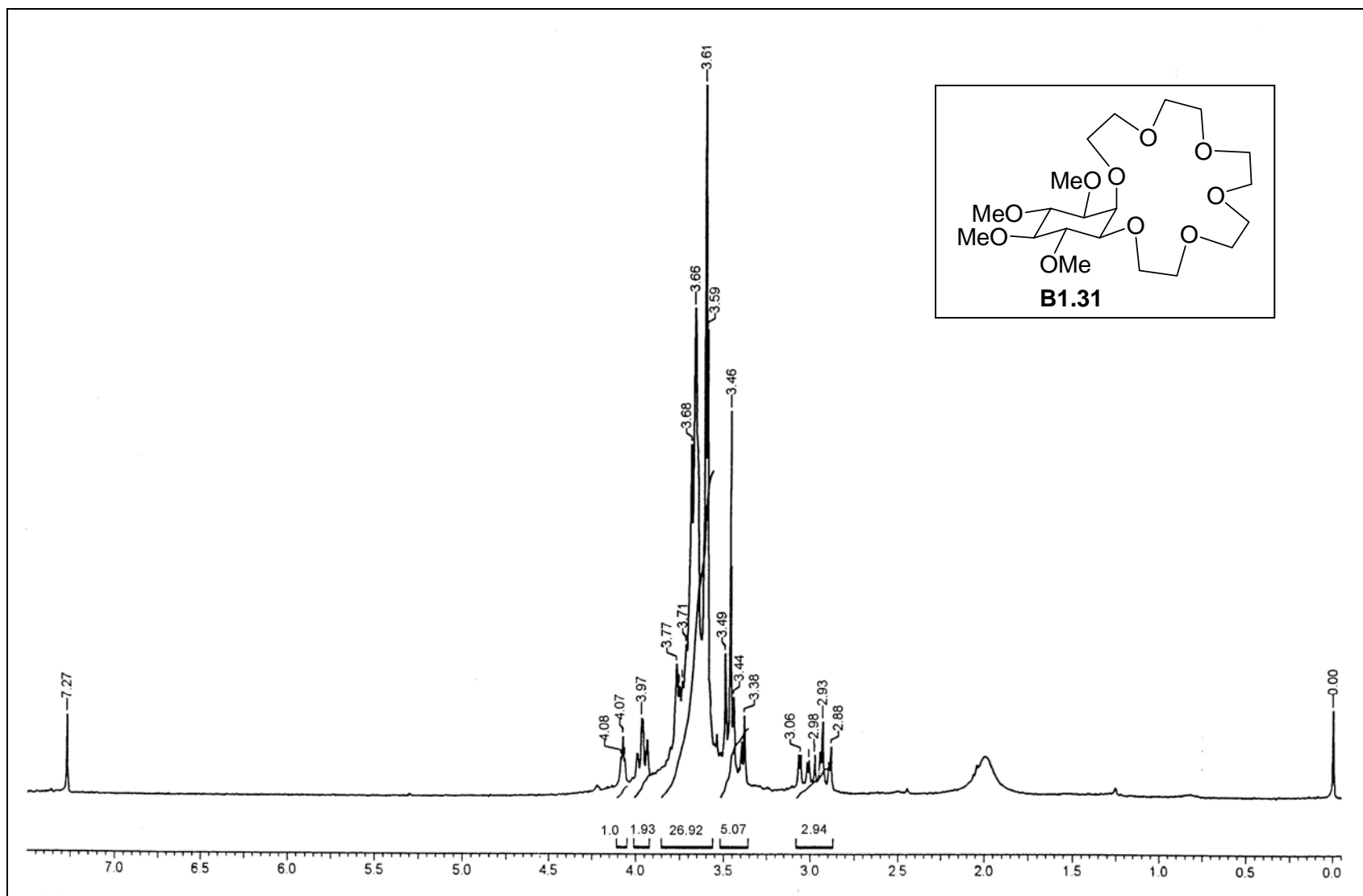


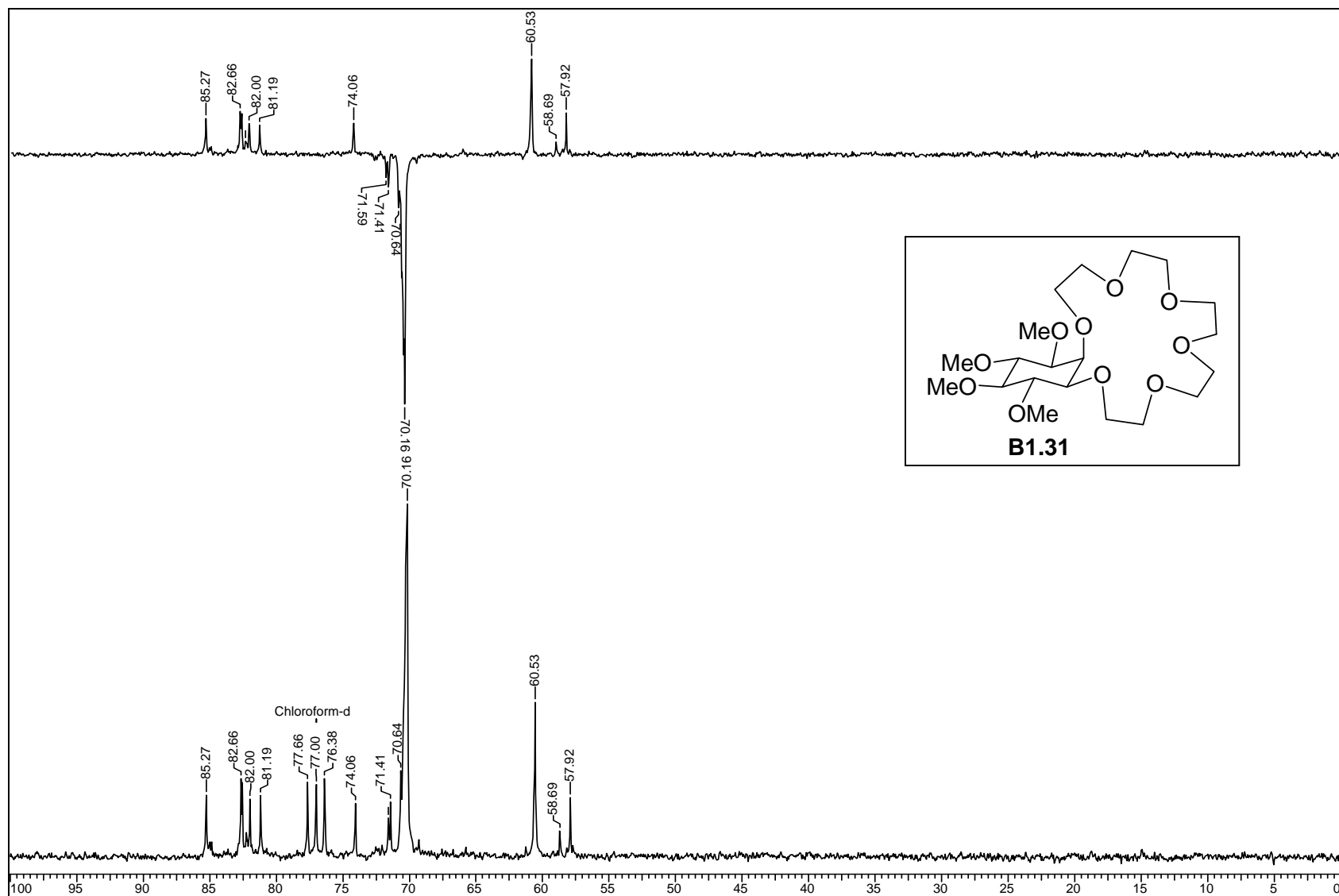


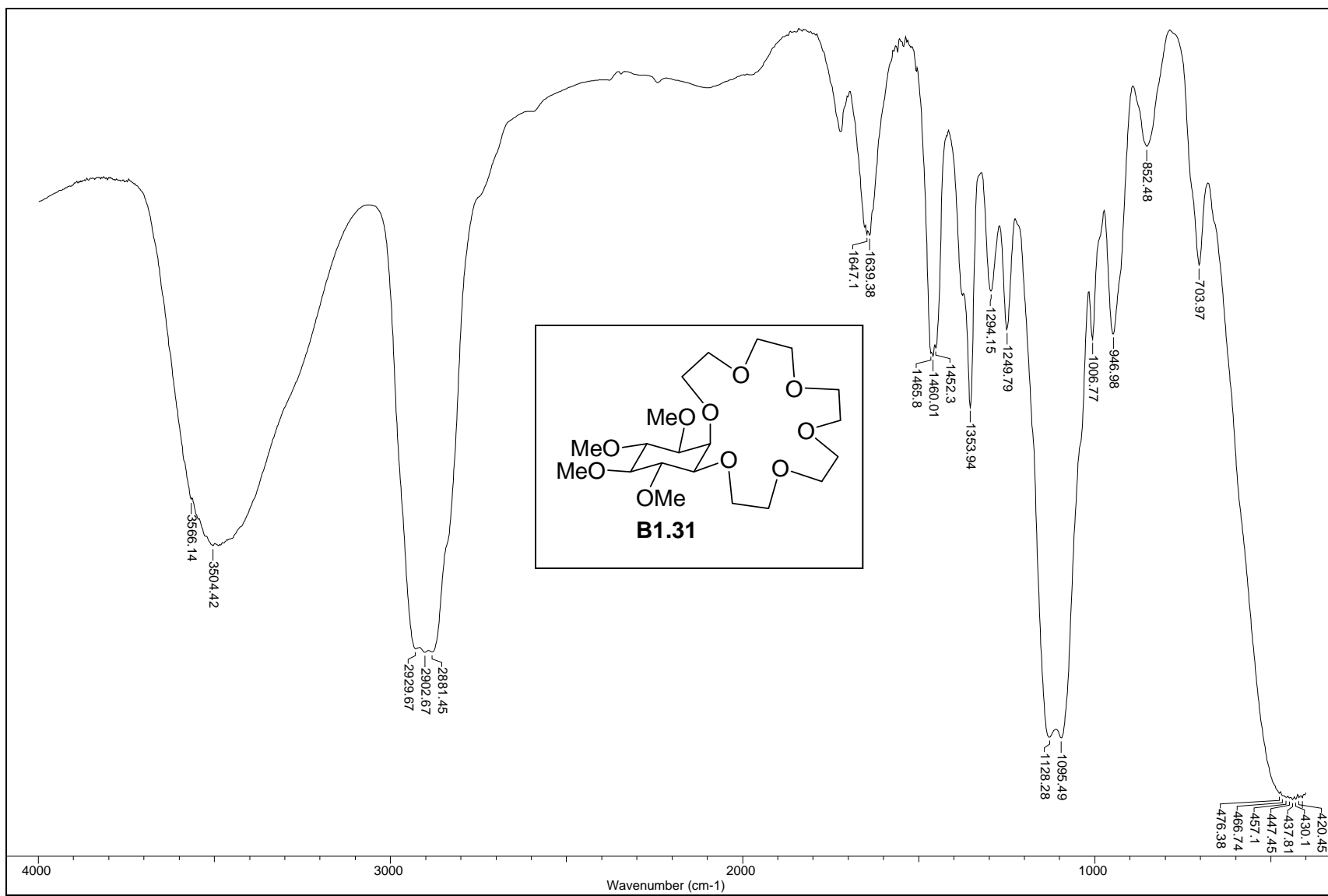


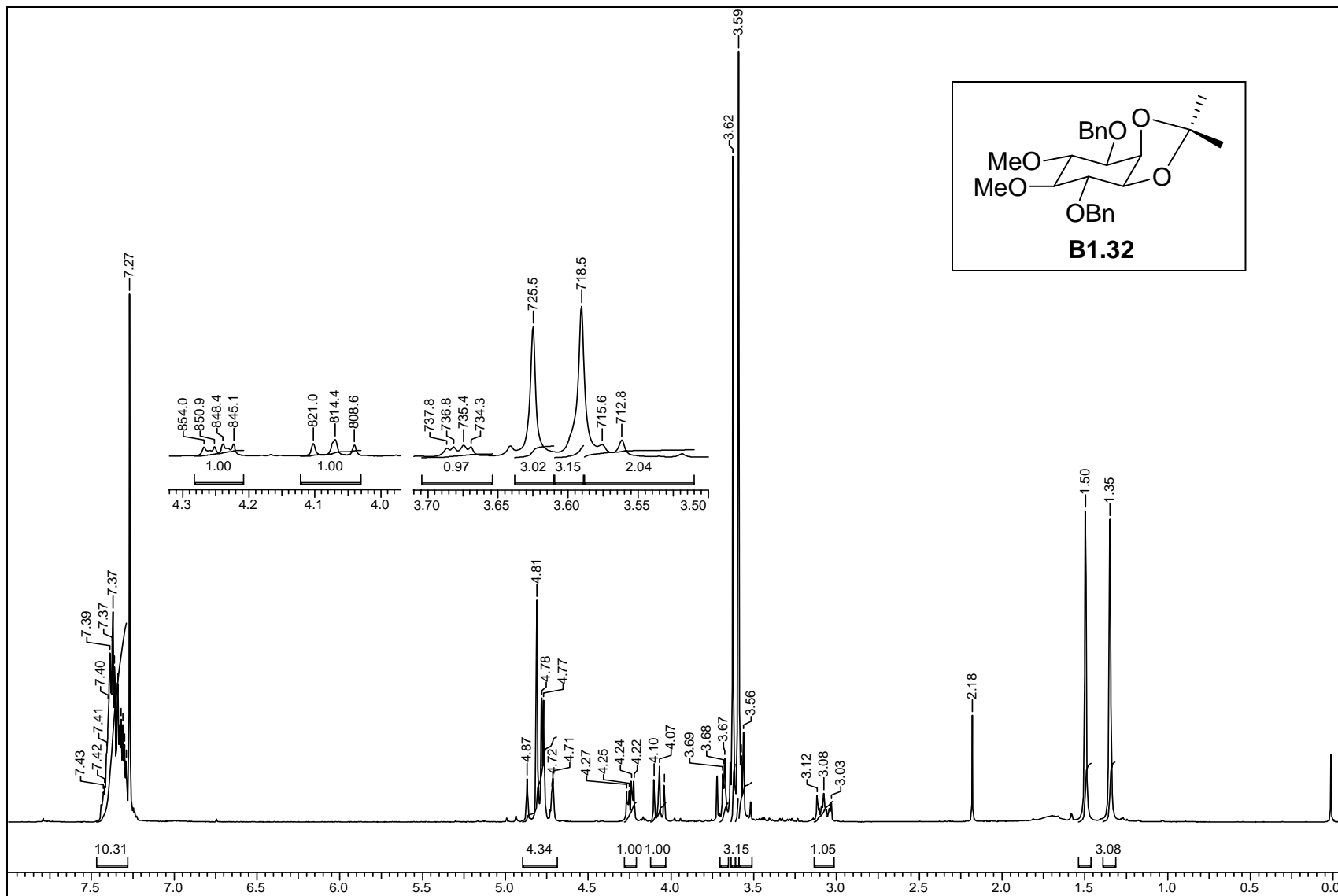
ORTEP diagram of **B1.30**Crystal data table of **B1.30**

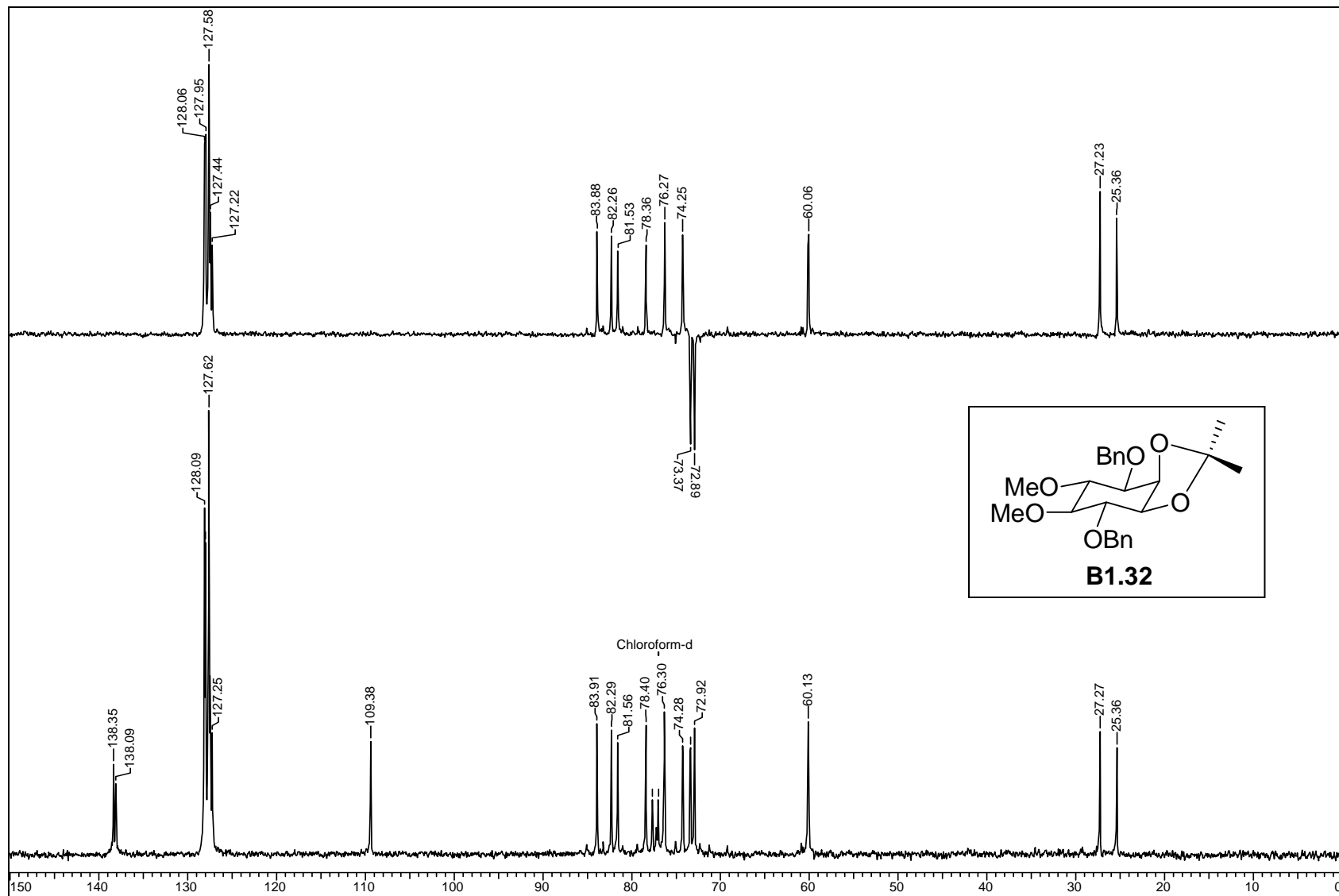
Identification code	B1.30 (crystallized from ethyl acetate: light petroleum)
Empirical formula	C ₁₀ H ₂₀ O ₆
Formula weight	236.26
Temperature	297(2) K
Wavelength	0.71073 Å
Crystal system, space group	Orthorhombic, Pbc _a
Unit cell dimensions	a = 8.860(7) Å, α = 90° b = 13.568(11) Å, β = 90° c = 20.390(18) Å, γ = 90°
Volume	2451(4) Å ³
Z, Calculated density	8, 1.281 Mg/m ³
Absorption coefficient	0.105 mm ⁻¹
F(000)	1024
Crystal size	0.78 x 0.14 x 0.07 mm
θ range for data collection	2.92 to 25.00°
Limiting indices	-10 ≤ h ≤ 10, -15 ≤ k ≤ 16, -24 ≤ l ≤ 24
Reflections collected / unique	16201 / 2157 [R(int) = 0.0559]
Completeness to θ = 24.99	99.9 %
Absorption correction	Semi-empirical from equivalents
Max. and min. transmission	0.9927 and 0.9224
Refinement method	Full-matrix least-squares on F ²
Data / restraints / parameters	2157 / 0 / 181
Goodness-of-fit on F ²	1.101
Final R indices [I > 2σ (I)]	R1 = 0.0463, wR2 = 0.1247
R indices (all data)	R1 = 0.0681, wR2 = 0.1401
Largest diff. peak and hole (ρ _{max} & ρ _{min})	0.205 and -0.178 e. Å ⁻³

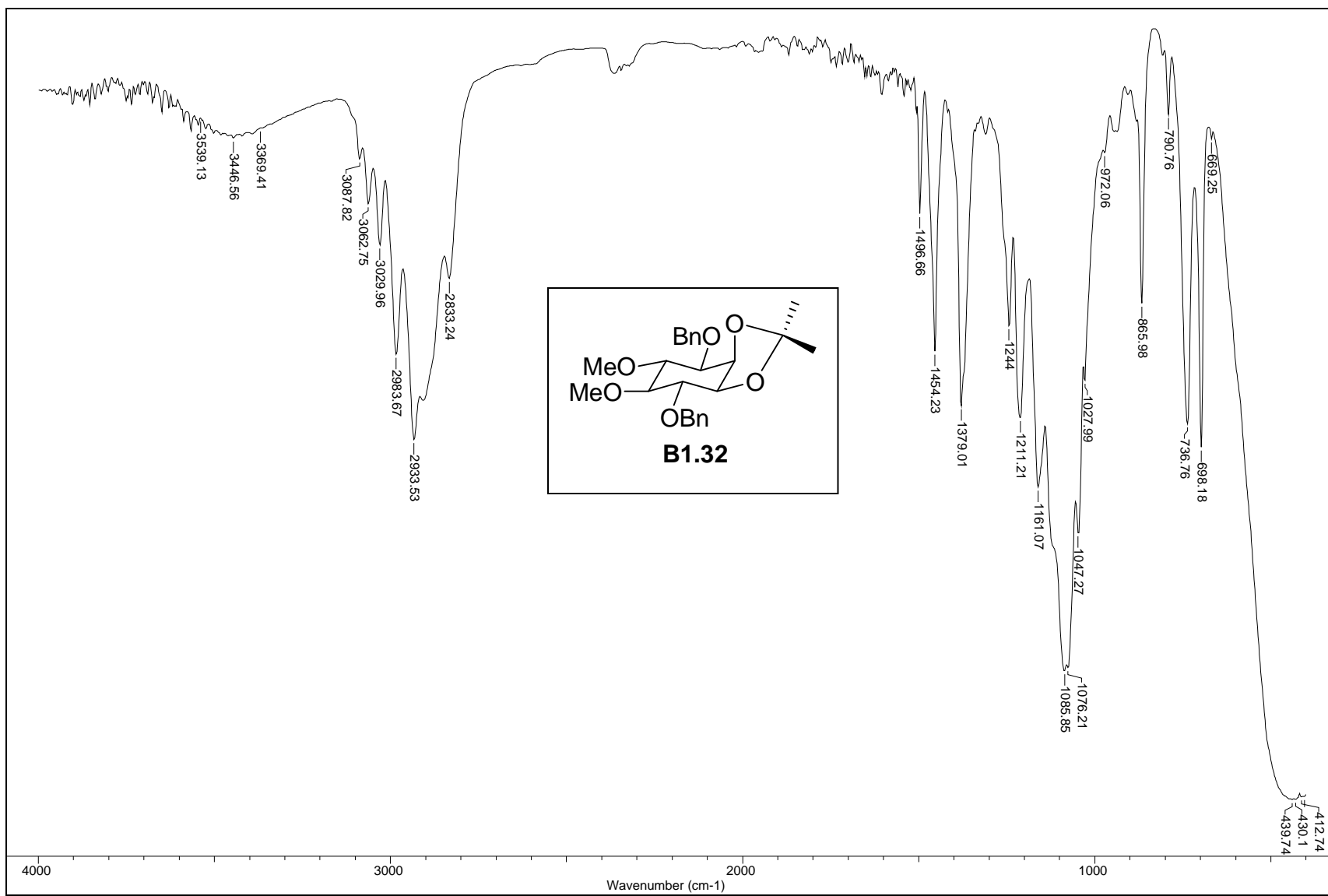


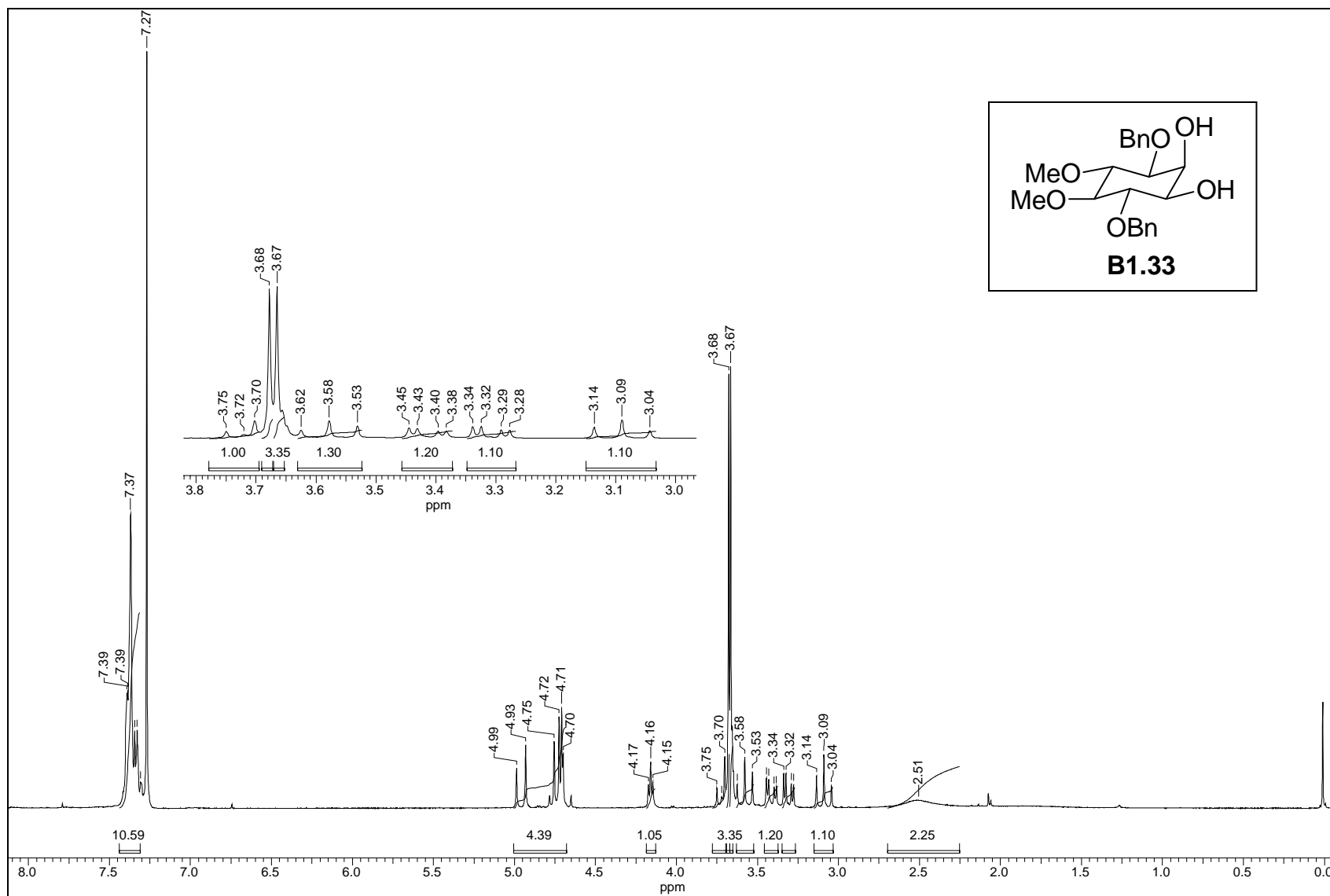


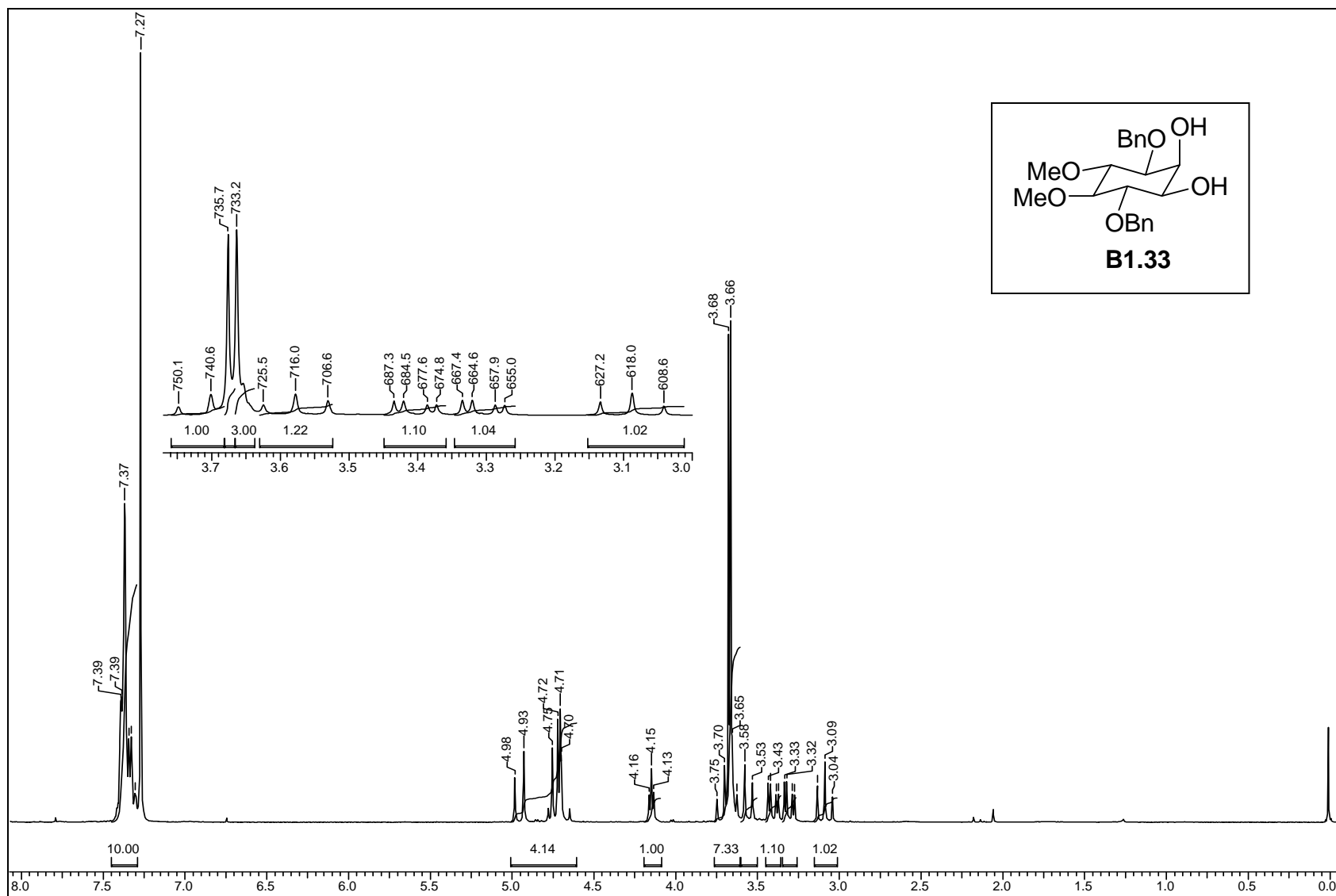


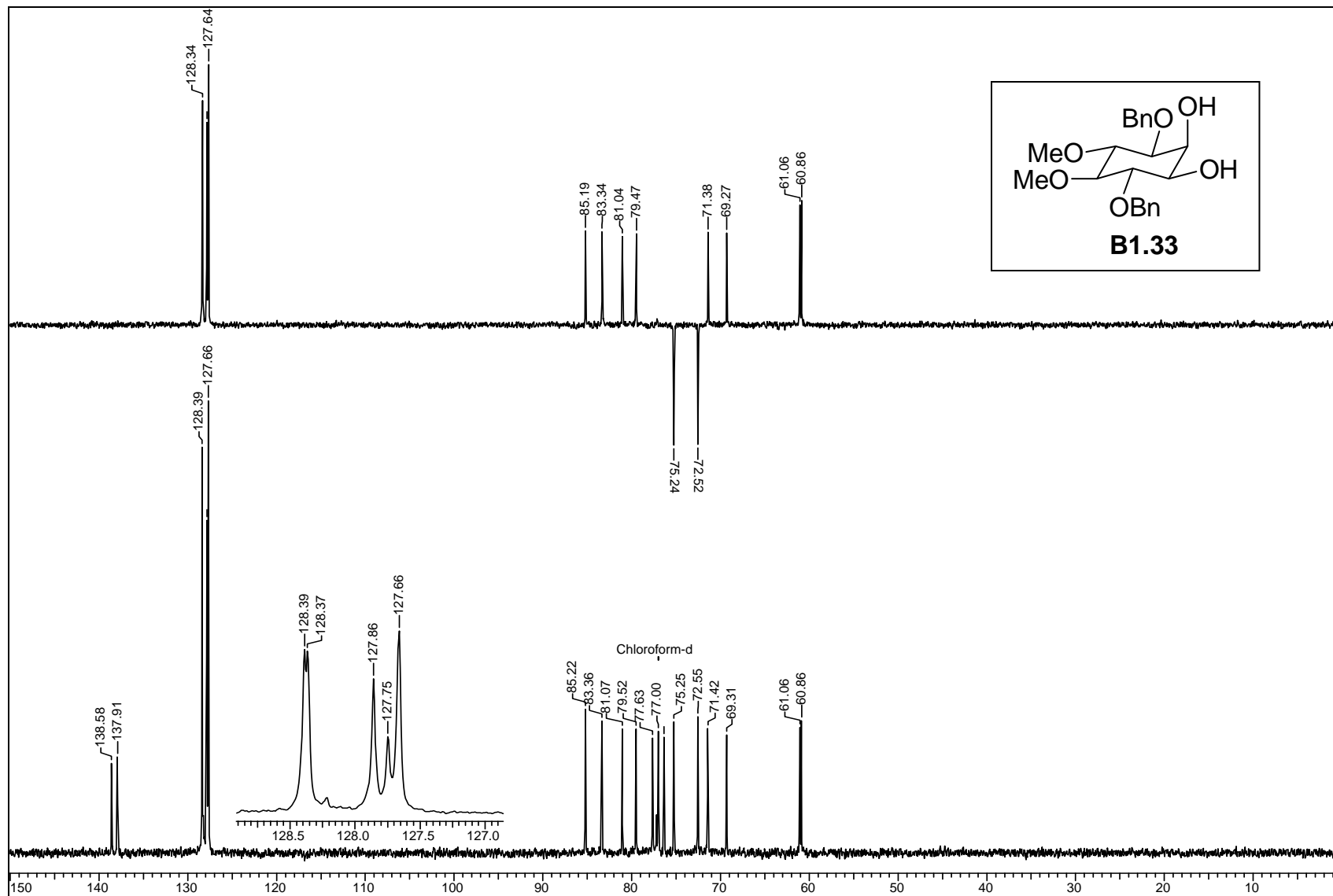


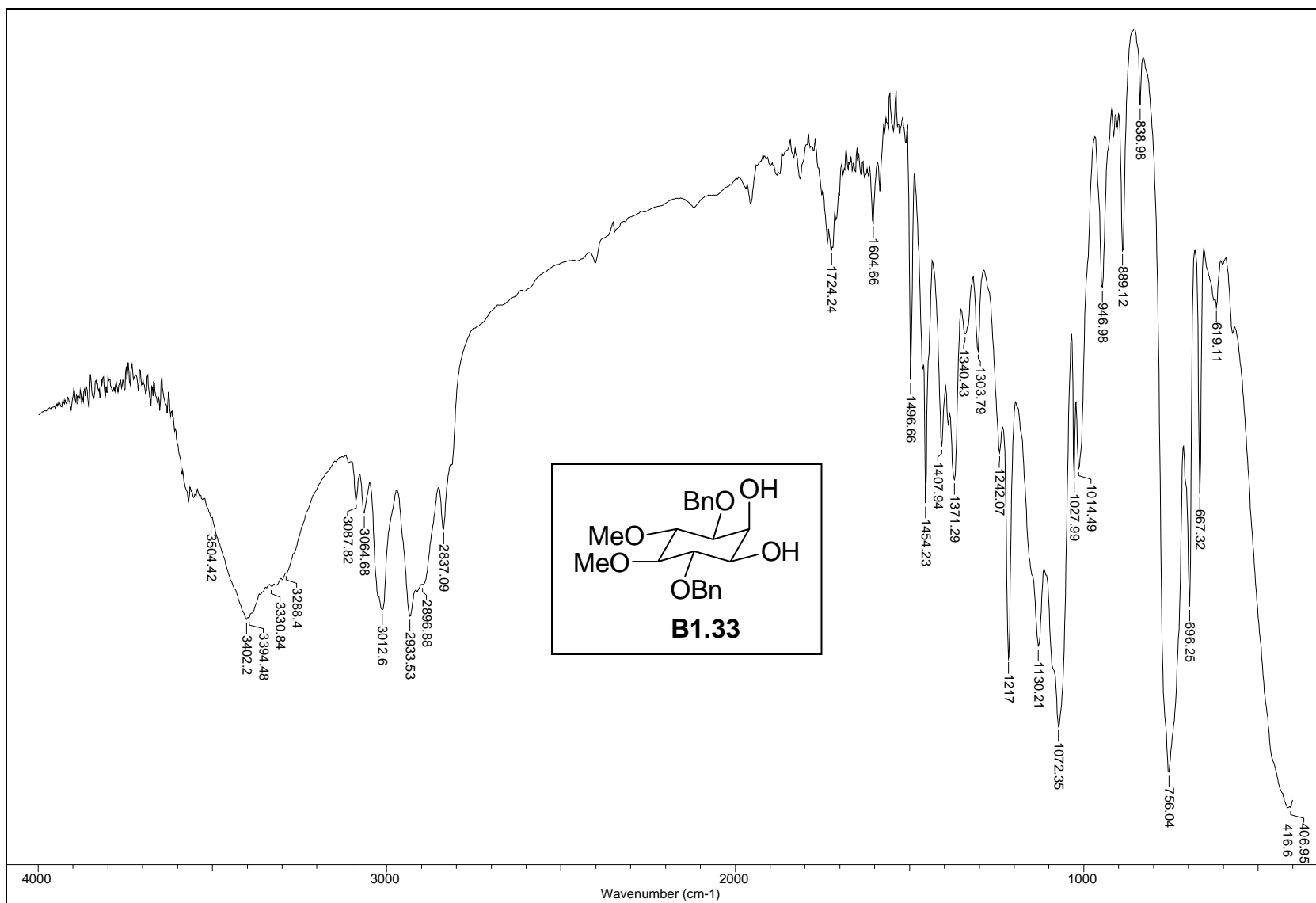


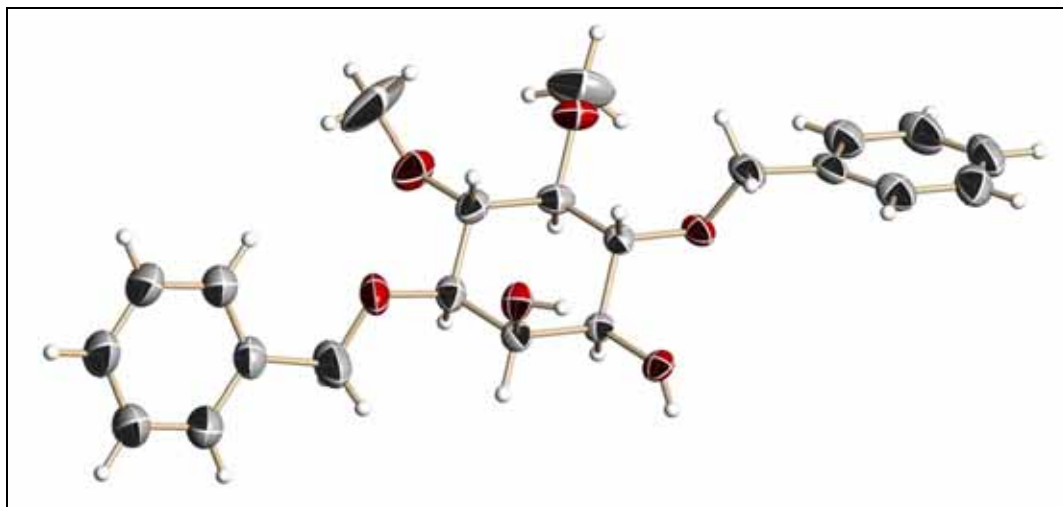




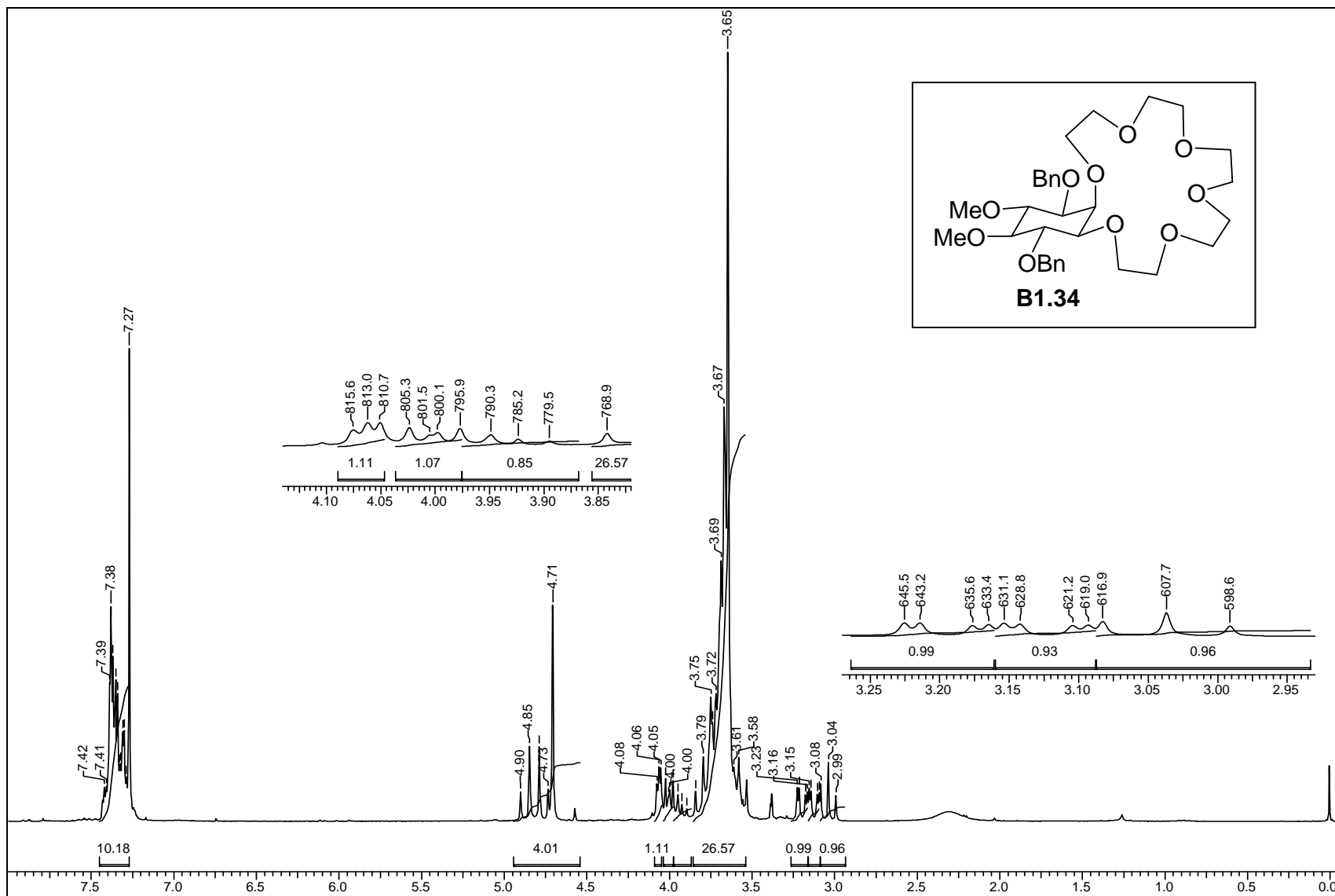


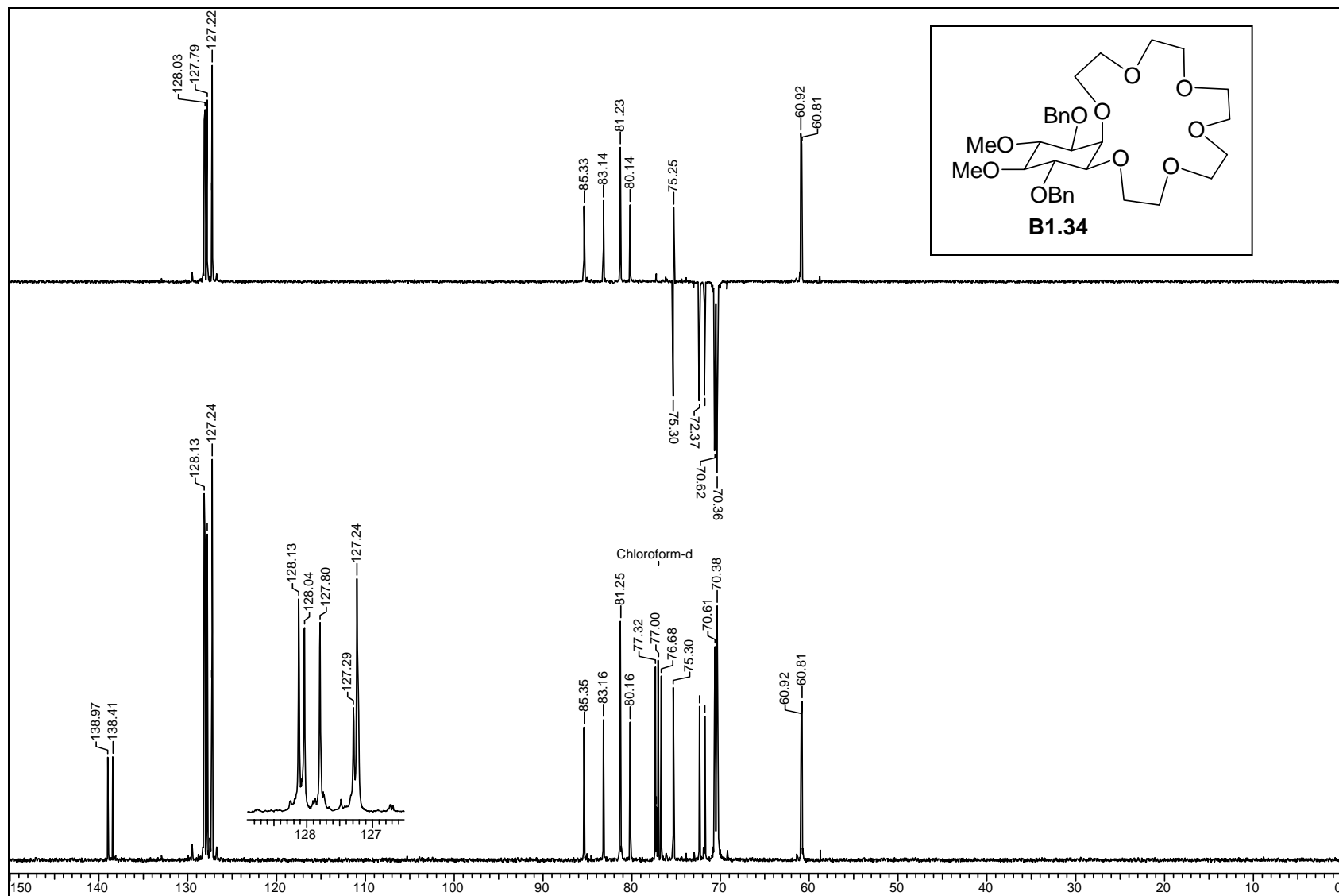


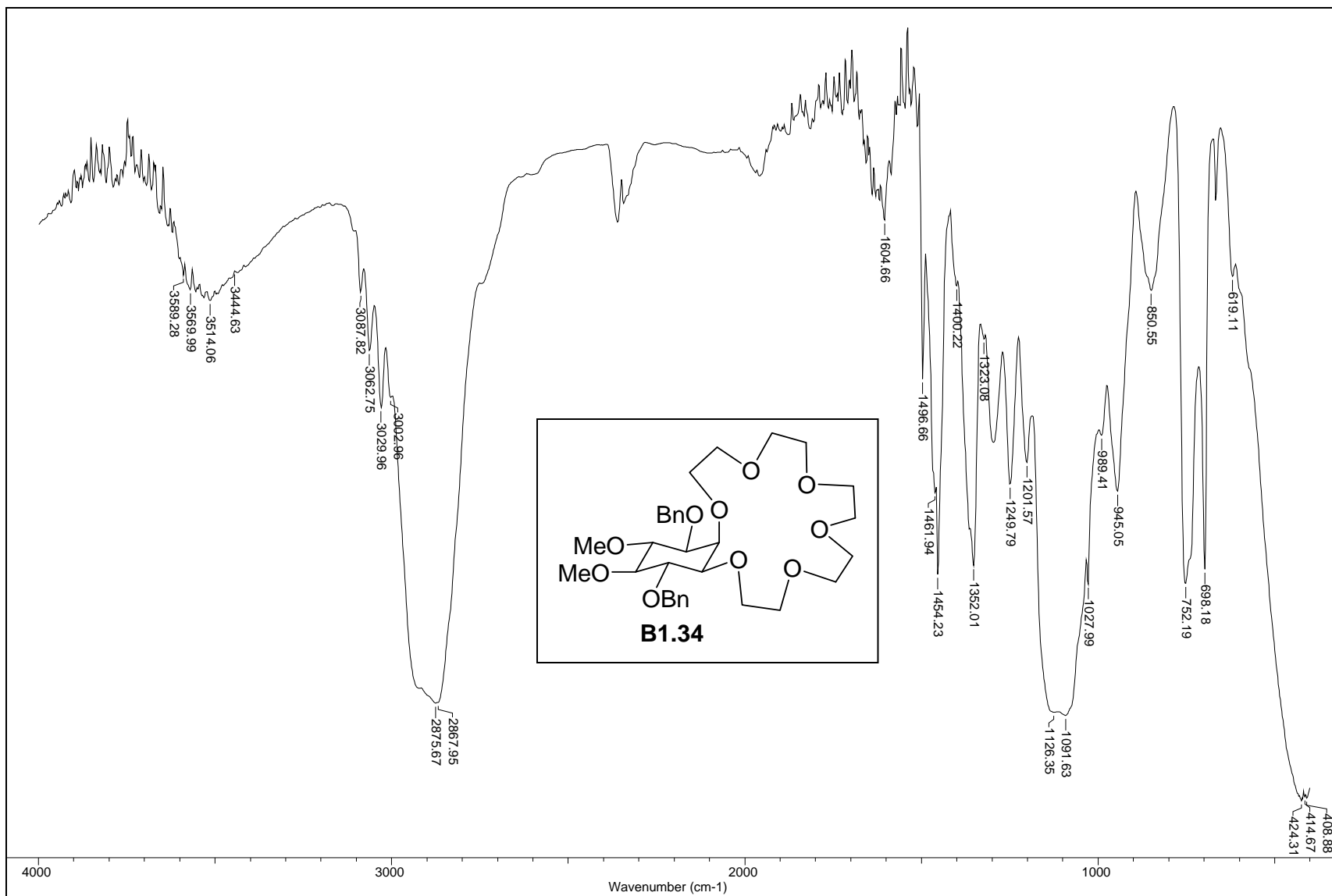


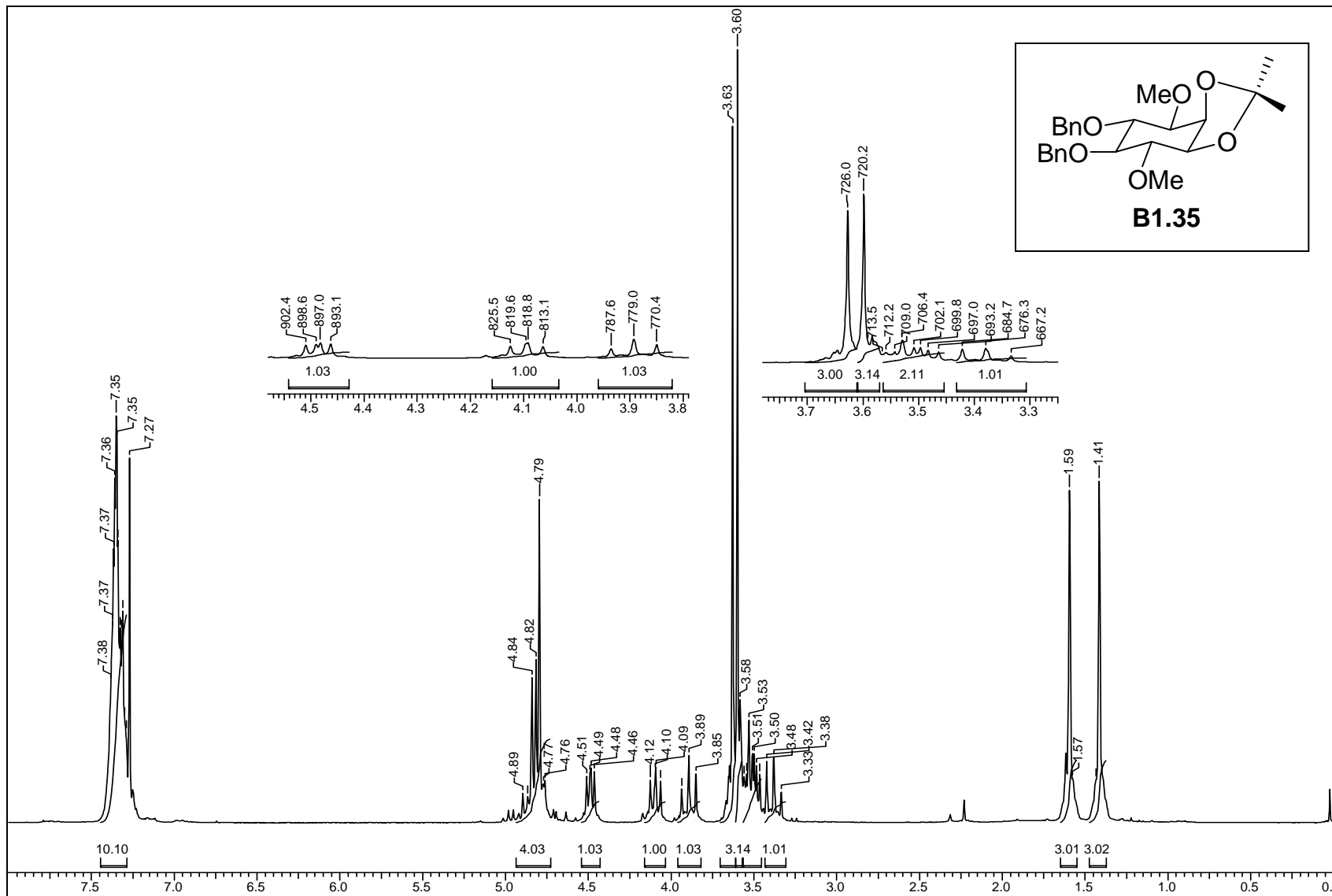
ORTEP diagram of **B1.33**Crystal data table of **B1.33**

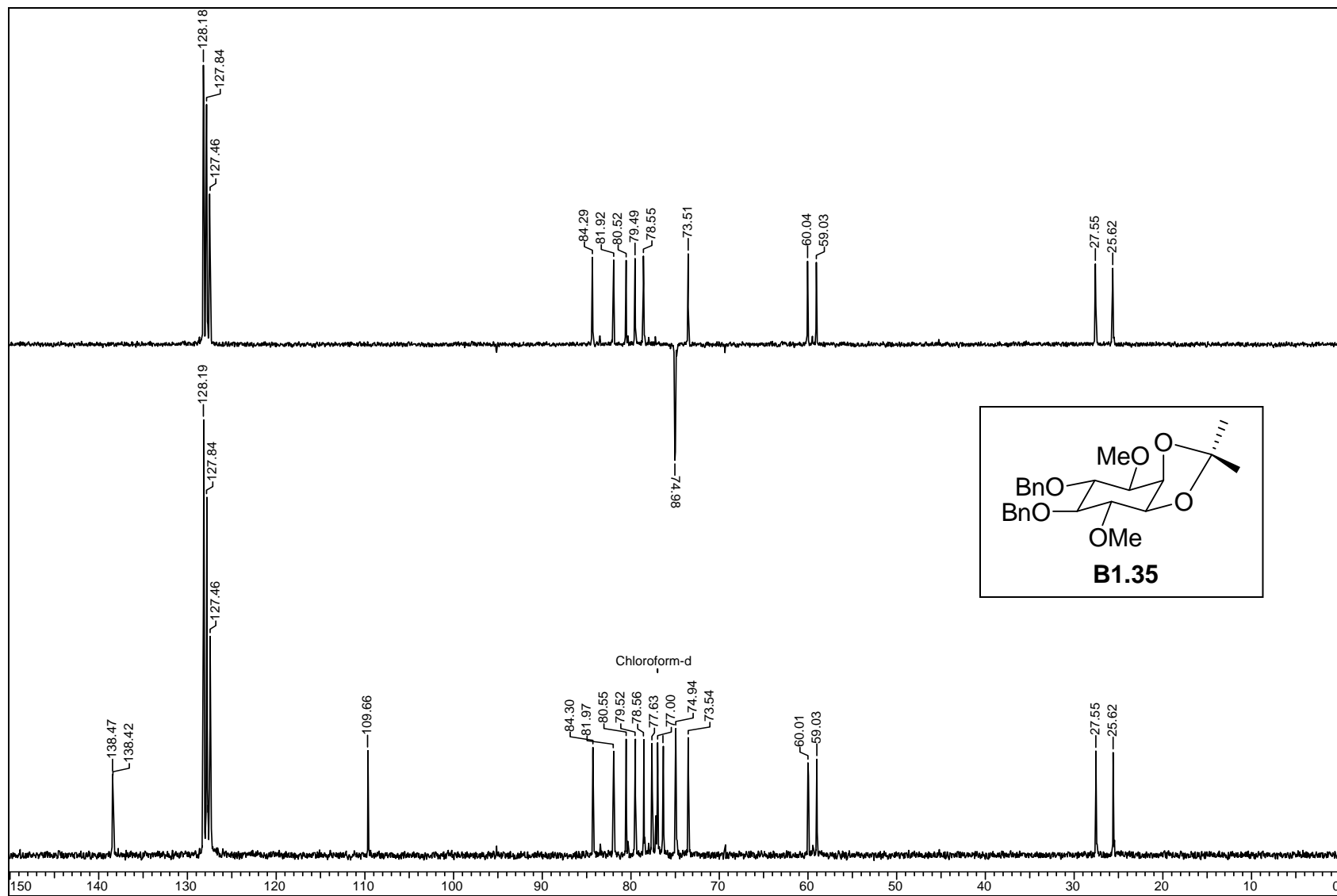
Identification code	B1.33 (crystallized from DCM: light petroleum)
Empirical formula	C ₂₂ H ₂₈ O ₆
Formula weight	388.44
Temperature	297(2) K
Wavelength	0.71073 Å
Crystal system, space group	Monoclinic, P 21/c
Unit cell dimensions	a = 5.7184(10) Å α = 90° b = 30.639(5) Å β = 102.938(3)° c = 12.321(2) Å γ = 90°
Volume	2103.9(6) Å ³
Z, Calculated density	4, 1.226 Mg/m ³
Absorption coefficient	0.088 mm ⁻¹
F(000)	832
Crystal size	0.78 x 0.11 x 0.09 mm
θ range for data collection	1.82 to 25.00°
Limiting indices	-6 ≤ h ≤ 6, -36 ≤ k ≤ 36, -12 ≤ l ≤ 14
Reflections collected / unique	15109 / 3709 [R(int) = 0.0369]
Completeness to θ = 25.00°	99.9 %
Absorption correction	Semi-empirical from equivalents
Max. and min. transmission	0.9921 and 0.9342
Refinement method	Full-matrix least-squares on F ²
Data / restraints / parameters	3709 / 0 / 257
Goodness-of-fit on F ²	1.022
Final R indices [I > 2σ (I)]	R1 = 0.0635, wR2 = 0.1404
R indices (all data)	R1 = 0.1002, wR2 = 0.1583
Largest diff. peak and hole (ρ _{max} & ρ _{min})	0.392 and -0.205 e. Å ⁻³

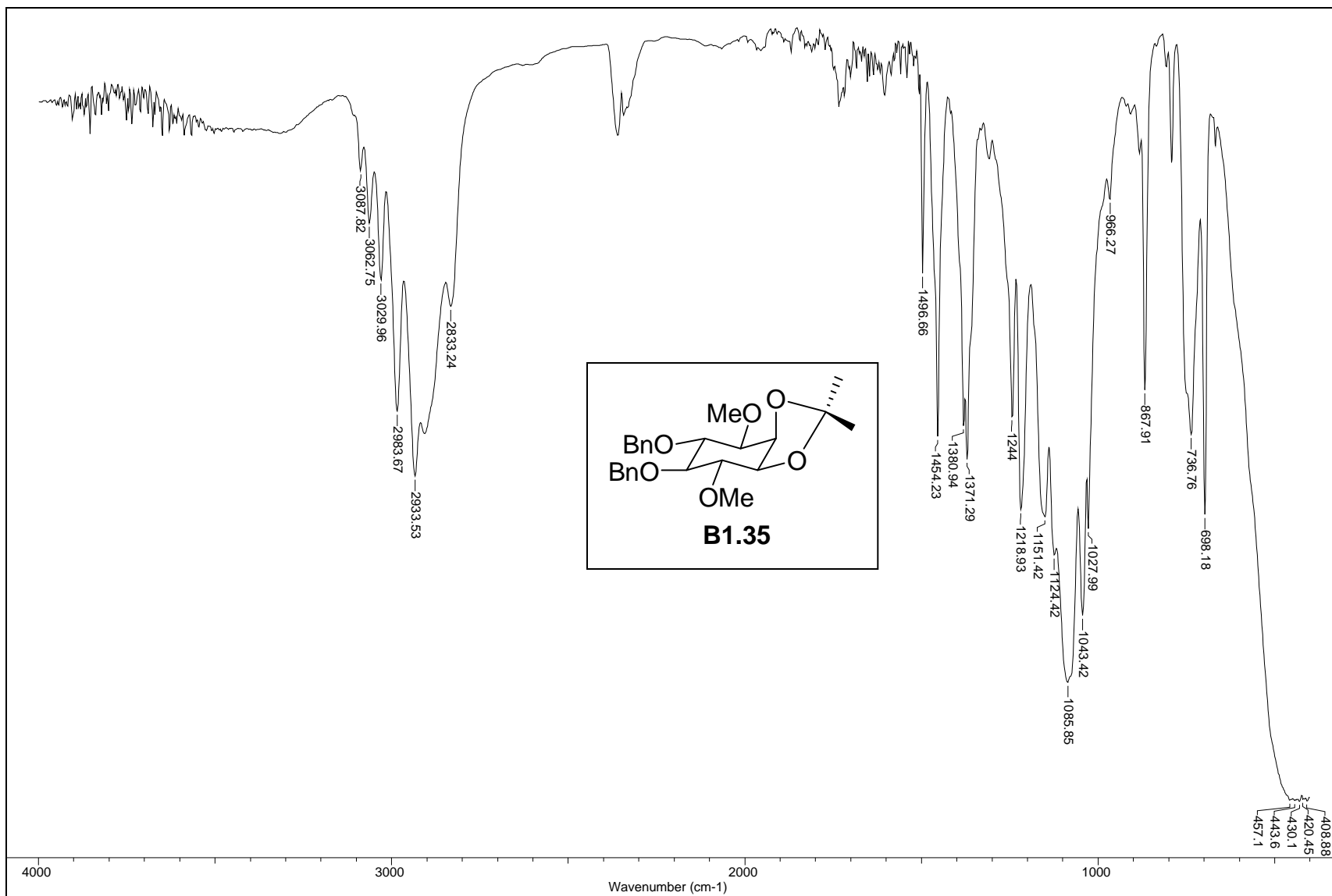


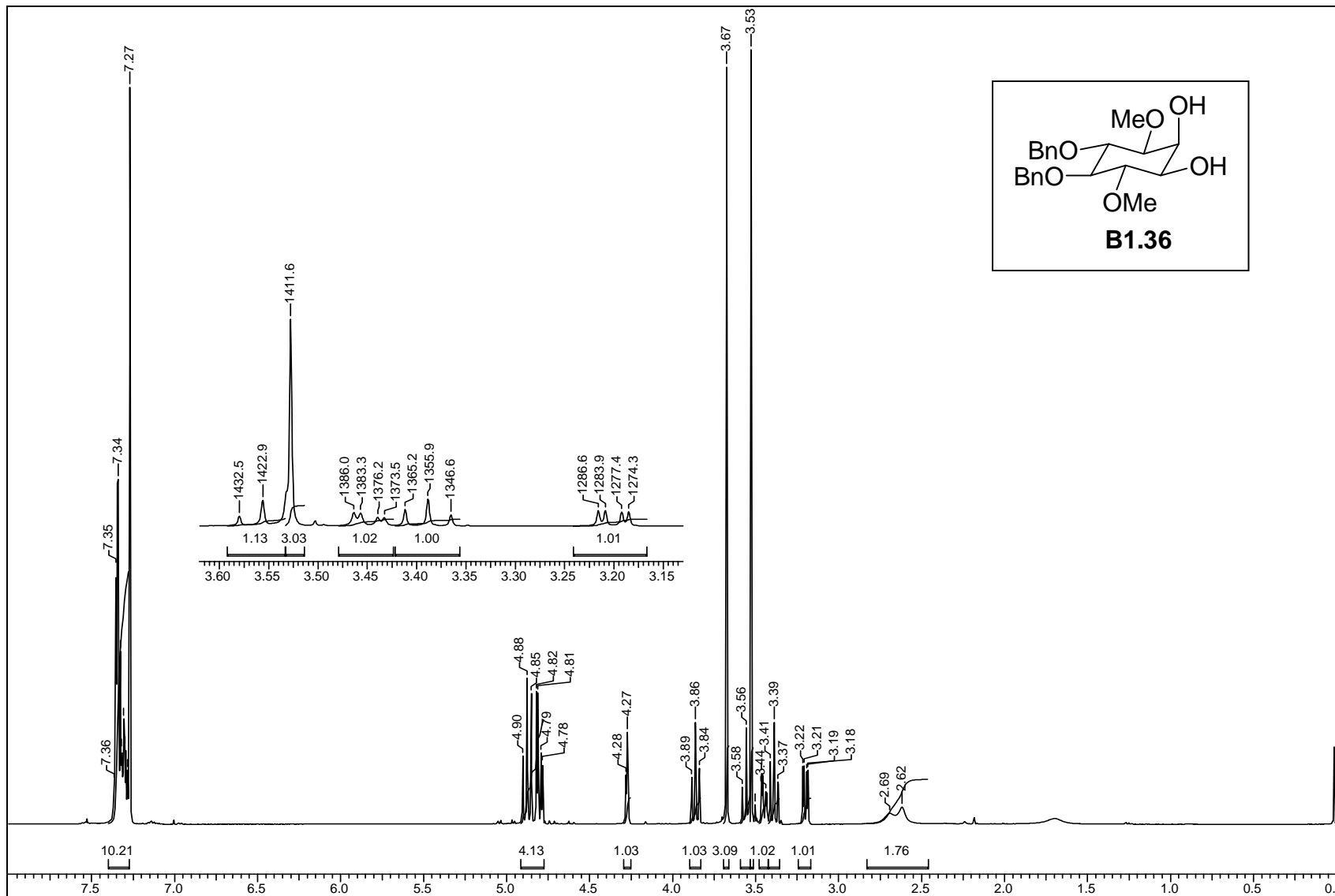


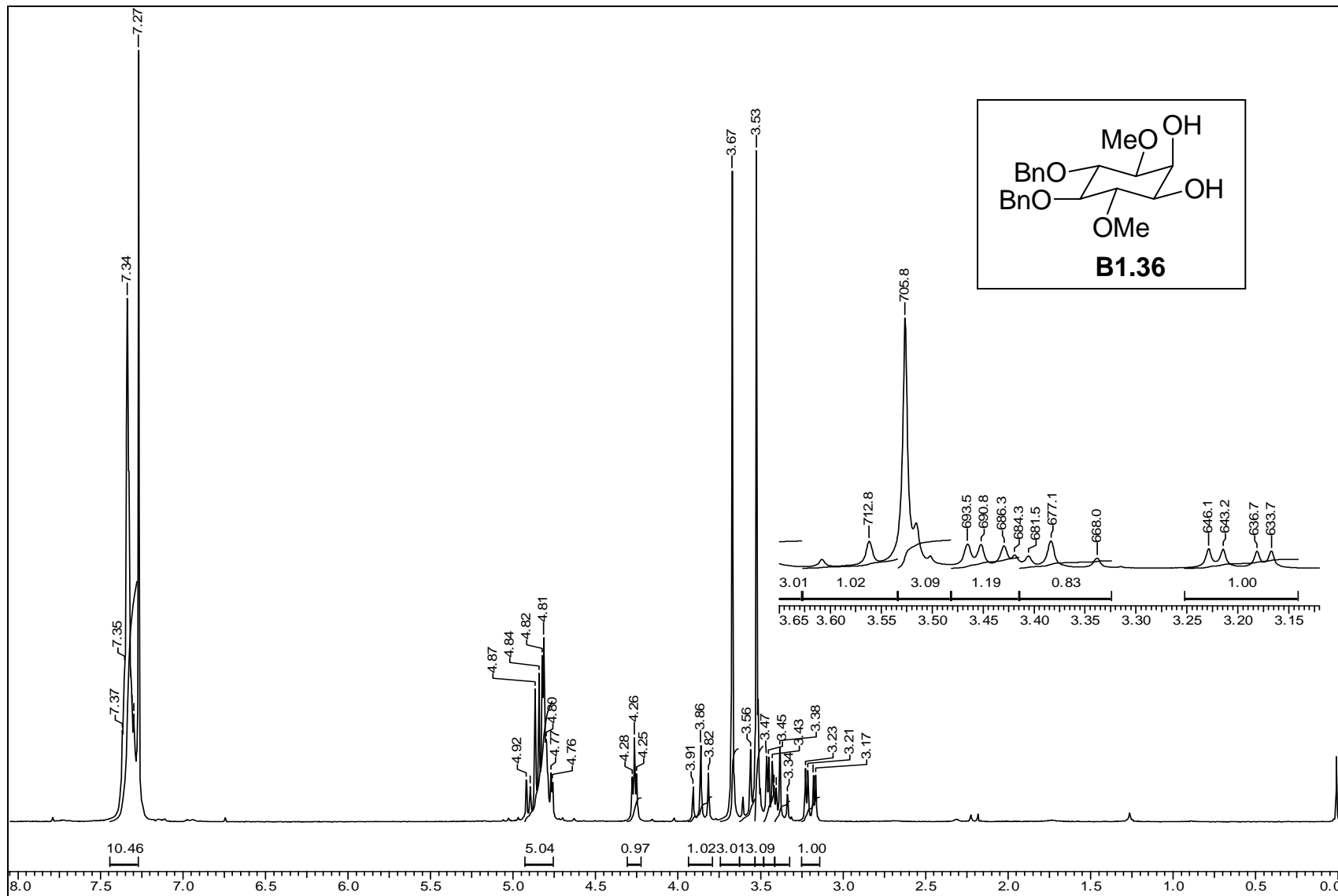


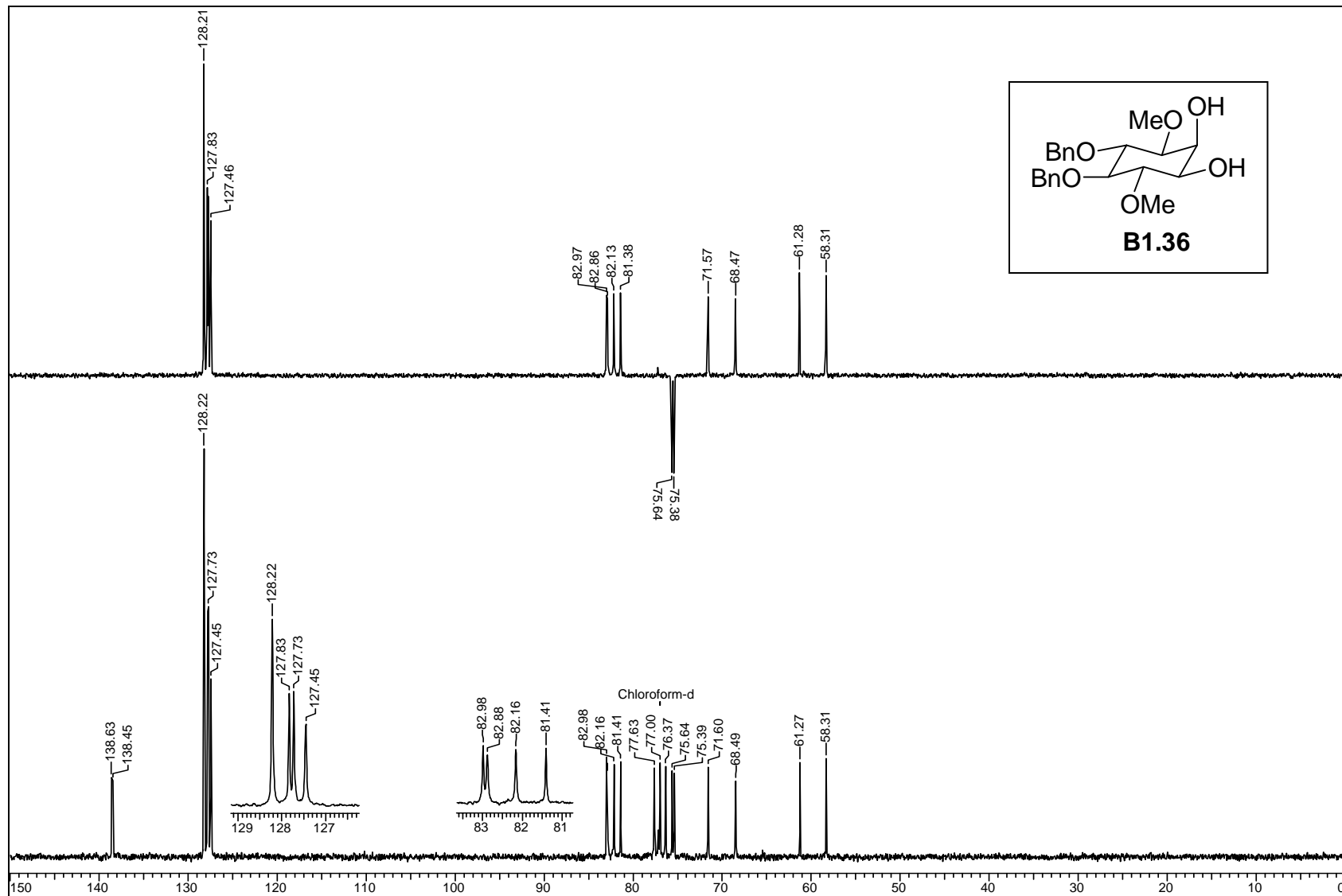


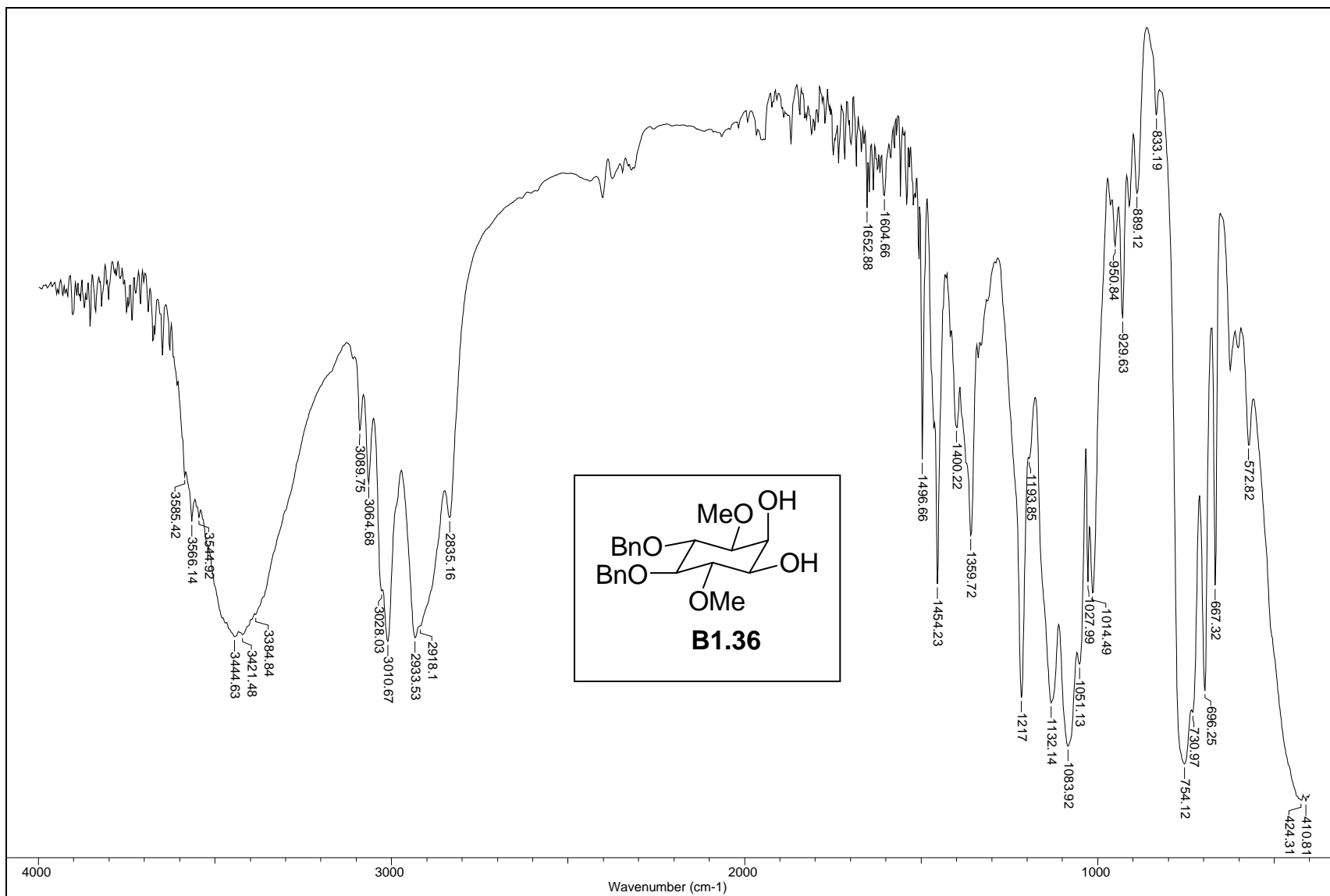


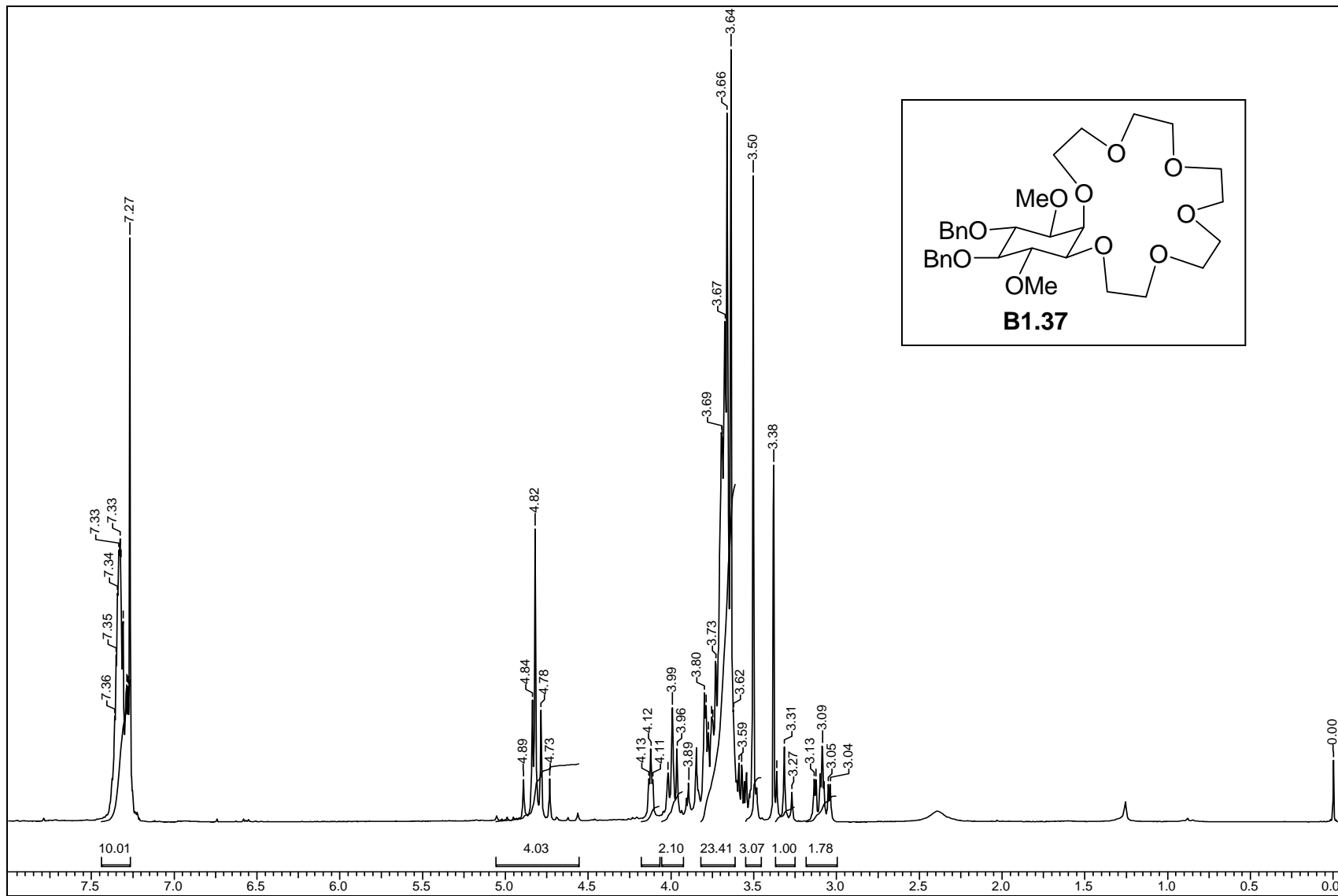


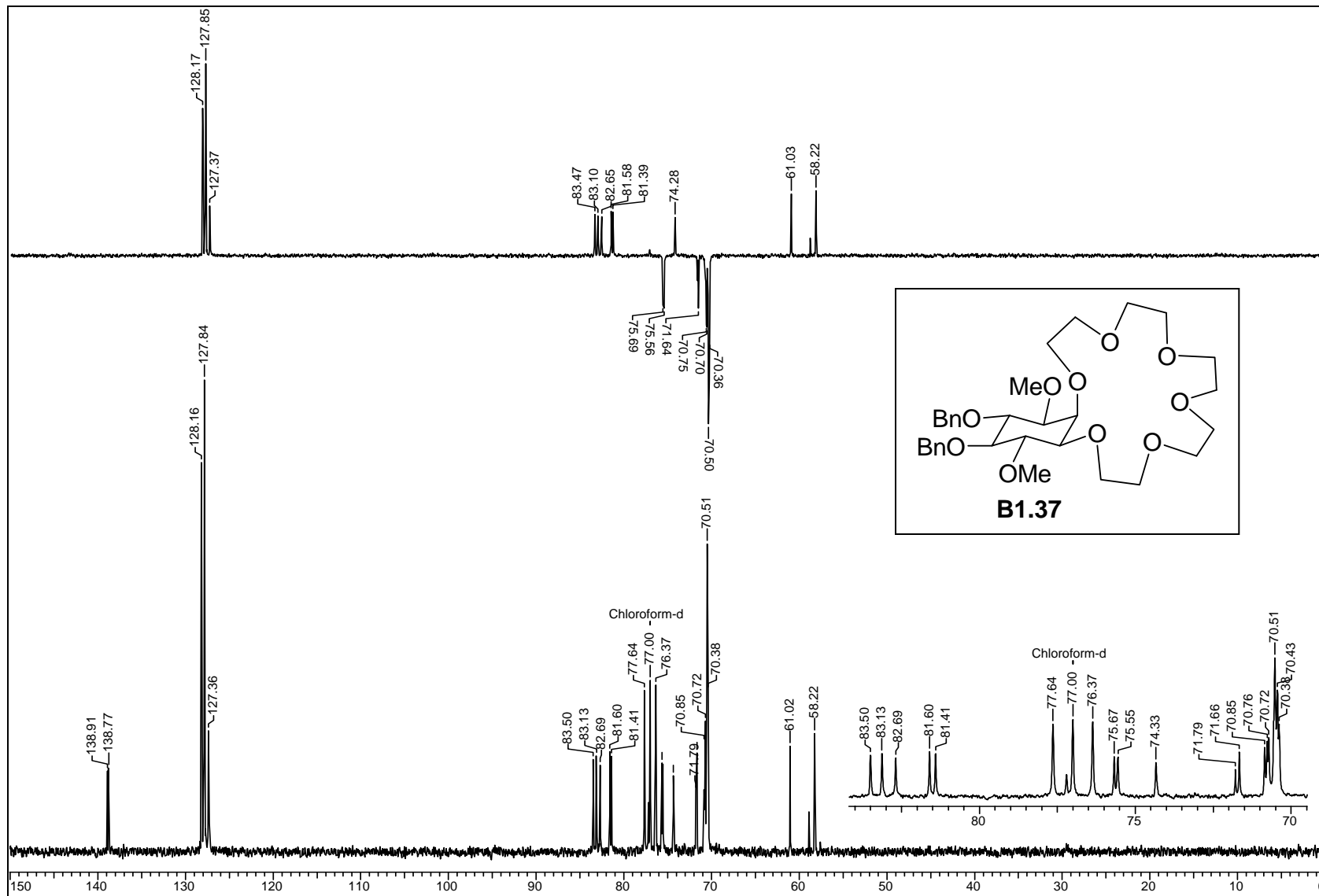


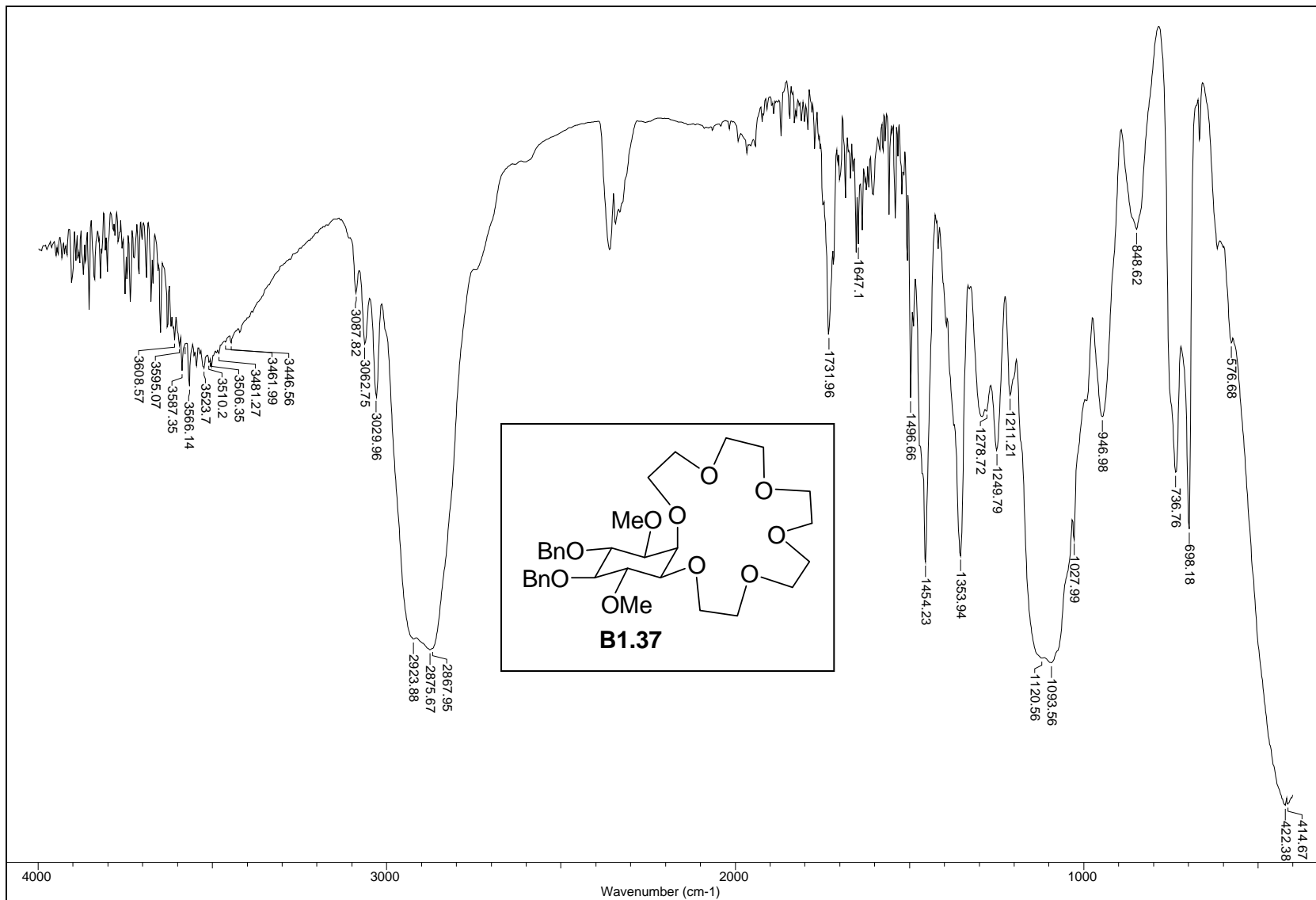












PART-B

Chapter 2

***scyllo*-Inositol based crown ethers: A comparative study with *myo*-inositol based crown ethers.**

A new scientific truth does not triumph by convincing its opponents and making them see the light, but rather because its opponents eventually die, and a new generation grows up that is familiar with it.

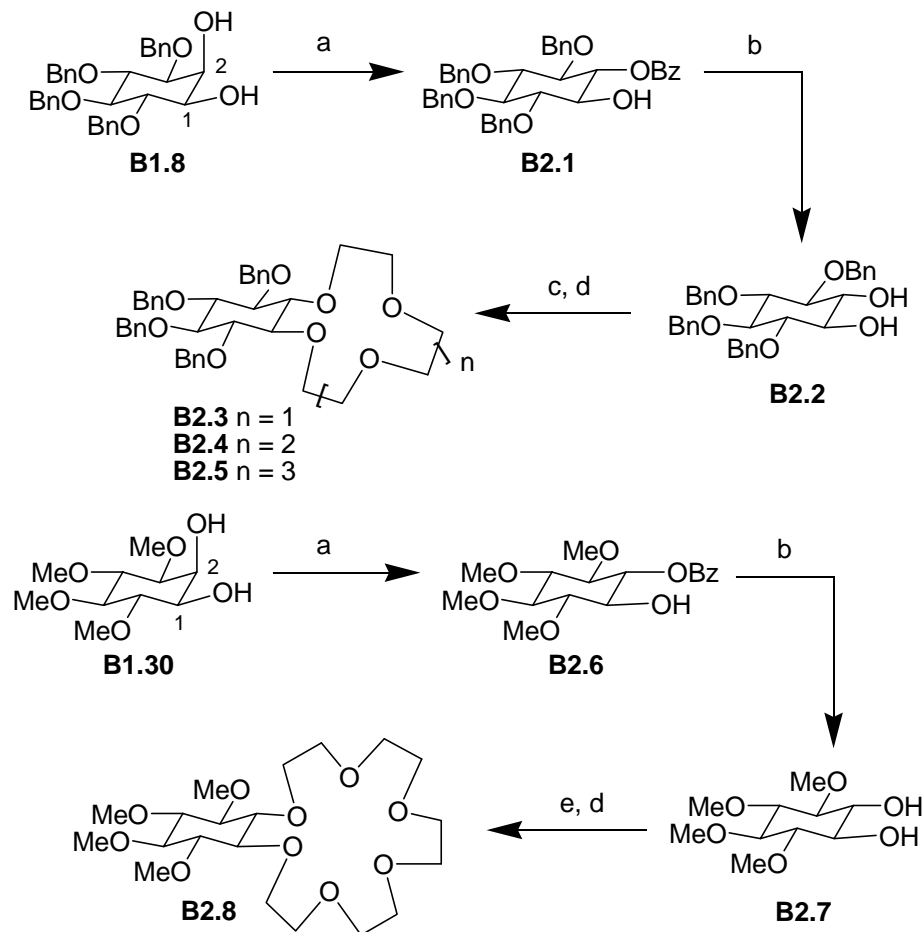
-Max Planck

2.1 Introduction

In the previous chapter the cation binding ability of *myo*-inositol derived crown ethers with varying structures were compared. The results showed that the cation binding ability of these crown ethers could be influenced by the relative stereo disposition of some of the crown ether oxygen atoms and also by the auxiliary groups present on the oxygen atoms that are not a part of the crown ether. Although crown ethers with different auxiliary groups, had the relative stereo disposition of the crown ether oxygen atoms same (e.g. crown-4 ethers **B1.14** and **B1.22**; crown-5 ethers **A.91** and **B1.25**; crown-6 ethers **A.94** and **B1.31**), the crown ethers with different relative stereo disposition of the crown ether oxygen atoms did not have identical substitution on the other oxygen atoms (e.g. *cis*-crown ethers **A.93**, **A.94**, **B1.9** had four benzyl groups, *trans*-crown ethers **A.91**, **A.92**, **B1.5** had two benzyl groups while orthoester crown ether **A.95**, **A.96**, **B1.14** had one benzyl group; similarly *cis*-crown ether **B1.31** had four methyl groups, *trans*-crown ether **B1.25** had two methyl groups while orthoester crown ether **B1.22** had one methyl group). Similarly, although a comparison of the metal ion binding ability of *myo*-inositol orthoformate derived crown ethers (**B1.14** and **B1.22**) reported in the previous chapter revealed the effect of the C2-O substituent on their metal ion binding ability, no information could be obtained on the effect of relative orientation of the C2-substituent (with respect to the crown ether moiety) on the cation binding ability of the 1,3-diaxial crown ether. Hence in order to understand the effect of only the relative stereo disposition of the crown ether oxygen atoms (while maintaining auxiliary groups same) on their cation binding ability, we undertook (a) the preparation and estimation of the cation binding ability of *scyllo*-inositol derived crown ethers and a comparison of these results

with analogous *myo*-inositol derived crown ethers; (b) the preparation and estimation of the cation binding ability of *scyllo*-inositol orthoformate derived crown ethers and a comparison of these results with analogous *myo*-inositol orthoformate derived crown ethers. A comparison between *myo*- and *scyllo*-inositol derived crown ethers, clearly highlight the significance of the relative orientation of oxygen atoms in the crown ethers as well as the auxiliary groups present on the inositol ring, on their cation binding ability.^{1,2}

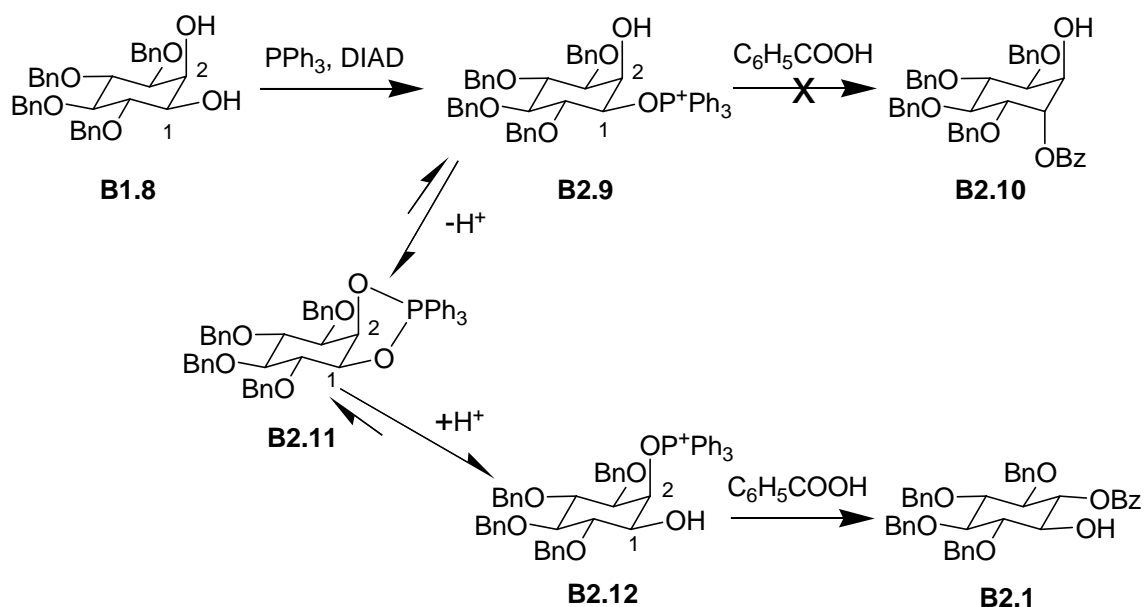
2.2 Results and Discussion



SCHEME B2.1. Reagents and conditions: (a) Benzene, PPh_3 (1.2 eq.), $\text{C}_6\text{H}_5\text{COOH}$, DIAD, 3\AA molecular sieves, $80\text{ }^\circ\text{C}$, 4 h (79% for **B2.1**), 16 h (68% for **B2.6**); (b) MeOH,

NaOH, reflux, 3 h (87% for **B2.2**), 2 h (77% for **B2.7**); (c) THF, NaH, TsOCH₂(CH₂OCH₂)_nCH₂OTs, reflux, 24 h; (d) MeOH, NaOMe, reflux, 12 h (13% for **B2.3**; 57% for **B2.4**; 75% for **B2.5**; 56% for **B2.8**); (e) THF, NaH, TsO(CH₂CH₂O)₅Ts, reflux, 24 h.

The *scyllo*-inositol derived crown ethers **B2.3**, **B2.4**, **B2.5** and **B2.8** were prepared from the diols **B2.2** and **B2.7** as shown in scheme B2.1. The *scyllo*-inositol derivative **B2.1** was obtained by inverting the axial hydroxyl group in **B1.8** by Mitsunobu reaction.³

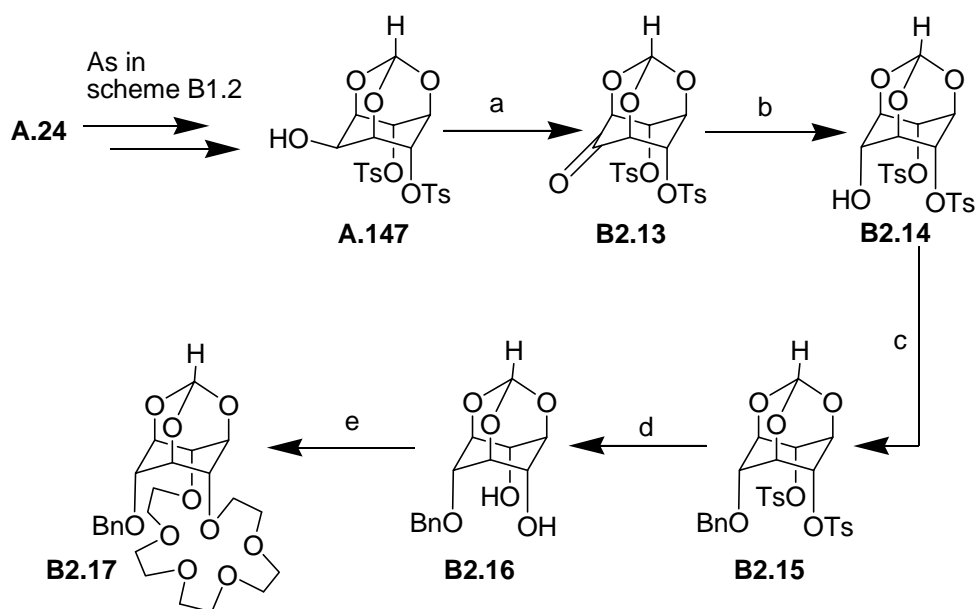


SCHEME B2.2.

It is interesting to see that only the C2-axial hydroxyl group of the diols **B1.8** and **B1.30** was inverted while the C1-hydroxyl group remained undisturbed during the Mitsunobu reaction. This observation can be rationalized by a mechanism⁴ as shown in scheme B2.2. **B2.1** probably arises from the attack of the nucleophile on the phosphonium salt **B2.12**. Initial formation of **B2.9** is depicted since it is well known that the equatorial hydroxyl group of a *cis*-1,2-diol (such as **B1.8**) is more nucleophilic than the axial hydroxyl group.⁵ Conversion of **B2.9** to **B2.11** is suggested since the formation

of the alcohol **B2.10** (which would arise from the attack of a nucleophile on **B2.9**) was not observed. Cyclic phosphoranes like **B2.11** have earlier been postulated as intermediates in Mitsunobu reactions involving diols.^{6,7} Protonation of **B2.11** leads to **B2.12**, which gives the *scyllo*-inositol derivative **B2.1**.

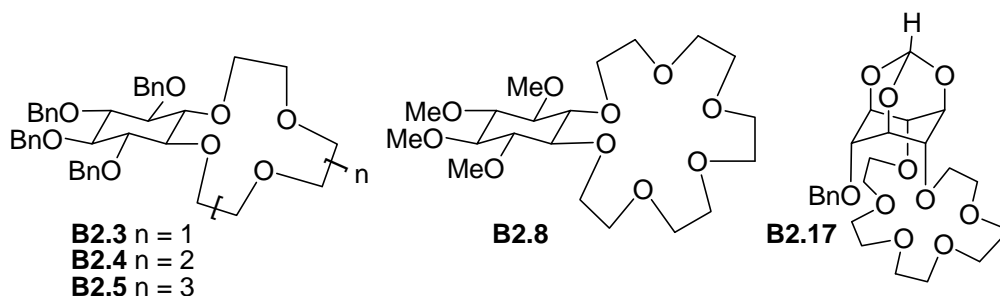
The *scyllo*-inositol orthoformate⁸ derived crown ether **B2.17** was prepared (Scheme B2.3) from the ditosylate **B2.14** which was obtained by inverting the hydroxyl group in **A.147** by sequential oxidation and reduction.⁹



SCHEME B2.3. *Reagents and conditions:* (a) DMSO, dichloromethane, $(\text{COCl})_2$, -78°C , 2 h. then Et_3N , rt; (b) THF:Methanol (1:4), NaBH_4 , rt, 30 min, 92%, (for two steps); (c) DMF, BnBr , NaH , rt, 10 min, 97%; (d) MeOH, NaOMe , reflux, 24 h, 97%; (e) THF, NaH , $\text{TsO}(\text{CH}_2\text{CH}_2\text{O})_5\text{Ts}$, reflux, 15 h, 53%.

The metal picrate extraction constants obtained by Cram's method¹⁰ for the newly synthesized *scyllo*-inositol based crown ethers are tabulated in Table B2.1.

TABLE B2.1. Association constants ($K_a \times 10^{-4} \text{ dm}^3 \text{ mol}^{-1}$) of *scyllo*-inositol derived crown ethers with metal picrates in CDCl_3 at 27 °C.



Crown	Li^+	Na^+	K^+	Cs^+	NH_4^+	Ag^+
B2.3	32.74	1.54	0.66	0.69	0.77	9.98
B2.4	13.15	2.31	1.45	3.22	1.60	12.54
B2.5	6.34	2.14	8.51	8.84	86.37	1900
B2.8	5.38	1.74	6.83	1.98	1.58	21.34
B2.17	17.25	58.04	722.58	22.49	193.47	245.18

Among the *scyllo*-inositol derived crown ethers, the crown-4 ether **B2.3** showed highest binding to lithium picrate, while the crown-6 ethers **B2.5** and **B2.8** showed highest binding to lithium picrate. The *scyllo*-inositol orthoester derived crown ether **B2.17** on the other hand bound potassium picrate best.

TABLE B2.2. Ratio of association constants between metal picrates for a given *scyllo*-inositol derived crown ether.^a

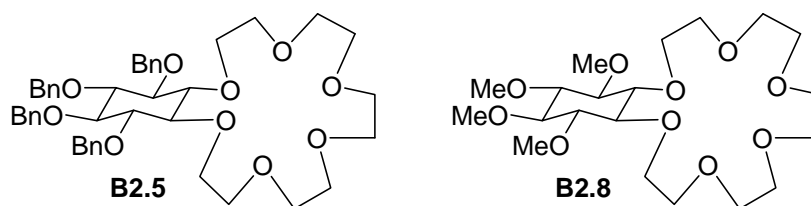
Crown	Li ⁺ /Na ⁺	Li ⁺ /K ⁺	Li ⁺ /Cs ⁺	Li ⁺ /NH ₄ ⁺	Li ⁺ /Ag ⁺
B2.3	21.30	49.41	47.30	42.26	3.28
B2.4	5.68	9.07	4.08	8.22	1.05
	K ⁺ /Li ⁺	K ⁺ /Na ⁺	K ⁺ /Cs ⁺	K ⁺ /NH ₄ ⁺	K ⁺ /Ag ⁺
B2.8	1.27	3.92	3.45	4.33	0.32
B2.17	41.88	12.45	32.13	3.73	2.95
	Ag ⁺ /Li ⁺	Ag ⁺ /Na ⁺	Ag ⁺ /K ⁺	Ag ⁺ /Cs ⁺	Ag ⁺ /NH ₄ ⁺
B2.5	299.7	887.3	223.3	214.8	22.0
B2.8	3.96	12.26	3.12	10.77	13.52

^a For a complete list of ratios see Table B2.7, Experimental section, page 218.

Ratio of association constants for the binding of picrates to a given crown ether, (Table B2.2) revealed the selectivity exhibited by the given crown ether. The crown-4-ether **B2.3** was more selective to lithium-picrate as expected ($\text{Li}^+/\text{K}^+ \approx 49$; $\text{Li}^+/\text{Na}^+ \approx 21$), whereas the crown-5-ether **B2.4** was selective for lithium-picrate to a lesser extent ($\text{Li}^+/\text{K}^+ \approx 9$; $\text{Li}^+/\text{Na}^+ \approx 6$); the crown-6-ether **B2.5** was selective to silver picrate ($\text{Ag}^+/\text{Li}^+ \approx 300$; $\text{Ag}^+/\text{Na}^+ \approx 887$). On the other hand the tetramethyl crown-6 ether **B2.8** showed almost no selectivity to silver ($\text{Ag}^+/\text{Li}^+ \approx 4$; $\text{Ag}^+/\text{Na}^+ \approx 12$; $\text{Ag}^+/\text{K}^+ \approx 3$). It was surprising to see that the crown-6 ether **B2.8** practically showed no selectivity for binding to potassium ($\text{K}^+/\text{Na}^+ \approx 4$; $\text{K}^+/\text{NH}_4^+ \approx 4$; $\text{K}^+/\text{Li}^+ \approx 1$). The diaxial crown-6 ether **B2.17**

however showed better selectivity for potassium ($K^+ / Li^+ \approx 42$; $K^+ / Na^+ \approx 12$) as compared to **B2.8**. A comparison of the ratio of association constants between the crown-6 ethers **B2.5** and **B2.8** (Table B2.3) shows that the presence of benzyl groups in *scyllo*-inositol derived crown-6 ether aids the binding of ammonium and silver-picrates ($K_{B2.5} / K_{B2.8}$ for $NH_4^+ \approx 55$ for $Ag^+ \approx 89$). For selectivity between Ag^+ and K^+ which have more or less same ionic radii, the tetrabenzyl crown-6 ether **B2.5** is much more selective to silver ($K_{(Ag^+)} / K_{(K^+)} \approx 223$) as compared to the tetramethyl- crown-6 ether **B2.8** ($K_{(Ag^+)} / K_{(K^+)} \approx 3$ see Table B2.2).

TABLE B2.3. Influence of protecting groups of the *scyllo*-inositol derived crown ethers on their binding to metal picrates.



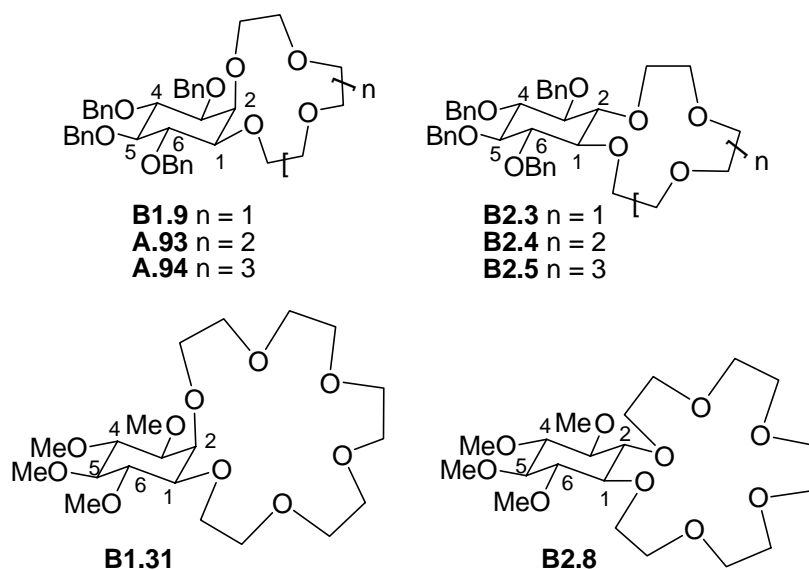
Picrate	Li^+	Na^+	K^+	Cs^+	NH_4^+	Ag^+
B2.5/ B2.8	1.18	1.23	1.24	4.46	54.66	89.03

scyllo-Inositol derived crown ethers vs *myo*-inositol derived crown ethers.

The crown ethers **B2.3**, **B2.4**, **B2.5**, **B2.8** and **B1.9**, **A.93**, **A.94**, **B1.31** only differ in the disposition of the C2-oxygen, which is axial in *myo*-inositol derived crown ethers and equatorial in *scyllo*-inositol derived crown ethers. This difference appears to matter considerably for the metal picrate extraction ability of these molecules (Table B2.4). A comparison of the metal picrate extraction constants shows that by and large *myo*-inositol

derived crown ethers extract metal picrates better than the corresponding crown ether with *scyllo*- configuration.

TABLE B2.4: Comparison of association constants ($K_a \times 10^{-4} \text{ dm}^3 \text{ mol}^{-1}$) of *myo*-inositol crown ethers with *scyllo*-inositol crown ethers.



Picrate	Li^+	Na^+	K^+	Cs^+	NH_4^+	Ag^+
B1.9	19.90	3.95	0.97	2.12	3.97	15.9
B2.3	32.74	1.54	0.66	0.69	0.77	9.98
A.93	12.9	64.7	6.7	1.33	1.83	27.6×10^3
B2.4	13.15	2.31	1.45	3.22	1.60	12.54
A.94	16.3	45.5	35.2×10^3	11.8	586	49.5×10^5
B2.5	6.34	2.14	8.51	8.84	86.37	1900
B1.31	1.75	6.51	48	1.31	22.2	63.1
B2.8	5.38	1.74	6.83	1.98	1.58	21.34

The enhanced binding observed for lithium, sodium, potassium and silver picrates to *myo*-crown ethers **B1.9**, **A.93**, **A.94** respectively, is mainly due to the change in the disposition of one of the oxygen atoms of the inositol ring. If the enhanced picrate extraction was due to the presence of aromatic rings in the crown ether (*picrate effect*¹¹), *scyllo*-crown ethers should have exhibited comparable binding constants to those of *myo*-inositol crown ethers, since all the crown ethers possess four benzyl groups.

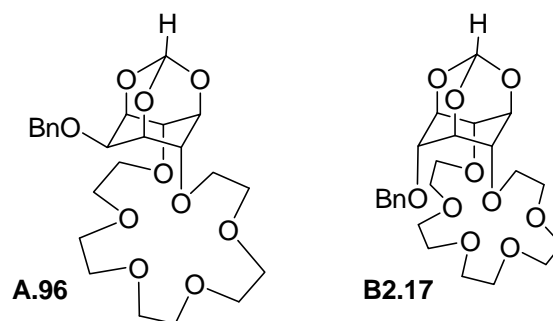
This is further supported by a comparison of the picrate extraction constants of **B1.31** and **B2.8**; the *myo*-crown ether shows better binding for sodium, potassium, ammonium and silver picrates as compared to the *scyllo*-crown ether **B2.8**. Results presented in earlier chapters of this thesis had shown that binding of *myo*-inositol crown ethers (such as **B1.31**) to metal picrates can be enhanced by replacing the methyl groups with benzyl groups. Although this effect is seen for *scyllo*-derived crown-6 ether also, the extent of increase is much smaller (for potassium-picrate $K_{B2.5}/K_{B2.8} \approx 1$ while $K_{A.94}/K_{B1.31} \approx 733$; for silver-picrate $K_{B2.5}/K_{B2.8} \approx 89$ while $K_{A.94}/K_{B1.31} \approx 78447$, see Table B2.3 and Table B1.10).

TABLE B2.5: Ratio of association constants for the binding of metal picrates between *myo*-inositol and *scyllo*-inositol derived crown ethers.

Picrate	Li ⁺	Na ⁺	K ⁺	Cs ⁺	NH ₄ ⁺	Ag ⁺
B1.9/ B2.3	6.08	25.65	14.70	30.72	51.56	15.93
A.93/ B2.4	0.98	28.00	4.62	0.41	1.14	2201
A.94/ B2.5	2.57	21.26	4136	1.33	6.78	2605
B1.31/ B2.8	0.32	3.74	7.02	0.66	14.05	2.95

The ratio of metal picrate association constants between crown ethers having *myo*- and *scyllo*- configuration are shown in Table B2.5. These values reveal that stereochemical disposition of one oxygen atom in the inositol ring has very large effect for the extraction of potassium (**A.94**/ **B2.5** \approx 4136) and silver picrates (**A.93**/ **B2.4** \approx 2201; **A.94**/ **B2.5** \approx 2605). It is interesting to note that although the *myo*-crown-6 ether **A.94** exhibits very high binding constant with silver-picrate, the extent to which the picrate binding is affected due to change in stereochemistry from *scyllo*- to *myo*-configuration matters, is more for the binding of potassium than silver picrate (Table B2.5). For other metal picrates tested, the change in stereochemistry does not have as great an influence on their binding to crown ethers.

TABLE B2.6: Comparison of association constants of *myo*-inositol orthoformate crown ethers with *scyllo*-inositol orthoformate crown ethers.



Picrate	Li ⁺	Na ⁺	K ⁺	Cs ⁺	NH ₄ ⁺	Ag ⁺
A.96 ¹	9.71	6.28	757	1.11	171	89.1
B2.17	17.25	58.04	722.58	22.49	193.47	245.18
B2.17/ A.96 ¹	1.77	9.24	0.95	20.26	1.13	2.75

In orthoesters **A.96** and **B2.17** although two axial oxygen atoms form the crown ether, the C2-substituent is *anti*- with respect to the crown ether moiety in **A.96** but *syn*- with respect to the crown ether moiety in **B2.17**. A comparison of the metal picrate association constants for orthoester based crown ethers reveals that *scyllo*-crown ether **B2.17** is able to extract metal picrates slightly better than **A.96** (except for potassium-picrate, see Table B2.6). This could be due to the presence of three *syn*- axial oxygen atoms capable of ligating with metal ions in **B2.17** while **A.96** has only two axial oxygen atoms. However, there is no dramatic change in the metal picrate binding patterns on changing from *myo*- to *scyllo*- configuration (in orthoesters), perhaps because the size of the binding pocket in these crown ethers is not expected to vary much (due to the presence of 1,3-diaxial oxygen atoms). Also, the cooperative binding of metal ions to crown ether as shown in figure B2.1 (C and D) cannot be ruled out.

Instances of variation in the metal ion binding ability of neutral, metal ion complexing agents with variation in the relative disposition of metal ligating atoms have been reported earlier. Cyclohexane triol based spirotetrahydrofuran derivatives **A.64** (relative stereodisposition of three oxygen atoms similar to *scyllo*-inositol orthoformate derivatives **B2.14-B2.16**) and **A.68** (relative stereodisposition of three oxygen atoms similar to *myo*-inositol orthoformate derivatives **B1.11-B1.13**) exhibited contrasting alkali metal binding abilities (Figure B2.2); although **A.68** showed no measurable tendency to complex with alkali metal ions, **A.64** bound strongly to Li^+ , Na^+ and CH_3NH_3^+ ions^{12,13} (also see Part A of this thesis page 35).

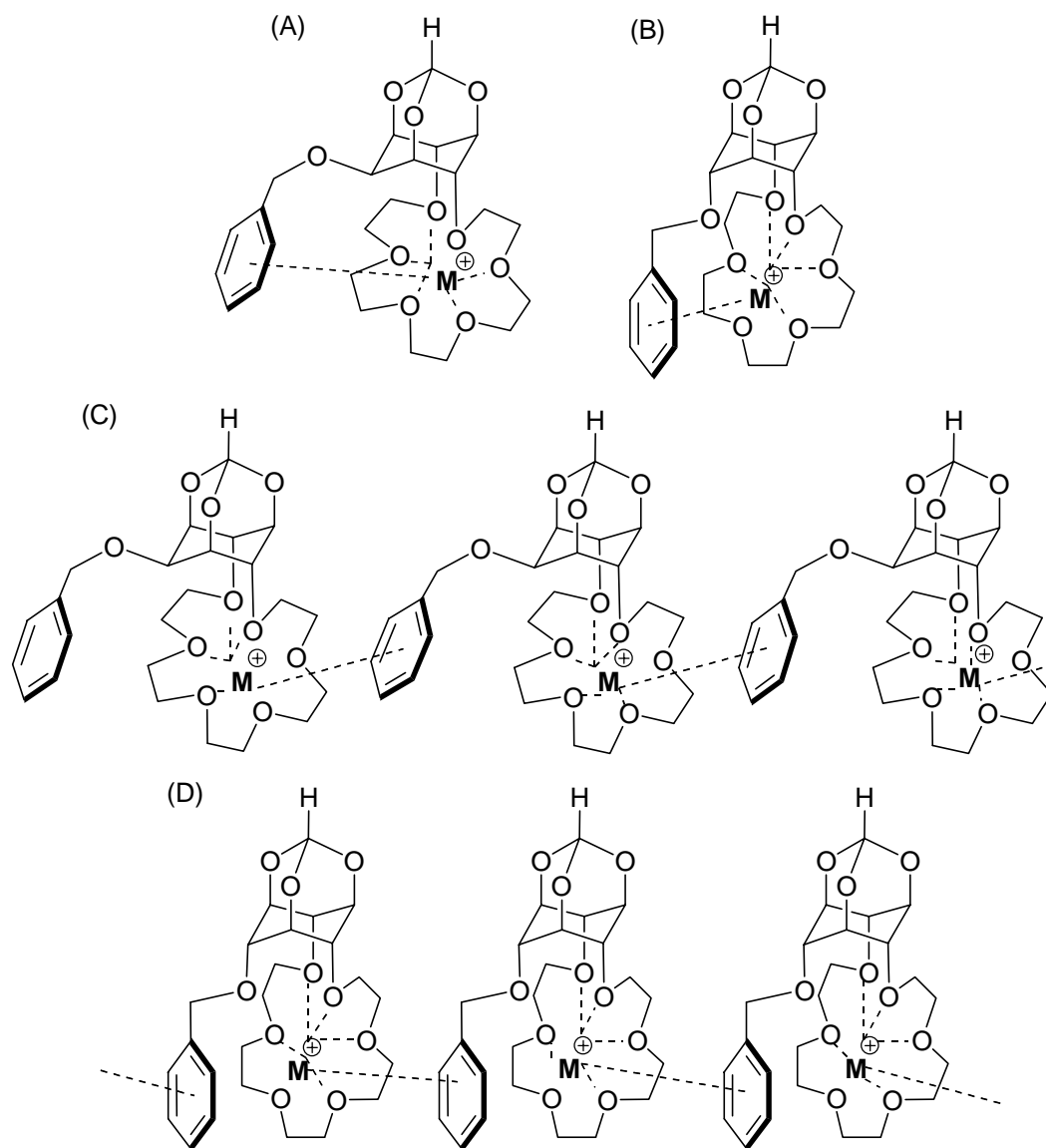


FIGURE B2.1. Possible modes of binding between metal picrate and *myo*- and *scyllo*-inositol orthoformate derived crown ethers containing benzyl groups.

Complexation of the crown ether **B2.19** with *S*-methyl phenylglycinate hydrochloride was better than with the crown ether **B2.18**. Evaluation by differential enantiomer transport of racemic methyl phenylglycinate hydrochloride through liquid membranes containing crown ethers **B2.18** and **B2.19** revealed preferential complex formation of **B2.18** and **B2.19** in 3% and 8% enantiomeric excess respectively.¹⁴

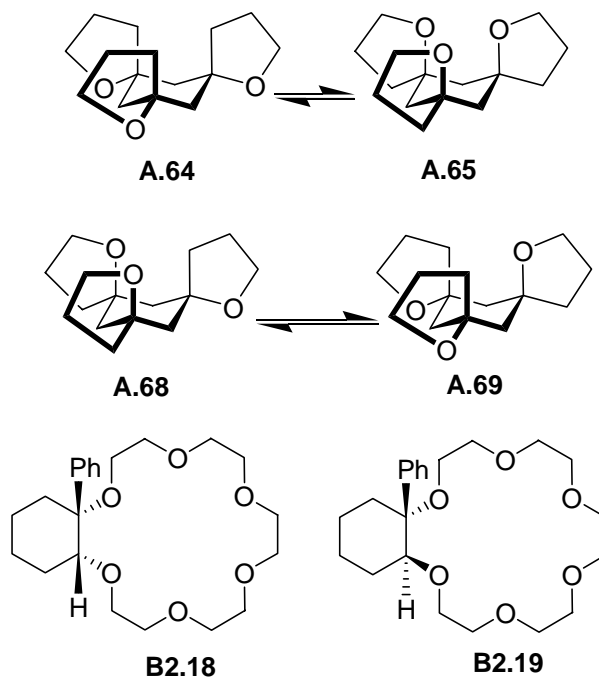


FIGURE B2.2.

2.3 Conclusions

Metal picrate binding ability of inositol derived crown ethers vary depending on the relative orientation of crown ether oxygen atoms in the inositol ring. The effect of such variation in the relative stereo-disposition of the inositol ring oxygen atoms influences the binding and selectivity of silver and potassium ions considerably. Auxiliary protecting groups on the inositol ring have greater influence on the binding of metal ions to crown ethers with *myo*-configuration as compared to crown ethers with *scyllo*-configuration. Change in the stereo-disposition of the C2-substituent in inositol orthoester derived crown ethers is more or less inconsequential for the binding of metal picrates.

2.4 Experimental Section

General: General methods are as mentioned in chapter 1, page 100. Racemic 1-*O*-benzoyl-2,3,4,5-tetra-*O*-benzyl-*scyllo*-inositol (**B2.1**) and the diol **B2.2** were prepared as reported.³ **A.147**, **B2.13** and **B2.14** were prepared as reported.⁹

Racemic 1,2-(12-crown-4)-3,4,5,6-tetra-*O*-benzyl-*scyllo*-inositol (B2.3**).** The diol **B2.2**³ (0.300 g, 0.55 mmol), sodium hydride (0.133 g, 3.33 mmol), triethyleneglycol ditosylate (0.331 g, 0.72 mmol) and dry THF (80 mL) were used to prepare (as in the general procedure on page 101) the crown ether **B2.3** (0.05 g, 13%); it was isolated as a white sticky solid by column chromatography (ethyl acetate-light petroleum, gradient elution).

IR (CHCl₃): $\tilde{\nu} = 3269\text{-}3517\text{ cm}^{-1}$ (H₂O).

¹H NMR (200 MHz; CDCl₃): $\delta = 3.22\text{-}3.37$ (m, 2H; Ins-H), $3.44\text{-}3.53$ (m, 4H; Ins-H), $3.54\text{-}4.09$ (m, 12H; OCH₂CH₂O), $4.43\text{-}5.00$ (m, 8H; CH₂Ph), $7.23\text{-}7.35$ (m, 20H; Ar-H).

¹³C NMR (50.3 MHz; CDCl₃): $\delta = 70.6$ (CH₂), 71.1 (CH₂), 72.9 (CH₂), 75.87 (CH₂), 75.93 (CH₂), 82.4 (Ins-C), 82.8 (Ins-C), 83.4 (Ins-C), 127.59 (Ar-C), 127.65 (Ar-C), 127.8 (Ar-C), 127.9 (Ar-C), 128.3 (Ar-C), 128.4 (Ar-C), 138.4 (Ar-C), 138.5 (Ar-C).

Elemental Analysis: Anal. Calcd. for C₄₀H₄₆O₈·1H₂O (672.82): C, 71.40; H, 7.19. Found: C, 71.79; H, 7.21.

Racemic 1,2-(15-crown-5)-3,4,5,6-tetra-*O*-benzyl-*scyllo*-inositol (B2.4**).** The diol **B2.2**³ (0.200 g, 0.37 mmol), sodium hydride (0.118 g, 2.96 mmol), tetraethyleneglycol ditosylate (0.214 g, 0.48 mmol) and dry THF (65 mL) were used to prepare (as in the general procedure on page 101) the crown ether **B2.4** (0.1473 g, 57%); it was isolated as a white solid by column chromatography (eluent 25% ethyl acetate in light petroleum).

m.p: 119-121 °C.

¹H NMR (200 MHz; CDCl₃): δ = 3.10-3.36 (m, 2H; Ins-H), 3.37-3.58 (m, 2H; Ins-H), 3.60-3.81 (m, 12H; OCH₂CH₂O), 3.83-3.95 (m, 2H; OCH₂CH₂O), 3.96-4.14 (m, 2H; OCH₂CH₂O), 4.43-5.00 (m, 8H; CH₂Ph), 7.25-7.40 (m, 20H; Ar-H).

¹³C NMR (50.3 MHz; CDCl₃): δ = 69.3 (CH₂), 70.5 (CH₂), 70.56 (CH₂), 70.6 (CH₂), 71.1 (CH₂), 73.0 (CH₂), 73.1 (CH₂), 75.8 (CH₂), 82.7 (Ins-C), 82.9 (Ins-C), 83.0 (Ins-C), 127.5 (Ar-C), 127.53 (Ar-C), 127.57 (Ar-C), 127.6 (Ar-C), 127.78 (Ar-C), 127.82 (Ar-C), 128.3 (Ar-C), 128.33 (Ar-C), 138.39 (Ar-C), 138.42 (Ar-C).

Elemental Analysis: Anal. Calcd. for C₄₂H₅₀O₉ (698.85): C, 72.18; H, 7.21. Found: C, 72.24; H, 7.20.

Racemic 1,2-(18-crown-6)-3,4,5,6-tetra-O-benzyl-scyllo-inositol (B2.5). The diol **B2.2**³ (0.200 g, 0.37 mmol), sodium hydride (0.088 g, 2.22 mmol), pentaerythritol ditosylate (0.263 g, 0.48 mmol) and dry THF (65 mL) were used to prepare (as in the general procedure on page 101) the crown ether **B2.5** (0.206 g, 75%); it was isolated as a white solid by column chromatography (ethyl acetate-light petroleum, gradient elution).

m.p: 107-109 °C.

¹H NMR (200 MHz; CDCl₃): δ = 3.22-3.39 (m, 2H; Ins-H), 3.40-3.52 (m, 4H; Ins-H), 3.60-3.79 (m, 16H; OCH₂CH₂O), 3.82-4.00 (m, 2H; OCH₂CH₂O), 4.09-4.23 (m, 2H; OCH₂CH₂O), 4.52-4.91 (m, 8H; CH₂Ph), 7.23-7.39 (m, 20H; Ar-H).

¹³C NMR (50.3 MHz; CDCl₃): δ = 70.5 (CH₂), 70.6 (CH₂), 70.7 (CH₂), 70.9 (CH₂), 73.0 (CH₂), 75.8 (CH₂), 82.58 (Ins-C), 82.62 (Ins-C), 83.2 (Ins-C), 127.49 (Ar-C), 127.52 (Ar-C), 127.8 (Ar-C), 127.9 (Ar-C), 128.25 (Ar-C), 128.27 (Ar-C), 138.4 (Ar-C), 138.5 (Ar-C).

Elemental Analysis: Anal. Calcd. for C₄₄H₅₄O₁₀ (742.90): C, 71.13; H, 7.32. Found: C, 70.77; H, 7.13.

Racemic 1-O-benzoyl-2,3,4,5-tetra-O-methyl-scyllo-inositol (B2.6). A mixture of the diol **B1.30**⁵ (0.600 g, 2.54 mmol), triphenyl phosphine (0.9387 g, 3.22 mmol), benzoic acid (0.389 g, 3.22 mmol), diisopropyl azidodicarboxylate (DIAD) (0.725 mL, 3.68 mmol) and 3Å molecular sieves in dry benzene (20 mL) was stirred at 80 °C for 16 h. The reaction mixture was allowed to come to ambient temperature and filtered. The filtrate was evaporated under reduced pressure to get a gum, which was purified by column chromatography (eluent, 25% ethyl acetate in light petroleum) to get **B2.6** (0.595 g, 68%) as a white solid.

m.p: 107-108 °C.

IR (CHCl₃): $\tilde{\nu} = 3337\text{-}3566\text{ cm}^{-1}$ (OH).

¹H NMR (200 MHz; CDCl₃): $\delta = 2.54$ (broad s, 1H; OH), 3.05-3.32 (m, 4H; Ins-H), 3.49 (s, 3H; OCH₃), 3.53-3.61 (m, 1H; Ins-H), 3.64 (s, 6H; OCH₃), 3.65 (s, 3H; OCH₃), 5.15 (t, $J = 10.0$ Hz, 1H; HCOBz), 7.35-7.65 (m, 3H; Ar-H), 8.08 (dd, $J_1 = 8$ Hz, $J_2 = 1.5$ Hz, 2H; Ar-H_{ortho}).

¹³C NMR (50.3 MHz; CDCl₃): $\delta = 60.7$ (OCH₃), 60.8 (OCH₃), 60.9 (OCH₃), 61.1 (OCH₃), 72.0 (Ins-C), 74.6 (Ins-C), 82.3 (Ins-C), 83.8 (Ins-C), 84.4 (Ins-C), 128.3 (Ar-C), 129.7 (Ar-C), 129.9 (Ar-C), 133.0 (Ar-C), 166 (C=O).

Elemental Analysis: Anal. Calcd. for C₁₇H₂₄O₇ (340.38): C, 59.98; H, 7.10. Found: C, 60.16; H, 7.13.

Racemic 1,2,3,4-tetra-O-methyl-scyllo-inositol (B2.7). The benzoate **B2.6** (0.590 g, 1.73 mmol) and sodium hydroxide (0.277 g, 6.93 mmol) were refluxed in methanol (15

mL) for 2 h. the reaction mixture was cooled to ambient temperature and neutralized with 2% HCl. Methanol was evaporated under reduced pressure to get a solid; this was extracted with ethyl acetate. The residue obtained by evaporation of the ethyl acetate extract was purified by column chromatography (ethyl acetate-light petroleum, gradient elution) to get **B2.7** (0.3148 g, 76%) as a white solid.

m.p: 129-131 °C.

IR (Nujol): $\tilde{\nu} = 3178\text{-}3521\text{ cm}^{-1}$ (OH).

¹H NMR (200 MHz; CDCl₃): $\delta = 2.78\text{-}3.12$ (m, 6H; 4 Ins-H and 2 OH), 3.31-3.40 (m, 2H; Ins-H), 3.62 (s, 6H; OCH₃), 3.64 (s, 6H; OCH₃).

¹³C NMR (50.3 MHz; CDCl₃): $\delta = 60.7$ (OCH₃), 60.9 (OCH₃), 73.4 (Ins-C), 83.7 (Ins-C), 84.9 (Ins-C).

Elemental Analysis: Anal. Calcd. for C₁₀H₂₀O₆ (236.27): C, 50.83; H, 8.53. Found: C, 50.74; H, 8.86.

Racemic 1,2-(18-crown-6)-3,4,5,6-tetra-O-methyl-scylo-inositol (B2.8). The diol **B2.7** (0.150 g, 0.635 mmol), sodium hydride (0.152 g, 3.80 mmol), pentaerythritol ditosylate (0.451 g, 0.82 mmol) and dry THF (100 mL) were used to prepare (as in the general procedure on page 101) the crown ether **B2.8** (0.1851 g, 66%); it was isolated as a gum by column chromatography (ethyl acetate-light petroleum, gradient elution).

IR (Nujol): $\tilde{\nu} = 3440\text{-}3560\text{ cm}^{-1}$ (H₂O).

¹H NMR (400 MHz; CDCl₃): $\delta = 2.93$ (dd, $J_1 = 7\text{ Hz}$, $J_2 = 2.6\text{ Hz}$, 1H; Ins-H), 2.95-3.08 (m, 2H; Ins-H), 3.10 (dd, $J_1 = 6.7\text{ Hz}$, $J_2 = 2.6\text{ Hz}$, 1H; Ins-H), 3.38 (s, 3H; OCH₃), 3.53-3.56 (m, 2H; OCH₂CH₂O), 3.60 (s, 6H; 2 OCH₃), 3.60-3.67 (m, 15H; OCH₃ and

OCH₂CH₂O), 3.67-3.78 (m, 6H; OCH₂CH₂O), 3.83-3.88 (m, 1H; Ins-H), 4.02-4.09 (m, 1H; Ins-H).

¹³C NMR (50.3 MHz; CDCl₃): δ = 58.8 (OCH₃), 60.7 (OCH₃), 60.8 (OCH₃), 70.29 (CH₂), 70.37 (CH₂), 70.39 (CH₂), 70.53 (CH₂), 70.58 (CH₂), 70.7 (CH₂), 71.7 (CH₂), 72.6 (CH₂), 82.9 (Ins-C), 84.18 (Ins-C), 84.26 (Ins-C).

Elemental Analysis: Anal. Calcd. for C₂₀H₃₈O₁₀·2H₂O (474.55): C, 50.62; H, 8.92. Found: C, 50.30; H, 9.09.

2-O-benzyl-4,6-(18-crown-6)-scyllo-inositol 1,3,5-orthoformate (B2.17). The diol **B2.16**¹⁵ (0.200 g, 0.713 mmol), sodium hydride (0.160 g, 4 mmol) and pentaerythritol ditosylate (0.438 g, 0.8012 mmol) were refluxed in dry THF (105 mL) for 15 h. Methanol (1 mL) was added to destroy excess of sodium hydride. The reaction mixture was cooled to ambient temperature and concentrated under reduced pressure to get a gum. This was dissolved in dichloromethane (30 mL), washed with water (15 mL × 2) followed by brine. The organic layer was dried over sodium sulphate and concentrated under reduced pressure to get gum. This gum was again dissolved in dichloromethane (5 mL) and stirred with water (5 mL); aqueous layer was replaced by fresh water every 1 h for 24 h. Dichloromethane layer was dried over anhydrous sodium sulphate and concentrated under reduced pressure to get **B2.17** as a gum (0.185 g, 53%).

IR (CHCl₃) $\tilde{\nu}$ = 3380-3604 cm⁻¹ (H₂O).

¹H NMR (CDCl₃, 200 MHz): δ = 3.40-3.96 (m, 22H; 2 Ins-H and OCH₂CH₂O), 4.20-4.30 (m, 2H; Ins-H), 4.42-4.55 (m, 2H; Ins-H), 4.60-4.69 (m, 2H; CH₂Ph), 5.49 (s, 1H; HCO₃), 7.27-7.47 (m, 5H; Ar-H).

^{13}C NMR (CDCl_3 , 50.3 MHz): δ = 68.4 (Ins-C), 68.5 (Ins-C), 69.6 (CH_2), 70.5 (CH_2), 70.6 (CH_2), 70.8 (CH_2), 72.00 (Ins-C), 73.6 (Ins-C), 102.9 (HCO_3), 127.4 (Ar-C), 128.2 (Ar-C), 138.1 (Ar-C).

Elemental Analysis: Anal. Calcd. for $\text{C}_{24}\text{H}_{34}\text{O}_{10} \cdot 0.25\text{H}_2\text{O}$ (487.035); C, 59.18; H, 7.14.

Found: C, 59.02; H, 7.29.

TABLE B2.7. Ratio of association constants between metal picrates for a given *scyllo*-inositol derived crown ether.

Crown Ether	Li^+/Na^+	Li^+/K^+	Li^+/Cs^+	$\text{Li}^+/\text{NH}_4^+$	Li^+/Ag^+
B2.3	21.30	49.41	47.30	42.26	3.28
B2.4	5.68	9.07	4.08	8.22	1.05
B2.5	2.96	0.74	0.72	0.07	3.3×10^{-3}
B2.8	3.1	0.79	2.72	3.41	0.25
B2.17	0.30	0.02	0.77	0.09	0.07
	Na^+/Li^+	Na^+/K^+	Na^+/Cs^+	$\text{Na}^+/\text{NH}_4^+$	Na^+/Ag^+
B2.3	0.05	2.32	2.22	1.98	0.15
B2.4	0.18	1.60	0.72	1.45	0.1845
B2.5	0.34	0.25	0.24	0.02	1.1×10^{-3}
B2.8	0.32	0.25	0.88	1.10	0.08
B2.17	3.36	0.08	2.58	0.30	0.24
	K^+/Li^+	K^+/Na^+	K^+/Cs^+	K^+/NH_4^+	K^+/Ag^+
B2.3	0.02	0.43	0.96	0.85	0.07
B2.4	0.11	0.62	0.45	0.90	0.11
B2.5	1.34	3.97	0.96	0.09	4.48×10^{-3}
B2.8	1.27	3.92	3.45	4.33	0.32
B2.17	41.88	12.45	32.13	3.73	2.95

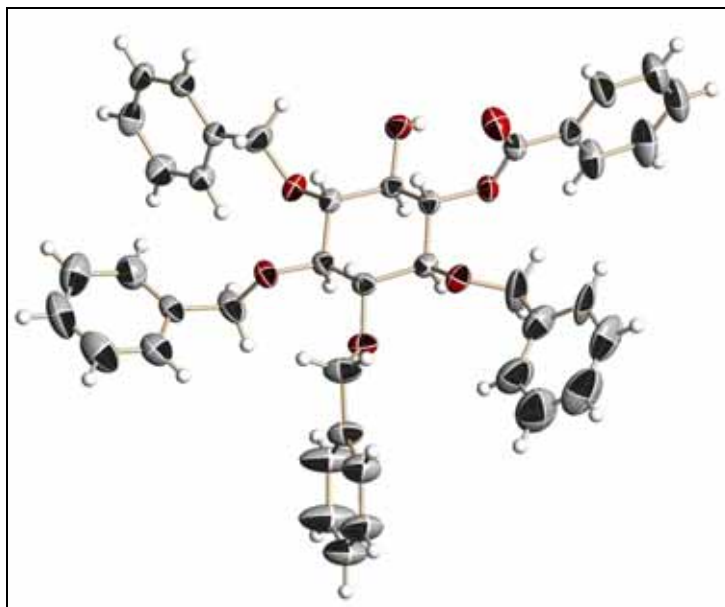
	Cs⁺/Li⁺	Cs⁺/Na⁺	Cs⁺/K⁺	Cs⁺/NH₄⁺	Cs⁺/Ag⁺
B2.3	0.02	0.45	1.04	0.89	0.07
B2.4	0.24	1.39	2.22	2.01	0.26
B2.5	1.39	4.13	1.04	0.10	4.65 × 10 ⁻³
B2.8	0.37	1.14	0.29	1.25	0.09
B2.17	1.30	0.39	0.31	0.12	0.09
	NH₄⁺/Li⁺	NH₄⁺/Na⁺	NH₄⁺/K⁺	NH₄⁺/Cs⁺	NH₄⁺/Ag⁺
B2.3	0.02	0.50	1.17	1.12	0.08
B2.4	0.12	0.69	1.10	0.50	0.13
B2.5	13.62	40.34	10.15	9.77	0.04
B2.8	0.29	0.90	0.23	0.80	0.07
B2.17	11.21	3.33	0.27	8.60	0.79
	Ag⁺/Li⁺	Ag⁺/Na⁺	Ag⁺/K⁺	Ag⁺/Cs⁺	Ag⁺/NH₄⁺
B2.3	0.30	6.50	15.06	14.41	12.88
B2.4	0.95	5.42	8.65	3.89	7.84
B2.5	299.7	887.3	223.3	214.8	22.0
B2.8	3.96	12.26	3.12	10.77	13.52
B2.17	14.21	4.22	0.34	10.90	1.27

2.5 References:

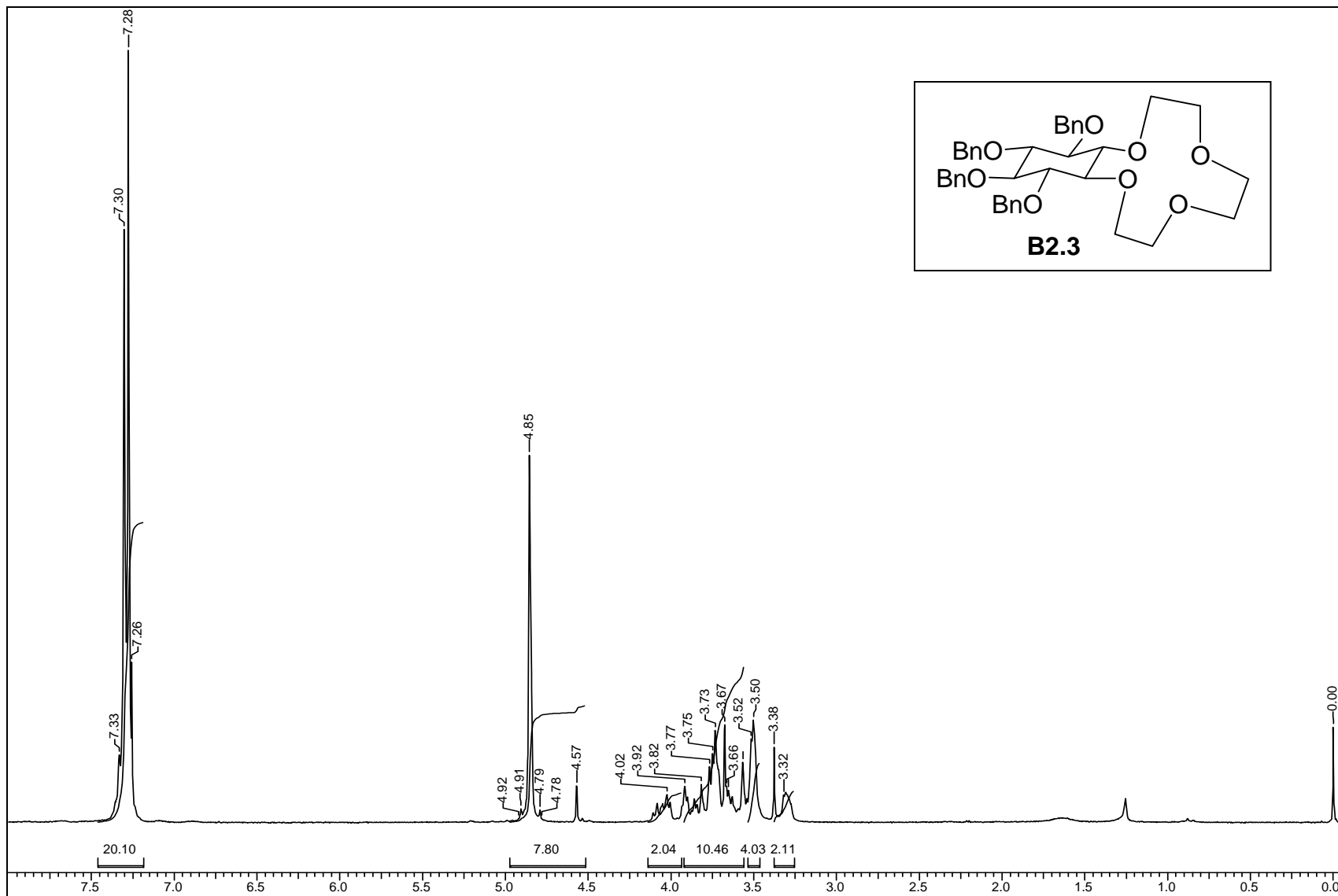
- 1 Sureshan, K. M.; Shashidhar, M. S.; Varma, A. J. *J. Org. Chem.* **2002**, *67*, 6884-6888.
- 2 Dixit, S. S.; Shashidhar, M. S.; Devaraj, S. *Tetrahedron* **2006**, *62*, 4360-4363.
- 3 Chung, S-K.; Kwon, Y-U.; Chang, Y-T.; Sohn, K-H.; Shin, J-H.; Park, K-H.; Hong, B-J.; Chung, I-H. *Bioorg. Med. Chem.* **1999**, *7*, 2577-2589.
- 4 Guidot, J. P.; Gall, T. L. *Tetrahedron Lett.* **1993**, *34*, 4647-4650.
- 5 Angyal, S. J.; Tate, M. E. *J. Chem. Soc.* **1965**, 6949-6955.
- 6 Castro, B. R. *Org. React.* **1983**, *29*, 1-162; see in particular pp 20-21.
- 7 Pautard, A. M.; Evans, Jr. A. E. *J. Org. Chem.* **1988**, *53*, 2300-2303.
- 8 Lee, H. W.; Kishi, Y. *J. Org. Chem.* **1985**, *50*, 4402-4404.
- 9 Sarmah, M. P.; Shashidhar, M. S. *Carbohydr. Res.* **2003**, *338*, 999-1001.
- 10 Moore, S. S.; Tarnowski, T. L.; Newcomb, M.; Cram, D. J. *J. Am. Chem. Soc.* **1977**, *99*, 6398-6405.
- 11 Talanova, G. G.; Elkarim, N. S. A.; Talanov, V. S.; Hanes, Jr. R. E.; Hwang, H-S; Bartsch, R. A.; Rogers, R. D. *J. Am. Chem. Soc.* **1999**, *121*, 11281-11290.
- 12 Paquette, L. A.; Tae, J.; Hickey, E. R.; Trego, W. E.; Rogers, R. D. *J. Org. Chem.* **2000**, *65*, 9160-9171.
- 13 Paquette, L. A.; Tae, J.; Hickey, E. R.; Rogers, R. D. *Angew. Chem., Int. Ed.* **1999**, *38*, 1409-1411.
- 14 Naemura, K.; Tobe, Y.; Kaneda, T. *Coord. Chem. Rev.* **1996**, *148*, 199-219.
- 15 Dixit, S. S.; Shashidhar, M. S. *Tetrahedron* **2007** (Accepted).

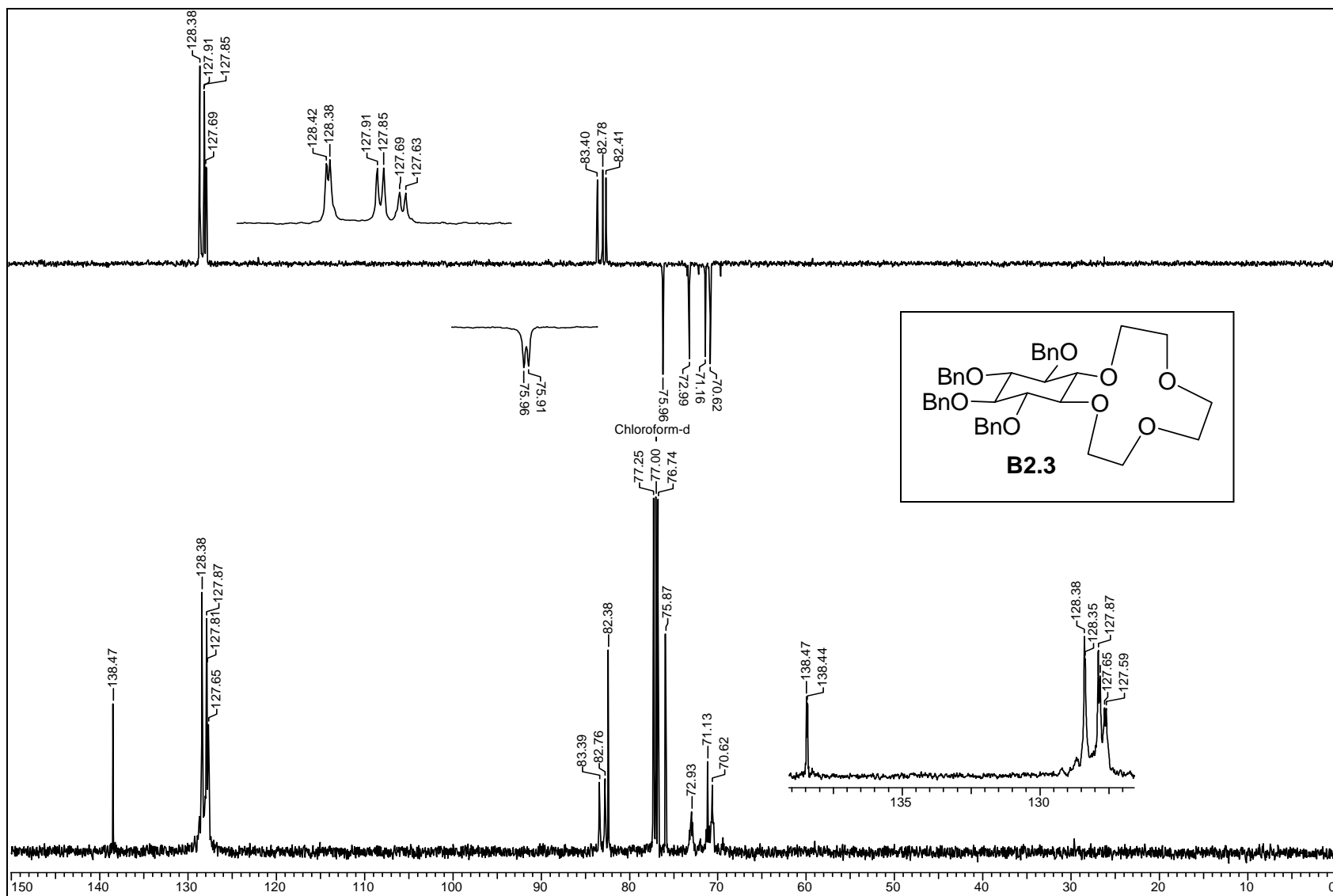
2.6 Appendix

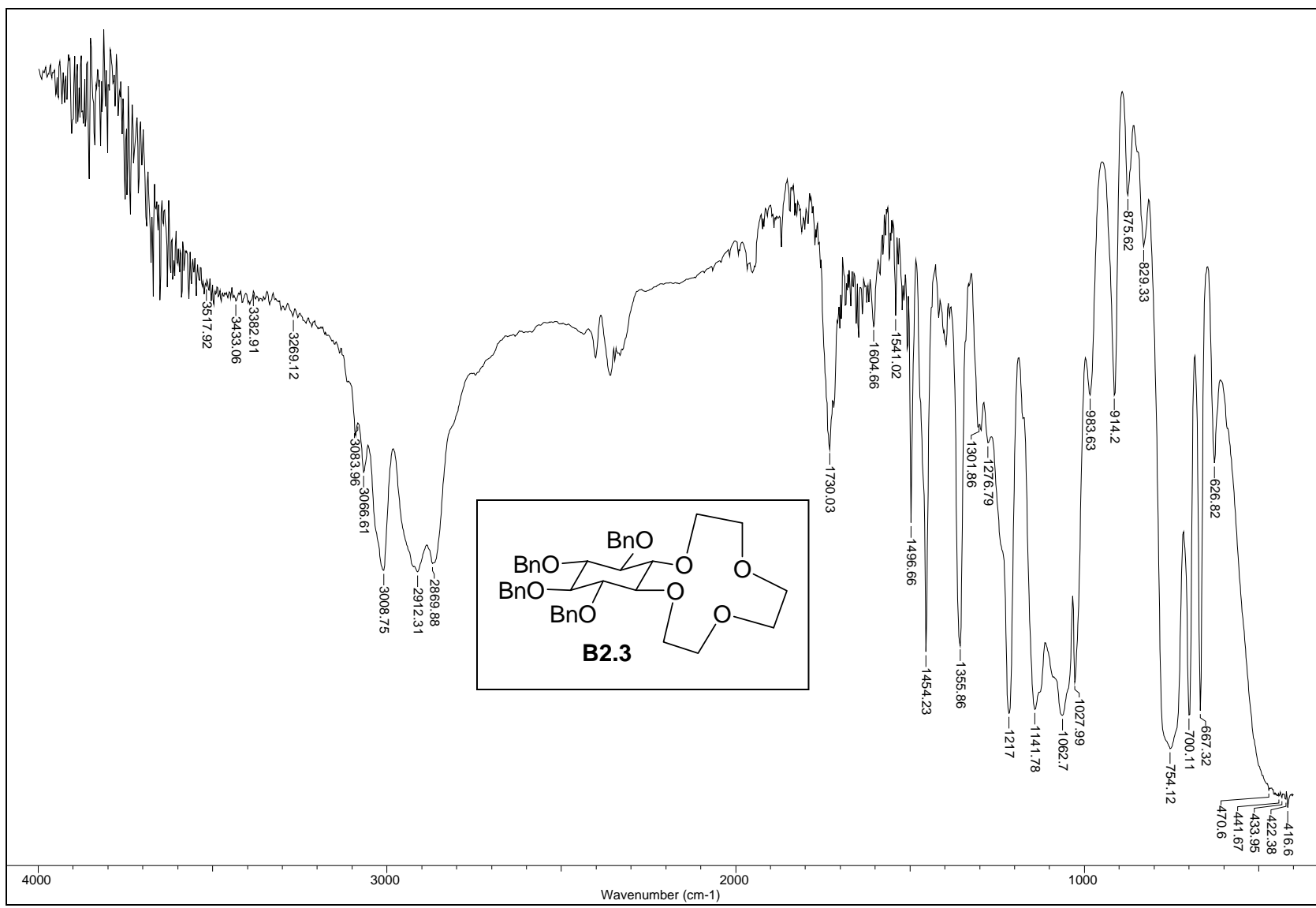
Sr. No	Index	Page No.
1	ORTEP, packing diagram and crystal data table of B2.1	222
2	^1H spectrum of B2.3	223
3	^{13}C and DEPT NMR spectra of B2.3	224
4	IR spectrum of B2.3	225
5	^1H spectrum of B2.4	226
6	^{13}C and DEPT NMR spectra of B2.4	227
7	IR spectrum of B2.4	228
8	^1H spectrum of B2.5	229
9	^{13}C and DEPT NMR spectra of B2.5	230
10	IR spectrum of B2.5	231
11	^1H spectrum of B2.6	232
12	D_2O exchange spectrum of B2.6	233
13	^{13}C and DEPT NMR spectra of B2.6	234
14	IR spectrum of B2.6	235
15	^1H spectrum of B2.7	236
16	D_2O exchange spectrum of B2.7	237
17	^{13}C and DEPT NMR spectra of B2.7	238
18	IR spectrum of B2.7	239
19	^1H spectrum of B2.8	240
20	^{13}C and DEPT NMR spectra of B2.8	241
21	IR spectrum of B2.8	242
22	ORTEP, packing diagram and crystal data table of B2.16	243
23	^1H spectrum of B2.17	244
24	^{13}C and DEPT NMR spectra of B2.17	245
25	IR spectrum of B2.17	246

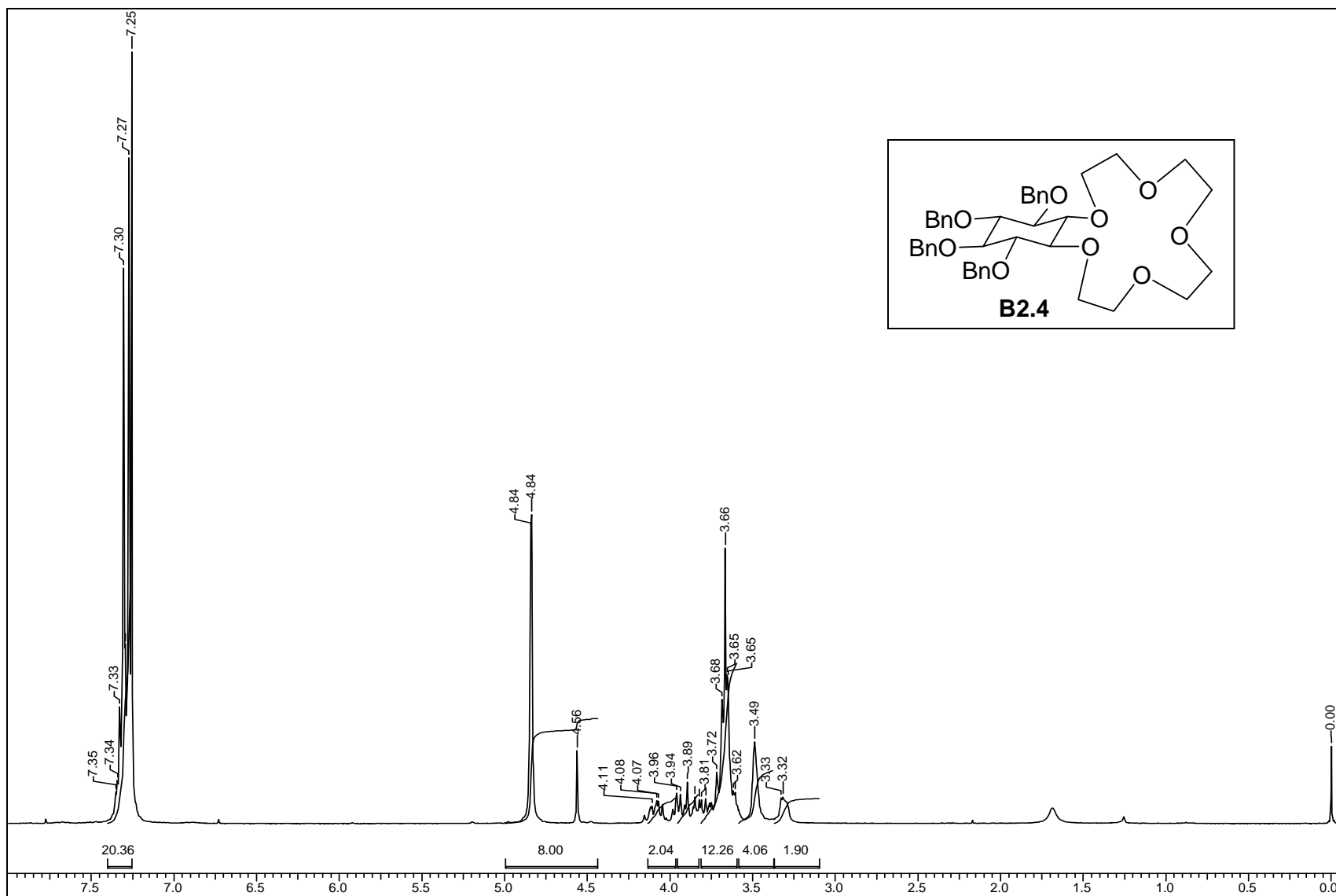
ORTEP diagram of **B2.1**Crystal data table of **B2.1**

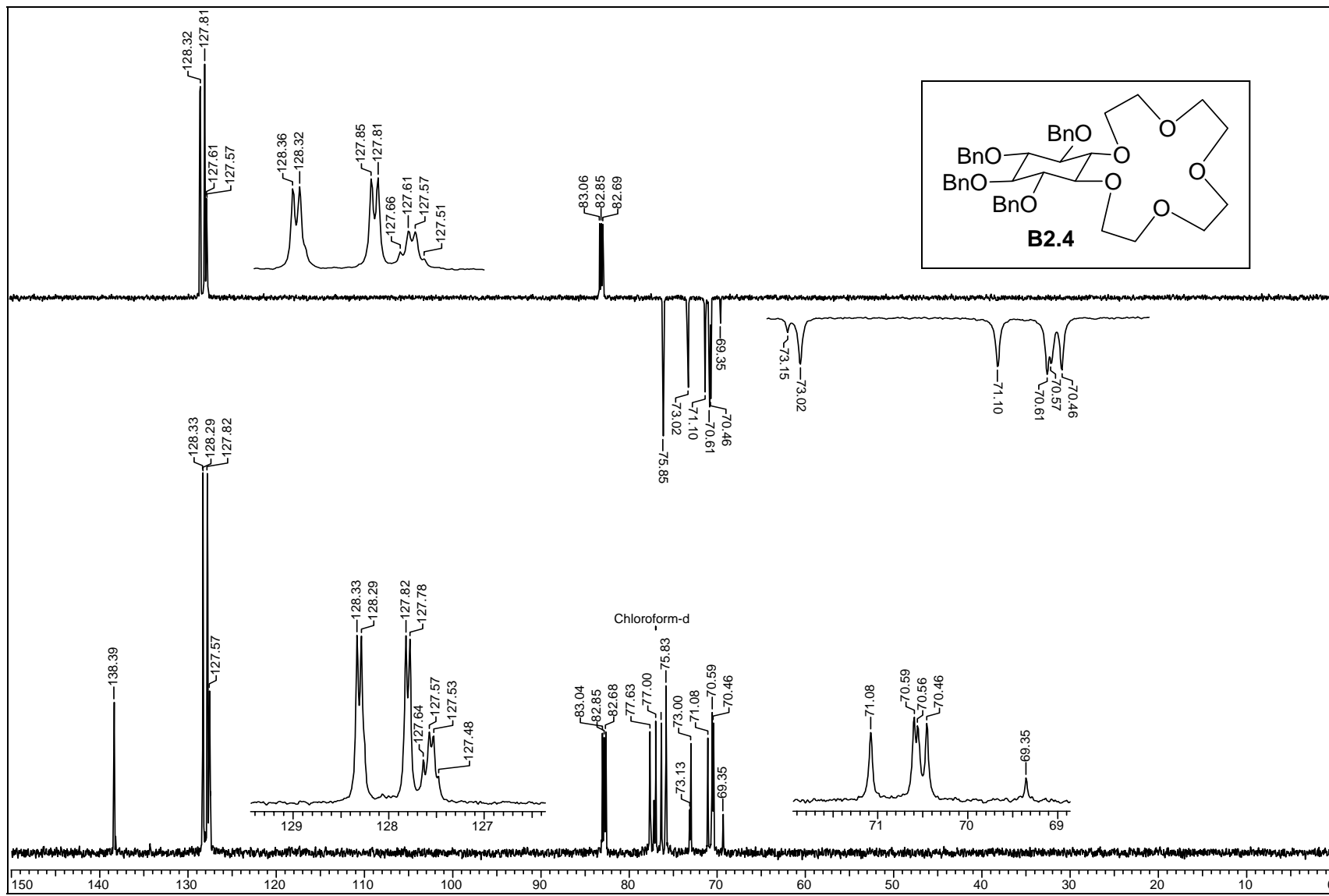
Identification code	B2.1 (crystallized from MeOH, DCM)
Empirical formula	C ₄₁ H ₄₀ O ₇
Formula weight	644.73
Temperature	297(2) K
Wavelength	0.71073 Å
Crystal system, space group	Triclinic, P-1
Unit cell dimensions	a = 10.742(5) Å α = 97.039(7)° b = 15.258(8) Å β = 90.842(12)° c = 21.937(10) Å γ = 98.888(9)°
Volume	3524(3) Å ³
Z, Calculated density	4, 1.215 Mg/m ³
Absorption coefficient	0.082 mm ⁻¹
F(000)	1368
Crystal size	0.88 x 0.14 x 0.12 mm
θ range for data collection	1.92 to 25.00°
Limiting indices	-12 ≤ h ≤ 12, -18 ≤ k ≤ 18, -26 ≤ l ≤ 26
Reflections collected / unique	34088 / 12372 [R(int) = 0.0498]
Completeness to θ = 25.00°	99.7 %
Absorption correction	Semi-empirical from equivalents
Max. and min. transmission	0.9900 and 0.9312
Refinement method	Full-matrix least-squares on F ²
Data / restraints / parameters	12372 / 171 / 933
Goodness-of-fit on F ²	0.968
Final R indices [I > 2σ (I)]	R1 = 0.0654, wR2 = 0.1545
R indices (all data)	R1 = 0.1609, wR2 = 0.2009
Largest diff. peak and hole (ρ _{max} & ρ _{min})	0.228 and -0.151 e. Å ⁻³

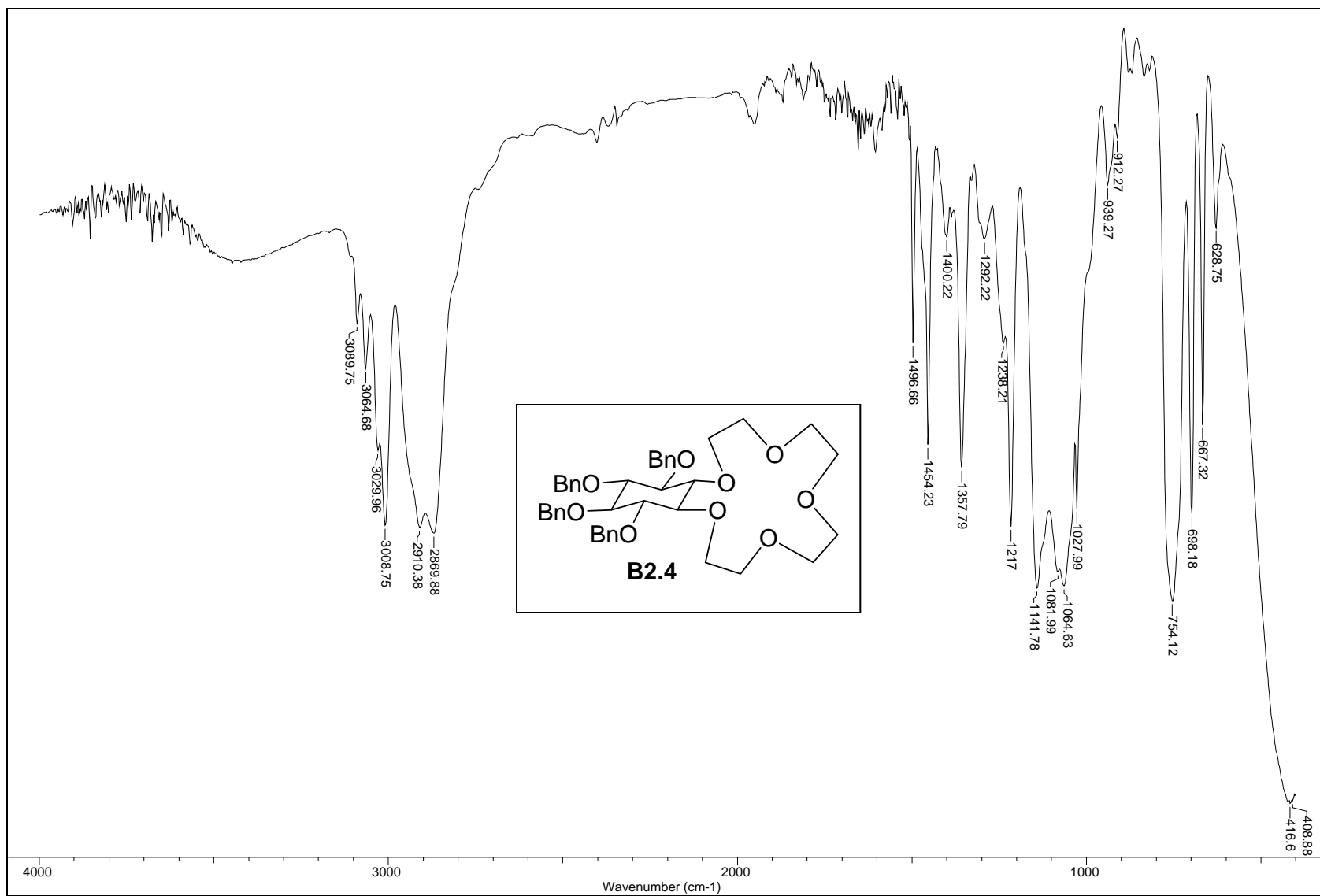


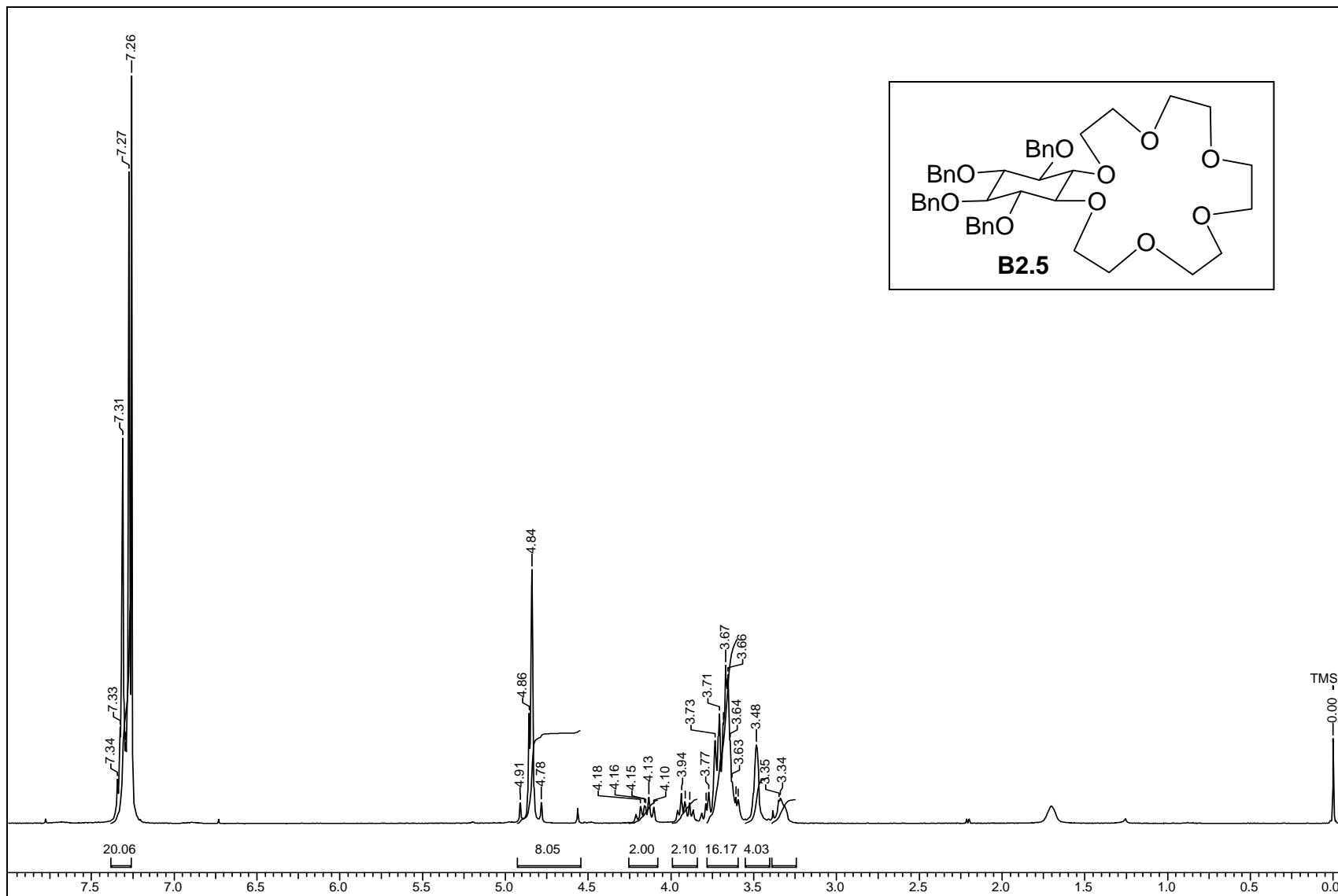


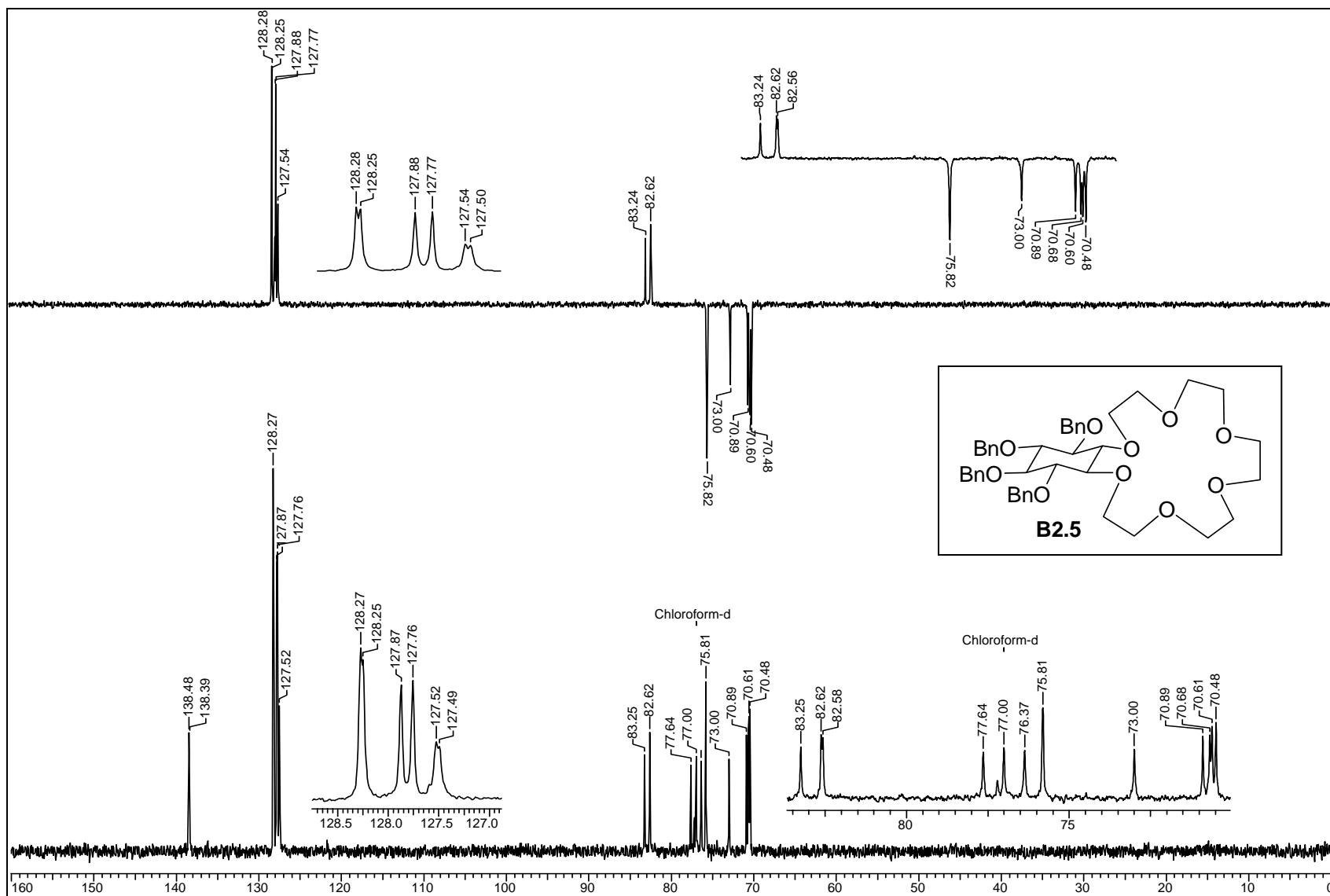


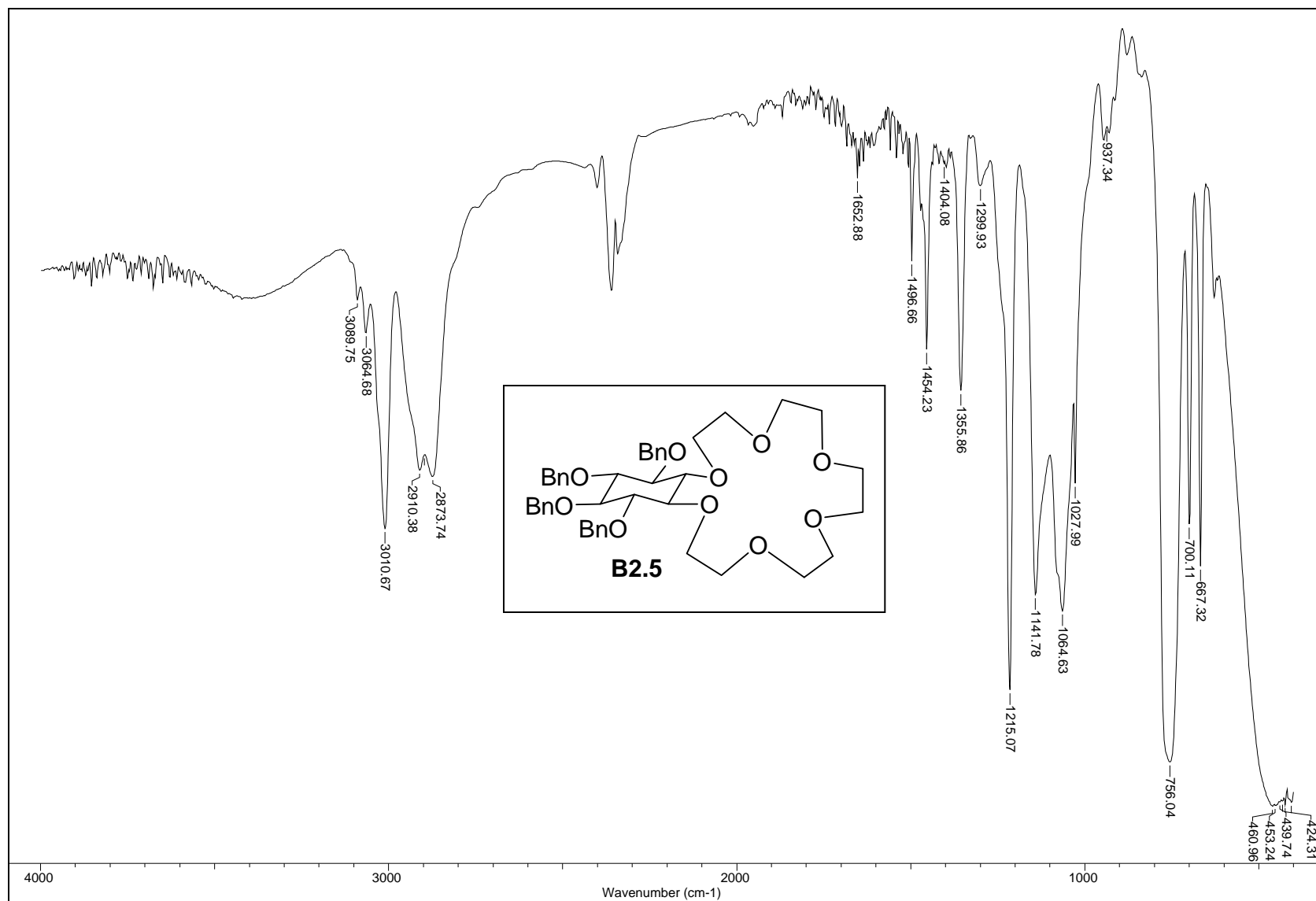


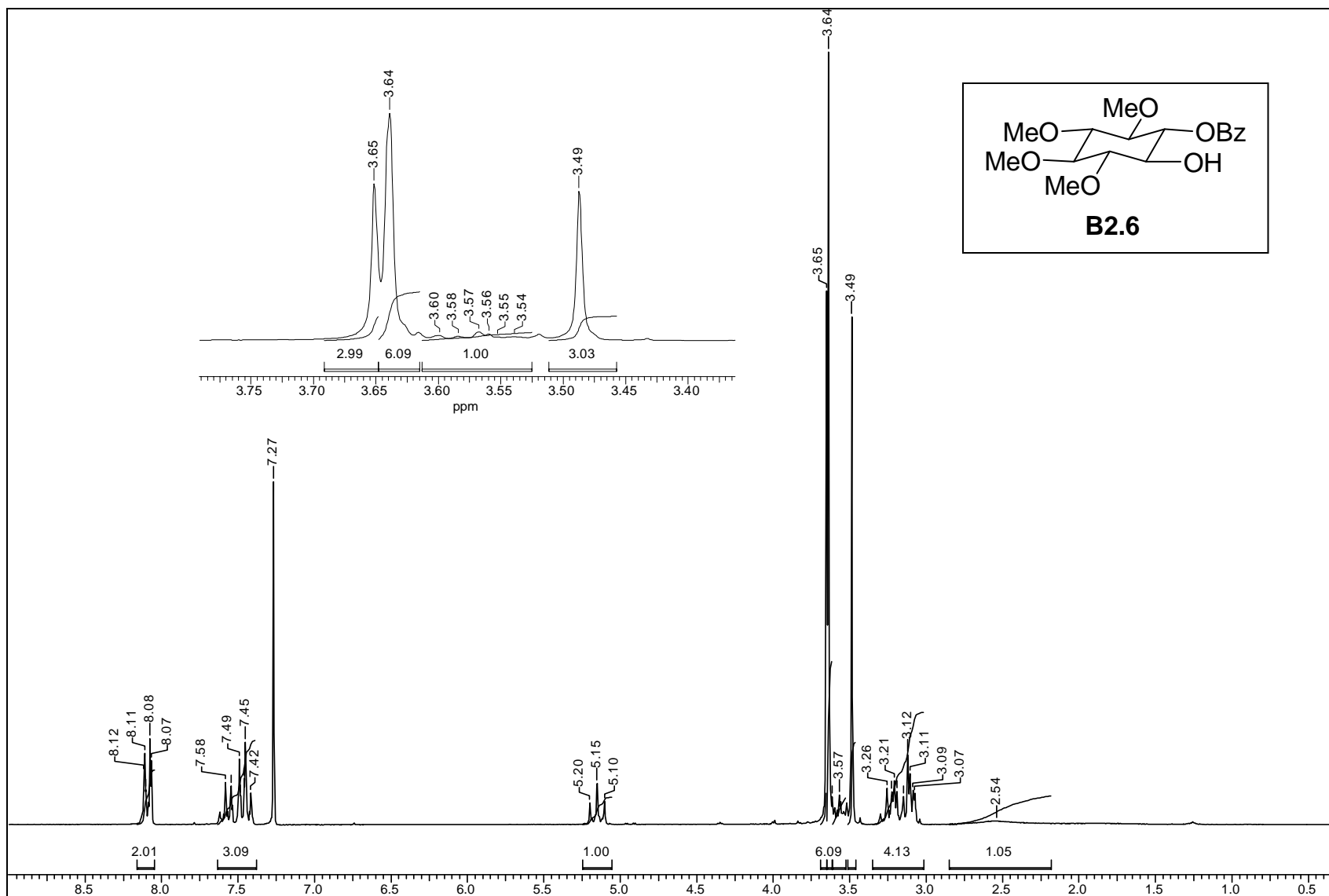


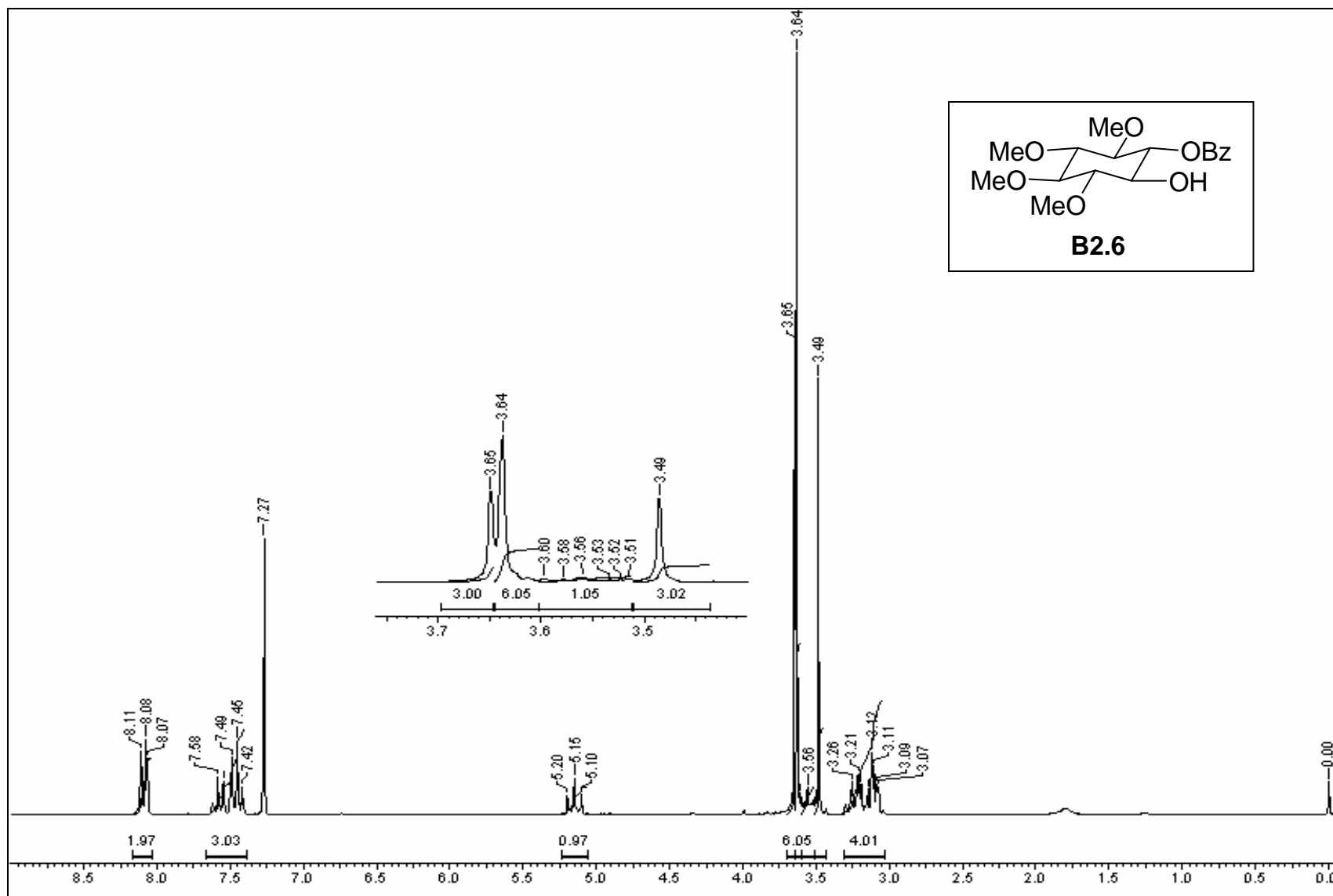


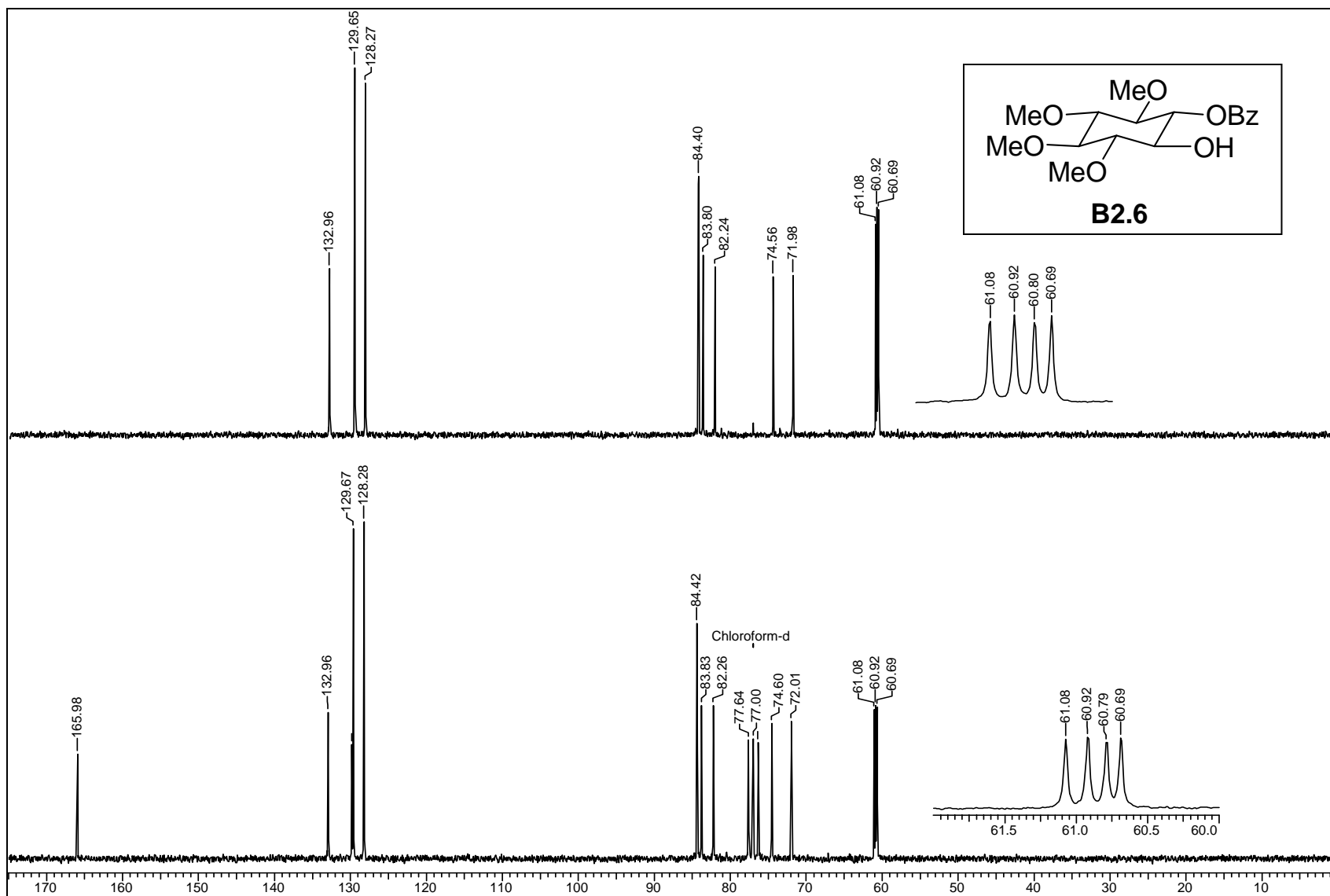


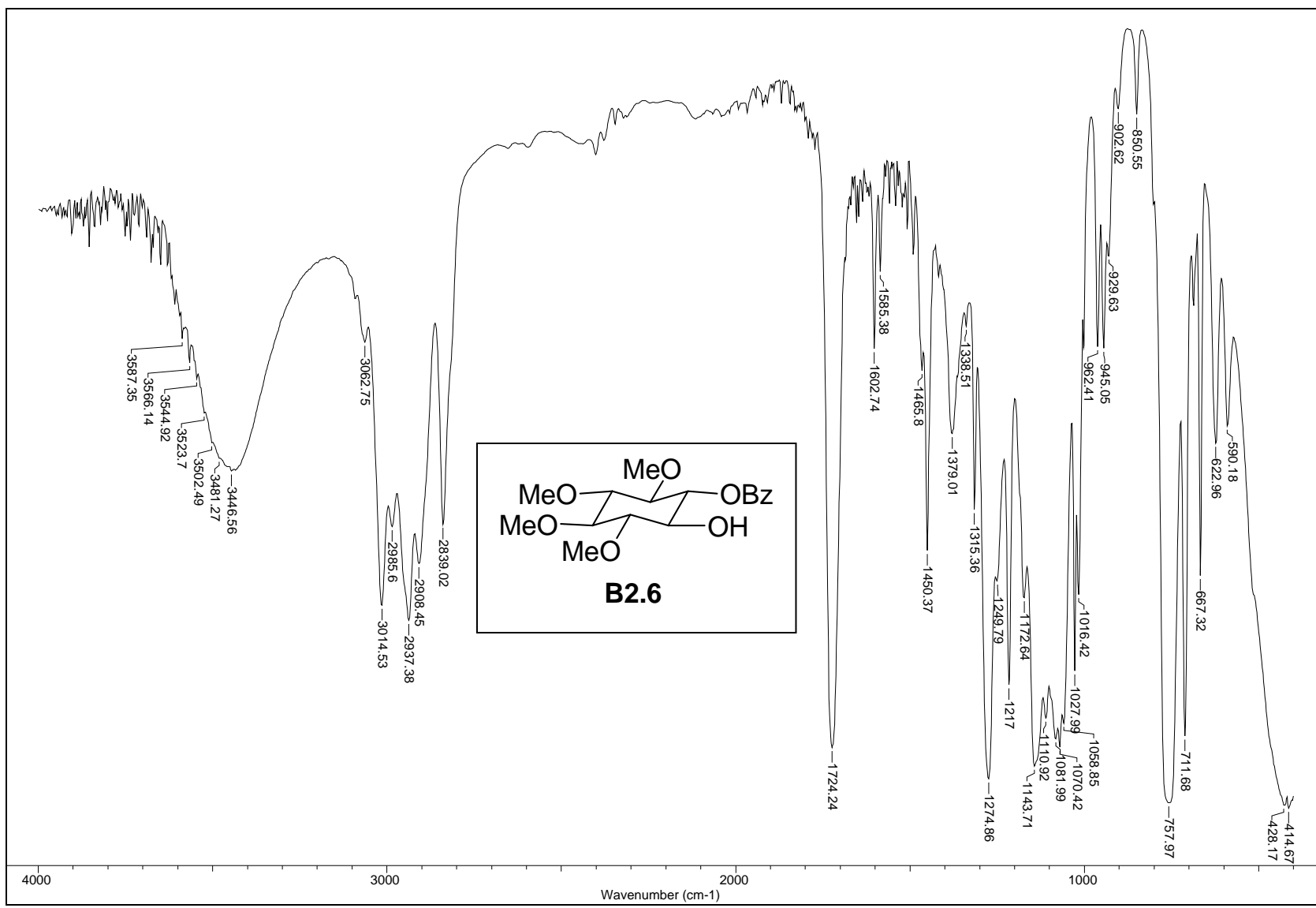


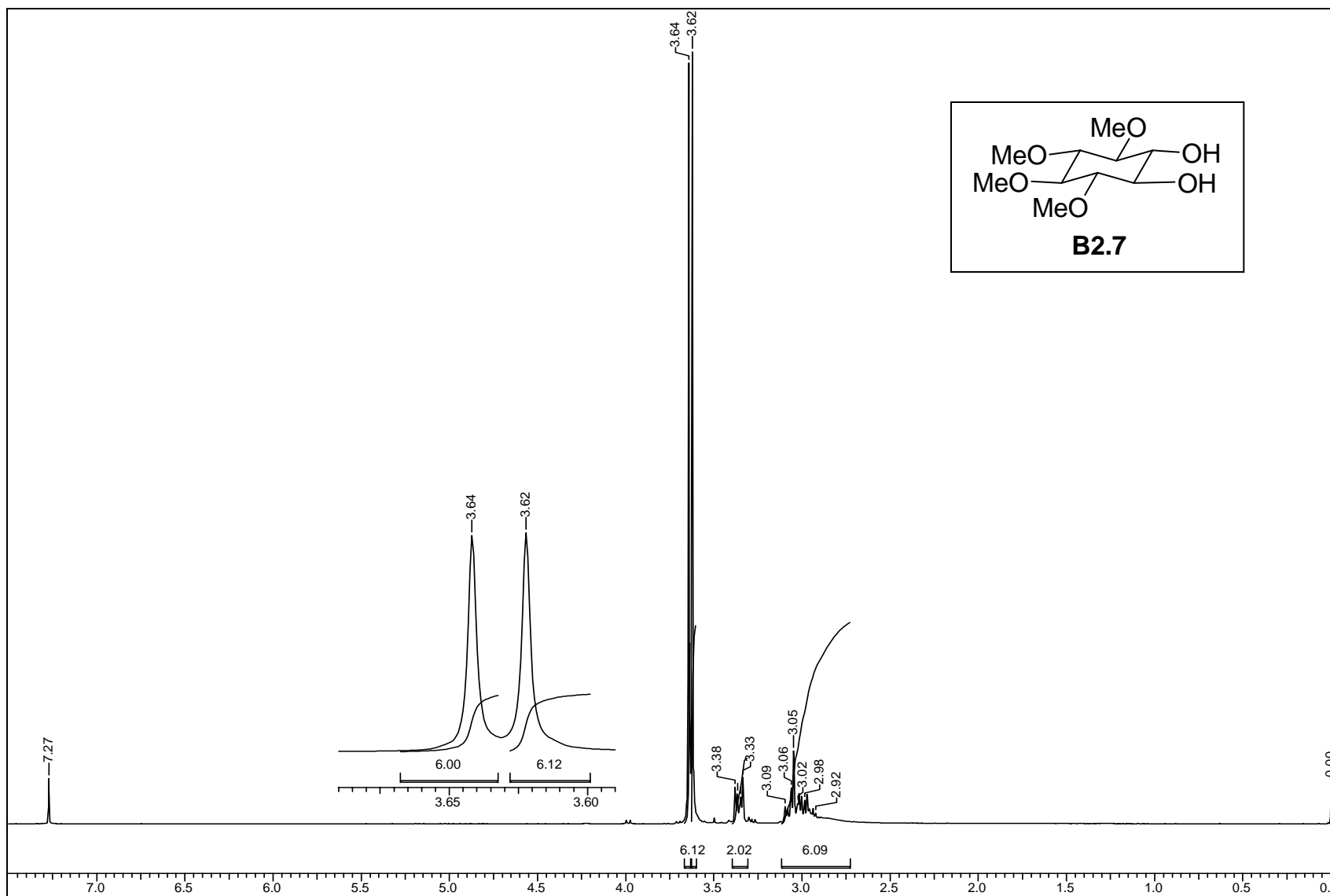


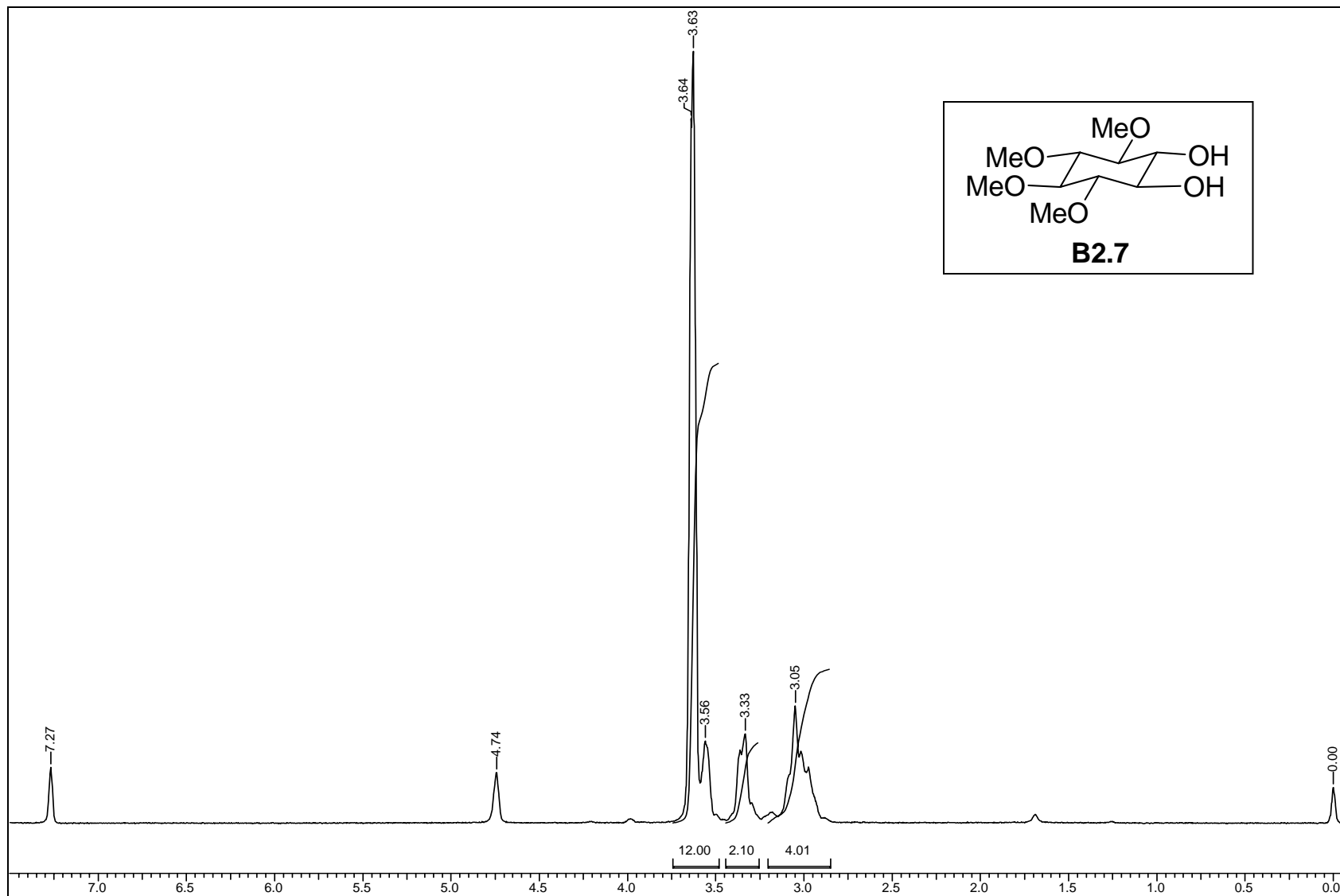


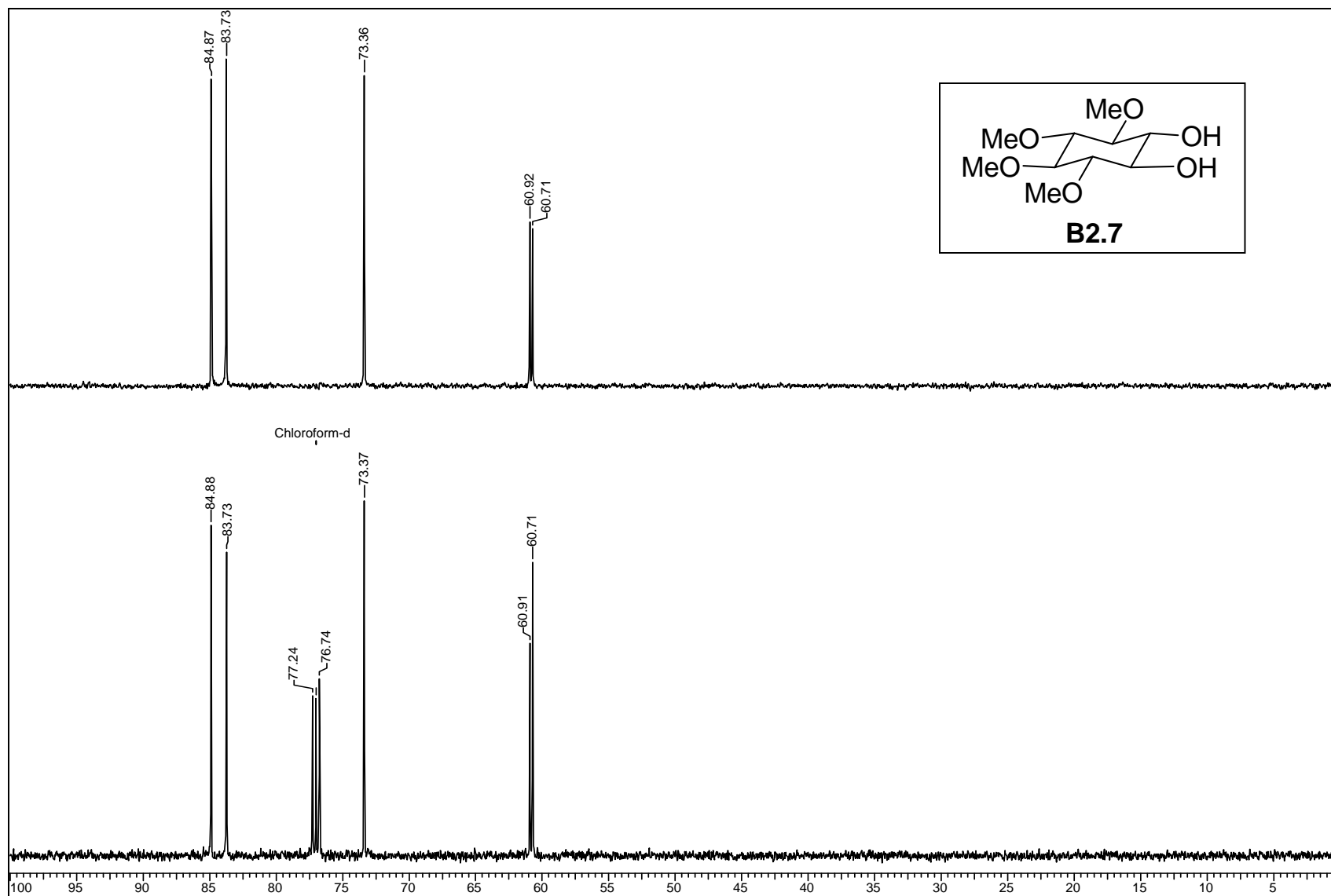


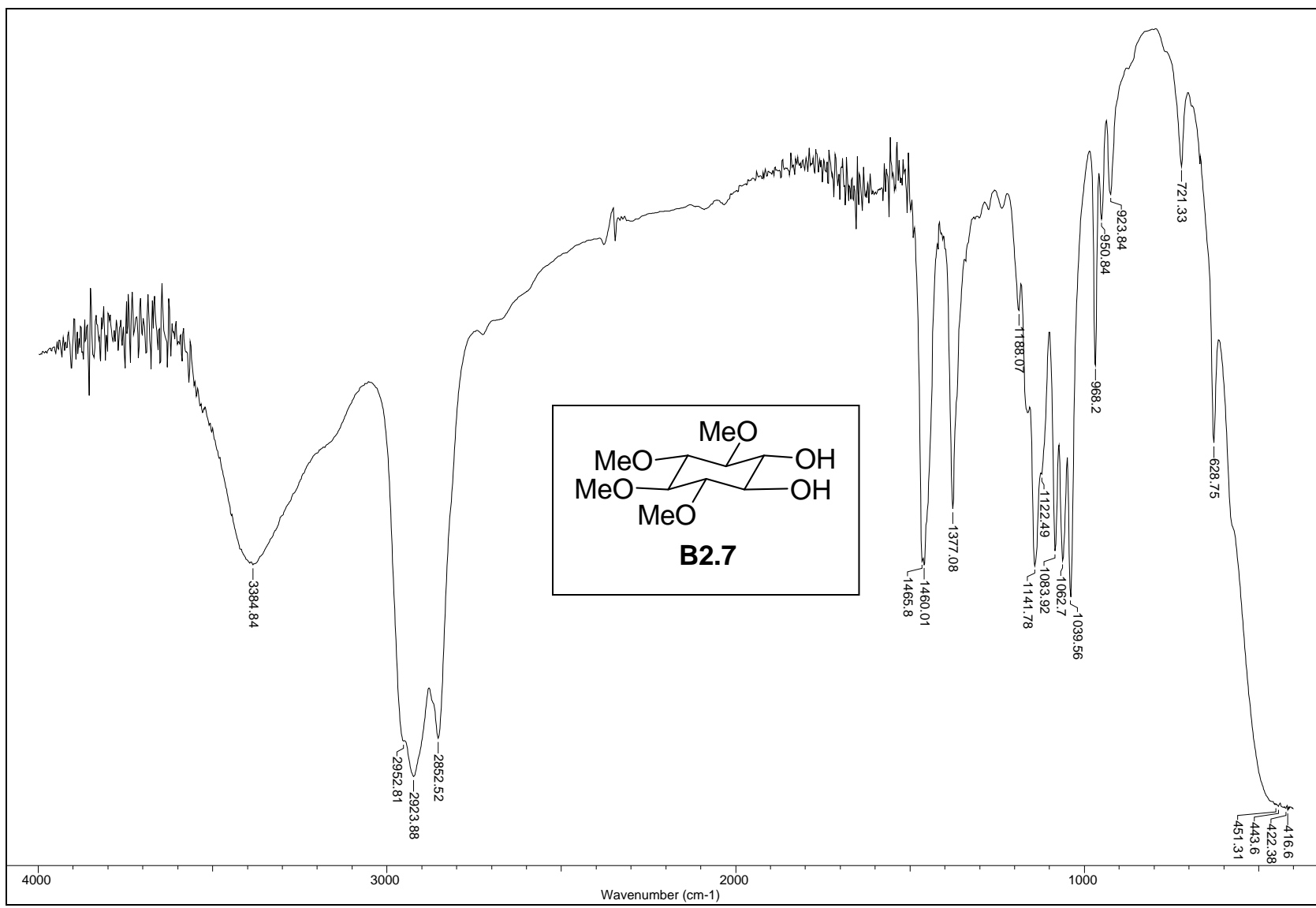


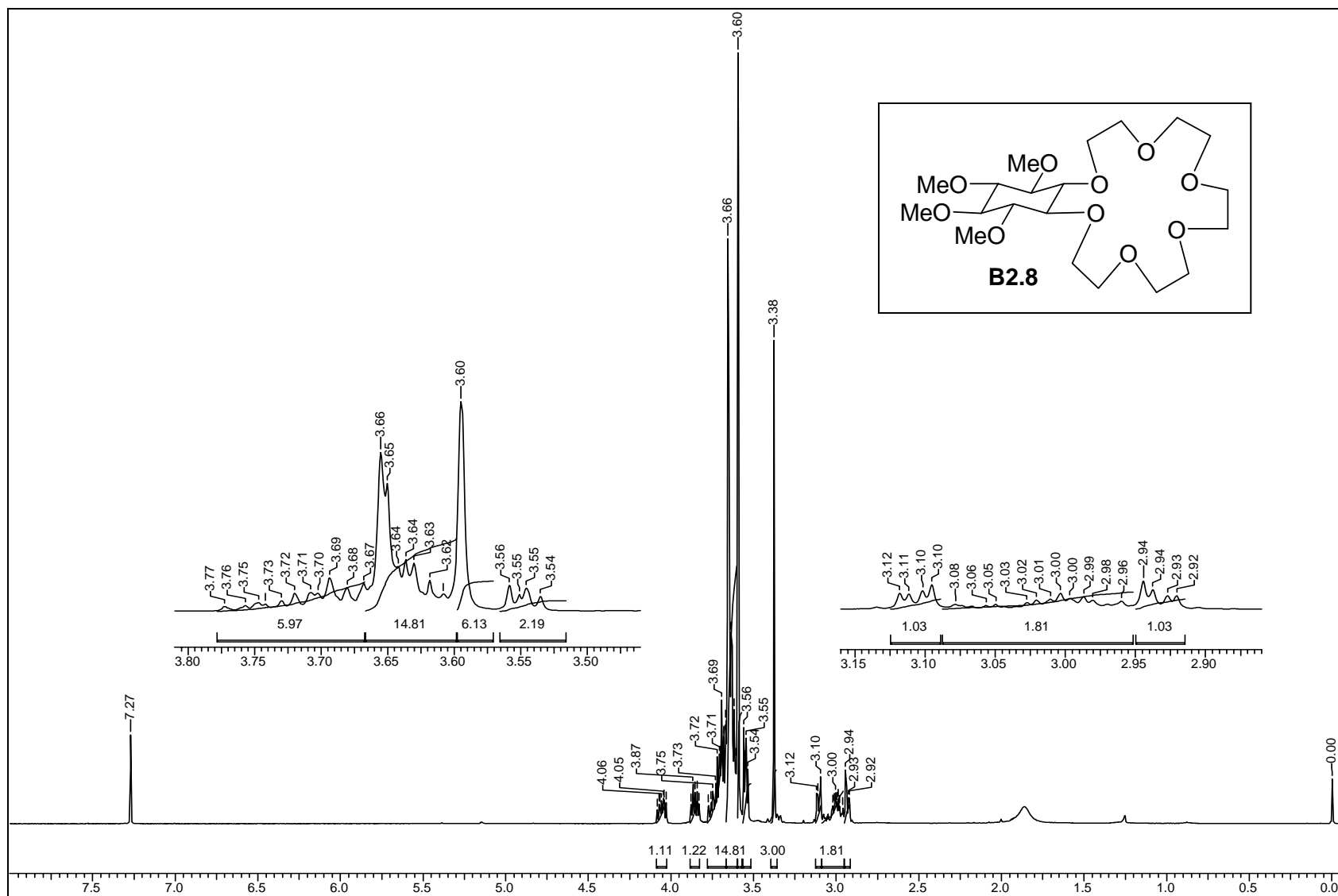


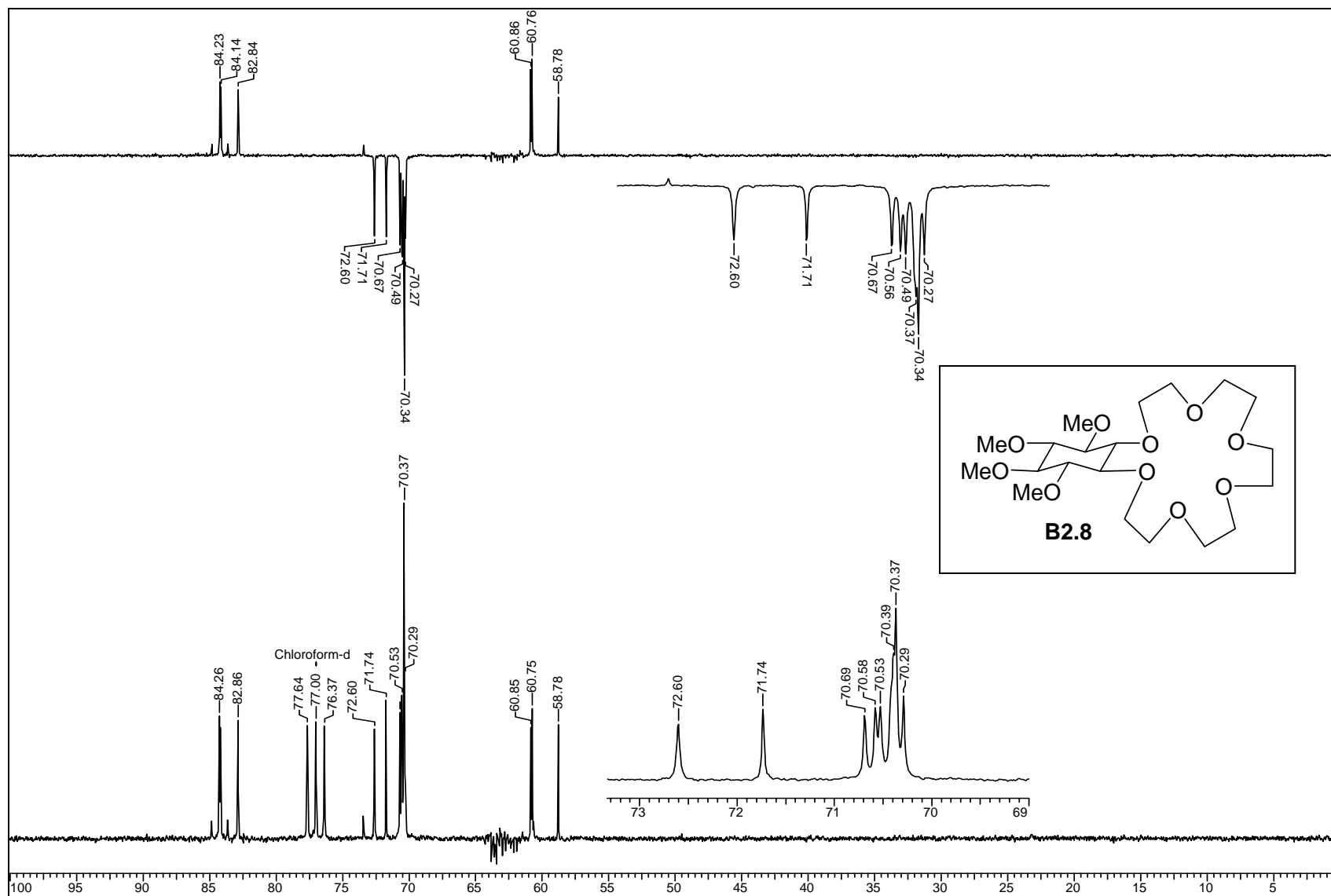


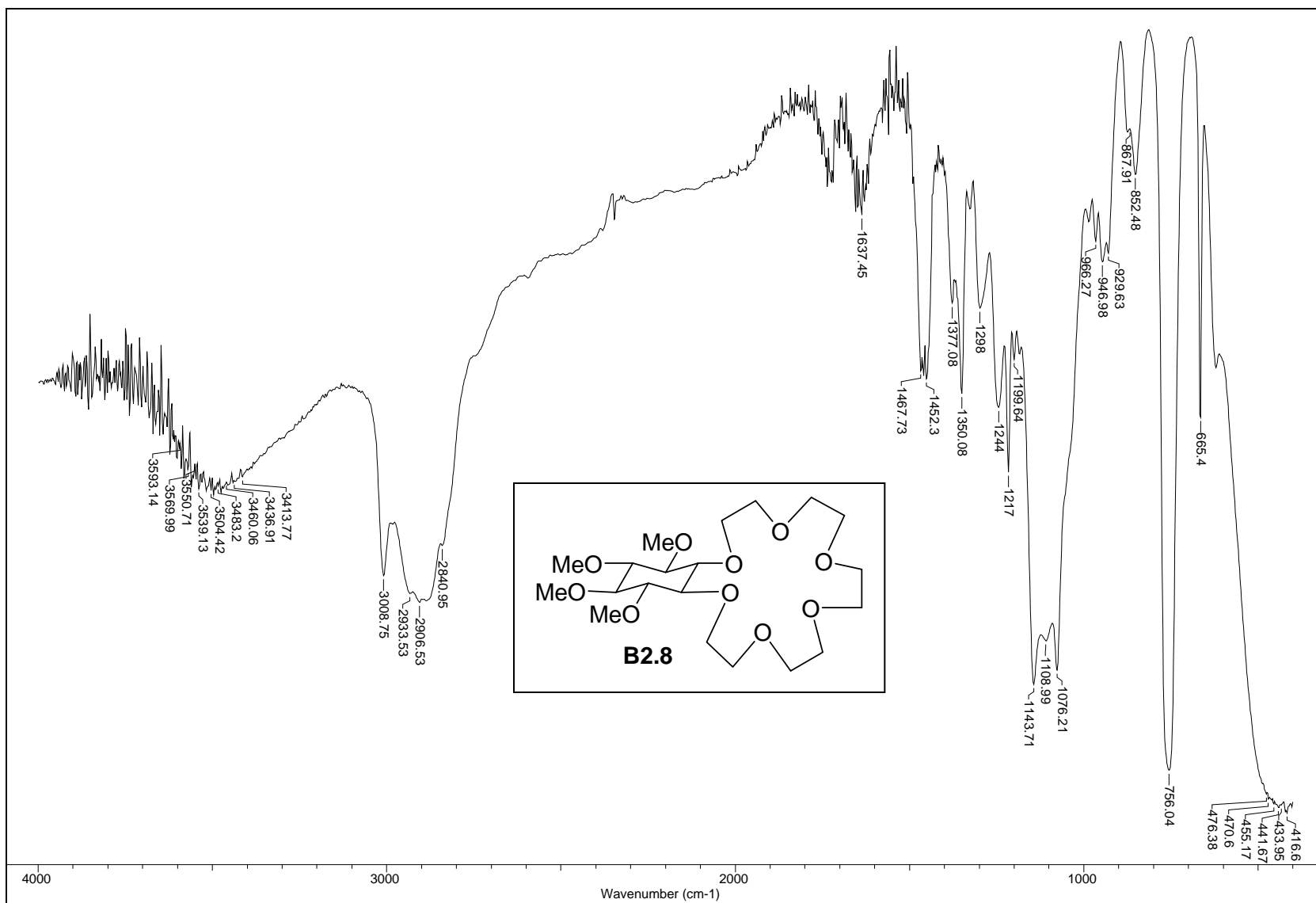


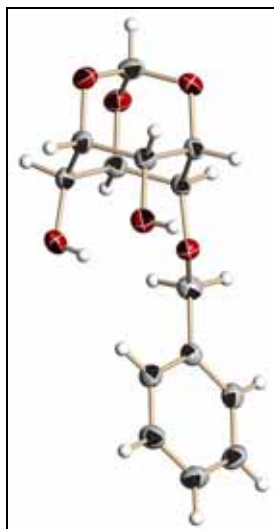




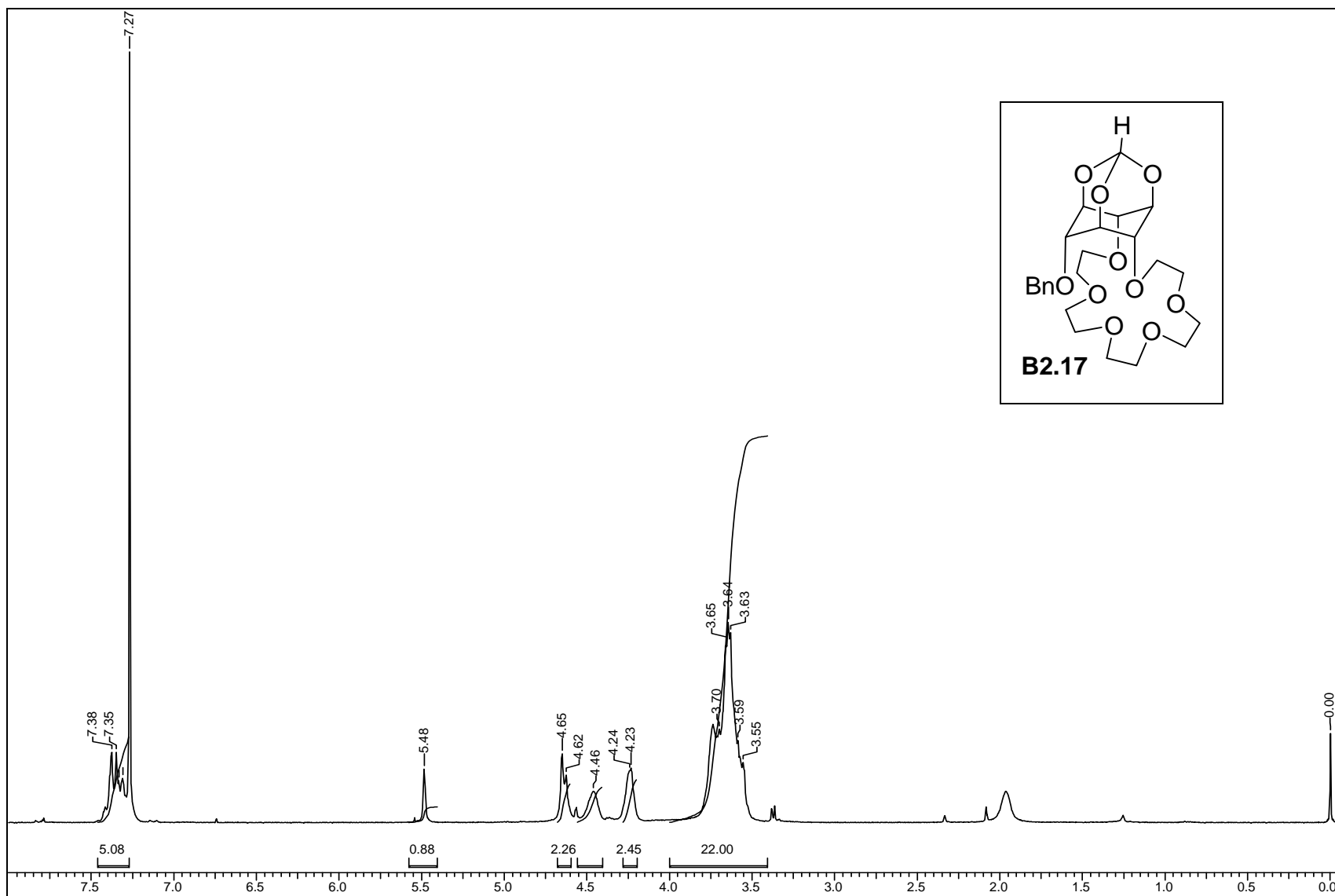


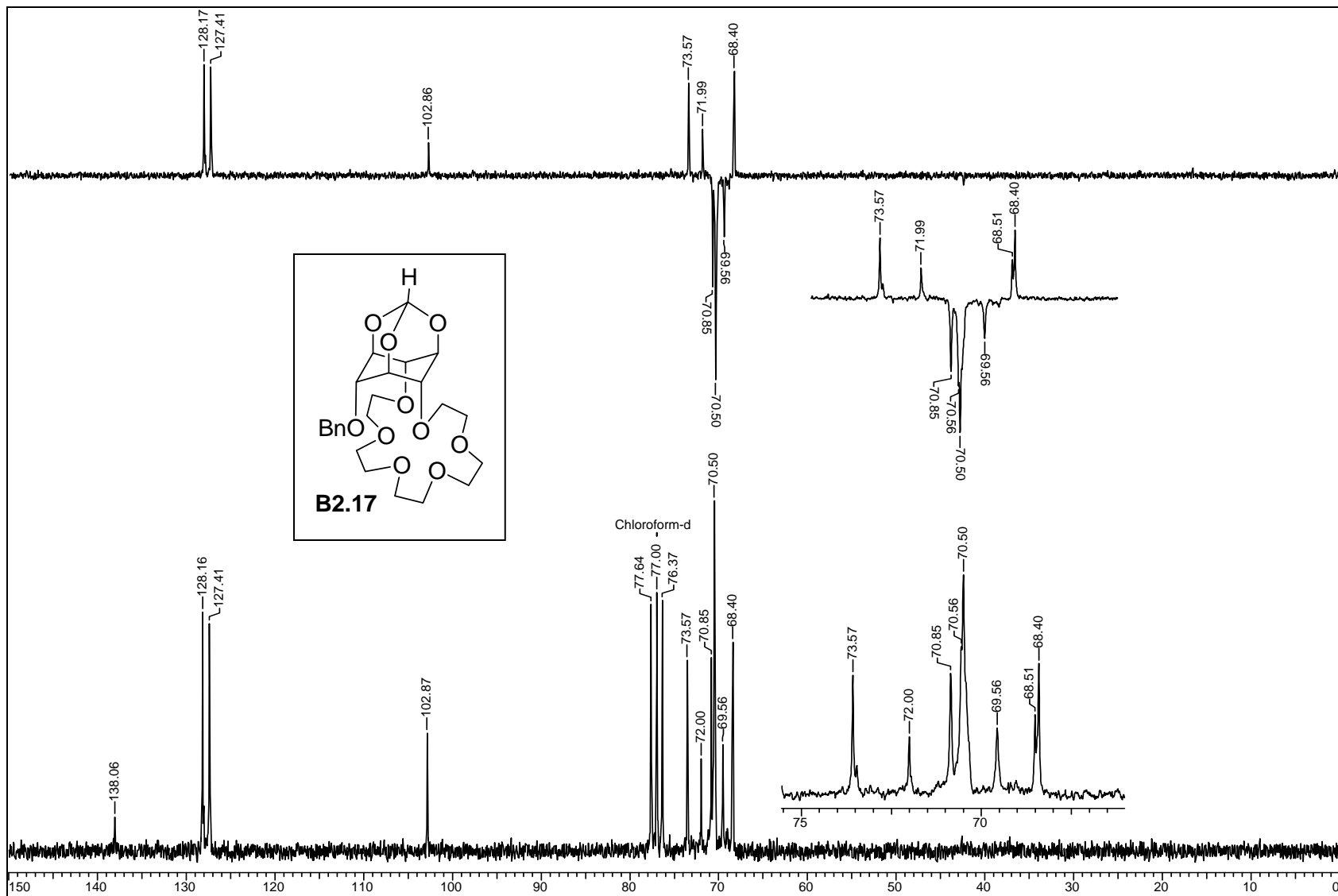


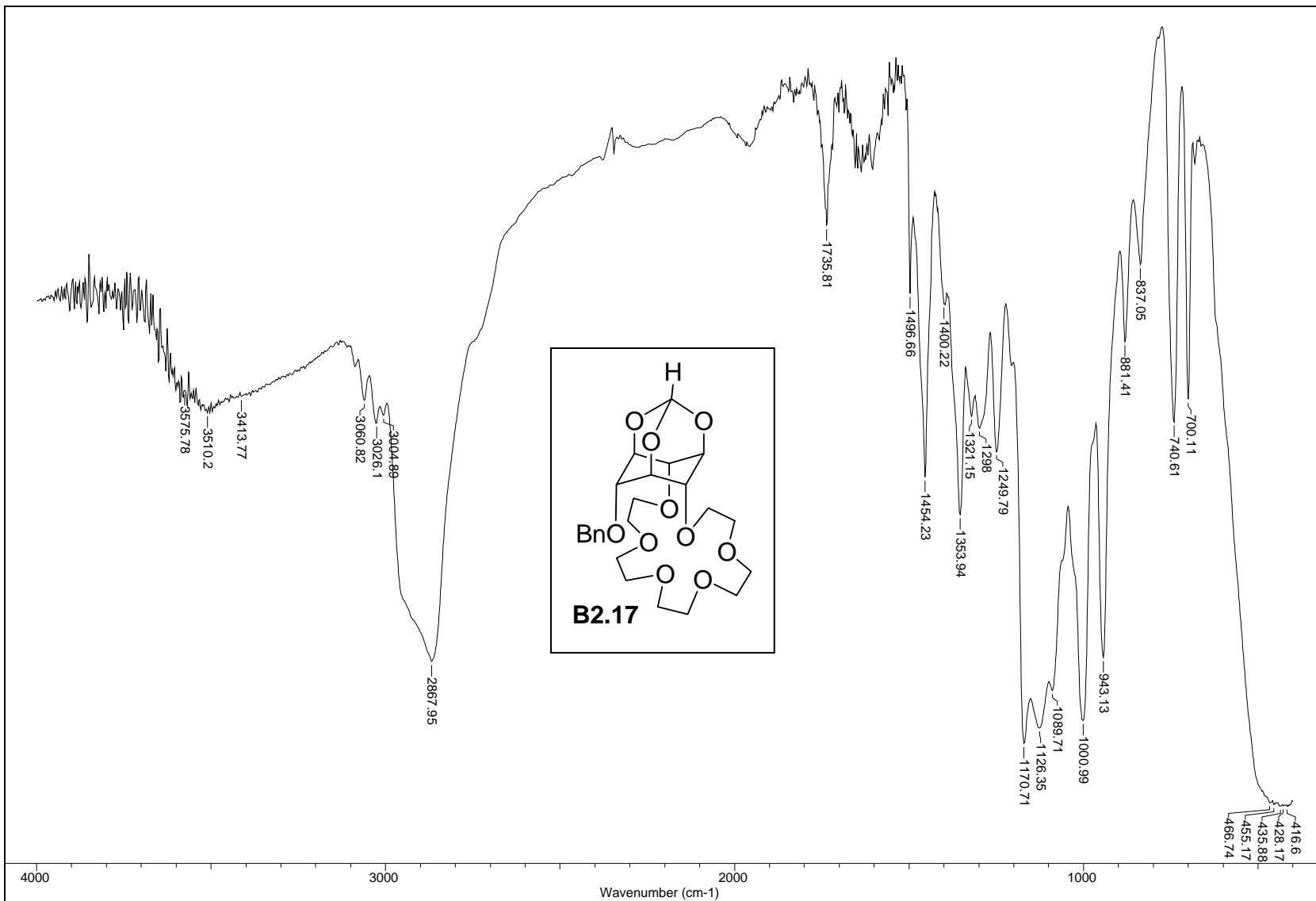


ORTEP diagram of **B2.16**Crystal data table of **B2.16**

Identification code	B2.16 (crystallized from DCM, light petroleum)
Empirical formula	C ₁₄ H ₁₆ O ₆
Formula weight	280.27
Temperature	297(2) K
Wavelength	0.71073 Å
Crystal system, space group	Triclinic, P-1
Unit cell dimensions	a = 9.929(6) Å α = 65.396(9)° b = 11.470(7) Å β = 75.295(9)° c = 12.539(7) Å γ = 87.527(10)°
Volume	1252.7(13) Å ³
Z, Calculated density	4, 1.486 Mg/m ³
Absorption coefficient	0.117 mm ⁻¹
F(000)	592
Crystal size	0.65 x 0.20 x 0.09 mm
θ range for data collection	2.70 to 25.00°
Limiting indices	-11 ≤ h ≤ 11, -13 ≤ k ≤ 13, -14 ≤ l ≤ 14
Reflections collected / unique	11917 / 4381 [R(int) = 0.0242]
Completeness to θ = 25.00	99.0 %
Absorption correction	Semi-empirical from equivalents
Max. and min. transmission	0.9901 and 0.9279
Refinement method	Full-matrix least-squares on F ²
Data / restraints / parameters	4381 / 0 / 365
Goodness-of-fit on F ²	1.111
Final R indices [I > 2σ(I)]	R1 = 0.0470, wR2 = 0.1195
R indices (all data)	R1 = 0.0554, wR2 = 0.1244
Largest diff. peak and hole (ρ _{max} & ρ _{min})	0.241 and -0.155 e. Å ⁻³







Chapter 3

Complexation of simple *O*-substituted inositol derivatives with metal ions and small molecules.

Happiness is the meaning and the purpose of life, the whole aim and end of human existence.

-Aristotle

3.1 Introduction

Realization of the existence of phosphoinositol based cellular signal transduction mechanisms in eukaryotic cells¹ and the role played by *myo*-inositol in the anchoring of certain proteins to the cell membranes² drove chemists to devise novel methods for the efficient synthesis of cyclitol derivatives (see introduction to Part B, Chapter 1 of this thesis).^{3,4,5} These synthetic investigations revealed that the regio- and stereoselectivity during the reactions of inositols and their derivatives depend on the reaction conditions and the reagents used.⁵ In particular, the unusual selectivity patterns observed during the reaction of *myo*-inositol or its derivatives, especially wherein the reagents used involved metal ions, were attributed to the chelation of inositol derivatives with metal ions (see part A, pages 47-50).^{6,7,8,9} These aspects prompted us to carry out metal picrate extraction experiments with simple inositol derivatives to investigate the extent of the binding of alkali metal ions and silver ions with inositol derivatives. Also, it was interesting to compare the metal ion binding ability of inositol derived crown ethers reported in previous chapters of this thesis, with simple inositol derivatives. Accordingly this chapter presents results on the binding of lithium, sodium and silver picrates to several inositol derivatives and a comparison of these results with the results presented in previous chapters.¹⁰

Yet another aspect that is closely related to the complexation of organic molecules with metal ions is their ability to form complexes with other small molecules either in solution or in the solid state. One of the well known examples is dioxanedibromide¹¹ (**B3.1**), which is a reagent used for the bromination of olefins. Some of the other examples of such phenomena are the formation of charge transfer complexes¹² (**B3.2**,

B3.3), formation of solvates¹³ (**B3.4**) and co-crystals^{14,15} (**B3.5**, **B3.6**), formation of Meisenheimer complexes^{16,17} (**B3.7**, **B3.8**), as well as the complexation of crown ethers with alkylammonium ions¹⁸ (**B3.9**, **B3.10**) and amino acid derivatives¹⁹ (**B3.11**). A few examples selected from the literature are shown in Figure B3.1.

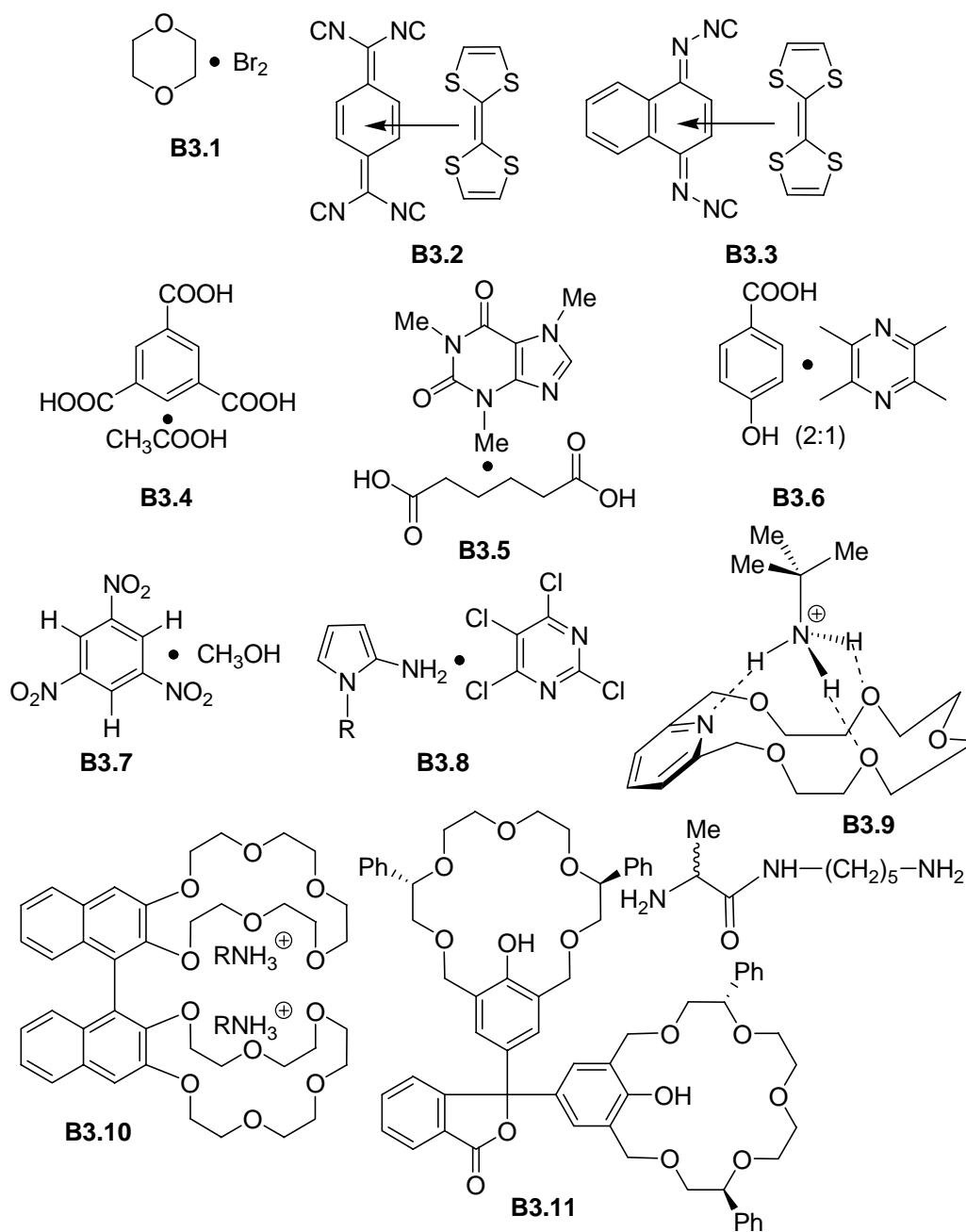


FIGURE B3.1. Selected examples of molecular complexes.

Past experience during the synthesis of inositol derivatives in our laboratory had shown that *myo*-inositol derivatives frequently form complexes with other small organic molecules in the solid state. Some of the examples from previous work in our laboratory are shown in Figure B3.2.

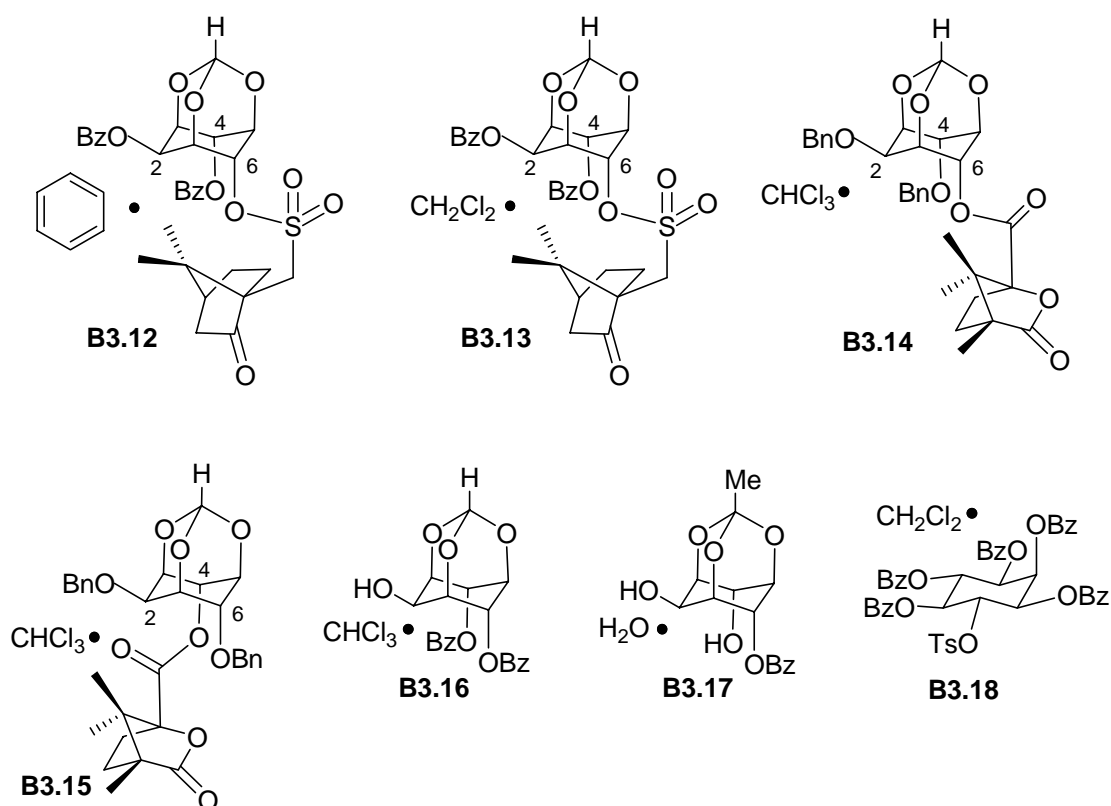


FIGURE B3.2. Selected examples of molecular complexes involving *myo*-inositol derivatives.

We have screened some of the inositol derivatives for their complexation with small organic molecules, since co-crystallization of organic compounds and determination of their physical and chemical properties are of current research interest in terms of their structure and reactivity in the solid state.^{20,21,22} Accordingly, this chapter also presents results on our attempts to obtain inositol derivative – neutral organic molecule complexes and their crystal structures.

3.2 Results and Discussion

Complexation of inositol derivatives with metal picrates

Simple inositol derivatives that were investigated for metal picrate binding studies are shown in Figure B3.3.

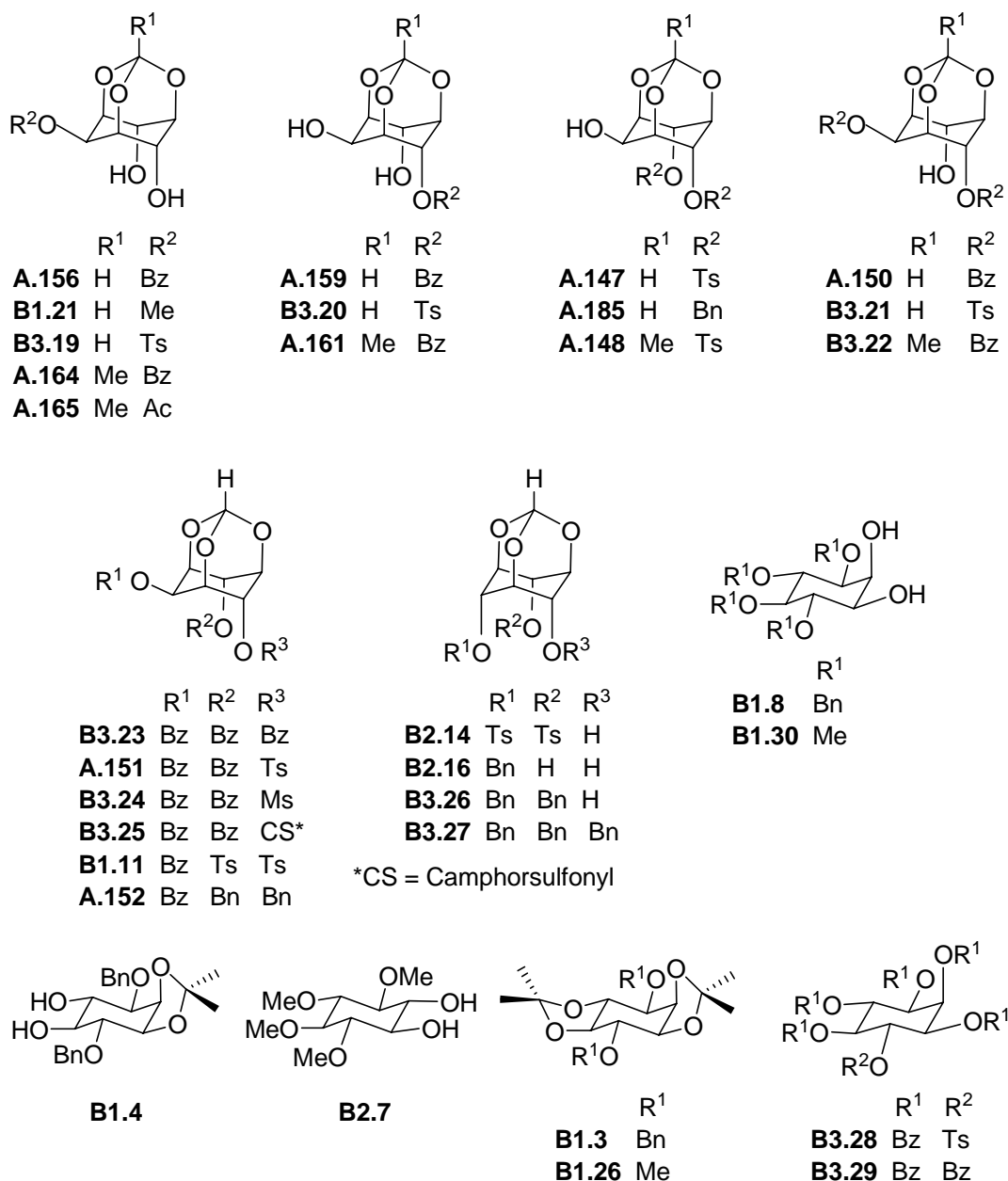
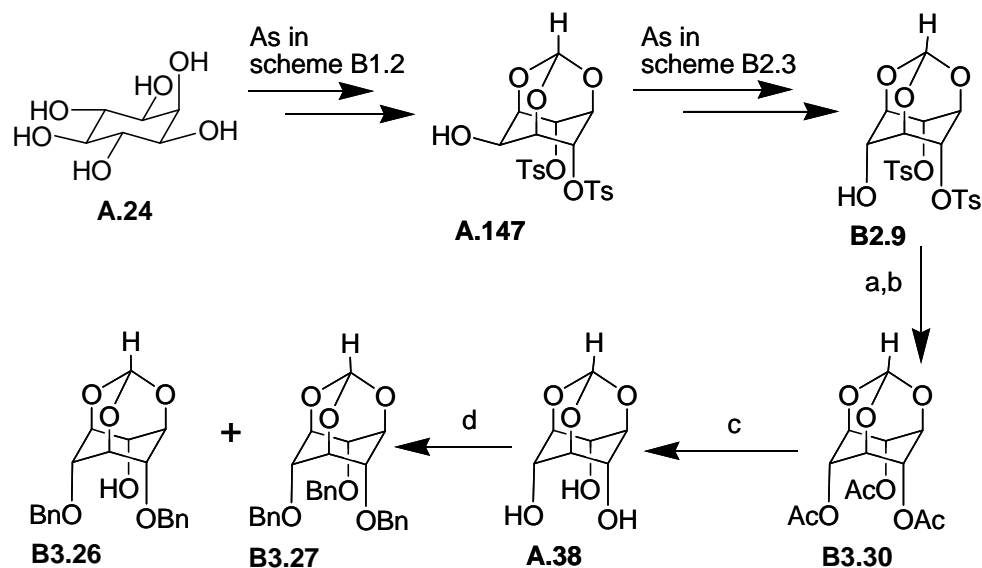


FIGURE B3.3. Inositol derivatives investigated for metal picrate binding studies.

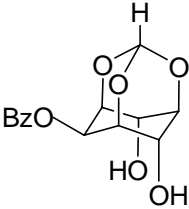
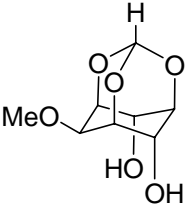
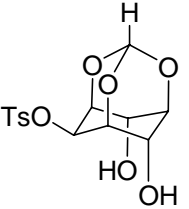
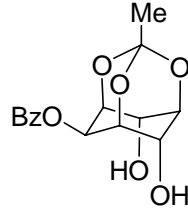
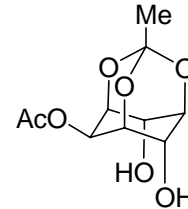
All the compounds shown in figure B3.3 except **B3.26** and **B3.27** were prepared as reported in the literature. The benzyl ethers **B3.26** and **B3.27** were prepared as shown in scheme B3.1.

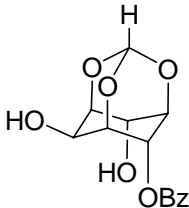
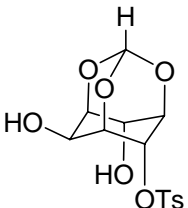
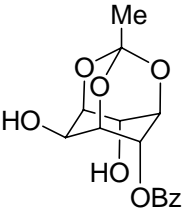
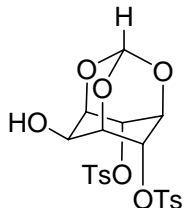
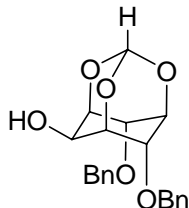


SCHEME B3.1. *Reagents and conditions:* (a) NaOMe, MeOH, reflux, 24 h; (b) Ac₂O, pyridine, rt, 24 h, 81% (for two steps); (c) *i*-BuNH₂, MeOH, reflux, 12 h, 85%; (d) DMF, BnBr, NaH, rt, 30 min (43% for **B3.26**; 21% for **B3.27**).

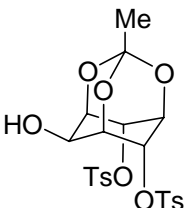
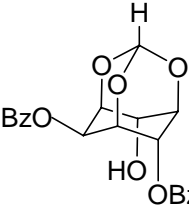
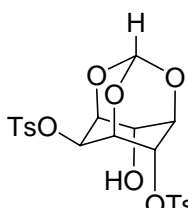
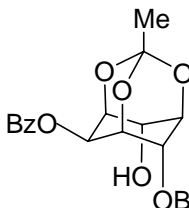
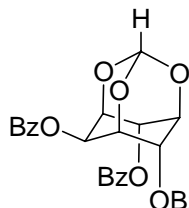
The association constants of the inositol derivatives with metal picrates are tabulated in Table B3.1. Some of these values are reproduced from the literature⁹ for comparison.

TABLE B3.1: Association constants ($K_a \times 10^{-4} \text{ dm}^3 \text{ mol}^{-1}$) of inositol orthoester derivatives with metal picrates in CDCl_3 at 27 °C.

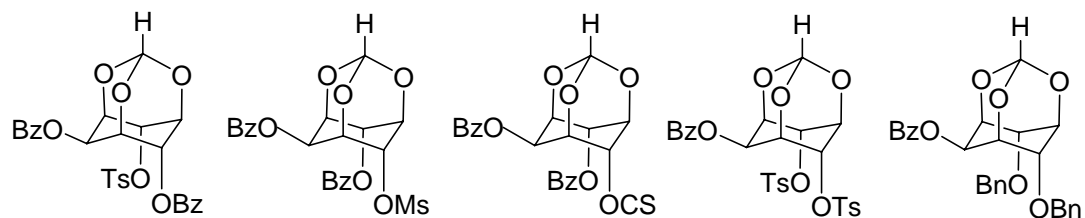
					
	A.156	B1.21	B3.19	A.164	A.165
Li	1115	242	194	14	59
Na	8.5	6.6	3.9	11	10.8
Ag	--	--	--	--	--

					
	A.159	B3.20	A.161	A.147	A.185
Li	102	1058	84	56	--
Na	13.5	15	12	1.7	--
Ag	--	15 ^a	--	--	8.3 ^a

^a These K_a values are from reference 9.

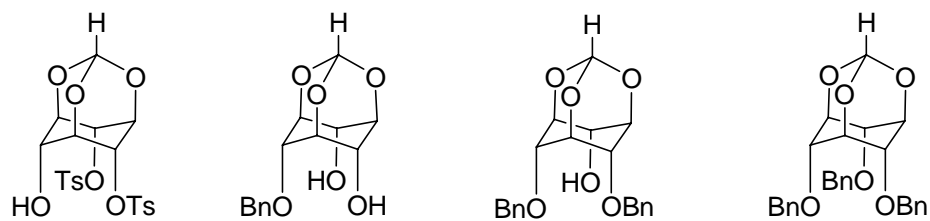
					
	A.148	A.150	B3.21	B3.22	B3.23
Li	39	127	480	19	315
Na	6.6	2.8	11.9	4.1	5
Ag	--	6.2 ^a	--	--	6.8

^a This K_a value is from reference 9.



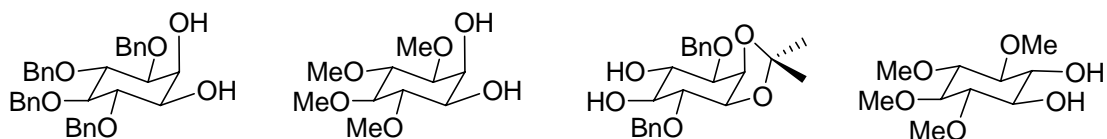
	A.151	B3.24	B3.25	B1.11	A.152
Li	85	--	--	72.6	--
Na	1.4	--	--	1.4	--
Ag	8.4 ^a	13.3	17.7 ^a	--	22.6 ^a

^a These K_a values are from reference 9.

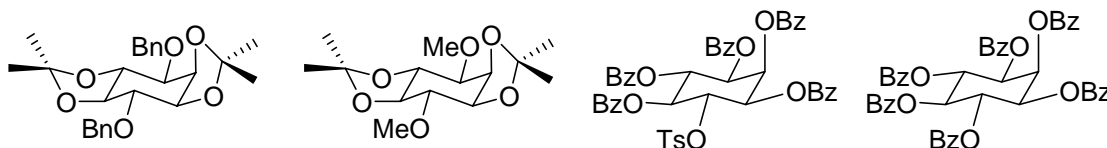


	B2.14	B2.16	B3.26	B3.27
Li	75.1	5.7	16.06	15
Na	2.8	2.7	7.9	0.586
Ag	--	0.96	1.24	2.94

TABLE B3.2: Association constants ($K_a \times 10^{-4} \text{ dm}^3 \text{ mol}^{-1}$) of simple inositol derivatives with metal picrates in CDCl_3 at 27 °C.



	B1.8	B1.30	B1.4	B2.7
Li	137	85	135.7	13.48
Na	1.1	0.8	2.6	1.12
Ag	--	--	--	1.44

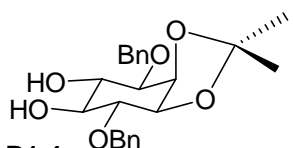
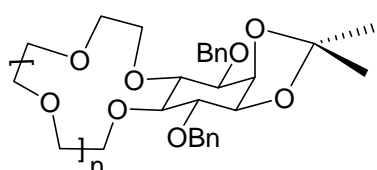
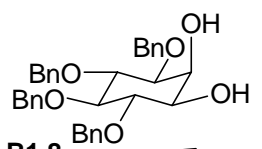
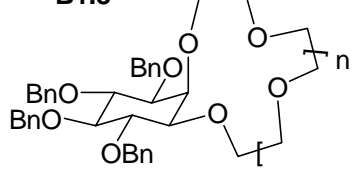
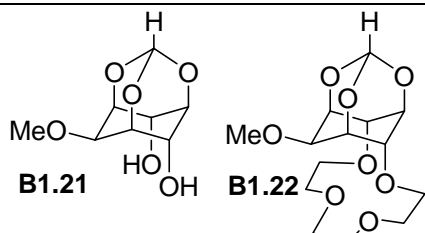


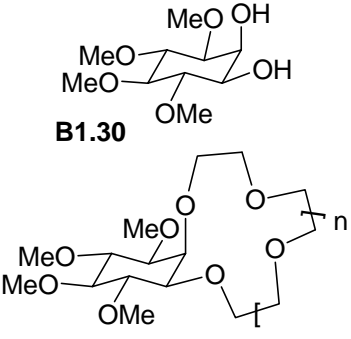
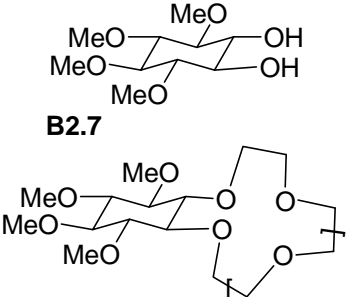
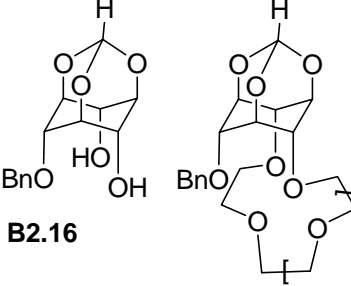
	B1.3	B1.26	B3.28	B3.29
Li	72	173	--	--
Na	3.1	2.9	--	--
Ag	--	--	8 ^a	19.9 ^a

^a These K_a values are from reference 9.

Results of these metal picrate extraction experiments suggest that the inositol derivatives bind lithium ions (a maximum of 130 times, **A.156** $K_{a(\text{Li}^+)}/K_{a(\text{Na}^+)} \approx 130$) better than sodium ions. These results give credence to the suggestion that the extent of chelation of metal ions by inositol derivatives is a major factor in deciding the observed regioselectivity²³ for the *O*-substitution reactions of many inositol derivatives (see Part B, Chapter 1, Scheme B1.3, page 78). A comparison of the association constants for the *myo*- and *scyllo*-diols **B1.30** and **B2.7** shows that the selectivity exhibited by **B1.30** ($K_{(\text{Li}^+)}/K_{(\text{Na}^+)} = 106$) for binding to lithium ion (as compared to sodium ion) is better than the selectivity exhibited by **B2.7** ($K_{(\text{Li}^+)}/K_{(\text{Na}^+)} = 12$). This result compliments the mode of binding (to lithium and sodium picrates) of the corresponding crown ethers with *myo*- and *scyllo*-configurations (results presented in Chapter 2, pages 208-209). Similar comparison could not be made for the tetrabenzyl ethers **B1.8** and **B2.2** since an estimate of the picrate binding constants for the diol **B2.2**, could not be made. This was because, mixing of a solution of **B2.2** and a solution of metal picrate resulted in immediate formation of a precipitate, making spectrophotometric determination of picrate concentration unreliable.

TABLE B3.3: Ratio of association constants of diols and the corresponding inositol crown ethers.

Structure	Compound	Li ⁺	Na ⁺
 <p>B1.4</p>	B1.4/B1.5	1.357	0.130
 <p>B1.5 Crown 4, n = 1 A.91 Crown 5, n = 2 A.92 Crown 6, n = 3</p>	B1.4/A.91	14.17	0.587
	B1.4/ A.92	30.63	0.558
 <p>B1.8</p>	B1.8/ B1.9	6.88	0.278
 <p>B1.9 Crown 4, n = 1 A.93 Crown 5, n = 2 A.94 Crown 6, n = 3</p>	B1.8/A.93	10.62	0.017
	B1.8/ A.94	8.40	0.024
 <p>B1.21 B1.22</p>	B1.21/ B1.22	15.51	2.76

 <p>B1.30</p> <p>B1.31 Crown 6, n = 3</p>	B1.30/ B1.31	48.57	0.123
 <p>B2.7</p> <p>B2.8 Crown 6, n = 3</p>	B2.7/B2.8	2.41	0.632
 <p>B2.16</p> <p>B2.17 Crown 6, n = 3</p>	B2.16/B2.17	0.330	0.046

We also calculated the ratio of the association constants for a given diol to the crown ethers derived from it (Table B3.3). These ratios revealed that the lithium picrate extractability does not improve much, due to the presence of the crown ether; most of the inositol derived diols bind lithium picrate better than the corresponding crown ethers. Only exception to this was the crown ether **B2.17** derived from *scyllo*-inositol orthoformate derivative **B2.16**, where in the metal picrate extraction is considerably improved due to the presence of the crown ether. A comparison of the extraction constants for *scyllo*-crown ethers with simple *scyllo*-inositol derivatives reveals that the

ditosylate **B2.14** extracts Li-picrate better than all the crown ethers. However this trend is reversed for the binding of sodium picrate; most of the inositol derived crown ethers bind sodium picrate better than the corresponding parent diol. These results suggest that the crown ether moieties contribute more towards the binding of sodium (and perhaps larger) ions as compared to lithium ions.

Complexation of inositol derivatives with small molecules

Simple inositol derivatives that were investigated for the complexation with small molecules are shown in Figure B3.4. We investigated the complexation behavior of a few *scyllo*- and *chiro*-inositol derivatives in order to obtain a comparison with *myo*-inositol derivatives which frequently^{24,25} show inclusion of small molecules in their crystals (Figure B3.2). But our attempts did not yield any co-crystals of *scyllo*- and *chiro*-inositol derivatives.

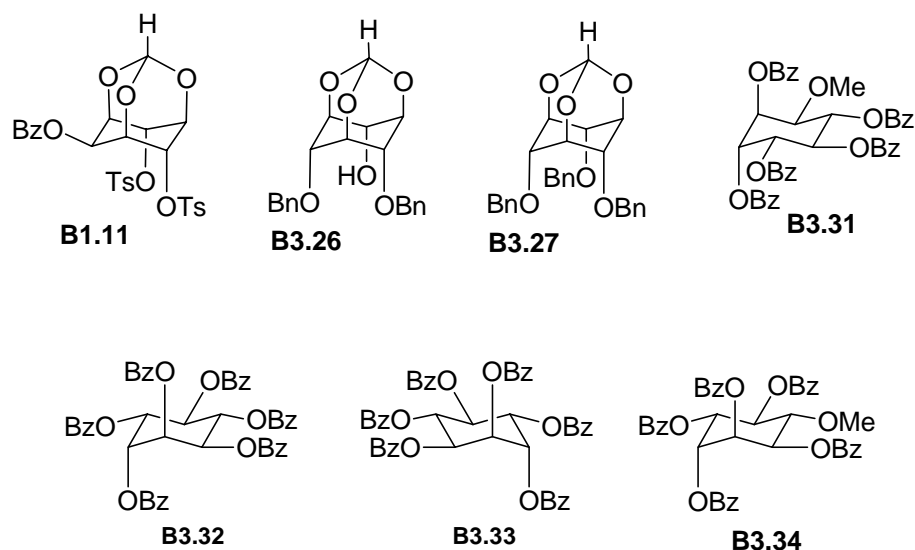
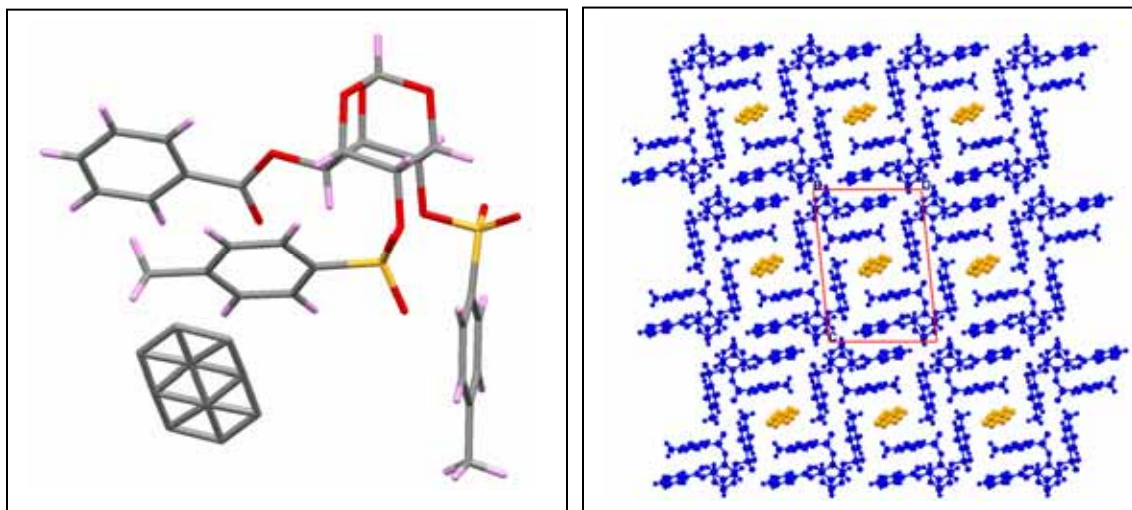


FIGURE B3.4. Inositol derivatives investigated for small molecule inclusion.

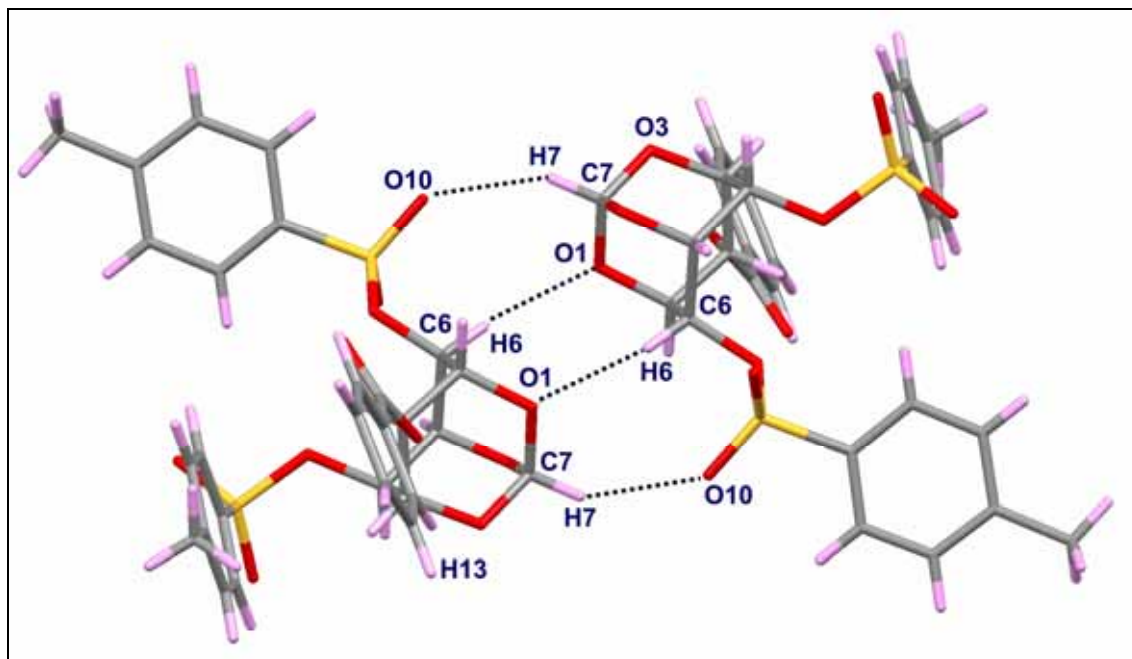
Crystallization of 2-*O*-benzoyl-4,6-di-*O*-tosyl *myo*-inositol orthoformate (**B1.11**) from various solvents showed that this ditosylate is capable of forming adducts with

toluene (**B3.35**), methanol (**B3.36**) and naphthalene (**B3.37**). For details on crystallization experiments see Table B3.4 in the experimental section, page 274. Toluene and methanol adducts **B3.35** and **B3.36**, were not very stable and the crystals turned opaque and amorphous on storing at ambient temperature, perhaps due to loss of toluene and methanol molecules from the crystal lattice. The naphthalene adduct (**B3.37** mp. 100-107 °C) was obtained on crystallization of the ditosylate **B1.11** (mp. 109-111 °C) from *p*-xylene. This was perhaps due to the presence of small quantities of naphthalene in commercial *p*-xylene. Addition of excess of naphthalene (one equivalent) during crystallization of **B1.11** from *p*-xylene did not increase the amount of naphthalene in the co-crystals. The single crystal X-ray crystal structure showed that the ratio of **B1.11**:naphthalene was 1:0.5 and elemental analysis showed that the ratio of **B1.11**:naphthalene was 1:0.45.



(a)

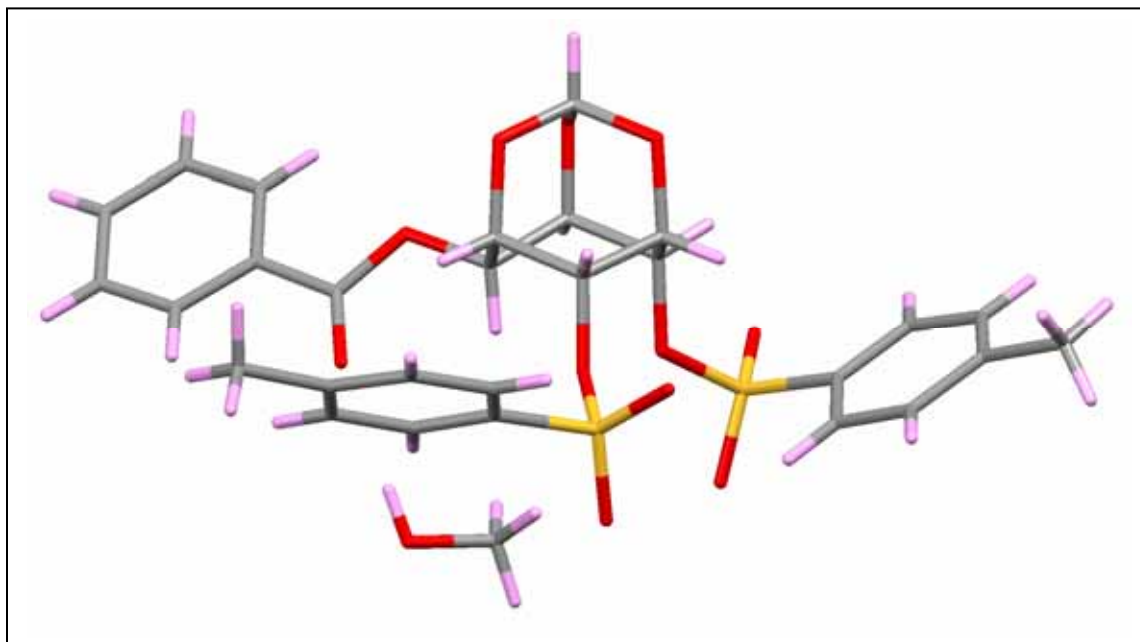
(b)



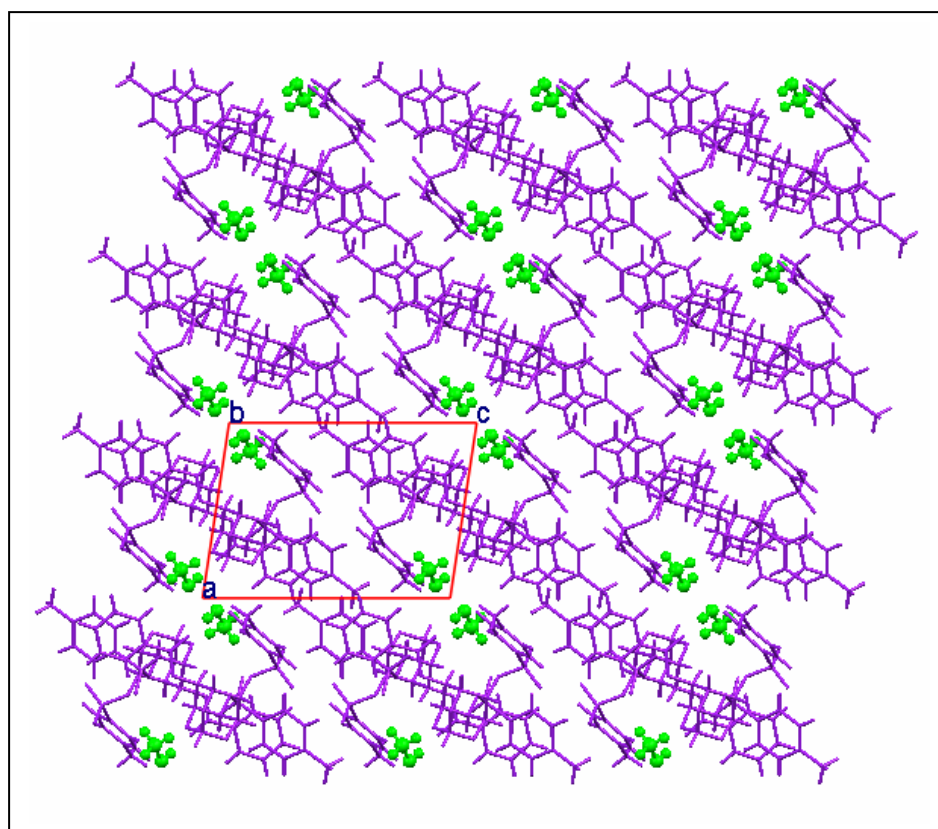
(c)

FIGURE B3.5. Crystal structure of toluene containing crystals, **B3.35** (a) structure of one molecule (toluene is disordered over two positions); (b) packing of molecules; (c) intermolecular interactions.

Figure B3.5 shows the structure of the toluene inclusion complex **B3.35** which has two independent molecules in the asymmetric unit. The molecules of **B1.11** form centrosymmetric dimers via two C-H...O interactions (C7-H7...O10 and C6-H6...O1) along the c-axis. These dimers are linked to other dimers along b-axis through centrosymmetric C13-H13...O3 contacts thereby creating voids. These voids accommodate toluene molecules which are disordered over two positions. The occupancy of toluene in **B3.35** crystals is 0.2. Elemental analysis data could not be obtained as **B3.35** crystals were unstable. The toluene molecules which occupy the channels formed by **B1.11** molecules do not make any significant non-covalent interactions with the host molecules.



(a)



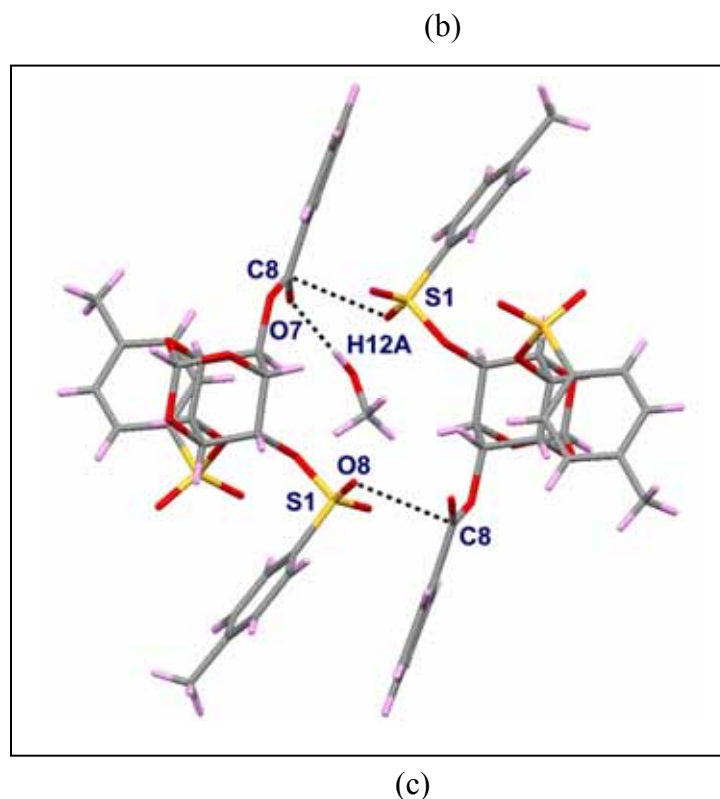
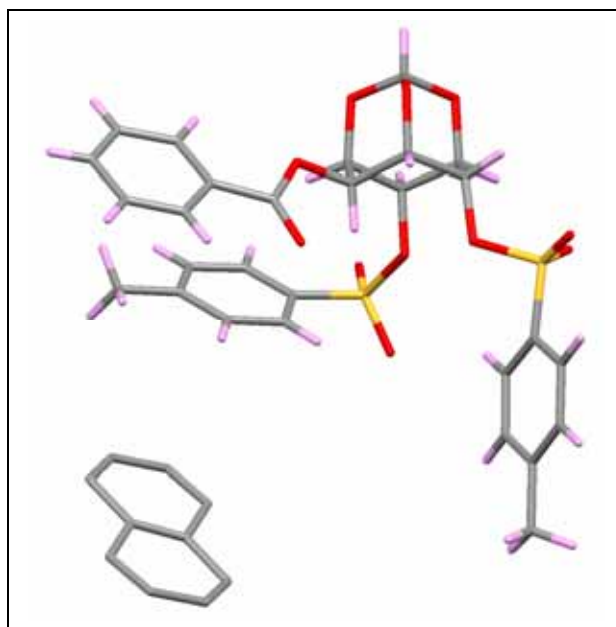


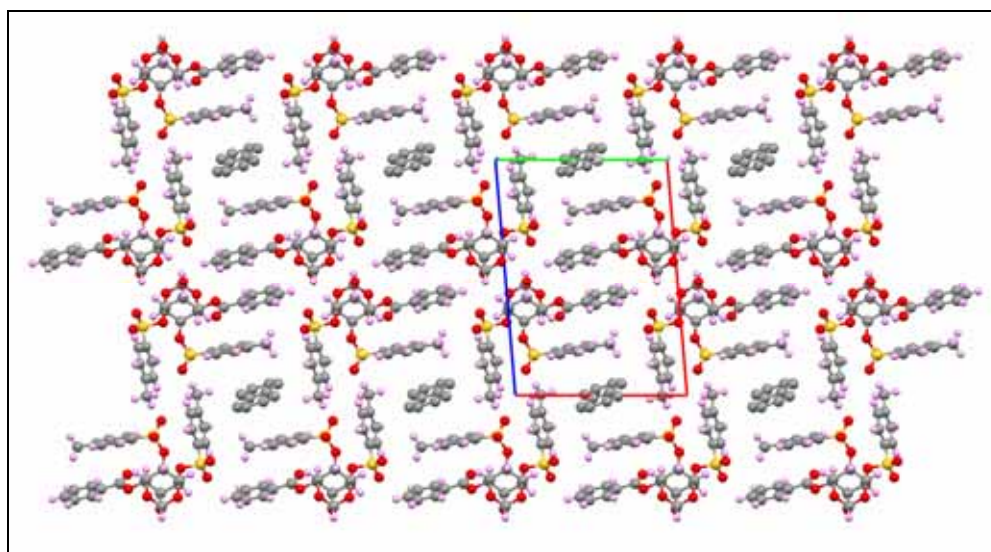
FIGURE B3.6. Crystal structure of methanol containing crystals, **B3.36** (a) structure of one molecule; (b) packing of molecules; (c) intermolecular interactions.

Figure B3.6 shows the structure of the methanol inclusion complex **B3.36**. There are two independent molecules of **B1.11** in the asymmetric unit. The molecules form centrosymmetric dimers via S1O8...C8O7 interactions along the a-axis. The methanol molecule in the crystal of **B3.36** forms hydrogen bond with the oxygen of the benzoate carbonyl group (O-H12A...O7). The occupancy of methanol in crystals of **B3.36** is 1.0. Elemental analysis could not be obtained as the crystals were unstable. The loss of weight in crystals of **B3.36** in thermogravimetric analysis was 5.9%. This corresponds to a ratio of 1:1 between **B1.11** and methanol in crystals of **B3.36**. The tosyl group (in crystals of **B3.36**) at C6-O- position shows a major conformational difference as compared to the toluene adduct. In toluene solvated crystals of **B3.35**, tosyl group at C6-O- position points

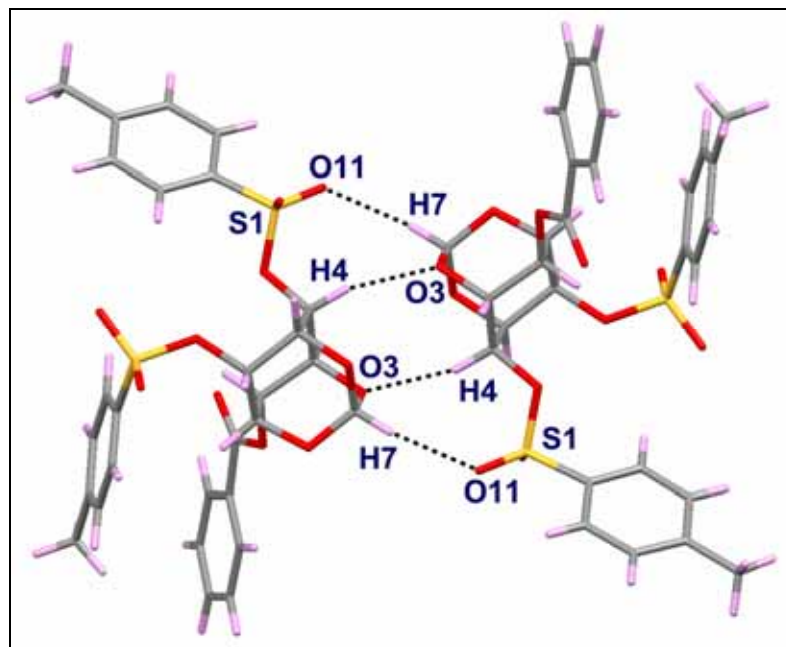
downwards (Figure B3.5(a)) whereas in methanol solvate crystals **B3.36** the same tosyl group is pointing upwards. Packing of molecules in crystals of **B3.35** and **B3.36** containing toluene and methanol respectively, show significant differences in organization of **B1.11** molecules.



(a)



(b)



(c)

FIGURE B3.7. Crystal structure of naphthalene containing crystals, **B3.37** (a) structure of one molecule; (b) packing of molecules; (c) intermolecular interactions.

Figure B3.7 shows the structure of the naphthalene inclusion complex **B3.37**. There are two independent molecules of **B1.11** in the asymmetric unit. These molecules form centrosymmetric dimers via two non-covalent interactions ($C4H4 \dots O3$ and $S1O11 \dots H7C7$) along the b-axis. Due to these interactions orthoformate groups from two adjacent molecules point towards each other in head to head fashion while the tosyl groups point away from each other thereby creating voids along the b-axis. These voids are capable of trapping naphthalene molecules without any significant non-covalent interaction with the host molecules. The occupancy of naphthalene in crystals of **B3.37** is 0.5. Conformation of **B1.11** molecules in its co-crystal with naphthalene (**B3.37**) was similar to that found in co-crystals with toluene (**B3.35**).

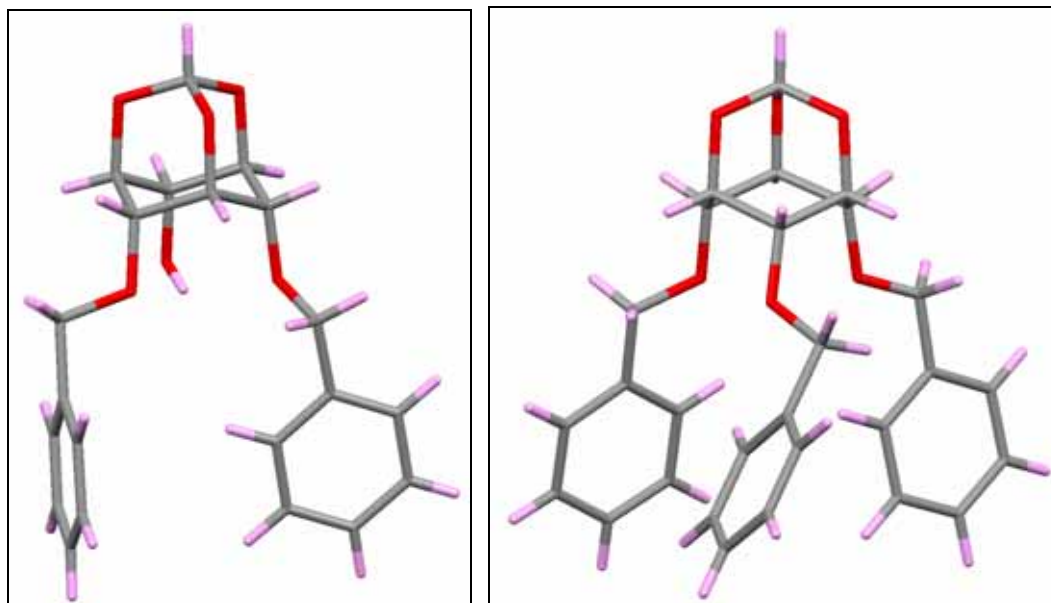
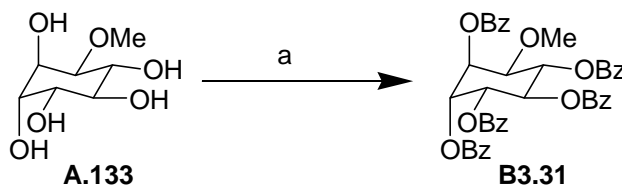


FIGURE B3.8. X-ray crystal structures of **B3.26** and **B3.27**.

The *scyllo*-inositol derivatives **B3.26** and **B3.27** did not show any solvent inclusion property. For crystallization details see Table B3.8 in the experimental section, page 281.

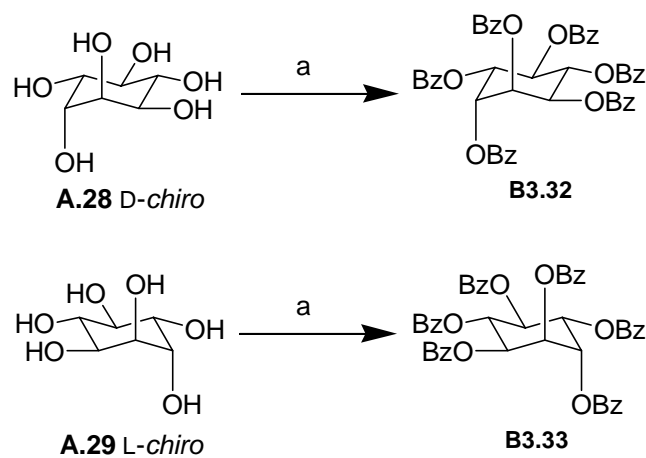
Quebrachitol penta benzoate²⁶ (**B3.31**) was prepared (scheme B3.2) from quebrachitol (**A.133**) using benzoyl chloride and pyridine. It was obtained as a glassy solid and our attempts to crystallize it from various solvents failed. For crystallization details see Table B3.14 in the experimental section, page 287.



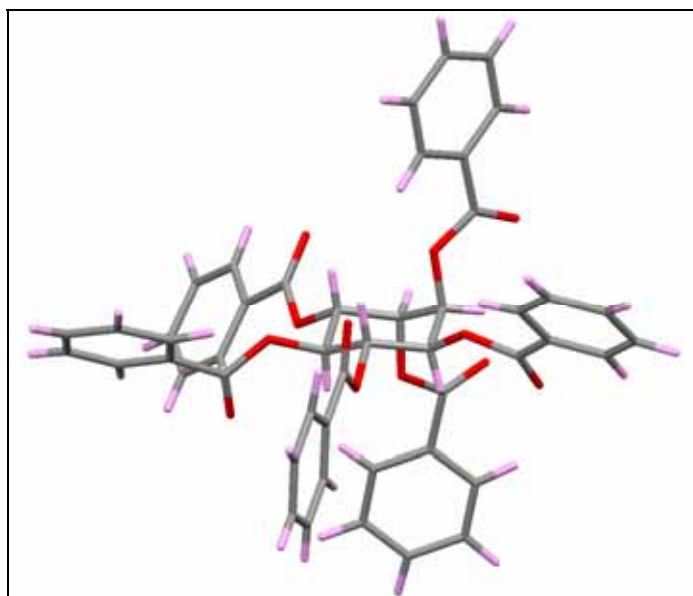
SCHEME B3.2. Reagents and conditions: (a) pyridine, BzCl, DMAP, rt, 36 h. 92%.

To study structural and solvent inclusion properties of *chiro*-inositol, hexabenzoates²⁷ both D- and L-*chiro*-inositols (**A.28** and **A.29**) were benzoylated to obtain the corresponding hexabenzoates **B3.32** and **B3.33**. Both the hexabenzoates gave

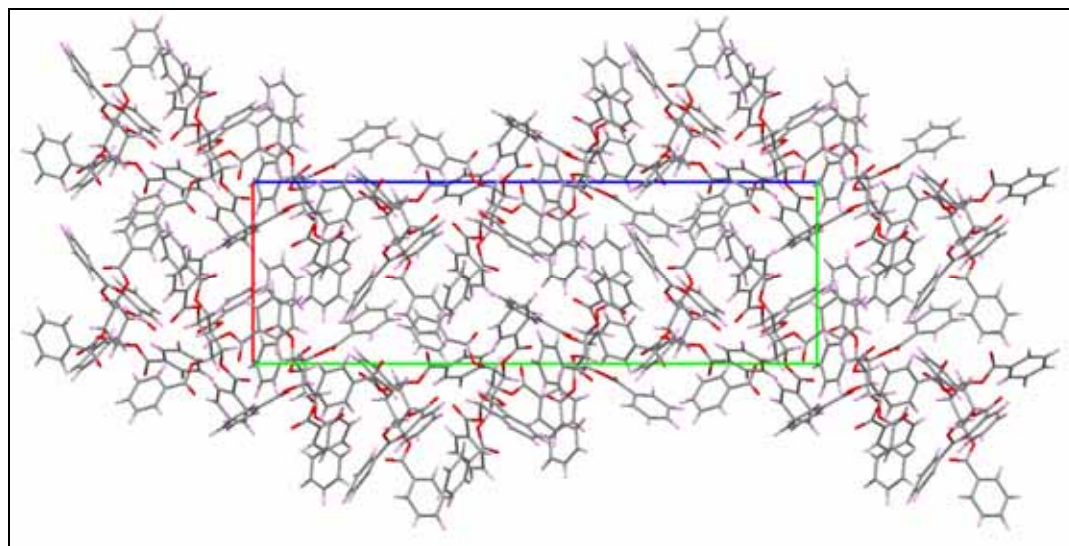
good quality crystals from acetonitrile as well as from chloroform - light petroleum mixture; most other solvents gave amorphous solids. But neither of these hexabenzoates showed solvent inclusion or polymorphism. For crystallization details see Table B3.11 in the experimental section, page 284.



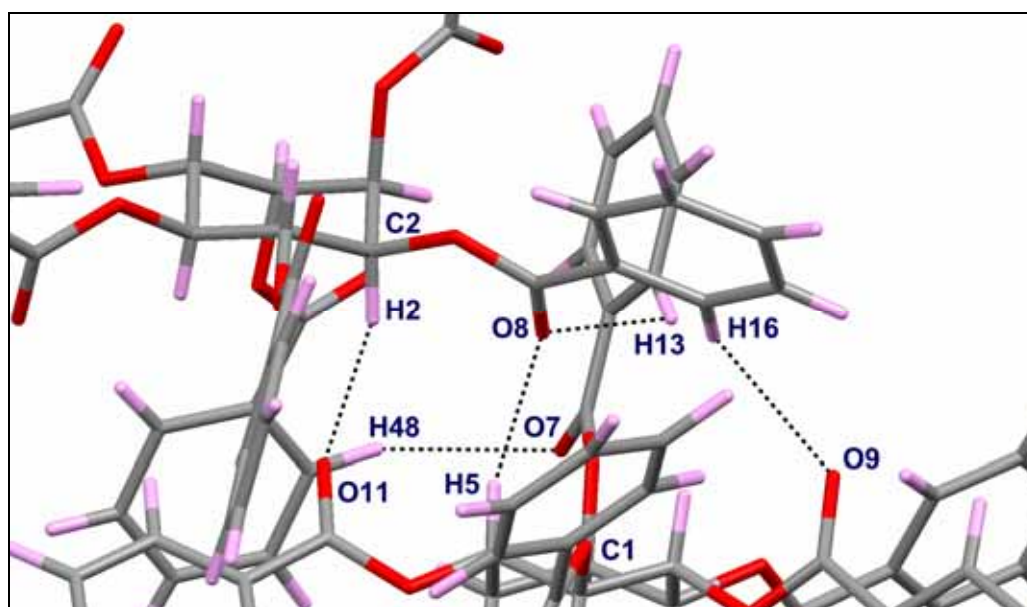
SCHEME B3.3. Reagents and conditions: (a) pyridine, benzoyl chloride, DMAP, rt, 48 h. 70% (for **B3.32**), 88% (for **B3.33**).



(a)



(b)

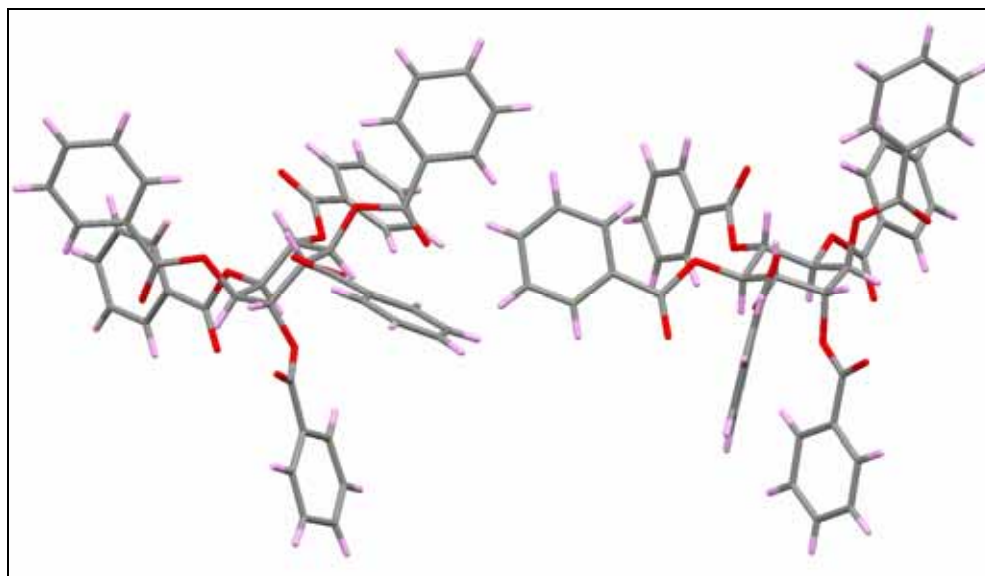


(c)

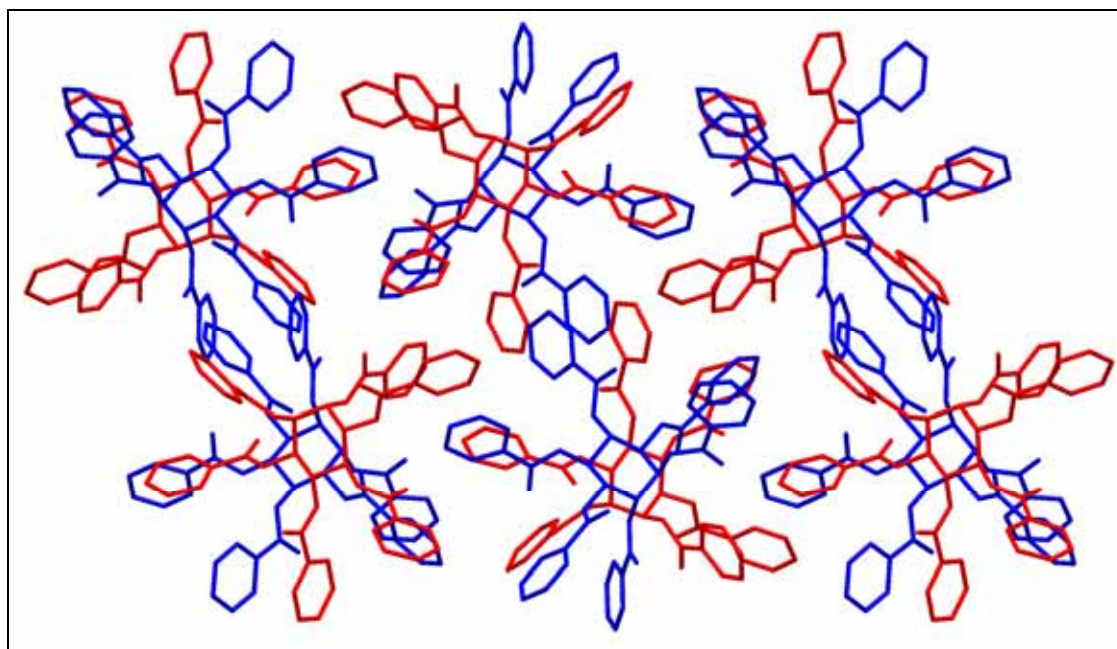
FIGURE B3.9. Crystal structure of **B3.33** (a) structure of one molecule; (b) packing of molecules; (c) intermolecular interactions.

Crystallization of a 1:1 mixture of D- and L-hexabenzoates **B3.32** and **B3.33** (racemic mixture) from acetonitrile deposited separate crystals of each enantiomer;

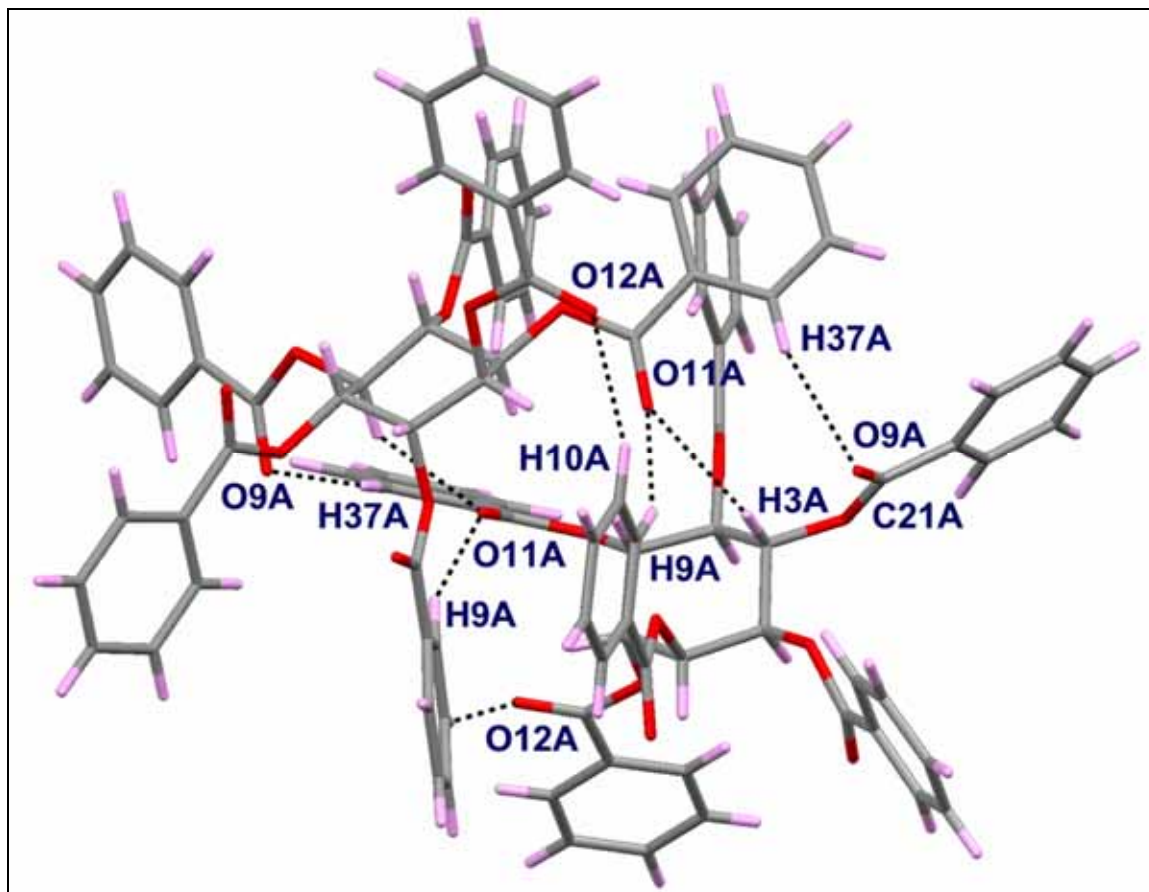
whereas crystallization of the same mixture from ethyl-acetate-petroleum ether mixture gave racemic crystals (**B3.38**).



(a)



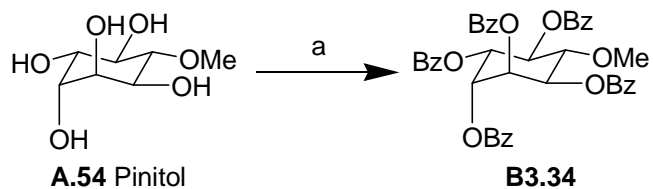
(b)



(c)

FIGURE B3.10. Crystal structure of racemic *chiro*-inositol hexabenzoate (**B3.38**) (a) one pair of enantiomers; (b) packing of molecules (down a-axis); (c) intermolecular interactions between two molecules of the same configuration.

The behavior of *chiro*-inositol hexabenzoate is in contrast to that of *myo*-inositol hexabenzoate which showed polymorphic²⁸ and pseudopolymorphic²⁰ (small molecule inclusion in crystals) behavior depending on the conditions of crystallization. Rapid crystallization of *myo*-inositol hexabenzoate yielded chiral crystals while slow crystallization yielded an achiral polymorph. Also the chiral crystals of *myo*-inositol hexabenzoate could be transformed to achiral crystals by heating.



SCHEME B3.4. *Reagents and conditions:* (a) pyridine, benzoyl chloride, DMAP, rt, 48 h. 39%.

Pinitol pentabenzoate²⁹ (**B3.34**) was prepared to study its crystal structure; however it was precipitated as glassy solid from all the solvents. For details see Table B3.15, page 288 in the experimental section.

3.3 Conclusions

Metal picrate extraction studies with simple inositol derivatives show that they complex lithium and sodium ions quite well. The construction of crown ether on the inositol ring appears to hinder the complexation of lithium ions but enhance the complexation of larger ions. The complexation of lithium ions by inositol derivatives is influenced considerably by the nature of the hydroxyl protecting groups. These results complement the differences in selectivity observed during the O-substitution reactions of inositol derivatives, with different reagents containing different alkali metal ions. Inositol derivatives also form complexes with small molecules in the solid state. Results available in the literature and from our laboratory suggest that *myo*-inositol derivatives form molecular complexes more frequently than derivatives of other isomers. Although, complexation ability of isomeric inositol derivatives (other than the *myo* isomer) have not been investigated as well as that of *myo*-inositol derivatives, preliminary results suggest that this property appears to be dependent on the relative disposition of the (protected) hydroxyl groups.

3.4 Experimental Section:

General: General methods and single crystal X-ray diffraction analysis are as mentioned in chapter 1, page 100. Compounds **A.147**, **A.148**,³⁰ **A.150**,³¹ **A.151**,⁹ **A.152**,⁶ **A.156**,⁶ **A.159**,⁷ **A.161**,⁷ **A.164**,⁷ **A.165**,⁷ **A.185**,³² **B1.3**,³³ **B1.4**,³³ **B1.8**,³⁴ **B1.11**,³⁵ **B1.21**,³⁶ **B1.26**,³⁶ **B1.30**,^{36,37} **B2.14**,³⁸ **B2.16**,³⁶ **B3.19**,³⁹ **B3.20**,⁸ **B3.21**,⁸ **B3.22**,³⁹ **B3.23**,⁶ **B3.24**,⁹ **B3.25**,⁹ **B3.28**,⁹ **B3.29**,⁴⁰ **B3.31**,²⁶ **B3.32**,²⁷ **B3.33**,²⁷ and **B3.34**,²⁹ were prepared as reported in the literature. Preparation of **B2.7**,³⁶ was presented in previous the chapter (Scheme B2.1).

2,4-di-O-benzyl-scylo-inositol 1,3,5 orthoformate (B3.26) and 2,4,6-tri-O-benzyl-scylo-inositol 1,3,5 orthoformate (B3.27): *scylo*-inositol 1,3,5 orthoformate (**A.38**,³⁸ 0.555 g, 2.92 mmol), sodium hydride (0.256 g, 6.4 mmol) and dry DMF (4 mL) were stirred at 0-5°C under nitrogen atmosphere for a few minutes. Then benzyl bromide (0.76 mL, 6.42 mmol) was added drop-wise. The reaction mixture was allowed to come to room temperature and stirred for further 30 min. The reaction was quenched by adding methanol (0.5 mL); DMF was removed under reduced pressure to get a solid. This solid was suspended in dichloromethane (40 mL), washed with water (10 mL × 3) followed by brine and the organic layer was dried over anhydrous sodium sulphate. The solvent was removed under reduced pressure; the residue was purified by column chromatography (eluent 10% ethyl acetate in light petroleum) to get the dibenzyl ether **B3.26**,⁴¹ (0.4675 g, 43 %) mp. 95-96 °C (lit. mp. 98-99 °C) and the tribenzyl ether **B3.27** (0.288 g, 21 %) as a solid.

Data for **B3.27**:

m.p: 111-112 °C (dichloromethane: petroleum ether).

¹H NMR (CDCl₃, 200 MHz): δ = 4.34 (dd, $J_1 = 4.4$ Hz, $J_2 = 2.8$ Hz, 3H; Ins-H), 4.55 (dd, $J_1 = 4.4$ Hz, $J_2 = 2.8$ Hz, 3H; Ins-H), 4.63 (s, 6H; CH₂Ph), 5.52 (s, 1H; HCO₃), 7.07-7.25 (m, 15H; Ar-H).

¹³C NMR (CDCl₃, 50.3 MHz): δ = 68.59 (Ins-C), 71.24 (CH₂), 72.51 (Ins-C), 103.09 (HCO₃), 127.38 (Ar-C), 127.77 (Ar-C), 128.09 (Ar-C), 137.84 (Ar-C).

Elemental Analysis: Anal. Calcd. for C₂₈H₂₈O₆ (460.53); C, 73.02; H, 6.12. Found: C, 72.73; H, 6.38.

General procedure for crystallization.

Procedure A. The inositol derivative was dissolved in a required warm solvent and the solution was kept in the crystallizing chamber, at ambient temperature. The solvent was allowed to evaporate slowly till the crystals appeared in the conical flask (generally after a few days).

Procedure B. The inositol derivative was dissolved in a mixture of two solvents and the solution was kept in the crystallizing chamber, at ambient temperature. The solvent was allowed to evaporate slowly till the crystals appeared in the conical flask (generally after a few days).

Procedure C. The inositol derivative was dissolved in a warm solvent and the solution was kept in the crystallizing chamber. Vapors of a different solvent (usually light petroleum) was allowed to diffuse into the solution of the inositol derivative at ambient temperature till crystals were formed.

Co-crystals of 2-O-benzoyl-4,6-di-O-tosyl myo-inositol orthoformate and toluene (B3.35). The ditosylate **B1.11** (10 mg) was crystallized from toluene (0.5 mL) according to procedure A, to get **B3.35** as needle shaped crystals (mp. 102-106 °C).

Co-crystals of 2-*O*-benzoyl-4,6-di-*O*-tosyl *myo*-inositol orthoformate and methanol (B3.36). **B1.11** (12 mg) was crystallized from methanol (0.5 mL) according to procedure A, to get **B3.36** as plate like crystals (mp. 63-66 °C).

Co-crystals of 2-*O*-benzoyl-4,6-di-*O*-tosyl *myo*-inositol orthoformate and naphthalene (B3.37). **B1.11** (20 mg) and naphthalene (4 mg) was crystallized from *p*-xylene (1 mL) according to procedure A, to get **B3.37** as plate like crystals (mp. 100-107 °C). **Elemental Analysis:** Anal. Calcd. for C₂₈H₂₆O₁₁S₂·0.45 C₁₀H₈ (661.23): C, 59.03; H, 4.51; S, 9.69. Found: C, 58.76; H, 4.24; S, 9.73.

TABLE B3.4: Crystallization of 2-*O*-benzoyl-4,6-di-*O*-tosyl *myo*-inositol orthoformate (**B1.11**) from different solvents.

Sr. No.	Conditions	Procedure	Result
1	Toluene	A	Co-crystals with toluene
2	Methanol	A	Co-crystals with methanol
3	Xylene	A	Co-crystals with naphthalene
4	Xylene + naphthalene (1 eq.)	A	Co-crystals with naphthalene
5	Benzene	A	Thin crystals ^a
6	DCM	A	Amorphous solid
7	Chloroform	A	Thin crystals ^a
8	Ethyl acetate	A	Crystals ^a
9	Nitromethane	A	Amorphous solid
10	Acetone	A	Amorphous solid

^a Not suitable for X-ray diffraction analysis.

Table B3.5: Crystal data for co-crystals of 2-*O*-benzoyl-4,6-di-*O*-tosyl *myo*-inositol orthoformate with toluene (**B3.35**).

Identification code	B3.35 (crystallized from toluene)
Empirical formula	C ₂₈ H ₂₆ O ₁₁ S ₂ · 0.2 C ₇ H ₈
Formula weight	614.62
Temperature	293(2) K
Wavelength	0.71073 Å
Crystal system, space group	Triclinic, P-1
Unit cell dimensions	a = 6.4485(10) Å α = 83.386(2)° b = 13.2459(19) Å β = 86.182(3)° c = 18.193(3) Å γ = 76.696(2)°
Volume	1500.9(4) Å ³
Z, Calculated density	2, 1.360 Mg/m ³
Absorption coefficient	0.236 mm ⁻¹
F(000)	640
Crystal size	1.06 x 0.11 x 0.08 mm
θ range for data collection	3.57 to 25.00°
Limiting indices	-7 ≤ h ≤ 7, -15 ≤ k ≤ 15, -21 ≤ l ≤ 20
Reflections collected / unique	18037 / 5262 [R(int) = 0.0382]
Completeness to θ = 25.00°	99.2 %
Absorption correction	Semi-empirical from equivalents
Max. and min. transmission	0.9818 and 0.7880
Refinement method	Full-matrix least-squares on F ²
Data / restraints / parameters	5262 / 34 / 392
Goodness-of-fit on F ²	1.111
Final R indices [I > 2σ (I)]	R1 = 0.0697, wR2 = 0.1936
R indices (all data)	R1 = 0.0896, wR2 = 0.2050
Largest diff. peak and hole (ρ _{max} & ρ _{min})	0.948 and -0.358 e. Å ⁻³

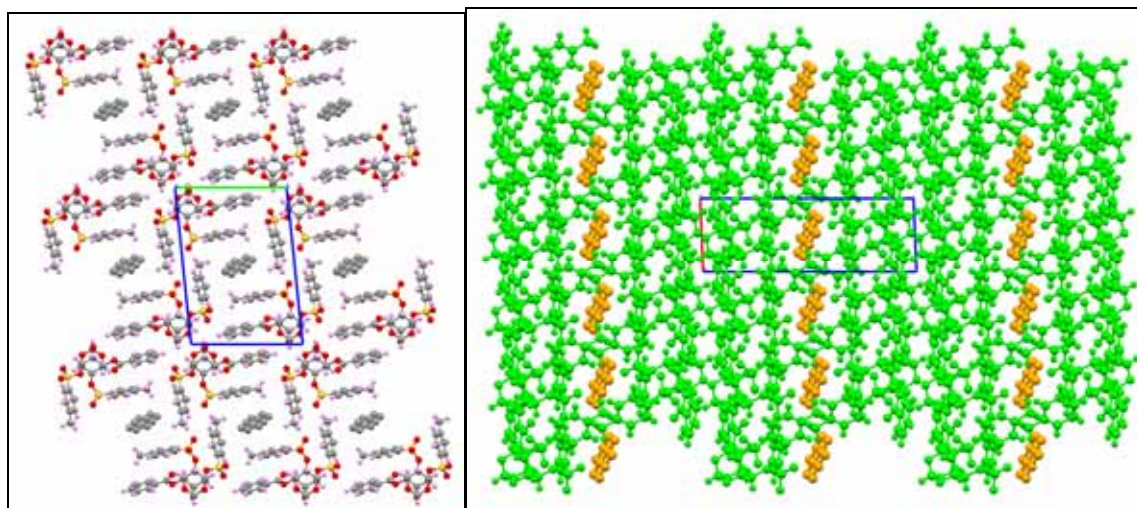
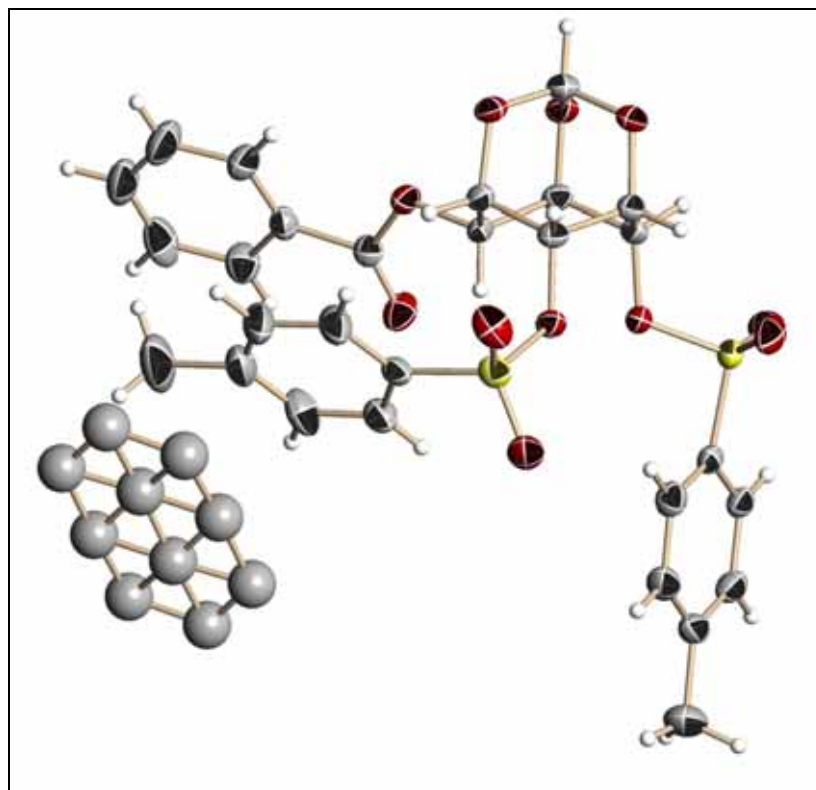


FIGURE B3.11. ORTEP, and packing diagram down a- and b-axis in crystals of **B3.35**.

Table B3.6: Crystal data for co-crystals of 2-*O*-benzoyl-4,6-di-*O*-tosyl *myo*-inositol orthoformate and methanol (**B3.36**).

Identification code	B3.36 (crystals from MeOH)
Empirical formula	C ₂₈ H ₂₆ O ₁₁ S ₂ · CH ₄ O
Formula weight	634.65
Temperature	297(2) K
Wavelength	0.71073 Å
Crystal system, space group	Triclinic, P-1
Unit cell dimensions	a = 10.293(12) Å α = 90.84(3)° b = 12.050(14) Å β = 97.82(2)° c = 13.537(19) Å γ = 110.60(3)°
Volume	1553(3) Å ³
Z, Calculated density	2, 1.357 Mg/m ³
Absorption coefficient	0.233 mm ⁻¹
F(000)	664
Crystal size	0.56 x 0.21 x 0.14 mm
θ range for data collection	1.52 to 25.00°
Limiting indices	-12 ≤ h ≤ 12, -14 ≤ k ≤ 13, -16 ≤ l ≤ 16
Reflections collected / unique	9449 / 5396 [R(int) = 0.0427]
Completeness to θ = 25.00°	98.6 %
Absorption correction	Semi-empirical from equivalents
Max. and min. transmission	0.9673 and 0.8814
Refinement method	Full-matrix least-squares on F ²
Data / restraints / parameters	5396 / 0 / 392
Goodness-of-fit on F ²	1.024
Final R indices [I > 2σ (I)]	R1 = 0.0635, wR2 = 0.1415
R indices (all data)	R1 = 0.1037, wR2 = 0.1616
Largest diff. peak and hole (ρ _{max} & ρ _{min})	0.298 and -0.240 e. Å ⁻³

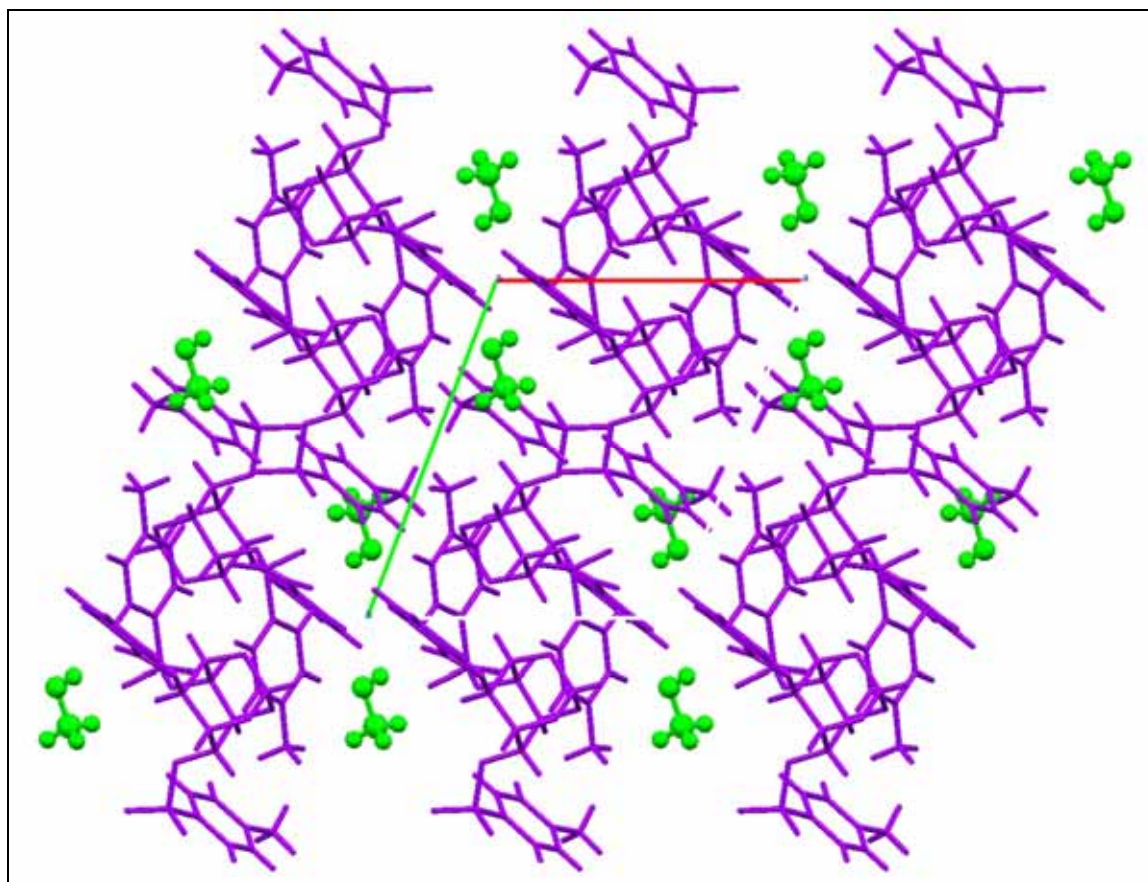
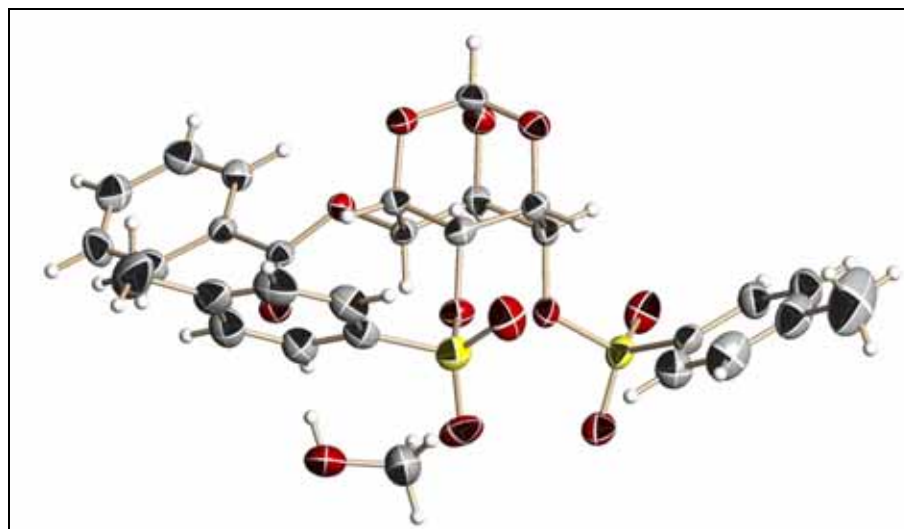


FIGURE B3.12. ORTEP, and packing diagram down c-axis in crystals of **B3.36**.

Table B3.7: Crystal data for co-crystals of 2-*O*-benzoyl-4,6-di-*O*-tosyl *myo*-inositol orthoformate and naphthalene (**B3.37**).

Identification code	B3.37 (crystals from <i>p</i> -xylene)
Empirical formula	C ₂₈ H ₂₆ O ₁₁ S ₂ ·0.5 C ₁₀ H ₈
Formula weight	632.63
Temperature	133(2) K
Wavelength	0.71073 Å
Crystal system, space group	Triclinic, P-1
Unit cell dimensions	a = 6.421(2) Å α = 84.400(6)° b = 13.242(5) Å β = 85.802(6)° c = 18.038(7) Å γ = 77.060(6)°
Volume	1485.5(10) Å ³
Z, Calculated density	2, 1.414 Mg/m ³
Absorption coefficient	0.241 mm ⁻¹
F(000)	658
Crystal size	0.44 x 0.22 x 0.05 mm
θ range for data collection	3.17 to 25.00°
Limiting indices	-7 ≤ h ≤ 7, -15 ≤ k ≤ 15, -21 ≤ l ≤ 21
Reflections collected / unique	14000 / 5197 [R(int) = 0.0467]
Completeness to θ = 25.00°	99.2 %
Absorption correction	Semi-empirical from equivalents
Max. and min. transmission	0.9871 and 0.9015
Refinement method	Full-matrix least-squares on F ²
Data / restraints / parameters	5197 / 5 / 392
Goodness-of-fit on F ²	1.159
Final R indices [I > 2σ (I)]	R1 = 0.0777, wR2 = 0.1758
R indices (all data)	R1 = 0.0987, wR2 = 0.1859
Largest diff. peak and hole (ρ _{max} & ρ _{min})	0.740 and -0.392 e. Å ⁻³

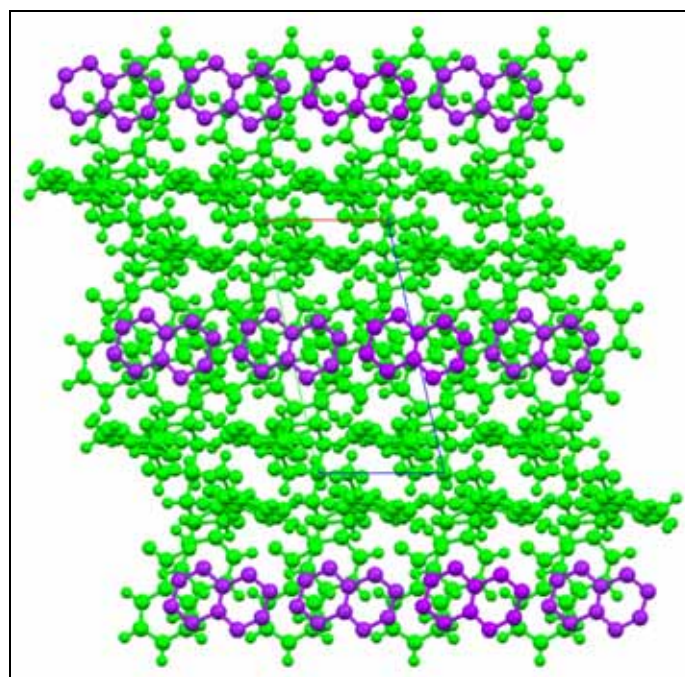
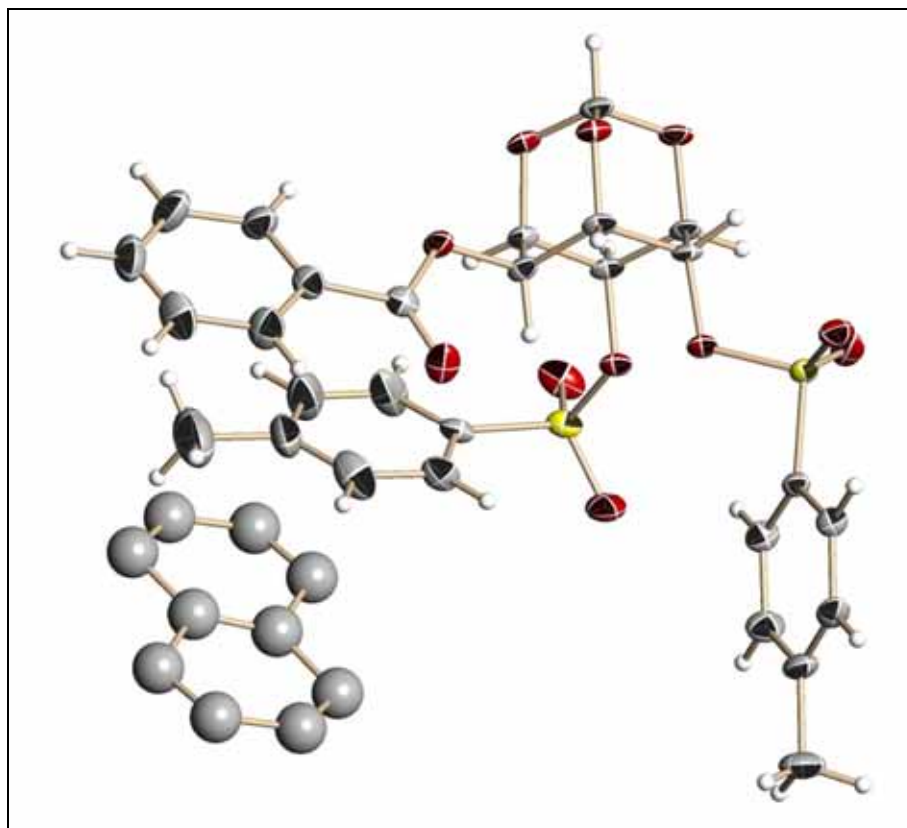


FIGURE B3.13. ORTEP, and packing diagram down c-axis of **B3.37**.

TABLE B3.8: Crystallization details of *scyllo*-inositol orthoformate di- and tri-benzyl ethers (**B3.26** and **B3.27**).

Sr. No.	Conditions	Procedure	Result
1	DCM	A	Amorphous solid
2	Methanol	A	Thin crystals ^b
3	Ethyl acetate + light petroleum ^a (1:1)	B	Thin crystals ^b
4	DCM + light petroleum ^a (1:1)	B	Crystals
5	Chloroform	A	Thin crystals ^b

^a Boiling range 60-80 °C. ^b Not suitable for X-ray diffraction analysis.

Table B3.9: Crystal data for *scyllo*-inositol orthoformate di-benzyl ether (**B3.26**).

Identification code	B3.26 crystals from DCM: light petroleum
Empirical formula	C ₂₁ H ₂₂ O ₆
Formula weight	370.39
Temperature	297(2) K
Wavelength	0.71073 Å
Crystal system, space group	Orthorhombic, Pbca
Unit cell dimensions	a = 8.2577(14) Å α = 90° b = 12.186(2) Å β = 90° c = 37.404(7) Å γ = 90°
Volume	3763.8(11) Å ³
Z, Calculated density	8, 1.307 Mg/m ³
Absorption coefficient	0.096 mm ⁻¹
F(000)	1568
Crystal size	0.74 x 0.33 x 0.09 mm
θ range for data collection	2.18 to 25.00°
Limiting indices	-9 ≤ h ≤ 9, -14 ≤ k ≤ 14, -44 ≤ l ≤ 44
Reflections collected / unique	25329 / 3323 [R(int) = 0.0385]
Completeness to θ = 25.00°	100.0 %
Absorption correction	Semi-empirical from equivalents
Max. and min. transmission	0.9918 and 0.9326
Refinement method	Full-matrix least-squares on F ²
Data / restraints / parameters	3323 / 0 / 245
Goodness-of-fit on F ²	1.050
Final R indices [I > 2σ (I)]	R1 = 0.0598, wR2 = 0.1414
R indices (all data)	R1 = 0.0794, wR2 = 0.1544
Largest diff. peak and hole (ρ _{max} & ρ _{min})	0.420 and -0.196 e. Å ⁻³

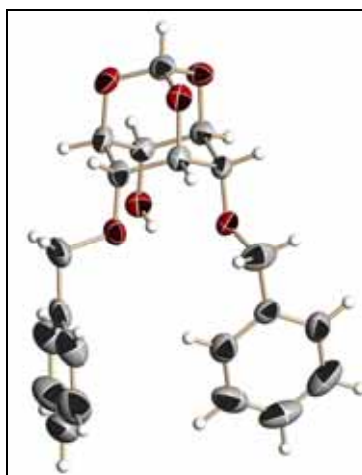
**FIGURE B3.14.** ORTEP diagram of **B3.26**.

Table B3.10: Crystal data for *scyllo*-inositol orthoformate tri-benzyl ether (**B3.27**).

Identification code	B3.27 crystals from DCM: light petroleum
Empirical formula	C ₂₈ H ₂₈ O ₆
Formula weight	460.50
Temperature	297(2) K
Wavelength	0.71073 Å
Crystal system, space group	Orthorhombic, Pccn
Unit cell dimensions	a = 16.827(3) Å α = 90° b = 37.365(7) Å β = 90° c = 7.5397(13) Å γ = 90°
Volume	4740.6(14) Å ³
Z, Calculated density	8, 1.290 Mg/m ³
Absorption coefficient	0.090 mm ⁻¹
F(000)	1952
Crystal size	0.62 x 0.25 x 0.13 mm
θ range for data collection	2.18 to 25.00°
Limiting indices	-20 ≤ h ≤ 20, -43 ≤ k ≤ 44, -8 ≤ l ≤ 8
Reflections collected / unique	42163 / 4164 [R(int) = 0.0566]
Completeness to θ = 25.00°	99.9 %
Absorption correction	Semi-empirical from equivalents
Max. and min. transmission	0.9884 and 0.9462
Refinement method	Full-matrix least-squares on F ²
Data / restraints / parameters	4164 / 0 / 307
Goodness-of-fit on F ²	1.055
Final R indices [I > 2σ (I)]	R1 = 0.0557, wR2 = 0.1234
R indices (all data)	R1 = 0.0762, wR2 = 0.1362
Largest diff. peak and hole (ρ _{max} & ρ _{min})	0.362 and -0.404 e. Å ⁻³

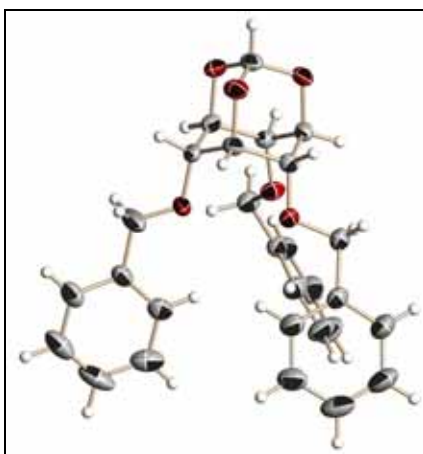
**FIGURE B3.15.** ORTEP diagram of **B3.26**.

TABLE B3.11: Crystallization details of D- and L-*chiro*-inositol hexabenzoates (**B3.32** and **B3.33**).

Sr. No.	Conditions	Procedure	Result
	B3.32		
1	Ethyl acetate	A	Amorphous solid
2	DCM + light petroleum ^a	C	Amorphous solid
3	Chloroform	A	Amorphous solid
4	Toluene	A	Amorphous solid
5	Acetonitrile	A	Crystals
6	DCM	A	Amorphous solid
7	Chloroform + light petroleum ^b	C	Crystals
	B3.33		
8	Chloroform	A	Amorphous solid
9	Ethyl acetate + light petroleum ^a (1:1)	B	Crystals
10	Acetonitrile	A	Crystals
	1:1 mixture of B3.32 and B3.33		
11	Acetonitrile	A	Separate crystals of each enantiomer
12	Ethyl acetate + light petroleum ^a (1:1)	B	Racemic crystals

^a Boiling range 60-80 °C; ^b Boiling range 40-60 °C.

Table B3.12: Crystal data for *L-chiro*-inositol hexabenzoate (**B3.33**).

Identification code	B3.33 (crystallized from acetonitrile)
Empirical formula	C ₄₈ H ₃₆ O ₁₂
Formula weight	804.77
Temperature	133(2) K
Wavelength	0.71073 Å
Crystal system, space group	Monoclinic, P 65
Unit cell dimensions	a = 13.910(8) Å α = 90° b = 13.910(8) Å β = 90° c = 37.20(4) Å γ = 120°
Volume	6234(8) Å ³
Z, Calculated density	6, 1.286 Mg/m ³
Absorption coefficient	0.093 mm ⁻¹
F(000)	2520
Crystal size	0.78 x 0.21 x 0.18 mm
θ range for data collection	2.36 to 25.00°
Limiting indices	-16 ≤ h ≤ 16, -16 ≤ k ≤ 16, -43 ≤ l ≤ 44
Reflections collected / unique	35981 / 6863 [R(int) = 0.0681]
Completeness to θ = 25.00°	94.1 %
Absorption correction	Semi-empirical from equivalents
Max. and min. transmission	0.9835 and 0.9311
Refinement method	Full-matrix least-squares on F ²
Data / restraints / parameters	6863 / 1 / 661
Goodness-of-fit on F ²	1.045
Final R indices [I > 2σ (I)]	R1 = 0.0433, wR2 = 0.0914
R indices (all data)	R1 = 0.0537, wR2 = 0.0950

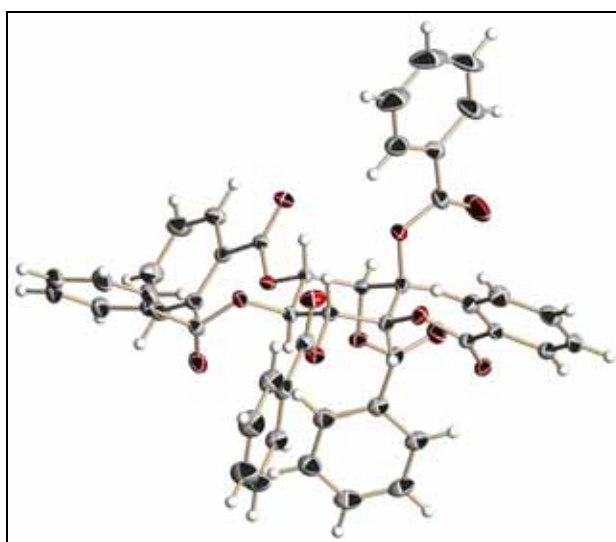
**FIGURE B3.16.** ORTEP diagram of **B3.33**

Table B3.13: Crystal data for racemic *chiro*-inositol hexabenzoate **B3.38**.

Identification code	B3.38 (crystals from ethyl-acetate-light petroleum)
Empirical formula	C ₄₈ H ₃₆ O ₁₂ .Unknown solvent
Formula weight	838.29
Temperature	293(2) K
Wavelength	0.71073 Å
Crystal system, space group	Monoclinic, C 2/c
Unit cell dimensions	a = 31.202(4) Å α = 90° b = 26.136(3) Å β = 109.126(3)° c = 23.270(3) Å γ = 90°
Volume	17929(4) Å ³
Z, Calculated density	16, 1.242 Mg/m ³
Absorption coefficient	0.090 mm ⁻¹
F(000)	6988
Crystal size	0.46 x 0.18 x 0.17 mm
θ range for data collection	1.04 to 25.00°
Limiting indices	-37 ≤ h ≤ 36, -31 ≤ k ≤ 16, -27 ≤ l ≤ 27
Reflections collected / unique	44735 / 15721 [R(int) = 0.0676]
Completeness to θ = 25.00°	99.5 %
Absorption correction	Semi-empirical from equivalents
Max. and min. transmission	0.9849 and 0.9599
Refinement method	Full-matrix least-squares on F ²
Data / restraints / parameters	15721 / 9 / 1117
Goodness-of-fit on F ²	1.015
Final R indices [I > 2σ (I)]	R1 = 0.0935, wR2 = 0.2433
R indices (all data)	R1 = 0.1656, wR2 = 0.2946
Largest diff. peak and hole (ρ _{max} & ρ _{min})	1.005 and -0.460 e. Å ⁻³

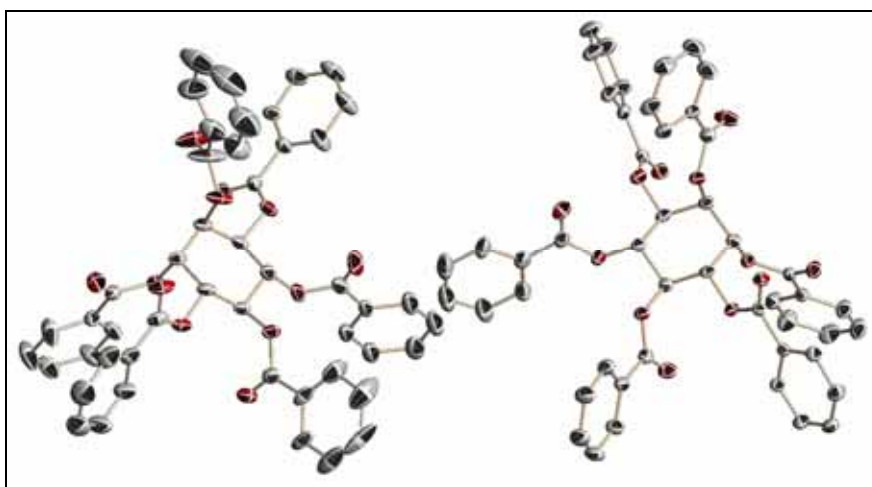
**FIGURE B3.17.** ORTEP diagram of **B3.38**

TABLE B3.14: Crystallization details of quebrachitol penta-benzoate (**B3.31**).

Sr. No.	Conditions	Procedure	Result
1	DCM + light petroleum	C	Glassy solid
2	Ethanol	A	Glassy solid
3	Methanol	A	Glassy solid
4	Toluene	A	Glassy solid
5	Carbontetrachloride	A	Glassy solid
6	Ethanol + drop of H ₂ O, rt.	B	Glassy solid
7	Ethanol + drop of H ₂ O, 0-5 °C	B	Glassy solid
8	Chloroform + light petroleum ^a (1:1)	B	Glassy solid
9	Chloroform + light petroleum ^b (1:1)	B	Glassy solid
10	Chloroform + Ethyl acetate	C	Glassy solid
11	CH ₃ CN + light petroleum ^a (1:1)	B	Glassy solid

^a Boiling range 60-80 °C; ^b Boiling range 40-60 °C.

TABLE B3.15: Crystallization details of pinitol penta benzoate (**B3.34**).

Sr. No.	Conditions	Procedure	Result
1	DCM + light petroleum ^a	C	Glassy solid
2	Ethyl acetate + light petroleum ^a	C	Glassy solid
3	Toluene	A	Glassy solid
4	Carbontetrachloride	A	Glassy solid
5	Chloroform + light petroleum ^a	C	Glassy solid
6	Acetonitrile + light petroleum ^a (1:1)	B	Glassy solid
7	Methanol	A	Glassy solid

^a Boiling range 60-80 °C.

3.5 References:

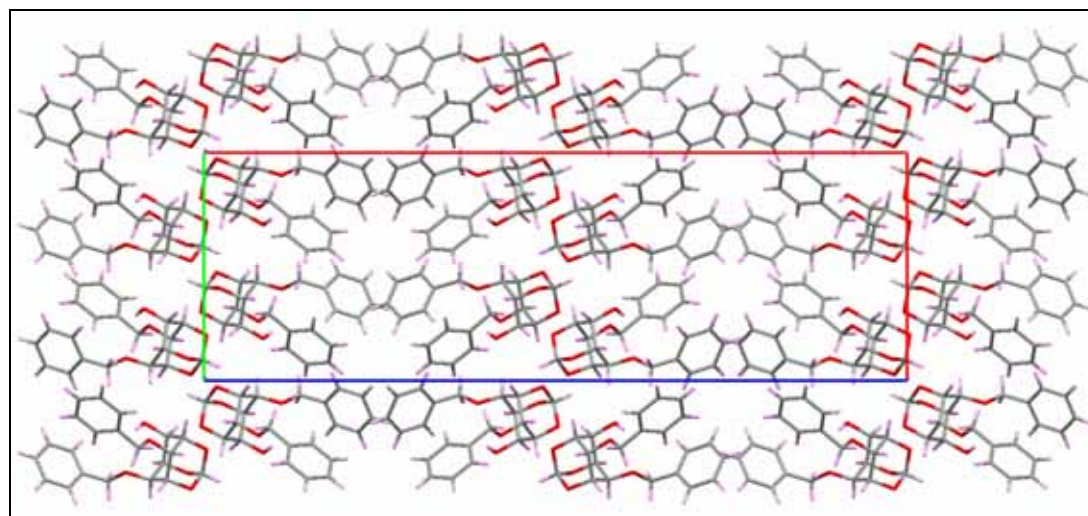
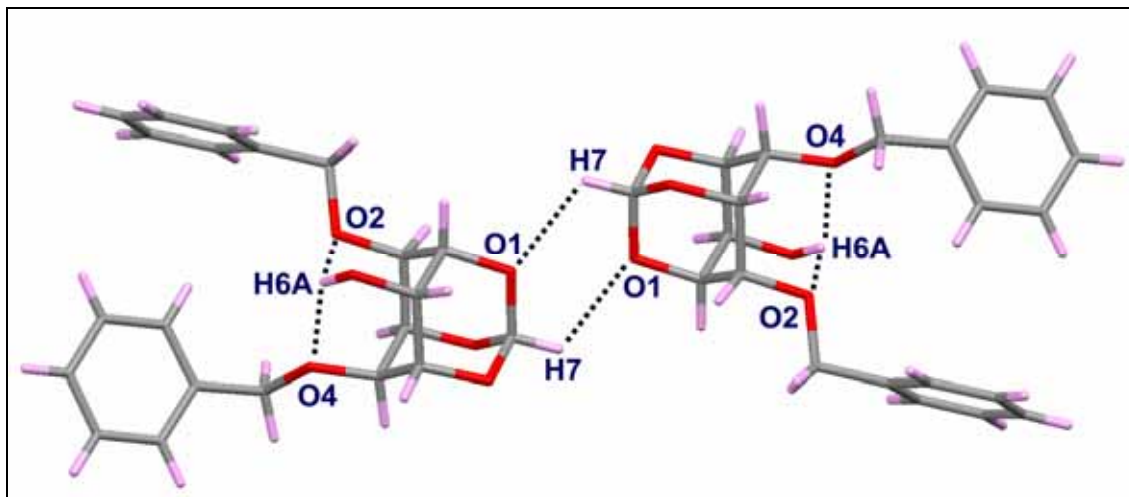
- 1 *Phosphoinositides: Chemistry, Biochemistry and Biomedical Applications*; Bruzik, K. S., Ed.; ACS Symposium Series 718; American Chemical Society: Washington DC, USA, **1999**.
- 2 Ferguson, M. A. J.; Williams, A. F. *Annu. Rev. Biochem.* **1988**, *57*, 285-320.
- 3 Billington, D. C. *The Inositol Phosphates. Chemical Synthesis and Biological Significance*; VCH: New York, NY, **1993**.
- 4 Potter, B. V. L.; Lampe, D. *Angew. Chem., Int. Ed. Engl.* **1995**, *34*, 1933-1972.
- 5 Sureshan, K. M.; Shashidhar, M. S.; Praveen, T.; Das, T. *Chem. Rev.* **2003**, *103*, 4477-4504.
- 6 Das, T.; Shashidhar, M. S. *Carbohydr. Res.* **1997**, *297*, 243-249.
- 7 Sureshan, K. M.; Shashidhar, M. S. *Tetrahedron Lett.* **2000**, *41*, 4185-4188.
- 8 Sureshan, K. M.; Shashidhar, M. S. *Tetrahedron Lett.* **2001**, *42*, 3037-3039.
- 9 Praveen, T.; Das, T.; Sureshan, K. M.; Shashidhar, M. S.; Samanta, U.; Pal, D.; Chakrabarti, P. *J. Chem. Soc., Perkin Trans 2* **2002**, 358-365.
- 10 Devaraj, S.; Shashidhar, M. S.; Dixit, S. S. *Tetrahedron* **2005**, *61*, 529-536.
- 11 Paul, S.; Gupta, V.; Gupta, R.; Loupy, A. *Tetrahedron Lett.* **2003**, *44*, 439-442.
- 12 Hünig, S.; Herberth, E. *Chem. Rev.* **2004**, *104*, 5535-5564.
- 13 Goldberg, I.; Bernstein, J. *Chem. Commun.* **2007**, 132-134.
- 14 Bučar, D-K.; Henry, R. F.; Lou, X.; Borchardt, T. B.; Zhang, G. G. *Z. Chem. Commun.* **2007**, 525-527.
- 15 Sreekanth, B. R.; Vishweshwar, P.; Vyas, K. *Chem. Commun.* **2007**, 2375-2377.

-
- 16 Chiavarino, B.; Crestoni, M. E.; Fornarini, S.; Lanucara, F.; Lemaire, J.; Maître, P. *Angew. Chem., Int. Ed.* **2007**, *46*, 1995-1998.
 - 17 De Rosa, M.; Arnold, D.; Medved', M. *Tetrahedron Lett.* **2007**, *48*, 3991-3994.
 - 18 Cram, D. J. *Angew. Chem., Int. Ed.* **1988**, *27*, 1009-1112.
 - 19 Tsubaki, K.; Tanima, D.; Nuruzzaman, M.; Kusumoto, T.; Fuji, K.; Kawabata, T. *J. Org. Chem.* **2005**, *70*, 4609-4616.
 - 20 Manoj, K.; Gonnade, R. G.; Bhadbhade, M. M.; Shashidhar, M. S. *Cryst. Growth Des.* **2006**, *6*, 1485-1492.
 - 21 Murali, C.; Shashidhar, M. S.; Gonnade, R. G.; Bhadbhade, M. M. *Eur. J. Org. Chem.* **2007**, 1153-1159.
 - 22 Sarmah, M. P.; Gonnade, R. G.; Shashidhar, M. S.; Bhadbhade, M. M. *Chem. Eur. J.* **2005**, *11*, 2103-2110.
 - 23 Dixit, S. S.; Shashidhar, M. S.; Devaraj, S. *Tetrahedron* **2006**, *62*, 4360-4363.
 - 24 Sureshan, K. M.; Shashidhar, M. S.; Gonnade, R. G.; Puranik, V. G.; Bhadbhade, M. M. *Chem. Commun.* **2001**, 881-882.
 - 25 Manoj, K.; Sureshan, K. M.; Gonnade, R. G.; Bhadbhade, M. M.; Shashidhar, M. S. *Cryst. Growth Des.* **2005**, *5*, 833-836.
 - 26 Angyal, S. J.; Odier, L. *Carbohydr. Res.* **1980**, *80*, 203-206.
 - 27 Lee, Y. J.; Lee, K.; Jung, S. I.; Jeon, H. B.; Kim, K. S. *Tetrahedron* **2005**, *61*, 1987-2001.
 - 28 Gonnade, R. G.; Bhadbhade, M. M.; Shashidhar, M. S. *Chem. Commun.* **2004**, 2530-2531.
 - 29 Ley, S. V.; Sternfeld, F. *Tetrahedron* **1989**, *45*, 3463-3476.

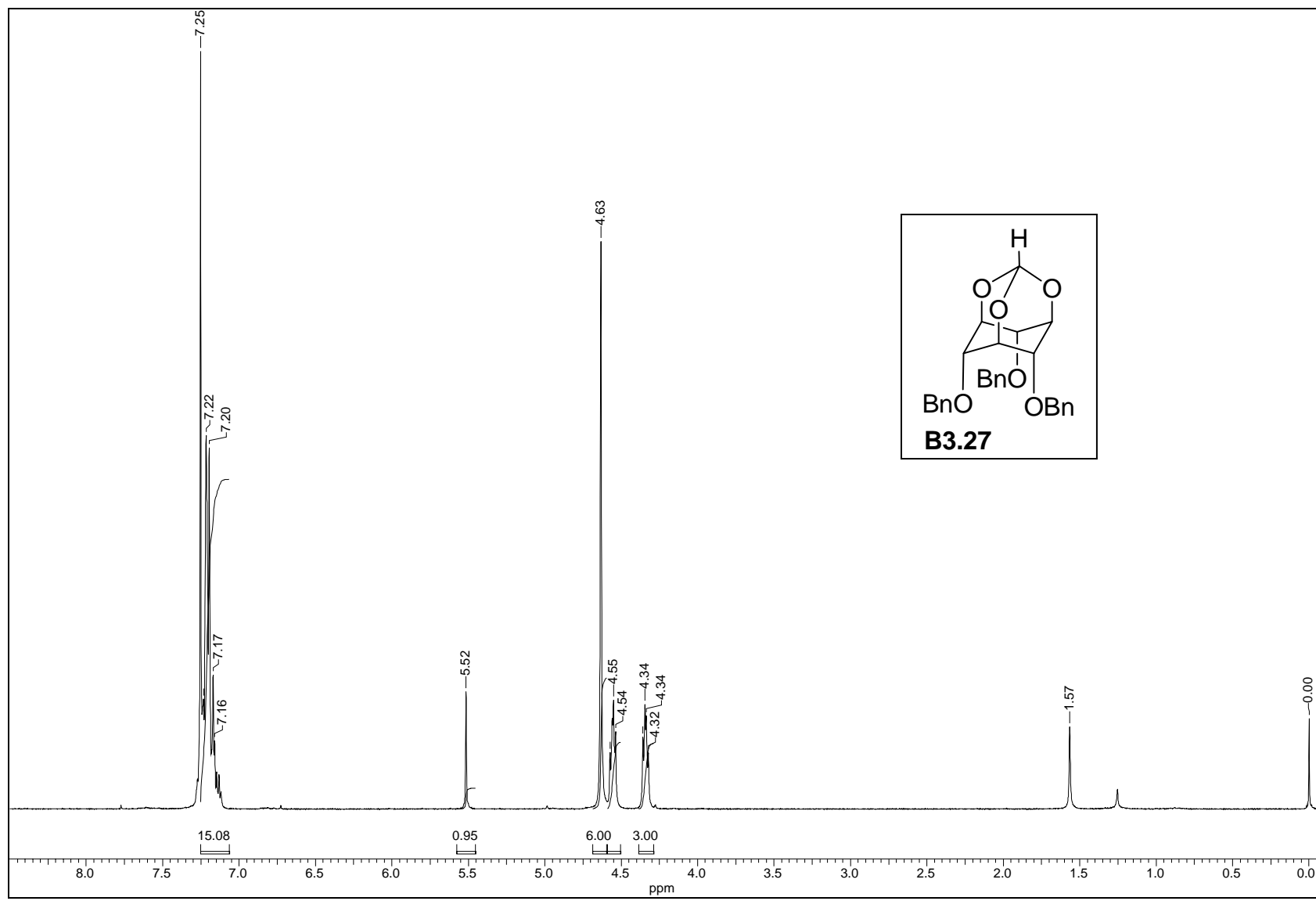
- 30 Sureshan, K. M.; Shashidhar M. S.; Praveen, T.; Gonnade, R. G.; Bhadbhade, M. M. *Carbohydr. Res.* **2002**, 337, 2399-2410.
- 31 Banerjee, T.; Shashidhar M. S. *Tetrahedron Lett.* **1994**, 35, 8053-8056.
- 32 Billington, D. C.; Baker, R.; Kulagowski, J. J.; Mawer, I. M.; Vacca, J. P.; deSolmes, S. J.; Huff, J. R. *J. Chem. Soc., Perkin Trans. I* **1989**, 1423-1429.
- 33 Gigg, J.; Gigg, R.; Payne, S.; Conant, S. *J. Chem. Soc., Perkin Trans. I* **1987**, 423-429.
- 34 Gigg, R.; Warren, C. D. *J. Chem. Soc.(C)*, **1969**, 2367-2371.
- 35 Sarmah, M. P. Ph.D. Thesis, *University of Pune*, **2005**.
- 36 Dixit, S. S.; Shashidhar M. S. *Tetrahedron* **2007**, Accepted.
- 37 Angyal, S. J.; Melrose, G. J. H. *J. Chem. Soc.* **1965**, 6494-6500.
- 38 Sarmah, M. P.; Shashidhar, M. S. *Carbohydr. Res.* **2003**, 338, 999-1001.
- 39 Sureshan K. M. Ph.D. Thesis, *University of Pune*, **2002**.
- 40 Stanacev, N. Z.; Kates, M. *J. Org. Chem.* **1961**, 26, 912-918.

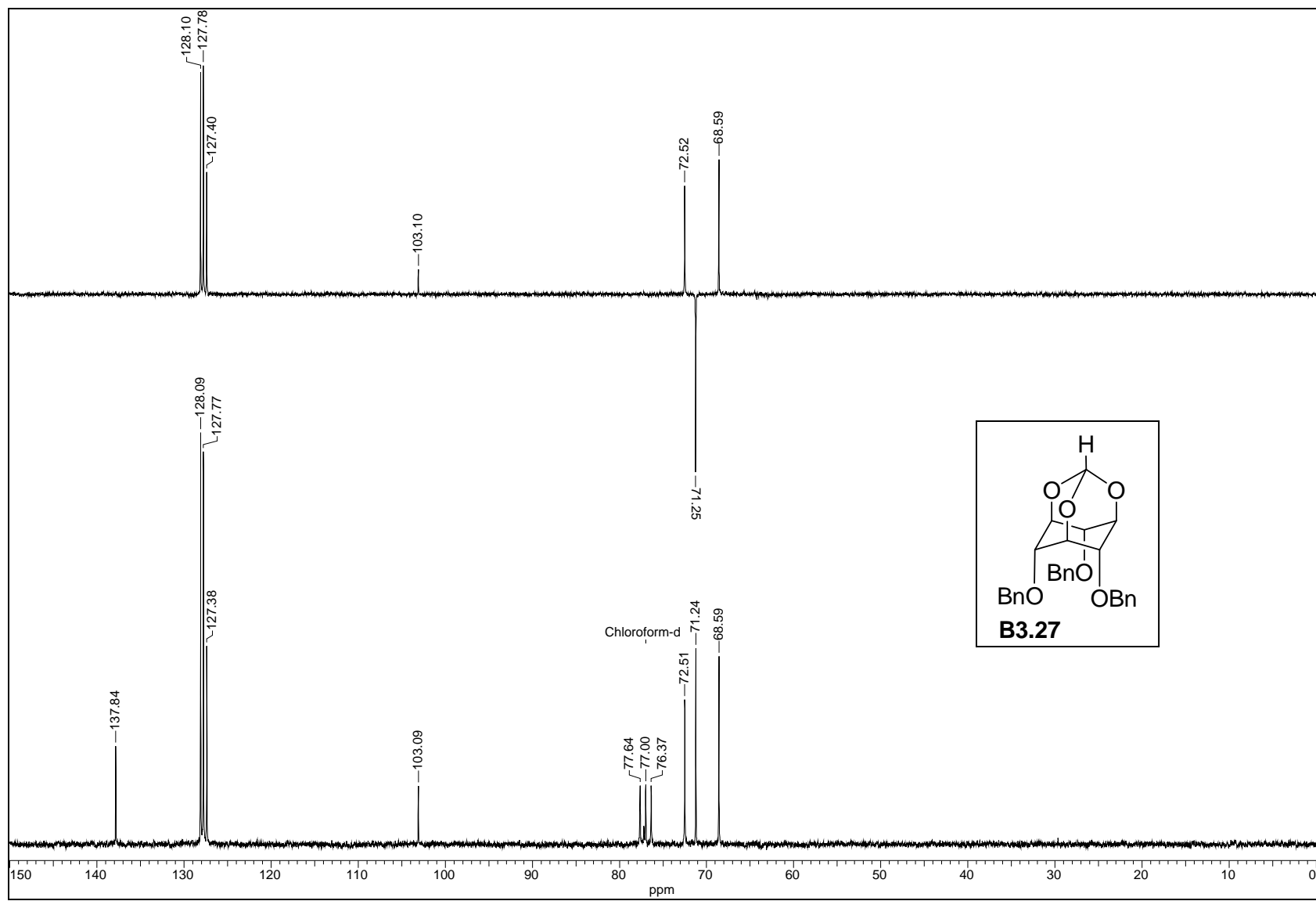
3.6 Appendix

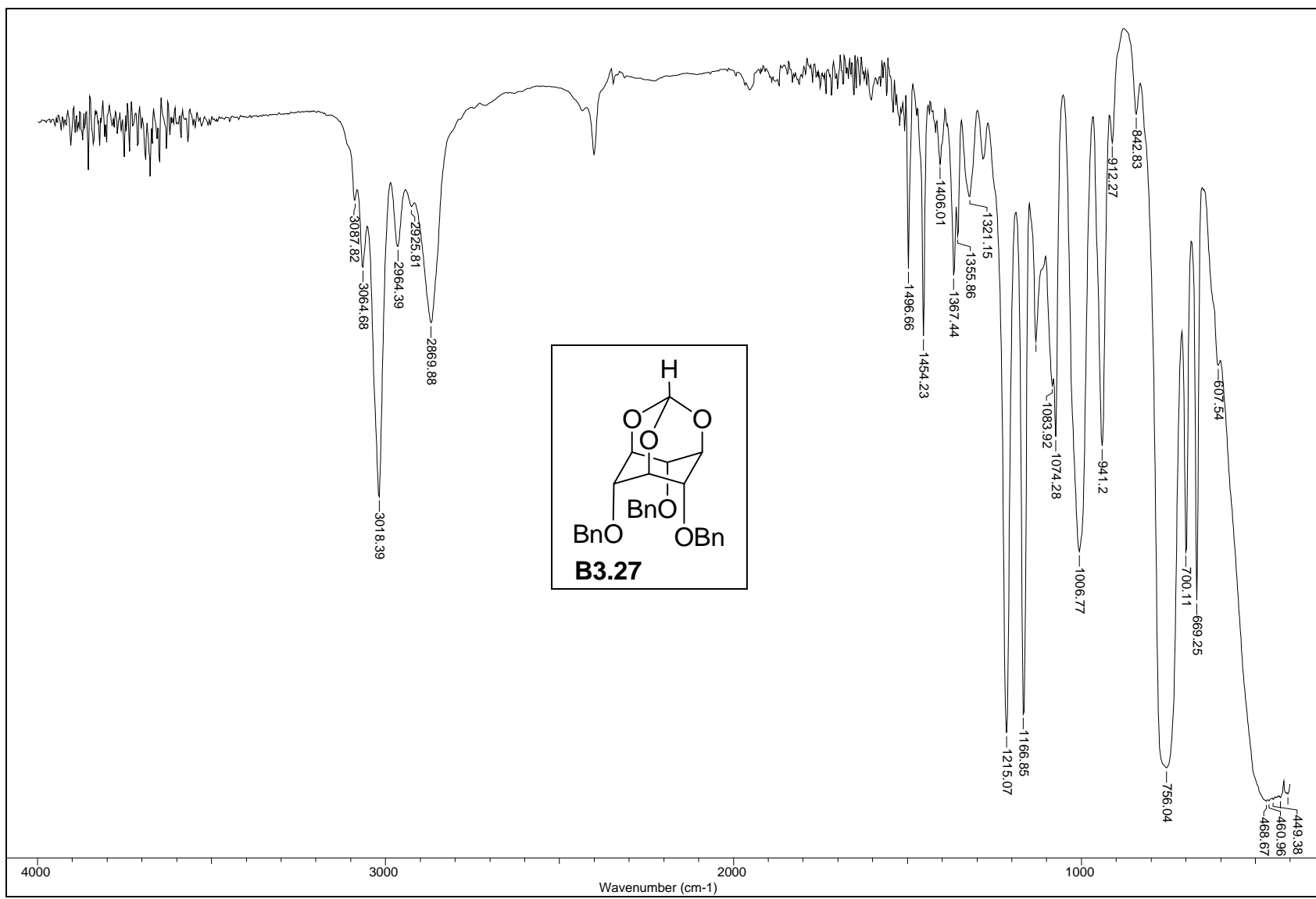
Sr. No	Index	Page No.
1	Molecular interactions and packing diagram of B3.26	293
2	¹ H spectrum of B3.27	294
3	¹³ C and DEPT NMR spectra of B3.27	295
4	IR spectrum of B3.27	296
5	Molecular interactions and packing diagram of B3.27	297
6	TGDTA graph of B3.35	298
7	TGDTA graph of B3.36	299
8	TGDTA graph of B3.37	300

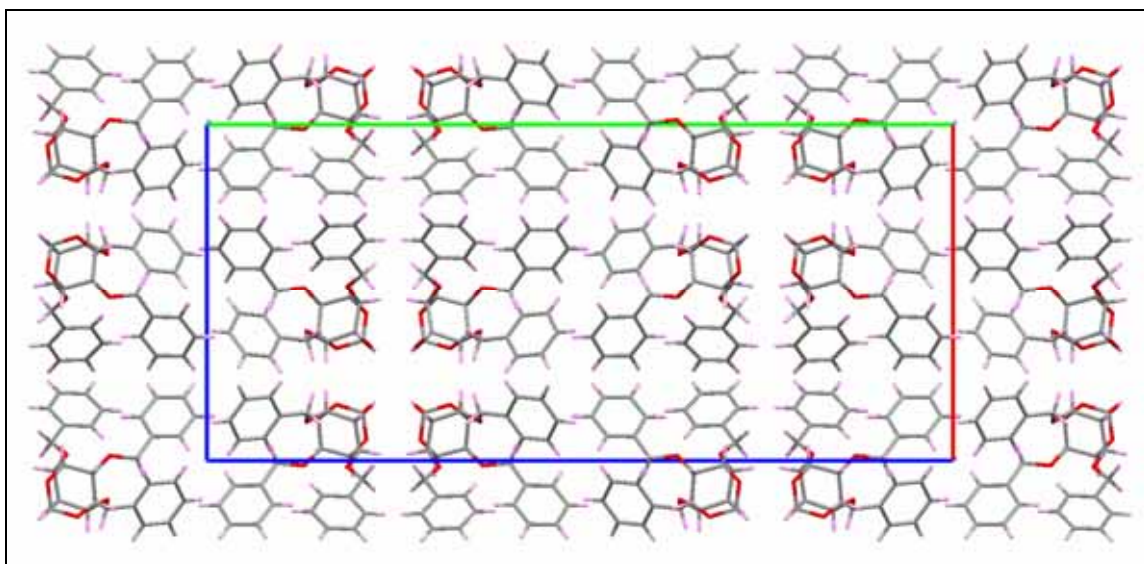
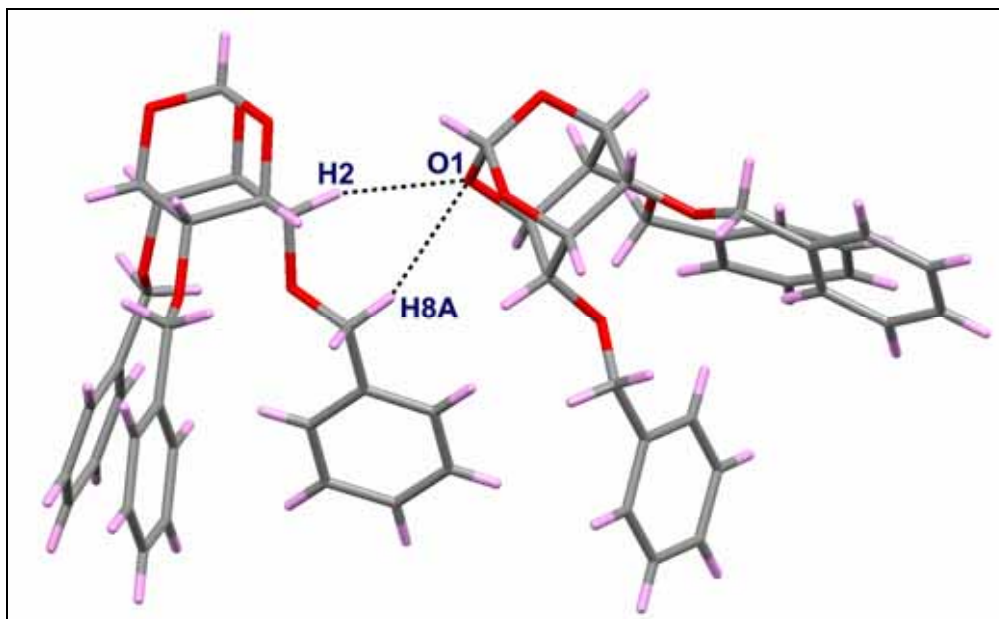


ORTEP, molecular interactions and packing diagram down a-axis of **B3.26**.









ORTEP, molecular interactions and packing diagram down c-axis of **B3.27**.

